Reinforcement Learning of Dynamic Collaborative Driving

by

Luke Ng

A thesis
presented to the University of Waterloo
in fulfillment of the
thesis requirement for the degree of
Doctor of Philosophy
in
Mechanical Engineering

Waterloo, Ontario, Canada, 2008

Author's Declaration

I hereby declare that I am the sole author of this thesis. This is a true copy of the thesis, including any required final revisions, as accepted by my examiners.

I understand that my thesis may be made electronically available to the public.

Abstract

Dynamic Collaborative Driving is the concept of decentralized multi-vehicle automated driving where vehicles form dynamic local area networks within which information is shared to build a dynamic data representation of the environment to improve road usage and safety. The vision is to have networks of cars spanning multiple lanes forming these dynamic networks so as to optimize traffic flow while maintaining safety as each vehicle travels to its destinations. A basic requirement of any vehicle participating in dynamic collaborative driving is longitudinal and lateral control. Without this capability, higher-level coordination is not possible.

This thesis investigates the issue of the control of an automobile in the context of a Dynamic Collaborative Driving system. Each vehicle involved is considered a complex composite nonlinear system. Therefore a complex nonlinear model of the vehicle dynamics is formulated and serves as the control system design platform. Due to the nonlinear nature of the vehicle dynamics, a nonlinear approach to control is used to achieve longitudinal and lateral control of the vehicle. This novel approach combines the use of reinforcement learning: a modern machine learning technique, with adaptive control and preview control techniques. This thesis presents the design of both the longitudinal and lateral control systems which serves as a basis for Dynamic Collaborative Driving. The results of the reinforcement learning phase and the performance of the adaptive control systems for single automobile performance as well as the performance in a multi-vehicle platoon is presented.

Acknowledgements

This thesis is the culmination of many years of hard work. This degree has allowed me to study different areas, make new friends, strengthen friendships and appreciate what real love, understanding and support are. I would like to thank all those who have helped me through this phase of my life. To my supervisor Dr. Jan Huissoon, thank you for your supervision, support and faith in my abilities and for giving me the opportunity to study with you. To my co-supervisor Dr. Christopher Clark, thank you for your advice, input and support.

To my loving wife Sharon, you gave your love, devotion, support, faith and wisdom generously throughout this endeavor. You are my rock and my best friend, without you, none of this would be possible.

To my family and friends: my mother-in-law, Connie, Matthew, Eric Lee, Paul Gray, Sang-Joon Park, Saleh Tabaneh, Josh Marshall and Jimmy Kuo, thank you for your encouragement and support throughout my studies.

To Dr. Gabriele D'Eleuterio, for giving me the opportunity to study at UTIAS. I have learned that despite my best efforts and continuous hard work over 4 years, it was not enough and I alone could not complete my studies at UTIAS. It is in these dark times I learned the true value of supervision.

To Dr. David Zingg thank you for your assistance and support during the most difficult times at UTIAS. To Dr. Peter Grant thank you for your support during my studies at UTIAS and your diligence in reviewing this thesis.

To Dr. Sangeev Bedi, Dr. Pascal Poupart, Dr. Fathi Ismail and Dr. Micheal Worswick thank you all for your advice, help and support throughout my studies at Waterloo.

Finally, I would like to thank NSERC and the Auto21 Centers of Excellence Program for financial funding of this research.

Dedication

This thesis is dedicated to my father-in-law Kam Shun Chau whose advice, love, endless support, and prayers allowed me to complete this long journey. I express my deepest thanks and gratitude to you.

Table of Contents

List of Figures

List of Tables

Chapter 1
Introduction

Dynamic collaborative driving is an automated driving concept that has the potential to significantly improve road transport safety and to reduce human casualties in motor vehicle accidents. This concept is based on the exchange of information between vehicles instrumented to perceive their surroundings so they may collaborate in dynamically formed groups. These vehicle groups, or ad-hoc networks, can form a collective driving strategy, which would require little if any operator intervention. This thesis introduces the idea of formulating the basic skills required in dynamic collaborative driving into finite *Markov Decision Processes* (MDP) which can be solved using *reinforcement learning* algorithms so as to produce a system which has the potential to continually adapt and learn to optimize its performance based on experience. When implemented in a group of vehicles linked with a communication system this allows for the possibility of an extremely adaptive multi-vehicle system which in turn can be more robust, reliable and efficient.

This introductory chapter of this thesis includes, i) the motivation behind this research, ii) the rationale of the study, iii) the definition of the research problem of this thesis, and iv) the research objectives. The next chapter provides the pertinent background material for this study. This includes a literature review and overview of some theoretical concepts. Chapter 3 discusses the vehicle dynamics modeling which is crucial to our simulation study. Chapter 4 describes the design of the control system. Chapter 5 describes the experimental portion of this study along with results. Chapter 6 states the conclusions of this thesis.

1.1 Motivation

In major cities throughout the world, urban expansion has led to an increase in traffic flow. The adverse effects associated with increased traffic flow are many and familiar to most. These include traffic congestion, driving stress, vehicle collisions, pollution, and logistical delays. Once traffic flow surpasses the capacity of the road system, it ceases to become a viable transportation option. One solution is to construct more roads or additional lanes to accommodate the peak traffic flow. This can be extremely costly and in some case infeasible (e.g. adding additional lanes on a mountain road). Additional complexity is also required to accommodate the new road or lanes into the existing system (i.e. signs, lights, and routing). Another solution is to use the existing road infrastructure but to increase the throughput of the road by having vehicles drive closer together and faster. However it is difficult for humans to safely drive automobiles at high speeds and maintain close inter-vehicle spacing, therefore, driving must be automated for this solution to be feasible.

1.2 Rationale

The concept of automated driving dates to the 1939 New York World's Fair, where General Motors designer, Norman Geddes showcased *Futurama*, a city set in what he envisioned would be 1959, where automated cars would drive people between their homes in the suburbs and their workplaces in the cities.

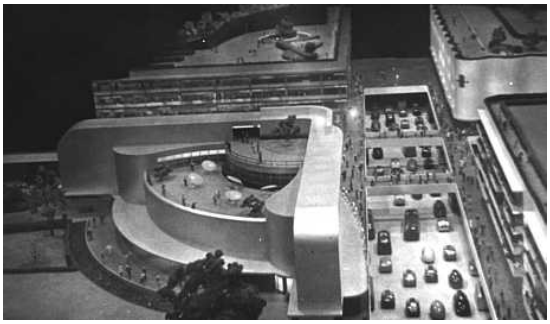

Figure 1.1 GM Futurama by Norman Geddes (NY, USA, 1939)

Since then, significant research has been accomplished in the area of automated driving throughout the world resulting in prototype systems, in Europe under the Chauffeur projects [Franke et al 1995] [Fritz et al 2004], in the United States during Demo '97 [Thorpe et al 1997] [Tan et al 1998] and in Japan during Demo 2000 [Tsugawa et al 2000] [Kato et al 2002]. Research continually flourished in Europe, US, and Japan, but despite all the research, automated driving today remains as a concept and not a reality. The acceptance of automated driving systems has not occurred with the general public, some of the reasons for which include: reliability, infrastructure, difficulty in deployment and integration with existing vehicles under human control [NAHS Research Program 1998].

In order to make automated driving a reality, many issues such as safety, fault-tolerance, and the coexistence of automated vehicles with human driven vehicles must be solved. These issues are evident in the prototype systems presented at Demo '97, Demo 2000 and the Chauffeur projects. The numbers of vehicles involved in these systems are limited to no more than eight vehicles. The vehicles involved are identical and formation control is centralized to a single lead vehicle. To address the shortcoming of these systems, new approaches to automated driving must be investigated that make use of decentralized control to gain fault tolerance and reliability. They must use adaptive controllers derived with the latest artificial intelligence methods. Sensor-fusion would be employed along with inter-vehicle communication and shared data. All this would make the vehicles *smarter* so that the system could accommodate human driven vehicles, offer increased reliability and to be scalable.

Promote Chauffeur
(E.U. 1994)

CalTrans PATH: Demo 97
(San Diego, USA 1997)

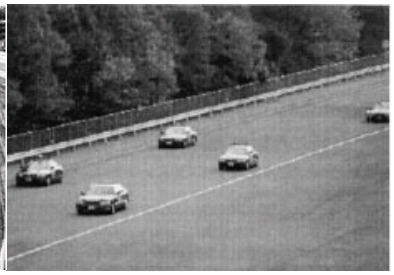

AIST : Demo 2000
(Tsukuba, Japan)

Figure 1.2 Global Research Efforts

The search for better automated driving approaches brings us to Dynamic Collaborative Driving, a concept that has multiple intelligent vehicles building dynamic local area networks. By sharing their sensory information, the vehicle group can build up a shared dynamic data representation of the environment. This larger representation allows the group to coordinate their movement so as to drive collaboratively. This multi-vehicle collaboration could lead to benefits such as improved traffic flow and improved safety. Since a dynamic collaborative driving system can be considered a multi-agent system under decentralized control, it has characteristics inherent of decentralized systems. Decentralized systems are known to be more scalable and not susceptible to individual vehicle failures, that is, they are more fault-tolerant [Parker 2000]. However, multi-agent systems under decentralized control are difficult to design and implement since the dynamics of the interacting agents are unknown. Individual agent controllers cannot simply be *hard-coded*; rather machine learning techniques are used by each agent to arrive at its own controller which will result in the desired emergent behavior. One example of such a technique is *reinforcement learning* which allows the systems to be more adaptable and to continuously integrate new experiences to develop an optimal control system [Sutton & Barto 1998]. By employing a decentralized approach and using reinforcement learning, a dynamic collaborative driving system could be designed to address the shortcomings of the previous generation of automated driving systems.

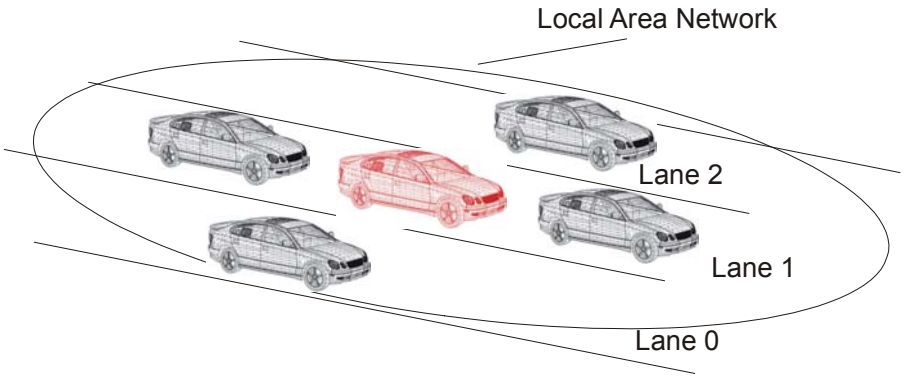

Figure 1.3 Dynamic Collaborative Driving

1.3 Research Definition

This thesis investigates the issue of multi-vehicle collaboration in dynamic collaborative driving under decentralized control. This issue can be stated as a research question, "How do you control the motion of vehicle within a group to share a common roadway?" Specifically, we wish to control how the vehicle interacts with the vehicles in its immediate vicinity. The most crucial capability for a vehicle to operate in any collaborative driving system is to be able to guarantee the following of a vehicle ahead both longitudinally and laterally. Once this basic skill is achieved, higher order commands with the aid of inter-vehicle communication can be issued to the vehicle to space the vehicles in a single lane formation or platoon, or to enter/exit other platoons in other lanes.

Previous research has demonstrated the use of conventional control strategies to achieve longitudinal control, lateral control and combined lateral and longitudinal control. These approaches make use of conventional control approaches which rely on state-space models to approximate the plant. The complexities and nonlinearities of the modern automobile which will be explained in Chapter 3, require equivalent state-space models that have a large number of states and may not model the system accurately. These state-space models are then used to derive controllers which are then tested on more complex numerical vehicle dynamics simulations [Maciuca & Hedrick 1995],[Pham et al 1997]. Although a rich simulation is available it is not used in the design process but as a means of evaluation. Why not incorporate the model into the design of the controller and capture the salient features of the vehicle dynamics model? To do this, a very different approach to control design is proposed. In this thesis, it is proposed that each agent involved with dynamic collaborative driving should determine its own control system on a continual basis either using real-time vehicle data or with the aid of a complex numerical vehicle dynamics simulation thus assuring a certain level of performance for various situation, in other words, machine learning is required.

The research objective of this thesis is to demonstrate that an individual vehicle agent can use reinforcement learning to determine its own decentralized adaptive motion control system capable of performing in a multi-vehicle environment for the task of Dynamic Collaborative Driving.

1.4 Contributions

This study shows how reinforcement learning can be applied to obtain an adaptive controller for the control of vehicle following. Although this is not the first study of reinforcement learning in collaborative driving [Laumonier et al 2006], it is the first in the literature that introduces the use and studies the feasibility of reinforcement learning for low-level motion control of an actual automobile modeled by a complex non-linear simulation vehicle model. The contributions achieved in this study are

1. A novel adaptive control design for the problem of automotive adaptive cruise control for dynamic collaborative driving which includes control of the throttle and braking response for a modern automobile.
2. A novel preview/adaptive control design for the problem of automotive steering control for dynamic collaborative driving for a modern automobile.

These controllers are machine learned using Monte Carlo reinforcement learning and based on the composite nonlinear vehicle model. The learning process, individual vehicle performance as well as multi-vehicle performance are demonstrated.

During the course of this research key software tools were developed in order to facilitate experimentation. In this thesis, the details of the design for these tools have been shared in hopes that other AI engineers can benefit in their research. The software tools developed in this thesis are

1. The design and formulation of a detailed composite nonlinear model of a modern automobile. Although parts of this model are based on a previous body of work, the model is applicable

throughout the performance envelope of the automobile and is used as a nonlinear control design platform. This model is implemented as both a C++ object library and a Matlab library which can be used by future engineers as an open standardized vehicle model of an automobile for the development of automotive control systems.

2. The design of an object-oriented programming (OOP) implementation of generalized Markov Decision Processes and reinforcement learning solution methods. The software is packaged as a C++ object library called RLtools and allows the user to modularize reinforcement learning functionality greatly simplifying the development process for future engineers.

This study adds to the area of intelligent vehicle research by demonstrating the viability of using machine learning approaches to address vehicle control problems that were formerly solved using conventional control theory. The introduction of reinforcement learning to vehicle control provides yet another avenue for the control system to achieve adaptability without complicating the controller design. Although, this study provides both the methodology and the software tools necessary for engineers to build future reinforcement learning based control systems for automobiles, the benefits of this research go beyond automotive control and can be applicable to any autonomous vehicle or robot.

Chapter 2
Background

2.1 Platooning

Research in automated driving in the United States during the 1990s was conducted under the PATH project (Partners for Advanced Transit and Highways). PATH introduced the concept of multi-vehicle coordination as platooning. Platooning is the concept of having vehicles in groups of 10-25 cars traveling in tight vehicle-string formations where the inter-vehicle spaces are in the order of 1-2m. The group is controlled by a leader and multiple platoons would be separated by larger distances for a greater degree of safety [Varaiya 1993], [Shladover et al 1991], [Hedrick et al 1994]. A prototype of this concept was demonstrated during Demo '97 in San Diego on a reserved 7-mile highway lane guided by magnets embedded in the roadway [Tan et al 1998], [Rajamani et al 2000]. Liu et al [2001] examined the robustness of conventional longitudinal controllers to communication delays and showed that string stability is seriously compromised by communication delays. Huppe and Michaud [2003] studied optimal control for platooning using Linear Quadratic Regulator and a 5^{th} order longitudinal following rule.

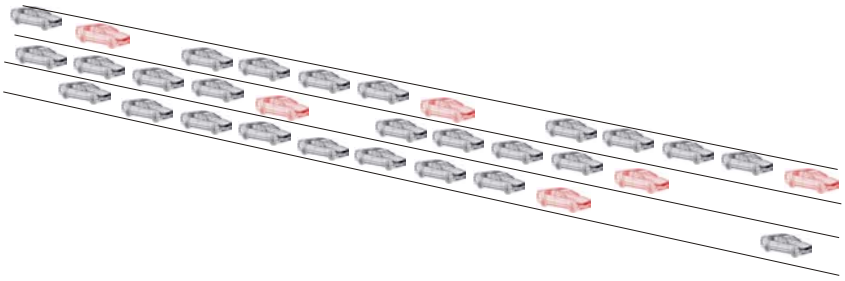

Figure 2.1 Concept of vehicle platooning

2.2 Longitudinal Control

The most basic level of control in platooning is longitudinal control, also referred to as autonomous intelligent cruise control (AICC). Ioannou and Chien [1993] describe an AICC system for automatic vehicle following, which is a stand-alone longitudinal control system using a linear vehicle following model. Raza and Ioannou [1997] implemented the AICC system on a real vehicle and evaluated it during Demo '97 to verify the performance obtained under simulation.

Studies in the mid 1990s at UC Berkeley [Maciuca and Hedrick 1995] [Maciuca et al 1994], [Gerdes et al 1995], [Swaroop & Hedrick 1994] focused on using sliding mode control to address the nonlinearities of longitudinal vehicle dynamics. The studies addressed vehicle dynamics simulation, string stability of linear formations and nonlinear control. Rajamani et al [2000] implemented sliding

surface control to longitudinal control during Demo '97. At Demo 2000, Kato et al [2002] demonstrated an adaptive proportional control law for longitudinal control. Recently, Zhang and Ioannou [2005] proposed an adaptive control approach to vehicle following with variable time headways, using a simplified first order linear vehicle model. The control system guarantees closed-loop system stability, and regulates the speed and separation errors towards zero when the lead vehicle is at a constant speed.

2.3 Lateral Control

Early research in automated driving began with lateral vehicle control for lane following on passenger vehicles conducted by General Motors and RCA in the late 1950s [Kargels 1960]. These studies included vehicle dynamics modeling, lane sensor development and the design of classical lateral controllers. Approaches to lateral control or automatic steering can be grouped into look-down and look-ahead systems, in terms of the measurement of lateral displacement. Look-down systems measure lateral displacement down from the front bumper using an electric wire [Fenton et al 1976] or magnetic markers [Zhang and Parsons 1990], these systems deal with the immediate lateral position of the vehicle, that is they do not rely on preview information [Guldner et al 1994] [Guldner et al 1997]. Thus, the performance is more speed dependent, leads to more sluggish performance and larger lateral errors. When experimentally verified, look-down systems are practical only at low speed of less than 20 m/s. Selim and Fenton [1984], [Fenton & Selim 1988] employed an optimal control approach to design a velocity-adaptive, lateral controller for the design goals of lateral-position tracking accuracy, robustness, and ride comfort. Guldner [1994] and Pham et al [1996] used sliding mode control without preview to achieve lateral control. Later, the coupling of the longitudinal control with lateral control led to sliding surface control [Pham et al 1994], [Pham et al 1997]. Rajamani et al [2000] implemented in hardware for Demo '97, a lateral control system incorporating both look-down and look-ahead control systems for integrated lane-keeping and lane-changing.

Alternatively, look-ahead systems replicate human driving by measuring lateral displacement ahead of the vehicle. With look-ahead system modalities such as machine vision [Jochem et al 1995] or radar [Unyelioglu et al 1996], it is possible to predict or anticipate where the vehicle is heading and provides a means of feed-forward control. Variya [1993] suggests that automatic steering systems should have some anticipatory capabilities. Prior to this, Peng and Tomizuka [1991] introduced a lateral feed-forward control algorithm which utilized preview information pertaining to road curvature as well as super-elevation angle. More recently, Netto et al [2004] conducted a simulation study to design a self-tuning linear regulator for lateral control. The controller is based on a simplified linear model of lateral vehicle dynamics. In this paper, a model predictive adaptive control system is introduced whereby the model is learned through reinforcement learning using a complex nonlinear vehicle dynamics model; this controller is considered a look-ahead system. Meier et al [2004] demonstrated a vision based tracking control system for lateral control for the INVENT research initiative in Germany.

Classical linear steering control was studied by Ackermann [1990] using a simplified lateral vehicle dynamics model which approximated the automobile as a bicycle. Mammar [2004]

demonstrated a gain scheduled H∞ controller for lateral control based on a simplified linear vehicle dynamics model (single track/bicycle model) which demonstrates quick lateral response in simulation. Recently, Khatir and Davison [2006] proposed a dual linear PID controller for longitudinal and lateral control assuming a simplified 6th order linear model and a bicycle model for vehicle dynamics.

2.4 Vehicle String Stability

The string stability of an interconnected system implies uniform boundedness of the state of all the systems being connected. For the application of automated vehicle-following, tracking errors such as inter-vehicle spacing and lateral offset should not amplify downstream from vehicle to vehicle. Early research [Levine & Athans 1966] [Melzer & Kuo 1971] sought optimal control solutions to the automated vehicle-following problem. However no precise definition of string stability was coined until Chu's work in 1974.

Chu [1974] defines string stability in the context of vehicle following for an infinite number of interconnected vehicles traveling in a single lane where the vehicle is considered a linear system. In the definition, all vehicles are assumed to be identical and the number of vehicles is assumed to be infinite. That is, there is no end to the string. In reality, the length of a string is always finite, considering that the system is a section of an infinite string, and adding fictitious vehicles that have no errors in their motion to the front and back end of the string section.

Swaroop and Hedrick [1996] generalize the concept of string stability to include nonlinear, non-identical interconnected systems. The concept of "weak coupling" conditions are presented that guarantee string stability for a class of interconnected systems and prove that every exponentially string-stable interconnected system is string stable in the presence of small perturbations (Lyapunov stability). Large perturbations do occur in collaborative driving such as when vehicles have collided or stopped, therefore empirical evaluations should be conducted to support the claim of stability by a given vehicle control system.

2.5 Linear Feedback Control

Control is the manipulation to the inputs of a system to achieve desired outputs or effects. Therefore a controller is another system which can provide the inputs to the system being controlled, which is called the plant, to produce the desired outputs. Inputs to the plant which are inaccessible by the controller can be considered disturbances. If the plant's properties are completely known and deterministic, then the controller need only provide appropriate input signals to achieve the desired output; this is called open-loop control because the control inputs are independent of the plant output. However in most cases, the plant's properties are partially known and disturbances may create unwanted responses which are desirable to reduce.

Feedback control is using the outputs of the plant to drive the inputs so that the desired output can be achieved. The outputs are said to be "fed back" to the plant, and this is referred to as close-

loop control. The advantages of feedback control are: i) increased accuracy as the error (desired output – measured output) can be driven to zero; ii) reduced sensitivity to changes in plant; iii) reduced effects of disturbances; and iv) increased speed of response and bandwidth [Stefani et al 1994].

A linear system is a system that can be modeled as a linear homogeneous differential equation with constant coefficients. These systems are particularly easy to solve by breaking up the differential equation into smaller easier to manage pieces, solving each of those pieces, and adding the solutions up. Therefore, linear systems satisfy the superposition property. However, most real systems are nonlinear as their effects are governed by nonlinear relationships between states or functions. Fortunately, a nonlinear system can be approximated as a linear system about an operating point with limited applicability and accuracy [Grantham & Vincent 1993].

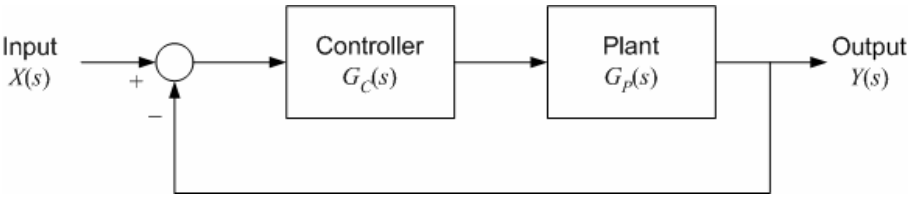

Figure 2.2 Block diagram of close-loop control

Figure 2.2 shows in block form of a plant under feedback control. Both the plant and the controller are considered as systems with inputs and outputs. The plant combined with the controller and the feedback loop is also considered a system with inputs and outputs. Each of these systems can be modeled as differential equations and can be expressed as Laplace transform "transfer" functions.

For a system, the transfer function $T(s)$ is the ratio of the Laplace transform $Y(s)$ of the output function in the time domain to the Laplace transform $X(s)$ of the input function in the time domain when all initial conditions are zero. For a single input single output (SISO) system, the output function in the time domain is $y(t)$ while the input function in the time domain is x(t).

$$T(s) = \left.\frac{Y(s)}{X(s)}\right|_0 = \frac{\mathcal{L}[y(t)]}{\mathcal{L}[x(t)]} = \frac{Output}{Input} \tag{2.1}$$

The transfer functions of the overall system, controller and plant are related using the following equation,

$$T_{desired}(s) = \frac{G_C(s)\,G_P(s)}{1 + G_C(s)\,G_P(s)} \tag{2.2}$$

which is equivalent to

$$G_C(s) = \frac{T_{desired}(s)}{G_P(s) - T_{desired}(s)\,G_P(s)}. \tag{2.3}$$

The challenge is to determine the controller transfer function $G_C(s)$ which will provide the desired overall system transfer function $T_{desired}(s)$. If $G_P(s)$, the transfer function of the plant is

known, then determining the controller transfer function, $G_C(s)$ is rather straightforward using Equation (2.3). This is assuming that the plant can be described with a linear differential equation. In most cases, there is not sufficient data to formulate an accurate linear model of the plant or the plant is nonlinear. Therefore, generic control laws are used and the parameters of these control laws are then tuned to match the plant to achieve the desired overall response.

A widely used control scheme is a cascade Proportional Integral Derivative (PID) compensation [Minorsky 1922]. The form of the transfer function of the PID compensator is

$$G_C(s) = K_p + \frac{K_i}{s} + K_d\, s \tag{2.4}$$

where K_p is the gain for the proportional (P) action, K_i is the gain for integral (I) action, and K_d is the gain for the derivative (D) action. The proportional action directly acts on the error signal and affects how quickly the error is eliminated. The effect of the integral action is to eliminate steady-state error due to an uncertain bias on the input. The derivative action introduces damping as the proportional action tries to reduce the error signal.

The above discussion assumes that the processes are in continuous time. However, this thesis deals with the computer control of discrete time systems. In continuous time systems, the transfer function is used to express the control system. In discrete time systems, a difference equation is used to express the control system which can readily be coded into a digital computer program. The difference equation for discrete PID control is

$$m_n = m_{n-1} + K_0 e_n + K_1 e_{n-1} + K_2 e_{n-2} \tag{2.5}$$

where

$$K_0 = K_p + K_i T + \frac{K_d}{T} \qquad K_1 = -K_p - 2\frac{K_d}{T} \qquad K_2 = \frac{K_d}{T}.$$

Assuming that a discrete process is to be controlled whose output c_n can be sampled at a period of T seconds and a desired output is r_n. The error in the processes output is determined using

$$e_n = r_n - c_n \tag{2.6}$$

and the discrete output of the controller is m_n where n is the current time step. The derivation of the difference equation for PID control is taken from Bollinger and Duffie [1988] and is shown in Appendix A.

2.6 Adaptive Control

To *adapt*, is to modify one's behavior according to changing circumstances. Therefore an adaptive controller is a controller that modifies its behavior in response to changes in the dynamics of the process and the character of the disturbances [Aström & Wittenmark 1994]. Although, adaptive control dates back to the 1950s it still lacks a formal definition. A pragmatic definition considers that an adaptive control system has adjustable parameters as well as a mechanism for adjusting the parameters. Due to the adjustment mechanism, the controller becomes nonlinear. The structure of an

adaptive controller is shown in block diagram form in Figure 2.3. Notice, there are two feedback loops, one is a normal feedback loop and the other is the parameter adjustment loop which is slower than the normal feedback loop.

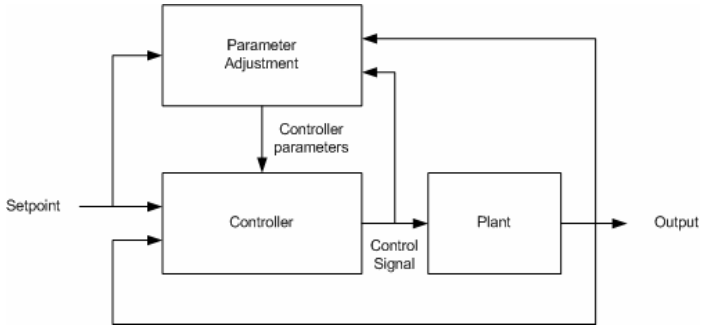

Figure 2.3 Block diagram of an adaptive system

Extensive research on adaptive control was pursued in the early 1950's for the design of autopilots for high-performance aircraft. These aircraft operate over a wide range of speeds and altitudes. Researchers found that ordinary constant-gain linear feedback control could work well in one operating condition but not over the whole flight regime. Therefore, a more sophisticated controller that could work well over a wide range of operating conditions was needed. For the application of flight control, it was possible to identify key measurable variables that correlated well with changes in flight dynamics. Thus a schedule of control parameters (gains) could be found for each flight condition. This technique is known as gain scheduling and has become the standard technique for high performance flight control systems.

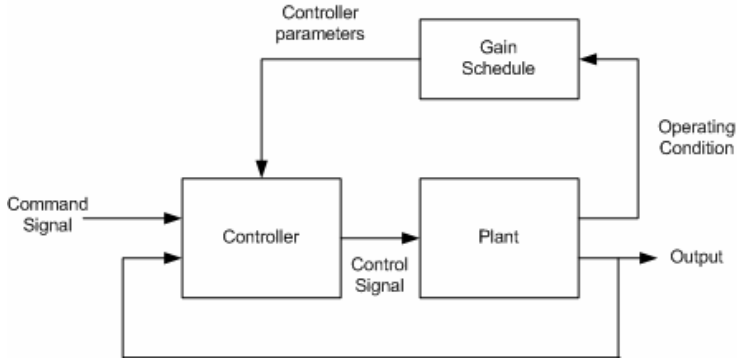

Figure 2.4 Block diagram of gain scheduling.

Gain scheduling is a powerful yet simple approach to adaptive control. The key problem is to find suitable scheduling variables that correlate well with measurable changes in process dynamics. The scheduling variables range is quantized over a number of discrete operating conditions. The controller parameters are then tuned for every operating condition and the parameters are stored in a table or schedule. Although significant effort is required to identify schedule variables and to build up the parameter table, normal operation requires only a facility for storing and recalling the parameters. Figure 2.4 illustrates the block diagram for gain scheduling. The system can be viewed

as having two loops, an inner feedback loop between the plant and the controller and an outer loop which adjusts the gains on the basis of operating conditions. One can consider the *Gain Schedule* to be a mapping or model from operating conditions to controller parameters.

2.7 Reinforcement Learning

The early research in the application of reinforcement learning to robotics was pursued by Mahadevan and Connell [1991a, 1991b] who used reinforcement learning to enable a mobile robot to learn the task of effectively pushing large boxes across a floor. This problem is characterized by immense uncertainty in the results of actions. The Q-learning reinforcement learning algorithm was used in conjunction with clustering techniques designed to enable a higher-dimensional input than a tabular approach would have permitted. The learning was extremely slow since it took place in real-time using hardware. The resulting control policy's performance was on par with a human-programmed solution.

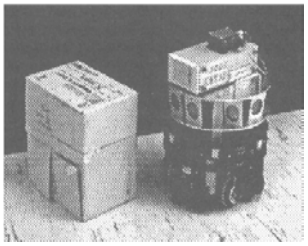

Figure 2.5 Mahadevan and Connell [1991a, 1991b]

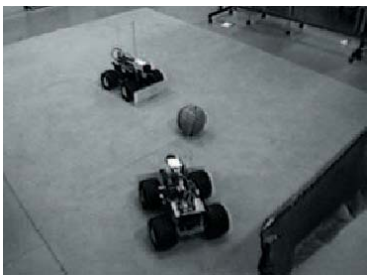

Uchibe [1999]

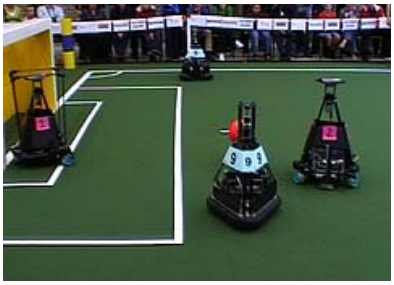

Reidmiller et al [2001]

Figure 2.6 Reinforcement learning and RoboCup

Figure 2.7 Reinforcement learning for helicopter flight control, Ng et al [2004]

Later, reinforcement learning was applied to the RoboCup soccer domain [Mackworth 1993] and resulted in some successful studies. Uchibe [1999] used reinforcement learning on an actual robot to learn to shoot a ball into a goal while avoiding an opponent. The task has a very well defined goal state, however the fact that it works on actual hardware makes it a notable achievement. Reidmiller et al [2001] use reinforcement learning to learn low-level skills such as kicking, interception, dribbling and cooperative scoring maneuvers (2 vs 2). A particularly successful implementation of reinforcement learning is for autonomous inverted helicopter flight control. Ng et al [2004] use a Monte Carlo reinforcement learning algorithm in combination with a neural network to control the inverted flight of the helicopter at low speeds. This is a particularly difficult non-linear control problem and is difficult for most humans to achieve. The learning was performed in a helicopter flight simulator and tested on an actual model helicopter.

2.7.1 Overview

Reinforcement learning (RL) is a machine learning approach that formulates a control problem using an agent that interacts with an environment. The agent senses the environment through its states *(s)* and responds to it through its actions *(a)* under the control of a policy, $a = \pi(s)$. This policy is modified iteratively using a reinforcement learning algorithm whose input is a numerical reward from the environment for the current state, $r = R(s)$. The challenge of reinforcement learning is to determine the actions which result in the maximum reward for every possible state, this state to action mapping is called the optimal policy π^*.

The environment supplies the next state based on the current state and the actions taken using the transition function or model, $s' = \sigma(s, a)$. Since it may be difficult to obtain a transition model of a plant, one can use average sampled experiences as an equivalent transition model. In this case, the *world* becomes the transition model and leads to real-time learning. One could also create a simulated world that provides the simulated experiences to the agent for the process of learning.

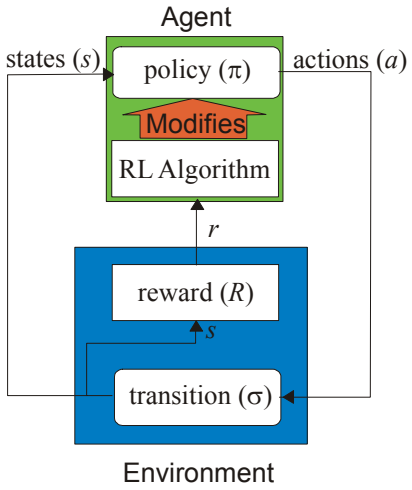

Figure 2.8 Overview of Reinforcement Learning

2.7.2 Markov Decision Processes

In reinforcement learning, the environment is typically formulated into a finite Markov Decision Process (MDP), a mathematical framework used in Machine Learning that lends itself well to iterative solutions [Bellman 1957b]. A finite MDP has states and actions which are discrete; therefore some form of discretization is required to convert continuous state and action values to their discrete equivalents. To formulate an MDP, the states s, actions a, reward $R(s)$ and transition model $s' = \sigma(s,a)$ must be defined. The key feature of an MDP is that to be considered Markov, its current state must be independent of previous states. This is so that for each visit to a state, the software agent is given a path independent reward. Subsequent actions will result in new states giving rise to different rewards. For the current state, actions that result in more favorable future states lead to higher rewards.

2.7.3 Policy

The solution to the reinforcement learning problem or MDP is the optimal policy π^*, which is determined iteratively through the process of learning. The agent's learning process begins with an initial policy π_0, such that when a new state is visited, a random action is taken, called an exploration start. For a greedy policy, if the state has already been visited, the agent chooses the action that previously resulted in the highest reward when compared with other actions taken from this state. This selection is based on $Q(s,a)$, the Q-value associated with the state-action pair $\{s,a\}$ and is not guaranteed to be the optimal action unless all possible actions have been previously tried for this state. Since the agent can only use what it knows, it will choose this suboptimal action every time it visits this state, therefore it is not learning. To allow exploration on a regular basis an ε-soft greedy policy is used in reinforcement learning. Instead of always using the previously taken action that resulted in the highest reward for the state at hand, the ε-soft greedy policy selects a random action with probability ε. . Thus it has the possibility of visiting every state-action pair infinite amount of times as $t \to \infty$. The importance of the concept will be clarified below in the next section.

2.7.4 Value Functions

For every visit to a state, the agent receives a specific reward based on the action taken. Subsequent actions will result in new states giving rise to different rewards. For the current state, actions that result in more favorable future states which lead to higher rewards are preferred. The favorability of a certain action given the current state is known as the Q-value.

The Q-value is defined as the expected reward E_r for taking action a in state s under a policy π, denoted by $Q^{\pi}(s, a)$.

$$Q^{\pi}(s,a) = E_{\pi}\{R_t \mid s_t = s, a_t = a\} = E_{\pi}\left\{\sum_{k=0}^{\infty} \gamma^k r_{k+t+1} \mid s_t = s, a_t = a\right\} \tag{2.7}$$

where γ is a discount factor for weighing future rewards r. As an agent experiences its environment, it updates the Q-value for each state-action pair it visits according to its reinforcement learning algorithm. As the agent repeatedly visits every state-action pair, it updates the policy so that the

highest valued state-actions will dominate. In this thesis, the reinforcement learning algorithm used is called *Monte Carlo ES* (Figure 2.9) where γ is set to 1 and $Q^{\pi}(s, a)$ is updated episodically by averaging the sampled expected returns for each visit to a specific state-action pair. Averaging the sampled $Q^{\pi}(s, a)$ eliminates variation due to the probabilistic nature of the environment.

The optimal policy is reached when every state-action pair in the current policy results in the highest reward possible, that is when $Q^{\pi}(s, a)$, the Q-value function for the current policy has been maximized. The convergence of this maximization process requires that all states and actions be visited infinitely many times in order for estimates of the Q-value to reach their optimal values. To ensure this convergence criterion, policies leading to π^* are ε-soft, meaning that there is a ε probability that a random action is selected. Therefore, all actions and states will be reached as $t \rightarrow \infty$.

2.7.5 Reward Function

The reward function expresses the desirability of being in a current state. It is the method of communicating to the agent the task to be performed. The challenge of the designer is to be able to come up with a reward function that captures the essence of the task so that learning can be achieved. The reward scalar can be either discrete (i.e., +1, -1, 0) or continuous. A negative reward indicates a punishment but reinforcement learning algorithms treat them symmetrically.

2.7.6 Solution Method

The solution method refers to the reinforcement learning algorithm used to update the Q-values for the current state-action pair which will drive the current policy towards the optimal policy. In this thesis, *Monte Carlo ES* reinforcement learning is used to learn control policies for adaptive control systems. Monte Carlo methods in the context of reinforcement learning are a collection of algorithms that can be used to compute optimal policies by averaging the returns of randomly sampled events. They do not require an accurate model of the environment but instead use *experience*, sampled sequences of states, actions and rewards from online or simulated interaction with an environment. This type of learning from on-line experience does not require any prior knowledge of the environment in order for the system to reach optimality. Learning from simulated experience does require a model, but the model need only generate the transitions of the samples, not every possible transition. To ensure accurate rewards are sampled, Monte Carlo methods are applied in an incremental episode-by-episode method. That is, the knowledge or rewards acquired from one episode can only be applied to the next. Therefore, Monte Carlo methods are applied only to episodic tasks. Episodic tasks are tasks that have a defined beginning and end (an episode) in which the performance of the task can be evaluated after completion. Improvement can only occur in the next repetition of the task [Sutton & Barto 1998]. A version of *Monte Carlo ES*-algorithm is shown in Figure 2.9 where the *ES* stands for the exploration start assumption; that is ε–soft policies must be used to ensure convergence to the optimal policy.

Initialize, for all $s \in S$, $a \in A(s)$:
$Q(s, a) \leftarrow$ arbitrary
$\pi(s) \leftarrow$ arbitrary
$Returns(s, a) \leftarrow$ empty list

Repeat forever:
(a) Generate an episode using exploring starts and π
(b) For each pair (s,a) appearing in the episode
$R \leftarrow$ return following the first occurrence of (s,a)
Append R to $Returns(s,a)$
$Q(s,a) \leftarrow$ average($Returns(s,a)$)
(c) For each s in the episode:
$\pi(s) \leftarrow \text{argmax}_a\ Q(s,a)$

Figure 2.9 *Monte Carlo ES*-algorithm

Chapter 3
Vehicle Modeling

The goal of this research is to demonstrate that reinforcement learning can be applied effectively to the decentralized control of dynamic collaborative driving. The ultimate deployment of the research is for wheeled ground vehicles such as cars, trucks, and buses. Due to the high costs associated with procuring large numbers of vehicles and the safety issues involved, full-scale vehicle studies can only be conducted through large scale government research projects in association with governments and automobile manufacturers such as Demo '97 [Thorpe et al 1997], [Tan et al 1998], [Rajamani et al 2000] and in Japan during Demo 2000 [Tsugawa et al 2000], [Kato et al 2002]. In Canada, smaller projects have used small mobile robots to model cars [Michaud et al 2006], however the cost and complexity associated with these mobile robot studies can also be quite high. In addition the vehicle dynamics of a mobile robot platform are significantly different from those of full-sized automobiles thereby limiting the applicability of those results.

Alternatively, simulation studies can be developed faster, they are more flexible, cost effective, have better repeatability and explore situations not easily achieved in reality. In 1989, the National Highway Traffic Safety Administration (NHTSA) began researching the use and construction of a new state-of-the-art driving simulator (Figure 3.1), the National Advanced Driving Simulator (NADS) [Haug 1990]. Since then, NADS has been used as a substitute for actual vehicle testing. The NHTSA's Vehicle Research and Test Center (VRTC) provides vehicle data for vehicles such as the 1994 Ford Taurus GL [Chrstos and Grygier 1994], the 1997 Jeep Cherokee [Salaani and Heydinger 2000], and the 1998 Chevrolet Malibu [Salaani et al 1998], which can be used to validate simulations. With the adoption of high fidelity simulation on modern computers, simulation has become the dominant method of study in this field.

Figure 3.1 NADS vehicle simulator

The main advantage of using a reinforcement learning approach to controller design is that a nonlinear complex numerical model can be used in the design of the control systems. For conventional control theory approaches, a linear approximation of the vehicle model must be assumed

in order to determine the control laws. With reinforcement learning, this requirement is eliminated as the agent can experience the model in order to infer the control policy.

This chapter describes the details of modeling a full-scale vehicle which will be used in the design and experimental portion of this thesis. One of the objectives of this chapter is to illustrate the complexities of an automobile model. Figure 3.2 illustrates an overview in block diagram form of the entire simulation. The entire simulation is a collection of several non-linear components from the engine to the tires with elaborate interconnections representing feedbacks resulting in a highly non-linear model of the automobile. The explanation of each component will give the reader an appreciation for the complexity in the controller needed to automate the driving of such a vehicle.

The basis of this simulation has its roots going back to the late 1980's. A significant amount of research was conducted at the Vehicle Dynamics Laboratory at the University of California at Berkeley by Hedrick under the PATH project. His group developed a complex numerical automobile model used to design and evaluate the performance of various controllers [McMahon & Hedrick 1989], [Peng & Tomizuka 1991], [Pham et al 1994]. Later work by Pham and Hedrick [Pham et al 1997] used this model to evaluate the performance of an optimal controller for combined lateral and longitudinal vehicle control. Therefore, this thesis follows this methodology and adopts the complex numerical automobile model developed by Hedrick so that our work can be bridged with his past research. The vehicle model developed is executed at a rate of 100 *Hz* or with a period of 10 *ms*.

This chapter on vehicle modeling is divided into four main sections. The first section discusses the modeling of the actuators for the control inputs, this includes i) steering, ii) throttle position, and iii) brake position. The second section describes the power-train, which comprises of the i) engine, ii) transmission, iii) steering geometry, iv) braking system, v) drive-train, vi) suspension, and vii) tires. The third section discusses the equations of motion and the numerical solution system used to determine the rigid body dynamics of the vehicle being modeled. The final section discusses the validation of the simulation.

3.1 Actuator Model

The control inputs to the vehicle model include a steering signal, a brake signal and a throttle signal. Each of these control signals has a respective actuator model which represents the linkages and hydraulics of these subsystems. Pham et al [1997] models all actuators as first-order elements with the following time constants.

Steering actuator: $\tau = 0.125$ms

Brake actuator: $\tau = 0.075$ ms

Throttle actuator: $\tau = 0.050$ms

A first-order element can be described with the following differential equation (3.1) and equivalent Laplace transformed continuous transfer function (3.2)

$$\tau\, \dot{x}(t) + x(t) = K\, u(t) \tag{3.1}$$

$$\frac{X(s)}{U(s)} = \frac{K}{\tau s + 1} \tag{3.2}$$

where $x(t)$ or $X(s)$ is the output of the actuator, $u(t)$ or $U(s)$ is the input and K is the gain. Effectively, each actuator delays the input signal by a certain amount of time and amplifies or reduces the signal. The outputs of the actuator models are fed to various power-train subsystems as seen in Figure 3.2.

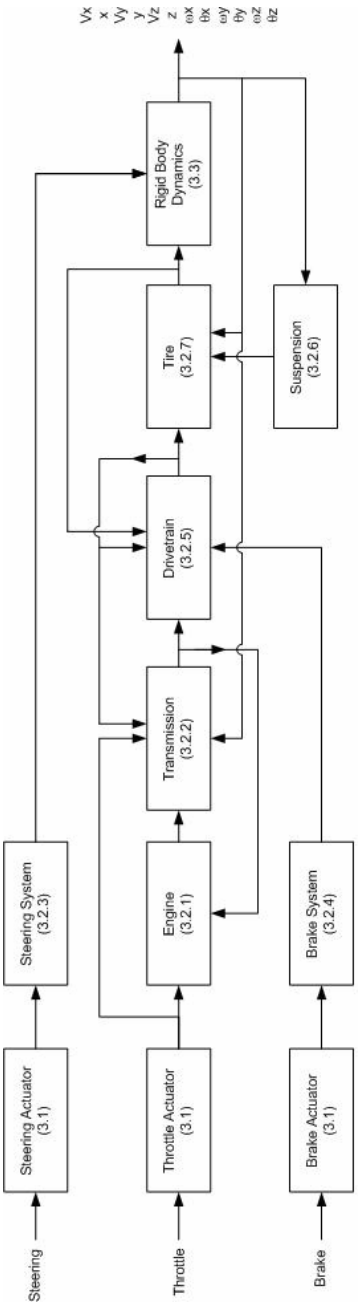

Figure 3.2 Vehicle Model Overview

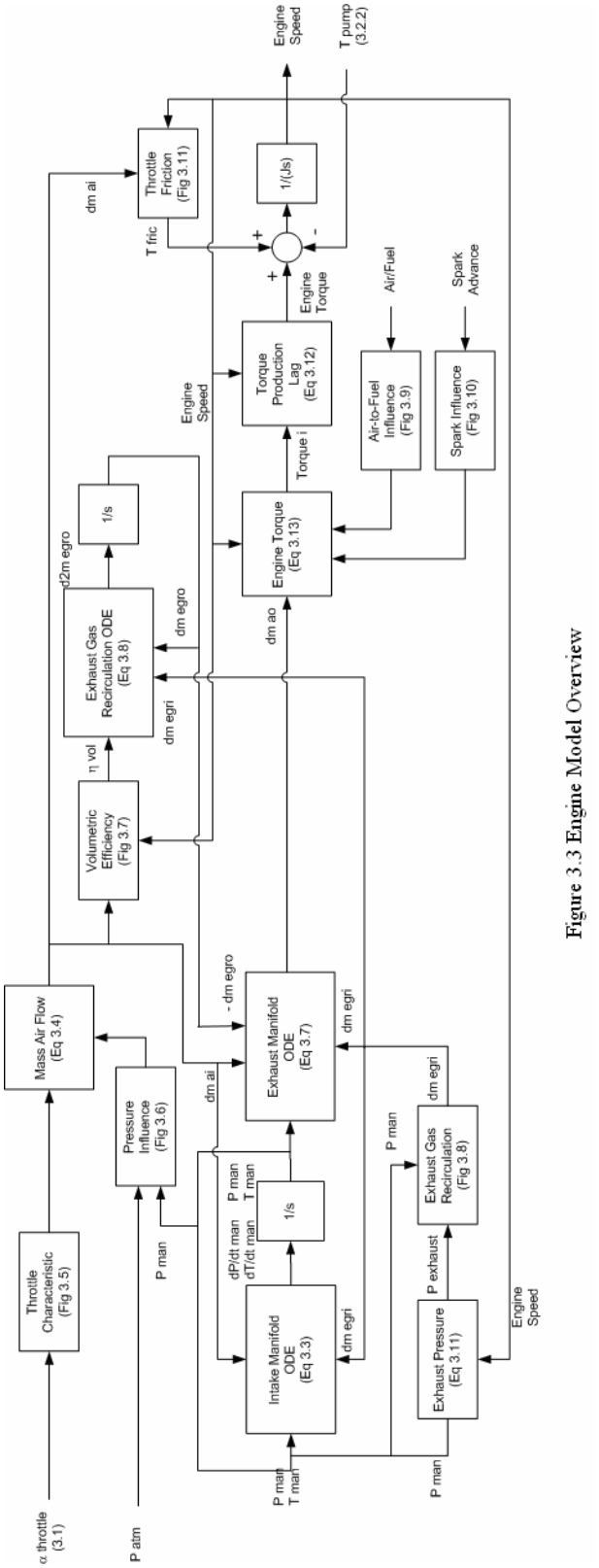

Figure 3.3 Engine Model Overview

3.2 Power-train

3.2.1 Engine Model

McMahon and Hedrick [1989], describes in detail a mathematical model of a Ford 3.4 liter V6 internal combustion engine. The main assumptions of this model are i) the mixture obeys the Ideal Gas Law and Dalton's Law of Non-Reacting Mixtures, ii) the temperature and pressure is uniform, and iii) complete mixture of air and exhaust gases, this *exhaust gas recirculation in/out* is abbreviated as *egri* or *egro*. Figure 3.2 illustrates in block diagram form the overall simulation of the engine. The control input to the engine is the throttle angle α, which is supplied by the throttle actuator model. The output of the engine model is the engine's crankshaft speed. In addition, a feedback term from the transmission model is required, in the form of the torque of the transmission pump which is connected to the engine's crankshaft. There are three differential equations which model the power generation process i) equation 3.3 which models the intake manifold, ii) equation 3.7 which models the exhaust manifold and iii) equation 3.13 which models torque production.

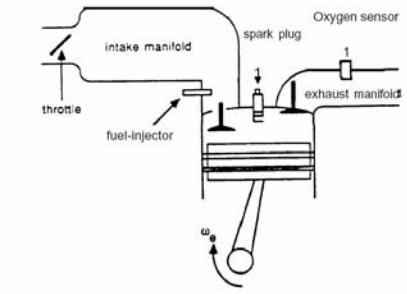

Figure 3.4 Engine Schematic [McMahon and Hedrick 1989]

The differential equation which models the state of the gas mixture in the intake manifold is given by

$$\dot{P}_m = \left(\left(\frac{\dot{T}_m}{T_m} \right) - 0.08873 \omega_e \eta_{vol} \right) P_m + \left(\frac{R T_m}{V_m} \right) \cdot \left(\dot{m}_{ai} + \dot{m}_{egri} \right) \qquad KPa/s \quad (3.3)$$

where P_m, and T_m are the manifold pressure and temperature. The manifold volume or engine displacement V_m is considered fixed at 3.4L or 0.0034 m^3. The mass rate of air entering the intake manifold is given by the relationship

$$\dot{m}_{ai} = MAX \cdot TC \cdot PRI \qquad kg/s \quad (3.4)$$

where *MAX* is the maximum flow rate which for this particular engine, *Max* = 0.335 kg/s. *TC* is the normalized throttle characteristic and is a function of throttle angle α.

$$TC = \begin{cases} 0.52 - 0.52\cos(2.1772\alpha + 7.6490) & for\ \alpha < 68.8^o \\ 1 & for\ \alpha \geq 68.8^o \end{cases} \quad (3.5)$$

The function *PRI* is the normalized pressure influence ratio and is a function of the pressure ratio $PR = P_m/P_{atm}$ and can be fit to the following 5th order polynomial equation

$$PRI = \begin{cases} A \cdot PR^5 + B \cdot PR^4 + C \cdot PR^3 + D \cdot PR^2 + E \cdot PR + F & PR > 0.38 \\ 1 & PR \le 0.38 \end{cases} \tag{3.6}$$

with the coefficients A = -9.3329, B = 19.4645, C = -15.6748, D = 5.3008, E = -0.6748, and F=1.0.

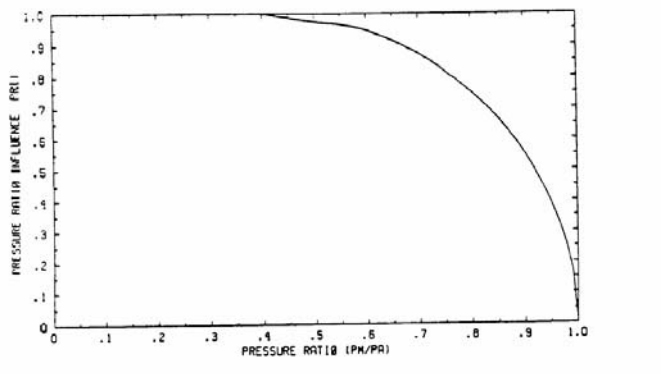

Figure 3.5 Pressure Ratio Influence function [McMahon and Hedrick 1989]

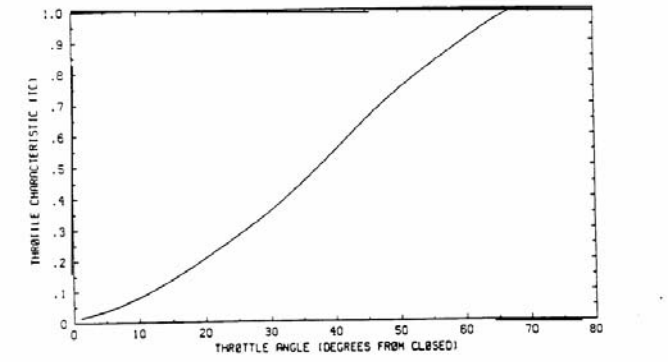

Figure 3.6 Graph of Throttle Characteristic function. [McMahon and Hedrick 1989]

The differential equation which models the state of the gas mixture in the exhaust manifold is

$$\dot{m}_{ao} = \dot{m}_{ai} + \dot{m}_{egri} - \dot{m}_{egro} + \left(\frac{P_m V_m}{R T_m}\right) \cdot \left(\frac{\dot{T}_m}{T_m} - \frac{\dot{P}_m}{P_m}\right) \qquad kg/s \tag{3.7}$$

The exhaust gas recirculation out of the exhaust manifold is described by the second order differential equation

$$\ddot{m}_{ergo} = 9.5 \times 10^{-5} \eta_{vol} \omega_e (\dot{m}_{ergi} - \dot{m}_{ergo}) \quad kg/s \tag{3.8}$$

The volumetric efficiency term η_{vol} of the engine is expressed as a surface (Figure 3.7) with a dependence on the mass of air flow rate $\dot{m}_{ai}$ into the intake manifold and the rotational speed of the engine ω_e.

$$\eta_{vol} = \eta_{vol}(\dot{m}_{ai}, \omega_e) \tag{3.9}$$

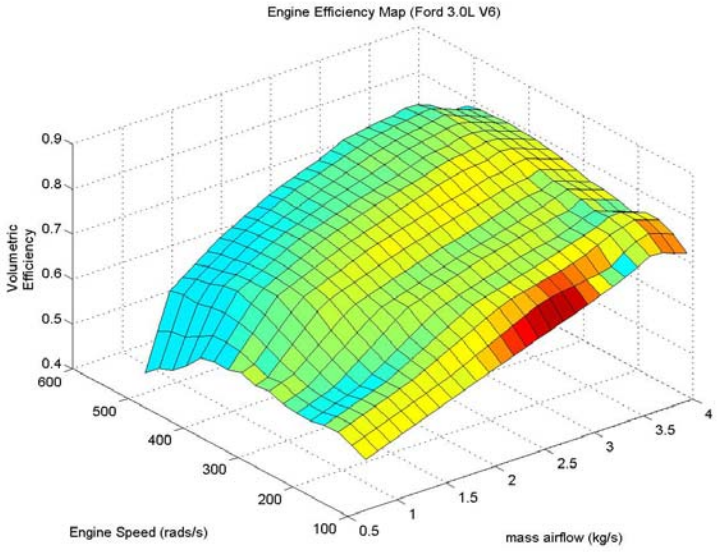

Figure 3.7 Volumetric efficiency function.

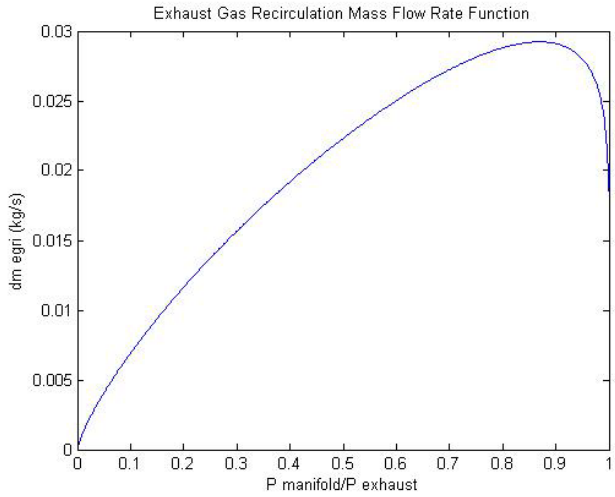

Figure 3.8 Exhaust Gas Recirculation into the manifold function

The mass flow rate of the exhaust gas into the exhaust manifold $\dot{m}_{egri}$ is provided by a lookup table illustrated in Figure 3.8 which is dependent on the ratio of manifold to exhaust pressure P_m/P_e

$$\dot{m}_{egri} = EGRI(P_m / P_e) \qquad kg/s \tag{3.10}$$

where pressure of the air in the exhaust manifold can be determined by the relationship

$$P_e = 102 + P_m \cdot \left(1.7 \times 10^{-3} \cdot \omega_e(t - \Delta_{it}) - 0.12\right) \qquad KPa \tag{3.11}$$

In this expression, engine speed is a function of time $\omega_e(t)$ where $t = t - \Delta_{it}$, which refers to a time delay Δ_{it}. This time delay is the intake to torque production delay resulting from the cyclic nature of the engine and is expressed as

$$\Delta_{it} = \frac{5.48}{\omega_e} \qquad s \tag{3.12}$$

The indicated engine torque produced is considered a discrete phenomenon due to the engine's cyclic nature; however it can be modeled in the continuous time domain for simplicity as

$$T_i = \frac{c_t \dot{m}_{ao}(t - \Delta_{it}) \cdot AFI(t - \Delta_{it}) \cdot SI(SA(t - \Delta_{it}))}{\omega_e(t - \Delta_{it})} \qquad N{\cdot}m \tag{3.13}$$

The constant c_t = 1175584 *N·m·s/kg* is the maximum torque capability of the engine and is specific to the engine and is provided by McMahon & Hedrick [1989]. The function *AFI*(*t*), is the air/fuel influence function shown in Figure 3.9. The function *SI*(*SA*), is the normalized spark influence function as a function of spark advance *SA(t)* from MBT or *minimum spark advance for best torque* and is expressed in equation (3.14) and shown in Figure 3.10. For the purpose of this simulation which follows McMahon & Hedrick [1989] the spark advance is set to constant value of *SA* = 0.3.

$$SI = 1.0 - 3.8 \times 10^{-4}(SA(t))^2 \tag{3.14}$$

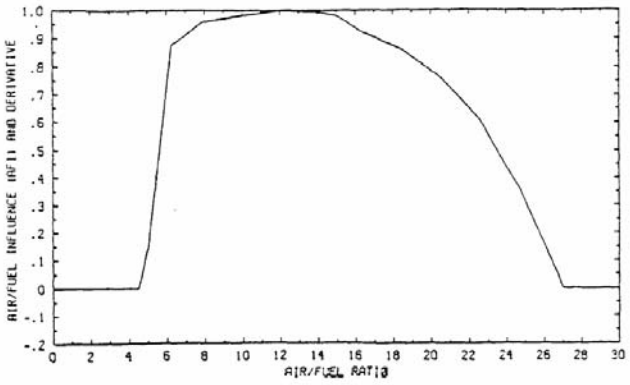

Figure 3.9 Air to Fuel Influence function [McMahon and Hedrick 1989]

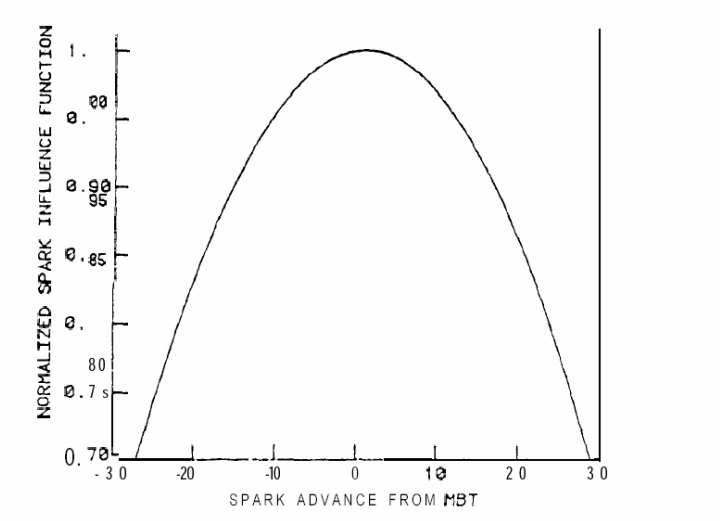

Figure 3.10 Spark Influence function [McMahon and Hedrick 1989]

The engine speed can be determined using the following torque balance or differential equation

$$J_e \dot{\omega}_e = T_i - T_f - T_p \quad N{\cdot}m \tag{3.15}$$

where $J_e = 0.2630\ kg{\cdot}m^2$ is the effective inertia of the engine and torque converter, T_i is the indicated torque produced by the engine obtained through equation (3.13), T_f is the engine friction torque which has the functional dependence and illustrated in Figure 3.11.

$$T_f = T_{fric}(\dot{m}_{ao}, \omega_e) \quad N{\cdot}m \tag{3.16}$$

and T_p is the torque converter pump torque which is modeled in the transmission subsystem model.

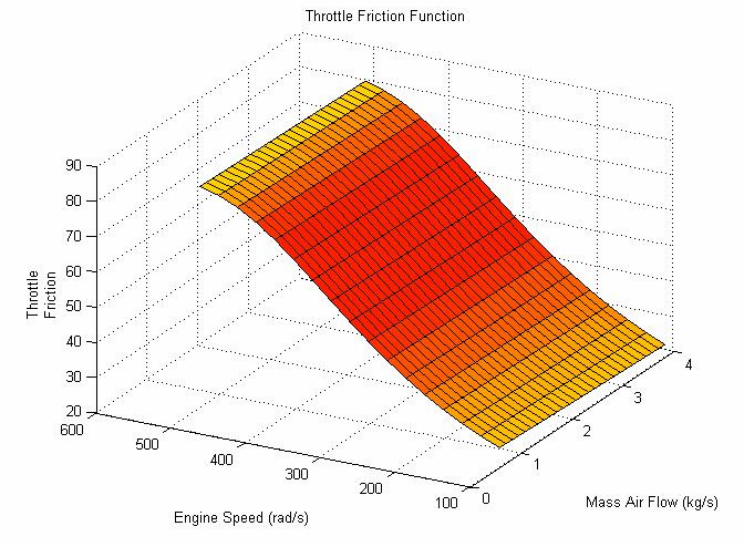

Figure 3.11 Throttle friction function

3.2.2 Transmission Model

McMahon and Hedrick [1989], describes the model of the automatic transmission subsystem which connects the engine to the driveshaft. The motion from the engine is transmitted through a gear-train that reduces the speed and increases the torque to the driveshaft.

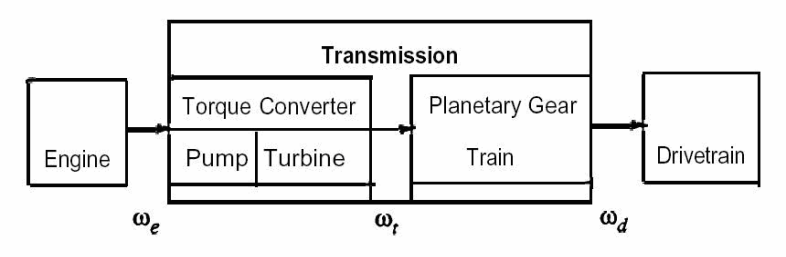

Figure 3.12 Schematic of Transmission System [McMahon and Hedrick 1989]

Figure 3.12 provides a functional illustration of the automatic transmission system. The engine is connected directly to the pump of the torque converter. The rotational motion of the fluid transmits the torque from the pump to the turbine. The turbine's output shaft is connected to the gear-train which is connected to the driveshaft. Since the gear-train is only connected to the engine through the transmission fluid, it is possible to change gears without disrupting the motion of the engine.

The block diagram of the transmission system model (Figure 3.13) can be divided into two sections. The top half of the diagram is concerned with the shifting of gears while the bottom half of the diagram is concerned with the torque transmission. The shifting of gears requires the longitudinal ground speed as well as the throttle position. The torque transmission requires the engine speed as input and provides as outputs both the torque of the driveshaft and the torque of the torque converter pump which provides a feedback to the engine model.

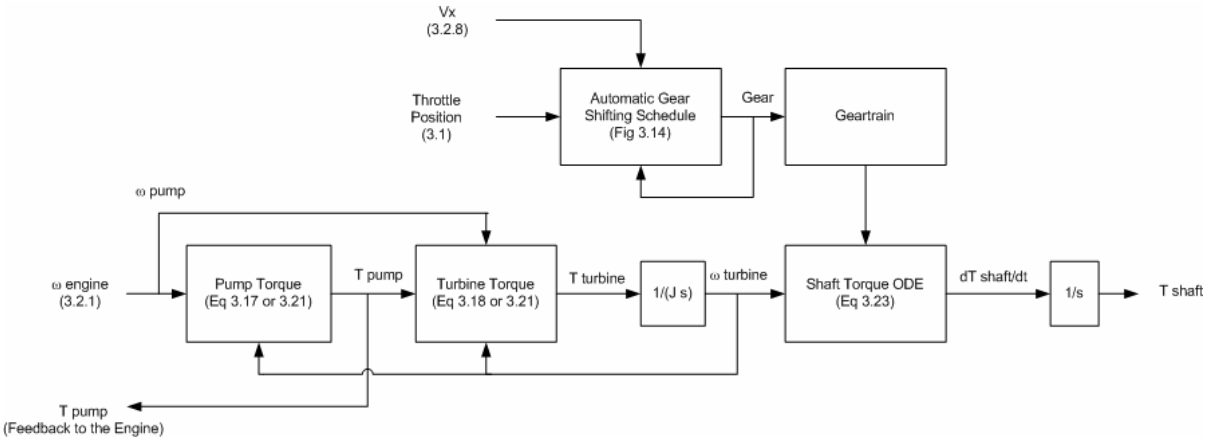

Figure 3.13 Block Diagram of Transmission System

The control of the gear selection of the gear train is managed by the *valve body*. The valve body senses hydraulic pressure and actuates servo pistons to select the proper gear ratios to optimize

engine performance. The behavior of the valve body can be modeled as a simple schedule which is dependent on both vehicle speed and throttle position as shown in Figure 3.14.

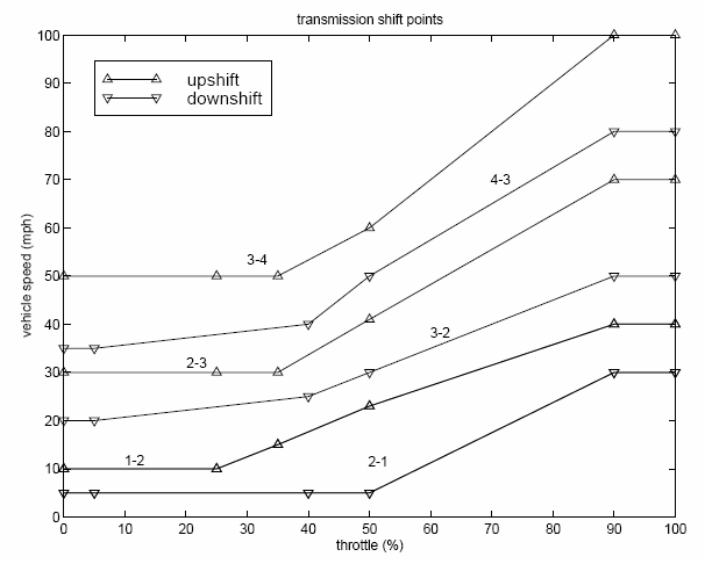

Figure 3.14 Automatic transmission model gear schedule

The torque transmission begins with the torque converter pump which has the same speed as the engine. The pump is connected to the turbine via transmission fluid. There are two phases of operation for the torque converter, the high torque phase (3.17 and 3.18) experienced when changing gears and the fluid coupling phase (3.21). The torque equations depend on the speed ratio of the turbine and pump ω_t/ω_p, the high torque phase satisfies the relationship $\omega_t/\omega_p < 0.9$. The torque of the pump T_p and the turbine T_t are expressed using the following equations

$$T_p = 3.4325\times10^{-3}\omega_p^2 + 2.21\times10^{-3}\omega_p\omega_{t,eff}^2 \qquad N{\cdot}m \tag{3.17}$$

$$T_t = 5.7656\times10^{-3}\omega_{p,eff}^2 + 0.3107\times10^{-3}\omega_{p,eff}\omega_t - 5.4323\times10^{-3}\omega_t^2 \ N{\cdot}m \tag{3.18}$$

where $\omega_{p,eff}$ and $\omega_{t,eff}$ satisfy the first order lag expressions

$$\dot{\omega}_{p,eff}\tau_p + \omega_{p,eff} = \omega_p \ \ rad/s \tag{3.19}$$

$$\dot{\omega}_{t,eff}\tau_t + \omega_{t,eff} = \omega_t \qquad rad/s \tag{3.20}$$

The fluid coupling phase exist when $\omega_t/\omega_p \geq 0.9$, therefore the torques for the turbine and pump are expressed as

$$T_t = T_p = -6.7644\times10^{-3}\omega_p^2 + 32.0084\times10^{-3}\omega_p\omega_t - 25.2441\times10^{-3}\omega_t^2 \ N{\cdot}m \tag{3.21}$$

Since the engine is connected directly to the pump, the rotational speed of the engine and pump are equal, $\omega_e = \omega_p$. To determine the angular speed of the turbine, ω_t, when the transmission is in gear, the following torque balance equation, also a first order differential equation is used

$$J_{tg}\dot{\omega}_t = T_t - R_g R_d T_s \quad N{\cdot}m \tag{3.22}$$

where J_{tg}= 0.07 $kg{\cdot}m^2$ is the rotational inertia, R_g is the gear ratio depending on which gear is used (i.e. 0.4167, 0.6817, 1, 1.4993) and R_d = 1 is the drive gear ratio. The shaft torque T_s can be determined from the following first order differential equation

$$\dot{T}_s = K_s(R_g R_d \omega_t - \omega_{wf}) \qquad N{\cdot}m/s \tag{3.23}$$

where K_s = 6742 $N{\cdot}m/rad$ is the shaft stiffness and ω_{wf} is the angular speed of the front wheel.

3.2.3 Steering Model

In this thesis an idealized steering model is used, a normalized steering command s_{steer} in the interval [-1, 1] is assumed to be provided by the control system and is passed through the steering actuator model. A linear mapping obtained by multiplying the normalized steering command to the maximum steering value of 15° is used to determine the steering angle δ with the range [-15°, +15°]. The equation is shown below

$$\delta = actuator_{steer}(s_{steer}) \cdot 15^{\circ} \quad degrees \tag{3.24}.$$

3.2.4 Braking System Model

McMahon and Hedrick [1989], describes a simplified model to determine the braking forces to apply to each wheel. Although the brake torques are largely dependent on the hydraulic system that makes up the braking system of the vehicle, according to McMahon & Hedrick a first order lag expression provides a sufficient simplified approximation to the system. A normalized brake command s_{brake} in the interval [0, 1] is assumed to be provided by the control system and is passed through the brake actuator model. The first order lag function, lag_{brake} which approximates the braking system is modeled using equations (3.1) and (3.2) with a time constant of τ = 0.072 s. The equation for the braking torques for the front T_{bf} and rear T_{br} are

$$T_{bf} = lag_{brake}\left(actuator_{brake}(s_{brake})\right) \cdot h_f F_{f\max} \quad N{\cdot}m \tag{3.25}$$

$$T_{br} = lag_{brake}\left(actuator_{brake}(s_{brake})\right) \cdot h_r F_{r\max} \quad N{\cdot}m \tag{3.26}$$

where $h_f = h_r$ = 0.3008 m are the heights from the ground to the front and rear axles. The maximum brake force $F_{f\,max}$ and $F_{r\,max}$ occurs during wheel lock (slip λ = 1) and can be determined using the following equations

$$F_{f\max} = \mu m g \cdot \left(l_f + h_f(\mu + f_{roll})\right) \quad N \tag{3.27}$$

$$F_{r\max} = \mu m g \cdot \left(l_r + h_r(\mu + f_{roll})\right) \quad N \tag{3.28}$$

where μ is the coefficient of friction between the road and the tire as specified in the tire subsystem model (Section 3.2.7), m = 1573 kg is the mass of the automobile, g = 9.807 m/s^2 is gravity, l_f = 1.034 m and l_r = 1.491 m is the longitudinal distance from the center of gravity to the front and rear axles

respectively and f_{roll} = 0.004908 is the coefficient of rolling resistance for the left and right tires combined.

3.2.5 Drive-train Model

Pham et al [1997] describes the model of the drive-train subsystem for a front wheel drive automobile. A torque balance about each wheel yields the first order differential equations for the front and the rear wheels

$$J_{w_i}\dot{\omega}_{w_i} = \tfrac{1}{2}T_s - \tfrac{3}{10}T_b - r_{w_i}F_{x_i} \qquad N{\cdot}m \qquad i = 1, 2 \text{ (front)} \tag{3.29}$$

$$J_{w_i}\dot{\omega}_{w_i} = \tfrac{2}{10}T_b - r_{w_i}F_{x_i} \qquad N{\cdot}m \qquad i = 3, 4 \text{ (rear)} \tag{3.30}$$

where T_s is the shaft torque calculated previously in the transmission subsystem model and T_b is the total braking torque available and F_x is the longitudinal force of each tire which is calculated in the tire model. An even distribution of the shaft torque is assumed by splitting half of the shaft torque to each of the front wheels. The total available brake torque is assumed to be distributed 60% to the front and 40% to the rear wheels.

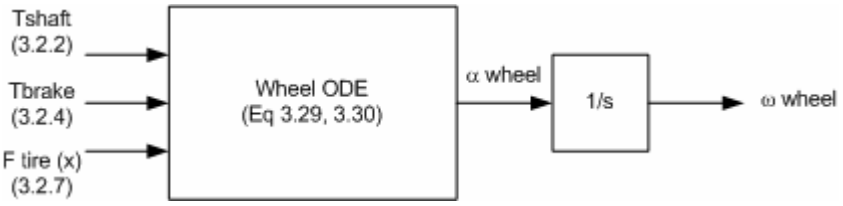

Figure 3.15 Overview of Drive-train Model

3.2.6 Suspension Model

Pham et al [1997] describes a simple one-dimensional quarter car model of an automotive suspension system with shock absorber and hardening spring [Peng 1992]. Neglecting the small coupling terms, the suspension forces can be completely determined by the local motion of each wheel [Tseng 1993]. Let e_i be the deflection at the i^{th} suspension joint.

$$e_1 = z_0 - z + h_5\theta + l_f\theta + \frac{s_f}{2}\phi \quad m, \qquad e_2 = z_0 - z + h_5\theta + l_f\theta - \frac{s_f}{2}\phi \quad m \qquad \text{(front)} \tag{3.31}$$

$$e_3 = z_0 - z + h_5\theta - l_r\theta - \frac{s_r}{2}\phi \quad m, \qquad e_4 = z_0 - z + h_5\theta - l_r\theta + \frac{s_r}{2}\phi \quad m \qquad \text{(rear)} \tag{3.32}$$

where z_0 is the nominal height, z is the current height of the vehicle, θ is the pitch angle, ϕ is the roll angle, h_5 = 0.1 m is the longitudinal distance from the center of gravity to pitch center, l_f = 1.034 m and l_r = 1.491 m is the longitudinal distance from the center of gravity to the front and rear axles respectively, and s_f = 1.450 m and s_r = 1.450 m are the front and rear axle track widths respectively.

The spring force F_s on each wheel is calculated using the following equation

$$F_{s_i} = C_1(e_1 + C_2 e_i^3) \qquad N \tag{3.33}$$

where C_1 = 40000 *N/m* and C_2 = 40000 m^{-4} are coefficients of the third order polynomial fit for the suspension spring. The damping force F_d on each wheel is calculated using the following equation

$$F_{d_i} = D_1 \dot{e}_i \qquad N \tag{3.34}$$

where the damping constant D_1 = 10000 *N·s/m*. A vertical force balance is used to determine the normal force F_N exerted on each wheel,

$$F_{N_i} = \tfrac{1}{2} m g \frac{l_f}{l_f + l_r} - F_{s_i} - F_{d_i} \quad N \tag{3.35}$$

where m = 1573 *kg* is the mass of the automobile and g = 9.807 m/s^2 is gravity.

3.2.7 Tire Model

Pham et al [1997] describes a simplified tire model referred to as the Bakker-Pacejka model adopted from the work of Peng [1992]. This model calculates the traction and cornering forces resulting from the road-tire interaction based on empirical curve-fitting with experimental data for a *Yokohama P205/60 R14 87H* tire [Peng 1992]. In this model, tire pressure, tire camber angle, and the road and tire physical parameters are fixed, but the forces generated at the tire are the functions of slip ratio λ, slip angle ν and the tire normal force F_N.

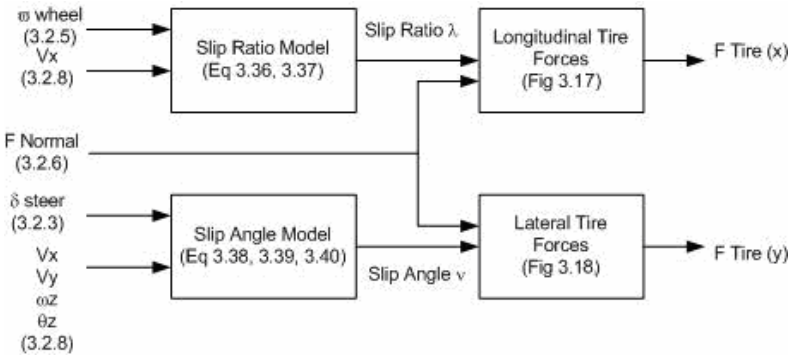

Figure 3.16 Overview of the Tire Model

The surfaces shown in Figure 3.17 and Figure 3.18 are plots for Equations (3.41) and (3.42) and are based on test data of the *Yokohama* tires under laboratory conditions for the ideal condition friction coefficient of μ = 1.0. According to Bakker et al [1987], road-tire interaction under non-ideal conditions can be extrapolated from the ideal curve by multiplying the ideal tire forces by the coefficient of friction μ. Typically for average freeway operation, μ = 0.8, for wet road conditions μ = 0.6, and for icy road conditions μ = 0.2.

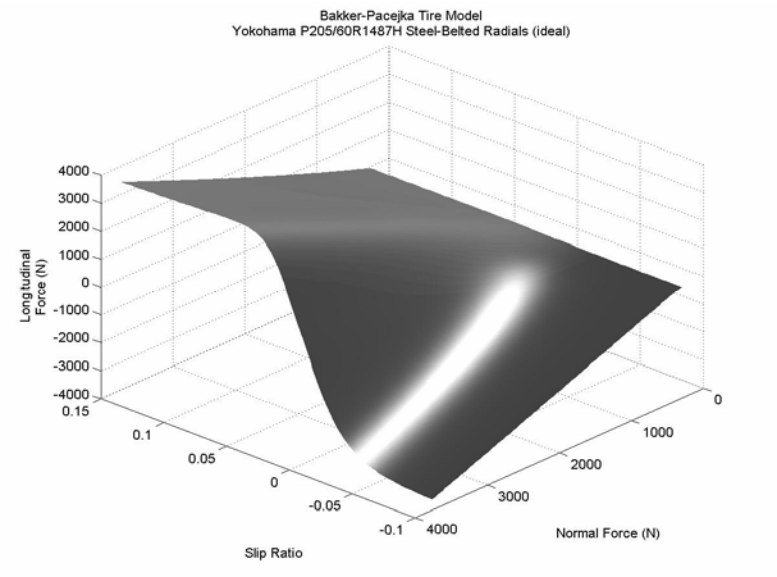

Figure 3.17 Longitudinal Force-slip characteristics of the *Yokohama* tire for $\mu = 1.0$ (ideal)

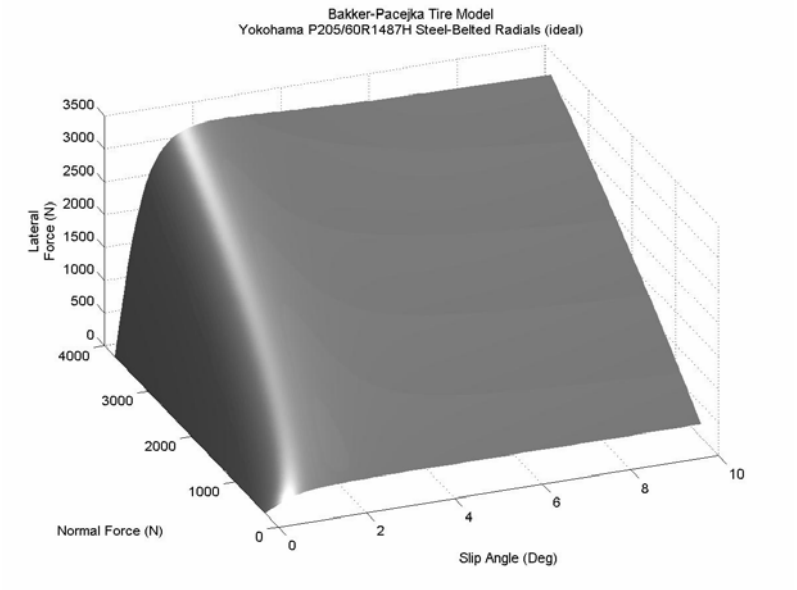

Figure 3.18 Lateral Force-slip characteristics of the *Yokohama* tire for $\mu = 1.0$ (ideal)

The calculation of the tire forces begins by determining the interaction with the road in the lateral and longitudinal direction, corresponding to the slip angle ν and the slip ratio λ respectively. The slip ratio λ is computed for traction and braking using the following equations

traction
$$\lambda = \frac{r_w \omega_w - V_x}{r_w \omega_w} \geq 0 \tag{3.36}$$

braking $$\lambda = \frac{r_w \omega_w - V_x}{V_x} < 0 \tag{3.37}$$

where ω_w is the rotational speed of each wheel determined in the drive-train subsystem model and the radius of the tire is $r_w = 0.301$ m.

If a moving reference frame is placed on the automobile with the x-axis aligned to the longitudinal axis of the car and the y-axis aligned with the lateral axis, then the slip angle ν is simply the difference in angle between the tire's orientation and its relative velocity vector angle ζ and can be determined with the following equation,

$$\nu_i = \delta_i - \zeta_i \qquad rad \tag{3.38}$$

where δ is the steering angle of the tire and $i = 1, 2, 3, 4$ refers to front left, front right, rear left and rear right tires respectively. Note that for the rear tires ($i = 3, 4$) the steering angle $\delta = 0$. The relative velocity angle ζ_i is calculated using the following equations

$$\zeta_1 = \arctan\left(\frac{V_y + l_f \dot{\psi}}{V_x - s_f \dot{\psi}}\right) \qquad rad \qquad \zeta_2 = \arctan\left(\frac{V_y + l_f \dot{\psi}}{V_x + s_f \dot{\psi}}\right) \qquad rad \tag{3.39}$$

$$\zeta_3 = \arctan\left(\frac{V_y - l_r \dot{\psi}}{V_x - s_r \dot{\psi}}\right) \qquad rad \qquad \zeta_4 = \arctan\left(\frac{V_y - l_r \dot{\psi}}{V_x + s_r \dot{\psi}}\right) \qquad rad \tag{3.40}$$

where V_x, V_y are the x and y components of the vehicle relative velocity vector, $\dot{\psi}$ is the vehicle's yaw rate, $l_f = 1.034$ m and $l_r = 1.491$ m is the longitudinal distance from the center of gravity to the front and rear axles respectively, and $s_f = 1.450$ m and $s_r = 1.450$ m are the front and rear axle lengths respectively.

Once the slip ratio λ_i and slip angle ν_i are determined for each tire, the longitudinal and lateral tire force can be calculated using the following equations

longitudinal $$F_x = \mu \cdot D_x \sin\left(C_x \arctan(B_x \phi_x)\right) + S_{vx} \qquad N \tag{3.41}$$

lateral $$F_y = \mu \cdot D_y \sin\left(C_y \arctan(B_y \phi_y)\right) + S_{vy} \qquad N \tag{3.42}$$

where μ is the coefficient of friction between the road and the tire, ϕ_x and ϕ_y are determined using the following curve fit equations

$$\phi_x = (1 - E_x) \cdot (\lambda + S_{hx}) + \frac{E_x}{B_x} \arctan\left(B_x (\lambda + S_{hx})\right) \qquad rad \tag{3.43}$$

$$\phi_y = (1 - E_y) \cdot (\nu + S_{hy}) + \frac{E_y}{B_y} \arctan\left(B_y (\nu + S_{hy})\right) \qquad rad \tag{3.44}$$

$$S_{hx} = 0 \qquad S_{vx} = 0 \qquad S_{hy} = 0 \qquad S_{vy} = 0 \tag{3.45}$$

and S_{hx}, S_{vx}, S_{hy} and S_{vy} are the offsets of the curve fits which are all zero in this case.

For the longitudinal force there are two cases based on the slip ratio, the traction case ($\lambda \geq 0$), and the braking case ($\lambda < 0$) where the coefficients of the curve fit are determined using

Traction ($\lambda \geq 0$):	Braking ($\lambda < 0$) :	
$B_x = 22 + \frac{F_z - 1940}{645}$	$B_x = 22 + \frac{F_z - 1940}{645}$	(3.46)
$C_x = 1.35 + \frac{F_z - 1940}{16125}$	$C_x = 1.35 + \frac{F_z - 1940}{16125}$	(3.47)
$D_x = 1750 + \frac{F_z - 1940}{0.956}$	$D_x = 1750 + \frac{F_z - 1940}{0.956}$	(3.48)
$E_x = -3.6$	$E_y = 0.1$	(3.49)

where F_z is the normal force on the tire determined by the suspension subsystem model (Section 3.2.6). For the lateral force the coefficients of the curve fit are determined using

$$B_y = 0.22 + \frac{5200 - F_z}{40000} \tag{3.50}$$

$$C_y = 1.26 + \frac{F_z - 5200}{32750} \tag{3.51}$$

$$D_y = -0.00003 F_z^2 + 1.0096 F_z - 22.73 \tag{3.52}$$

$$E_y = -1.6 \tag{3.53}$$

3.3 Rigid Body Dynamics

The purpose of the vehicle dynamics simulation is to determine the position and orientation of the vehicle in response to command inputs from a given controller. In the previous section, command inputs provided by a controller enter the power-train model and tire forces are computed. These tire forces are the primary external forces applied to the rigid body which is the vehicle. Other external forces include aerodynamic forces and gravity. This section describes how the kinematic states

$$[x, y, z, \phi, \theta, \psi] \tag{3.54}$$

where ϕ is the roll angle, θ is the pitch, and ψ is the yaw angle in radians, are calculated from the tire forces. The external forces on the vehicle are first transformed into equivalent external forces and moments for each axis (i.e. x, y, and z components). Next, equations of motions of the vehicle are formulated using the external forces and moments. These equations are in fact a set of simultaneous ordinary differential equations to be solved using a numerical solver described in section 3.3.2, thus providing the kinematic state of the vehicle.

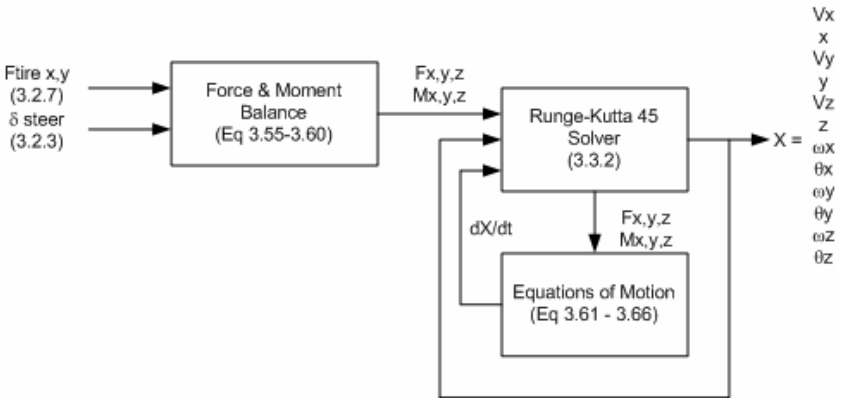

Figure 3.19 Rigid Body Dynamics Modeling Overview

3.3.1 Dynamics and Equations of Motion

The external forces for each axis of the rigid body exerted on each tire, $F_{X_i}, F_{Y_i}, F_{Z_i}$ are determined using the following equations

$$F_{X_i} = F_{x_i}\cos(\delta_i) - F_{y_i}\sin(\delta_i) \qquad N \qquad (3.55)$$

$$F_{Y_i} = F_{x_i}\sin(\delta_i) + F_{y_i}\cos(\delta_i) \qquad N \qquad (3.56)$$

$$F_{Z_i} = F_{N_i} \qquad N \qquad (3.57)$$

where i = 1,..,4 is the tire index, F_{x_i}, F_{y_i}, are the longitudinal and lateral tire forces as computed by the tire model and F_{N_i}, is the normal force computed by the suspension model and δ_i is the steering angle of the tire, for a front wheel drive vehicle, $\delta_3 = \delta_4 = 0$. The external moments for each axis of rotation M_x, M_y, M_z, due to the tire forces are

$$M_x = \left(\frac{s_f}{2} + h_2\phi\right)\cdot F_{Z_1} + \left(\frac{s_r}{2} + h_2\phi\right)\cdot F_{Z_3} - \left(\frac{s_f}{2} - h_2\phi\right)\cdot F_{Z_2} - \left(\frac{s_r}{2} + h_2\phi\right)\cdot F_{Z_4} - (z + h_5\theta)\cdot\sum_{i=1}^{4} F_{Y_i} \qquad N\cdot m \qquad (3.58)$$

$$M_y = (l_r + h_4\theta)\cdot(F_{Z_3} + F_{Z_4}) - (l_f - h_4\theta)\cdot(F_{Z_1} + F_{Z_2}) - (z - h_5\theta)\sum_{i=1}^{4} F_{X_i} \qquad N\cdot m \qquad (3.59)$$

$$M_z = (l_f - h_4\theta)\cdot(F_{Y_1} + F_{Y_2}) - (l_r - h_4\theta)\cdot(F_{Y_3} + F_{Y_4}) - \left(\frac{s_f}{2} + h_2\phi\right)\cdot F_{X_1} - \left(\frac{s_r}{2} + h_2\phi\right)\cdot F_{X_3} + \left(\frac{s_f}{2} - h_2\phi\right)\cdot F_{X_2} + \left(\frac{s_r}{2} - h_2\phi\right)\cdot F_{X_4} \qquad N\cdot m \qquad (3.60)$$

where $h_2 = 0.30\ m$ is the vertical distance from the center of gravity to the roll center, $h_4 = 0.25\ m$ is the vertical distance from the center of gravity to pitch center, $h_5 = 0.10\ m$ is the longitudinal distance from the center of gravity to pitch center, $l_f = 1.034\ m$ and $l_r = 1.491\ m$ is the longitudinal distance from the center of gravity to the front and rear axles respectively, and $s_f = 1.450\ m$ and $s_r = 1.450\ m$ are the front and rear axle lengths respectively.

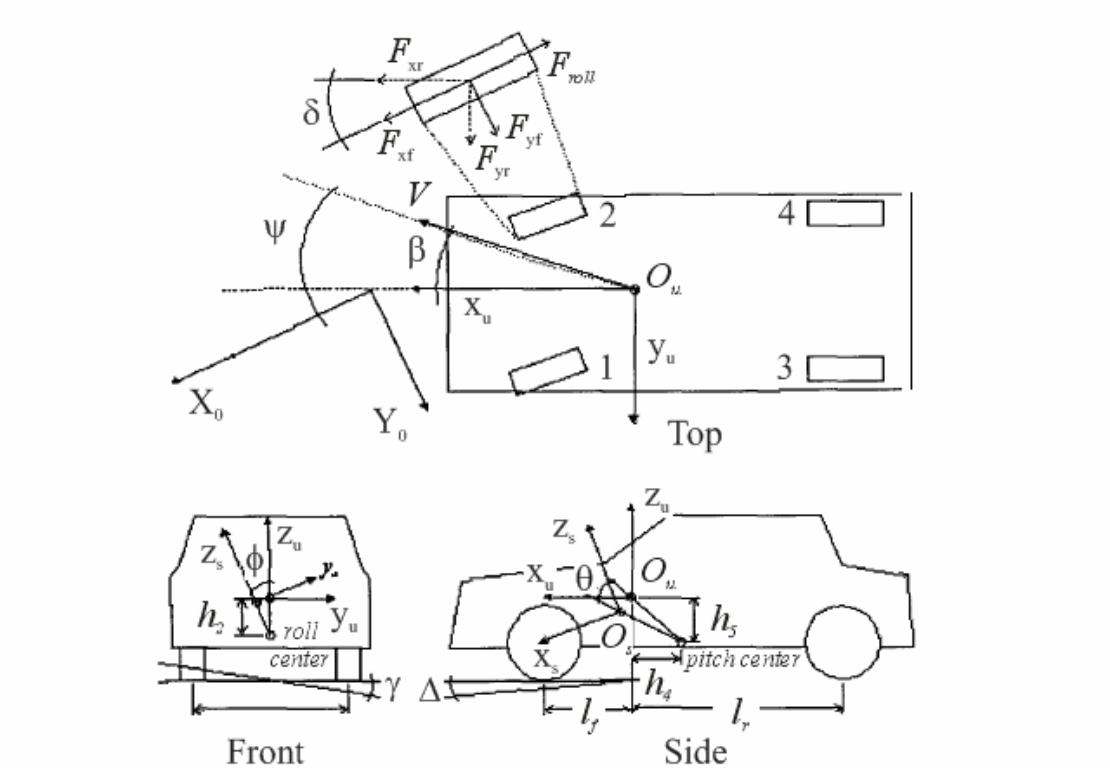

Figure 3.20 Schematic of vehicle reference frames

The following are the equations of motion for a sprung mass where the external forces and moments have been determined from equations 3.55 through 3.60. The rotational equations of motion are

$$\begin{aligned} &I_x\left[\ddot{\phi}+\ddot{\gamma}+\dot{\beta}\,\dot{\Delta}+\beta\,\ddot{\Delta}-(\Delta+\theta)\,\ddot{\psi}-(\dot{\Delta}+\dot{\theta})\,\dot{\psi}\right] \\ &-(I_y-I_z)\cdot\left(\dot{\theta}+\dot{\gamma}+\beta\dot{\Delta}-\{\Delta+\theta\}\dot{\psi}\right)\cdot\left(\theta\{\dot{\phi}+\dot{\gamma}\}-\phi\{\dot{\theta}+\dot{\Delta}\}+\dot{\psi}\right)=M_x-\theta M_z \end{aligned} \tag{3.61}$$

$$\begin{aligned} &I_y\left[\ddot{\phi}-\dot{\beta}\,\dot{\gamma}+\dot{\beta}\,\dot{\gamma}+\ddot{\Delta}+(\gamma+\phi)\,\ddot{\psi}-(\dot{\gamma}+\dot{\phi})\,\dot{\psi}\right] \\ &-(I_z-I_x)\cdot\left(\dot{\phi}+\dot{\gamma}+\beta\dot{\Delta}-\{\Delta+\theta\}\dot{\psi}\right)\cdot\left(\theta\{\dot{\phi}+\dot{\gamma}\}-\phi\{\dot{\theta}+\dot{\Delta}\}+\dot{\psi}\right)=M_y+\phi M_z \end{aligned} \tag{3.62}$$

$$\begin{aligned} &I_z\left[\dot{\theta}(\dot{\gamma}+\dot{\phi})+\theta(\ddot{\gamma}+\ddot{\phi})-\dot{\phi}(\dot{\Delta}+\dot{\theta})-\phi(\ddot{\Delta}+\ddot{\theta})+\ddot{\psi}\right] \\ &-(I_x-I_y)\cdot\left(\dot{\phi}+\dot{\gamma}+\beta\dot{\Delta}-\{\Delta+\theta\}\dot{\psi}\right)\cdot\left(\dot{\theta}+\beta\dot{\gamma}+\dot{\Delta}-\{\gamma+\phi\}\dot{\psi}\right)=M_x-\theta M_y+M_z \end{aligned} \tag{3.63}$$

where $I_x = 479.6\ kg{\cdot}m^2$, $I_y = 2549.3\ kg{\cdot}m^2$, $I_z = 2782.1\ kg{\cdot}m^2$ are the moments of inertia about each axis, Δ is the gradient angle of the road, β is the slip angle and γ is the super-elevation angle of the road in radians. The translational equations of motion are

$$m\left[\dot{V}_x - V_y\,\dot{\psi} + \left({}_u\ddot{\mathbf{r}}_{S/U}\right)_x\right] = \sum_{i=1}^{4} F_{X_i} - C_x V_x{}^2 - F_{roll} + \Delta\, mg \tag{3.64}$$

$$m\left[\dot{V}_y + V_x\dot{\psi} + \left({}_u\ddot{\mathbf{r}}_{S/U}\right)_y\right] = \sum_{i=1}^{4} F_{Y_i} - C_y V_y{}^2 - \gamma\, mg \tag{3.65}$$

$$m\left[V_y\,(\dot{\gamma} + \beta\,\dot{\Delta} - \Delta\dot{\psi}) - V_x\,(-\beta\,\dot{\gamma} + \dot{\Delta} + \gamma\,\dot{\psi}) + \left({}_u\ddot{\mathbf{r}}_{S/U}\right)_z\right] = \sum_{i=1}^{4} F_{Z_i} - mg \tag{3.66}$$

where ${}_u\ddot{\mathbf{r}}_{S/U}$ is the relative acceleration of the sprung mass (see equation B.15 in Appendix B), C_x = 0.45 and C_y = 2.1 are the aerodynamic coefficients of drag. The rolling resistance due to tire deformation F_{roll} = 274.7 N is specific to tire and the tire pressure, it is considered a constant for this simulation as it is independent of velocity [Gillespie 1992]. For a detailed derivation of the equations of motion see Appendix B: Equations of Motion.

3.3.2 Numerical Solution of Simultaneous Differential Equations

To solve the six equations with six unknown state variables, a numerical approach to solving the simultaneous differential equations is used. For each time step in the simulation, these six equations in six unknowns must be solved ($x, y, z, \phi, \theta, \psi$). For a 100 *Hz* simulation to be considered real-time the solution must be calculated in under 0.010 *s* for each vehicle. Therefore, assumptions are made to facilitate the solution. In the equations of motion (3.61) to (3.66), other than the state variable appear, these include the gradient angle of the road Δ, the slip angle with respect to motion β, and the super-elevation angle of the road γ, along with their corresponding first and second derivatives with respect to time.

$$\left[\Delta, \beta, \gamma, \dot{\Delta}, \dot{\beta}, \dot{\gamma}, \ddot{\Delta}, \ddot{\beta}, \ddot{\gamma}\right] \tag{3.67}$$

Let us consider, that the set of variables in (3.67) are considered constant for the given time interval that the numerical solution for the equations of motion are being calculated. Therefore, the first and second derivatives of Δ, β, and γ are calculated externally using a Backward Euler Approximation (3.68) prior to solving the equations of motion,

$$y'(t) \approx \frac{y(t) - y(t-h)}{h} \tag{3.68}$$

where h is the period of the simulation (i.e. 0.01 *s*).

The six equations of motion are second order differential equations, or simply there are second derivatives of the state variables. Since all derivatives are with respect to a single variable t time, the order can be reduced to order one by introducing additional state variables which correspond

to the first derivatives with respect to time. This increases the number of state variables to twelve (3.69) where X is the vector which represents the state variables.

$$X = \left[\dot{x}, x, \dot{y}, y, \dot{z}, z, \dot{\phi}, \phi, \dot{\theta}, \theta, \dot{\psi}, \psi\right]^T \tag{3.69}$$

Therefore, an additional 6 differential equations (3.70) need to be provided.

$$\begin{aligned} &\frac{dx}{dt} = \dot{x} \quad \frac{dy}{dt} = \dot{y} \quad \frac{dy}{dt} = \dot{z} \\ &\frac{d\phi}{dt} = \dot{\phi} \quad \frac{d\theta}{dt} = \dot{\theta} \quad \frac{d\psi}{dt} = \dot{\psi} \end{aligned} \tag{3.70}$$

This provides 12 differential equations with 12 state variables to be solved.

The equations of motion (3.61) to (3.66) are considered ordinary differential equations; that is there is only one independent variable t time. However, the differential equations are in the implicit form; that is the derivatives of the state variables with respect to time are not separate from the state variables. Examples of explicit differential equations are seen in the equations in (3.70) where the derivative of the state variable is an explicit function of the state variable. The general form of the system of implicit ordinary differential equations is shown below

$$A(t, X) \cdot \frac{dX}{dt} = G(t) \cdot X + C \tag{3.71}$$

$$\frac{dX}{dt} = \left[\ddot{x}, \dot{x}, \ddot{y}, \dot{y}, \ddot{z}, \dot{z}, \ddot{\phi}, \dot{\phi}, \ddot{\theta}, \dot{\theta}, \ddot{\psi}, \dot{\psi}\right]^T \tag{3.72}$$

where $A(t, X)$ is a matrix of terms in each differential equation which corresponds to the first derivatives of the state variable, $G(t)$ is a matrix of terms in each differential equation which to the state variables and C is a matrix corresponding to the constants of each differential equation.

Although numerical methods exist to solve implicit differential equations [Brenan et al 1989], their complexity leads to slower performance and difficulties in integration. It is possible to transform the system of implicit ordinary differential equations into system of explicit ordinary differential equations with initial values. Therefore, faster explicit standard numerical approaches to solving the equations of motion can be used. In this thesis, a standard library function from Sandia National Laboratories (USA), *Runge-Kutta-Fehlberg 45* (*rkf45*) [Fehlberg 1969], [Shampine et al 1976] is integrated into the simulation to solve the equations of motion. In order to use *rkf45*, the following explicit function is provided to approximate the derivatives of the state variables (3.72)

$$\frac{dX}{dt} = A^{-1}(t, X) \cdot G(t) \cdot X + A^{-1}(t, X) \cdot C \tag{3.73}$$

where $A^{-1}(t,X)$ is the inverted matrix of $A(t,X)$.

3.4 Model Validation

The vehicle simulation discussed above is a composite of various subsystems that does not correlate to an actual vehicle (i.e. Ford V6 3.0L engine, Yokohama 14" radial tires, Toyota Camry chassis dimensions). However, comparison vehicle response data supplied by the NHTSA's Vehicle Research and Test Center (VRTC) for a 1997 Jeep Cherokee [Salaani & Heydinger 2000] is presented to illustrate analogous behavior between an actual vehicle and the vehicle simulation.

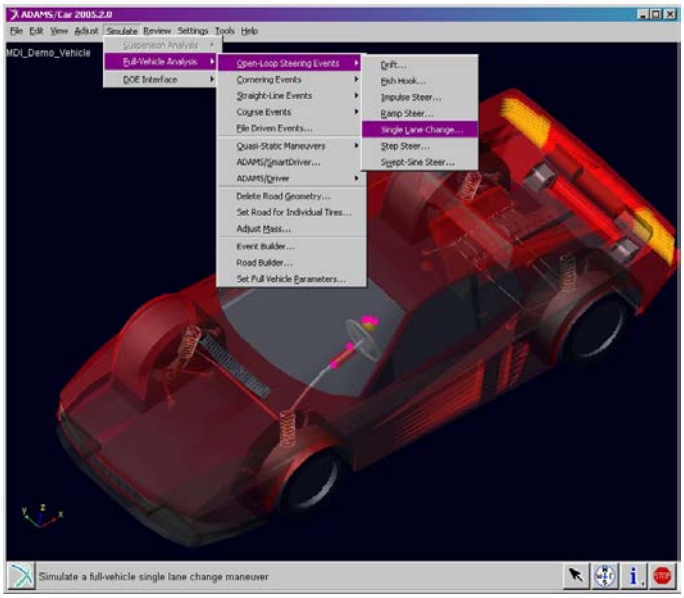

Figure 3.21 Screenshot of ADAMS/Car by MSC Software.

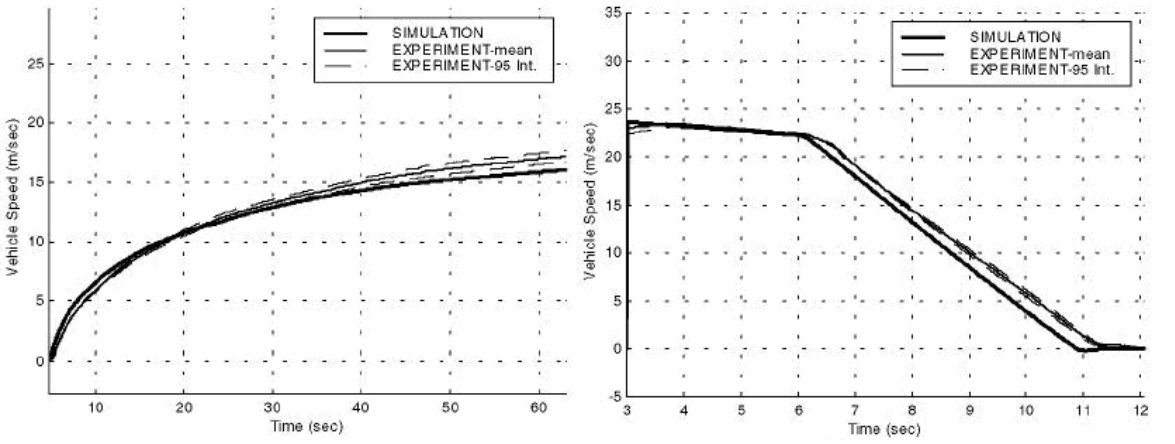

(a) (b)

Figure 3.22 1997 Jeep Cherokee throttle step and brake step response [Salaani & Heydinger 2000]

Unfortunately, the validation data provided by NHTSA is rather limited for both longitudinal and lateral vehicle dynamics. Figure 3.22a shows the actual vehicle's longitudinal velocity response

to a throttle step input in 1st gear. Notice a smooth increase in acceleration which saturates at the top speed for the specific gear. Figure 3.22b shows the actual vehicle's velocity response to a brake step input. From 0-6 *s* the throttle is released, this is known as power-off and results in a linear decrease in speed due to engine braking, at 6 *s* the brake is pressed and a linear decrease with a much steeper slope is seen.

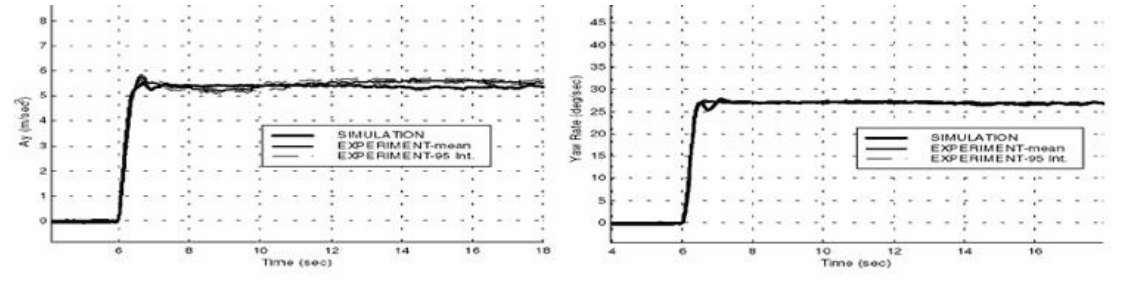

(a) (b)

Figure 3.23 1997 Jeep Cherokee steering step input responses [Salaani and Heydinger 2000]

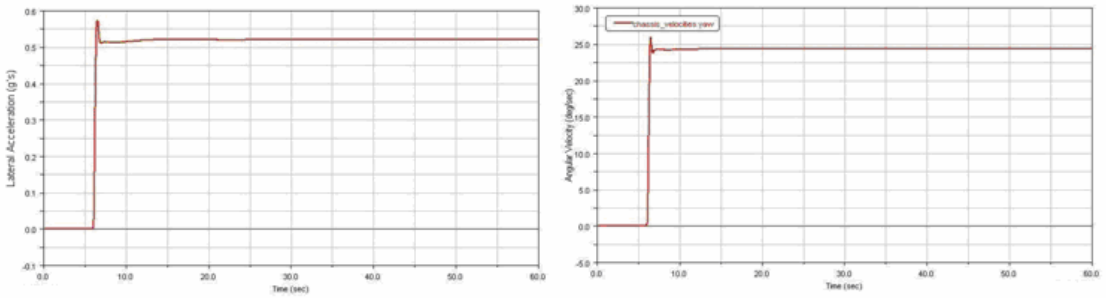

(a) (b)

Figure 3.24 Adams Car steering step input responses.

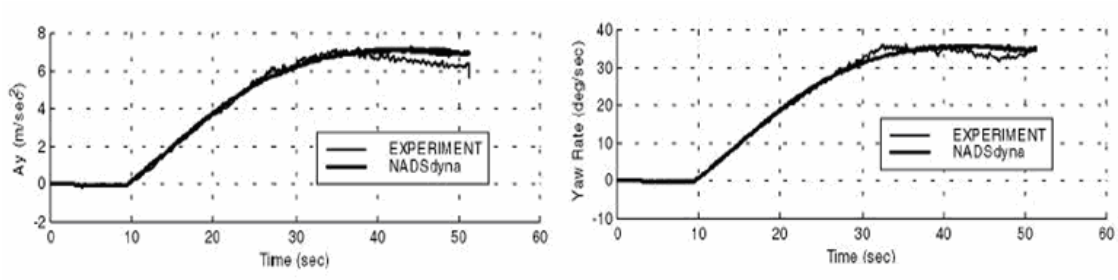

(a) (b)

Figure 3.25 1997 Jeep Cherokee steering ramp input responses [Salaani and Heydinger 2000]

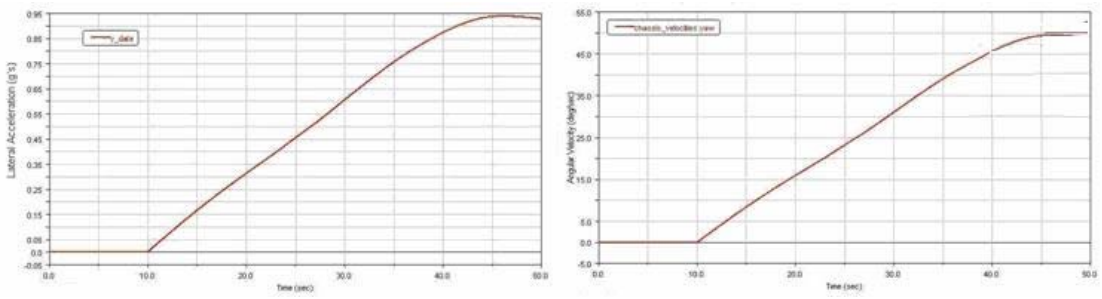

(a) (b)

Figure 3.26 Adams Car steering ramp input responses.

Figures 3.23 and 3.25 show the vehicle's lateral acceleration and yaw rate response to a step and ramp steering input for the actual vehicle and the VRTC simulation. The results are collected with the vehicle under cruise control for 12 *m*/*s* and 11 *m*/*s* respectively; however, our simulation does not include a driver model which performs cruise control.

To address the issue of limited performance data and the requirement for cruise control, a commercial mechanical simulation called Adams Car (MSC Software Corp.) is used to provide additional verification data for both straight-line (longitudinal) and steering tests (lateral). Figure 3.24 and 3.26 show the Adams Car simulation results for lateral acceleration and yaw rate in response step and ramp inputs for steering under cruise control to demonstrate the equivalence of the Adams Car simulation with the actual vehicle in lateral dynamics. Since the Adams Car simulation can provide data throughout the performance envelope, reference data for various straight-line and open-loop steering tests can be generated. The straight-line and open-loop steering performance of both the Adams Car and our simulation are shown side by side to establish equivalence. Although, the vehicle modeled in Adams Car is a high performance sports car, a comparison with our simulation will show the same behavior but the responses will be slower. It is not precision that is being compared rather accuracy in terms of behavior.

3.4.1 Straight Line Analysis

The straight-line analysis consists of subjecting the vehicle to step inputs and ramp inputs for either the throttle or the brake signal. The vehicle's longitudinal speed is recorded and compared. In Figure 3.25 and 3.26, the vehicle speed range is much larger since the simulation incorporates an automatic transmission system. The effects of the automatic transmission shifting can be seen as slight discontinuities in the response. Despite the differences, the step responses of both the actual vehicle and the simulation follow the same behavior. Figures 3.27, 3.28, 3.29, 3.30 and 3.31 show the simulation velocity responses to throttle step, throttle ramp, brake step, brake ramp and throttle power-off inputs respectively. The simulation responses match the vehicle responses in terms of behavior.

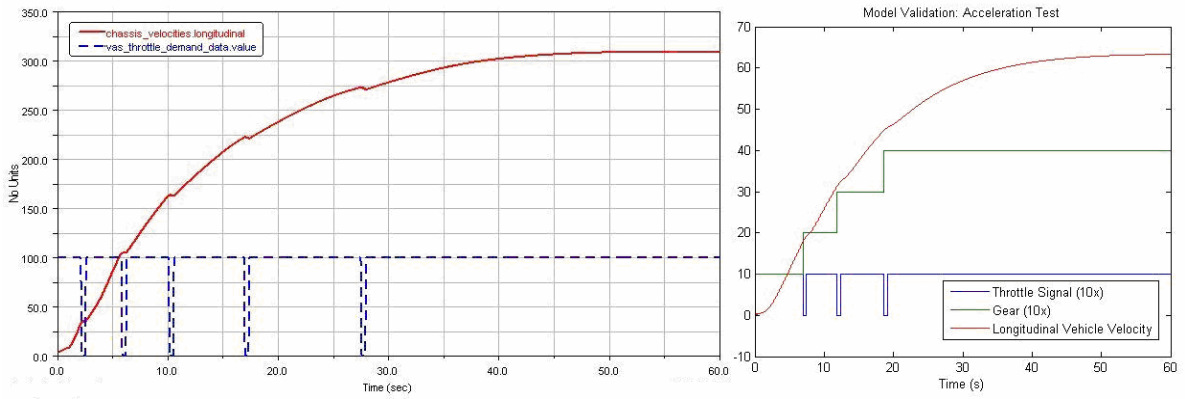

Figure 3.27 Adams Car (left) and Simulation (right) throttle step response.

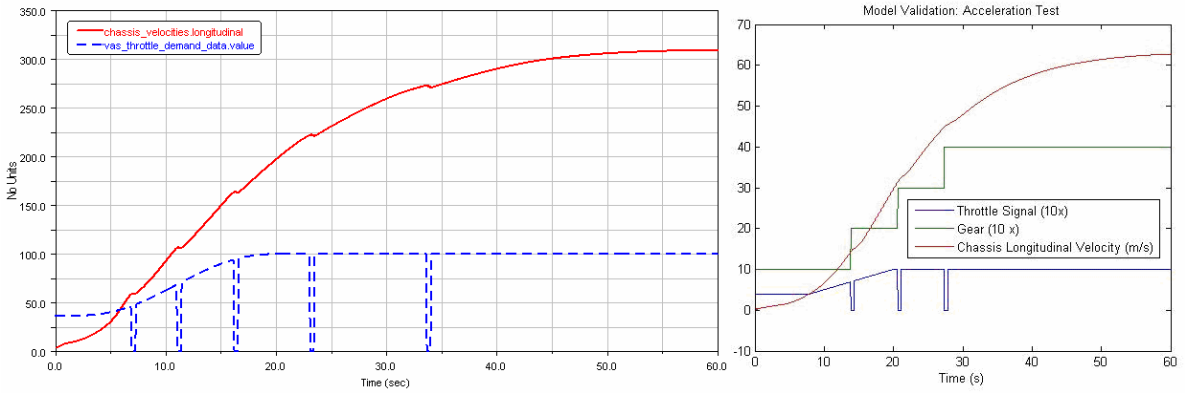

Figure 3.28 Adams Car (left) and Simulation (right) throttle ramp response.

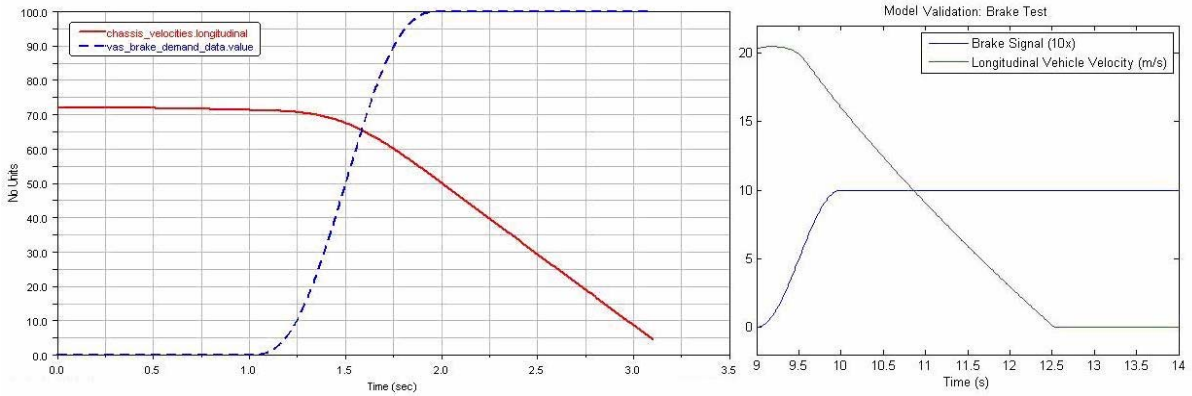

Figure 3.29 Adams Car (left) and Simulation (right) brake step response.

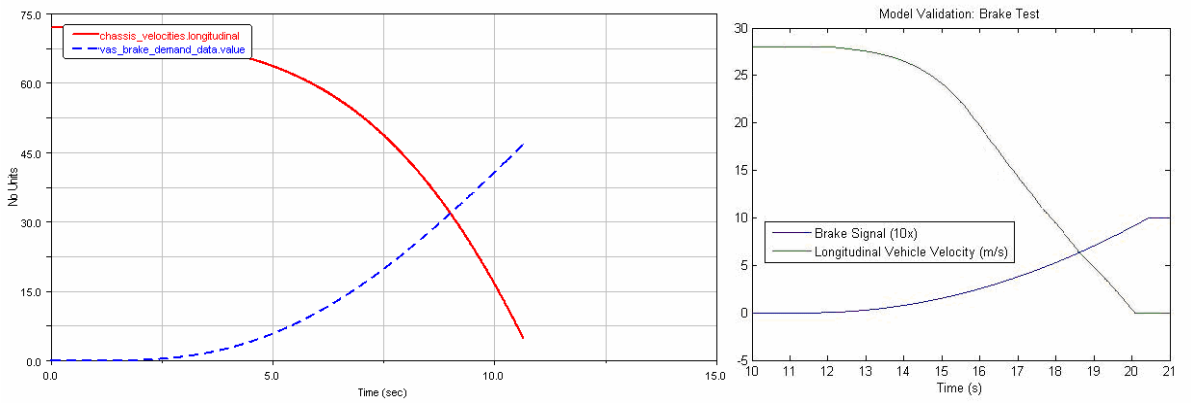

Figure 3.30 Adams Car (left) and Simulation (right) brake ramp response.

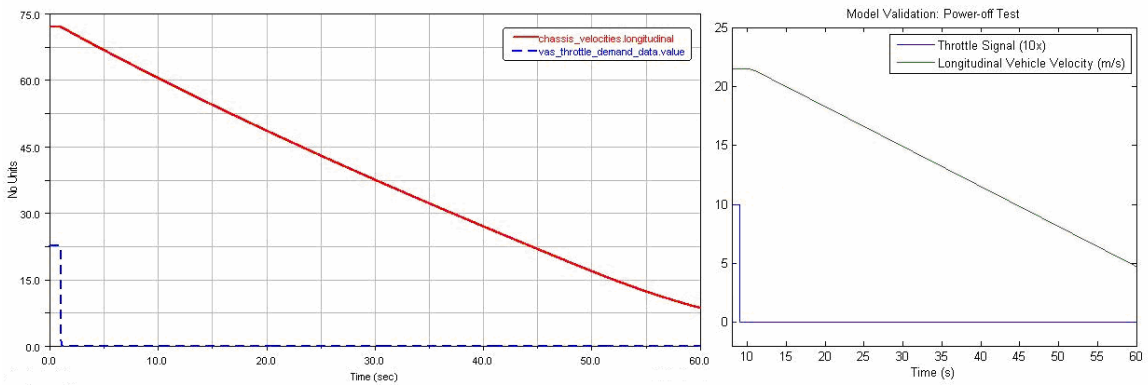

Figure 3.31 Adams Car (left) and Simulation (right) power-off response.

3.4.2 Open Loop Steering Analysis

To demonstrate the validity of our simulation in modeling lateral vehicle dynamics, our simulation and the Adams Car simulation are subjected to a battery of open-loop steering tests and their results compared side by side. These tests are accomplished without the use of cruise control. Figure 3.32 through 3.37 shows the vehicle path traveled when applying the following steering input signals i) impulse, ii) step, iii) ramp, iv) single sinusoid cycle for single lane change, v) sinusoidal with increasing frequency, and vi) ISO lane change. The Adams Car results are shown side by side with the results of our simulation for the various inputs. For each test, the Adams Car simulation and our simulation match. Note that for the ISO lane change test, Adams Car employs a driver model to execute the maneuver, our simulation does not have a driver model, therefore a piecewise combination of sinusoidal functions are used to emulate the maneuver, however, the responses do match.

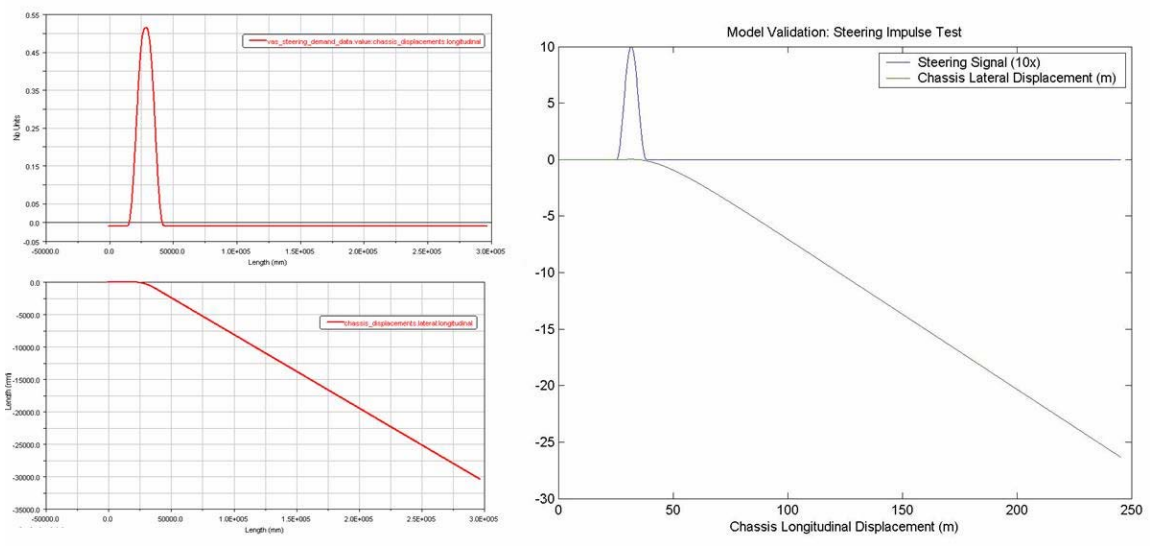

Figure 3.32 Adams Car (left) and Simulation (right) steering impulse input response.

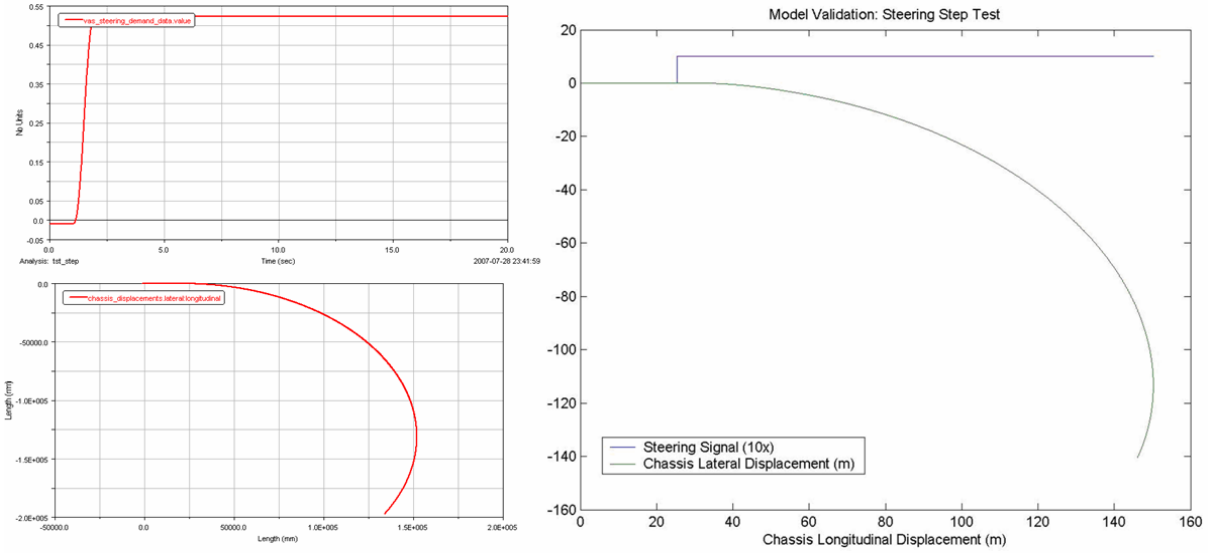

Figure 3.33 Adams Car (left) and Simulation (right) steering step input response.

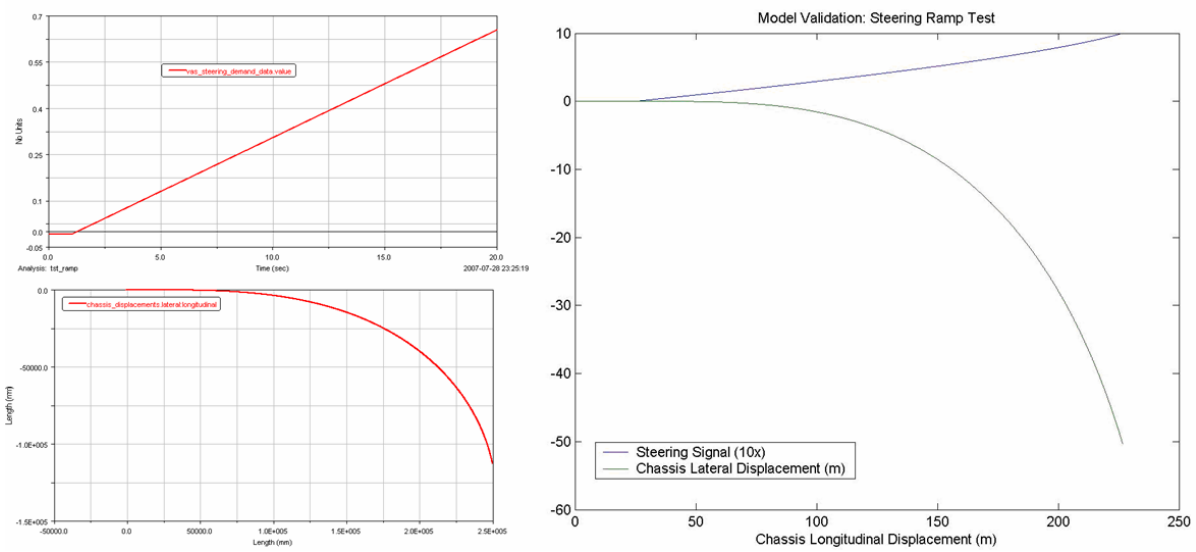

Figure 3.34 Adams Car (left) and Simulation (right) steering ramp input response.

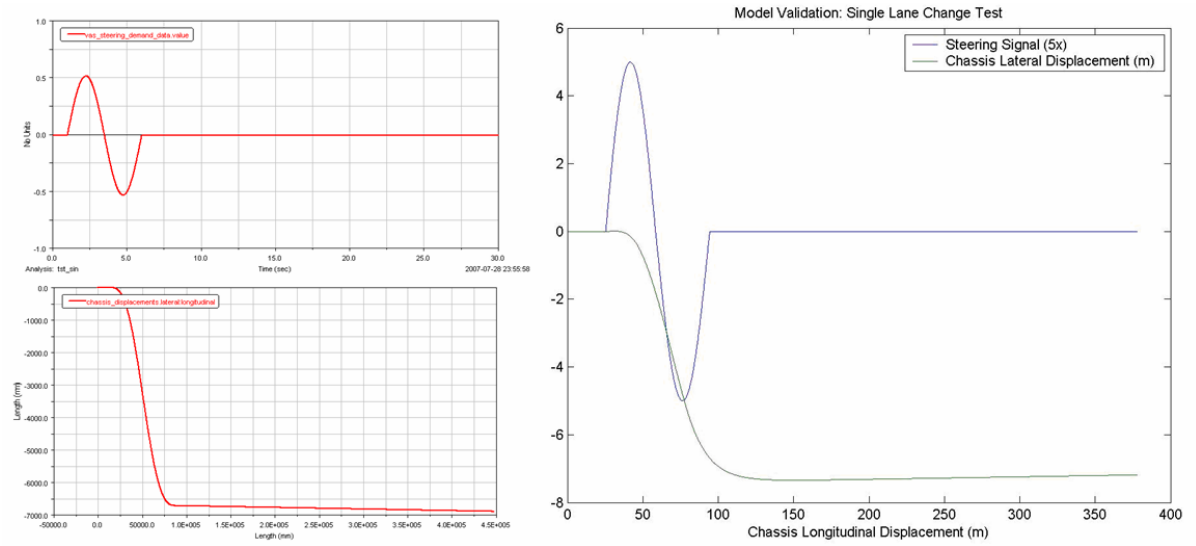

Figure 3.35 Adams Car (left) and Simulation (right) single lane change.

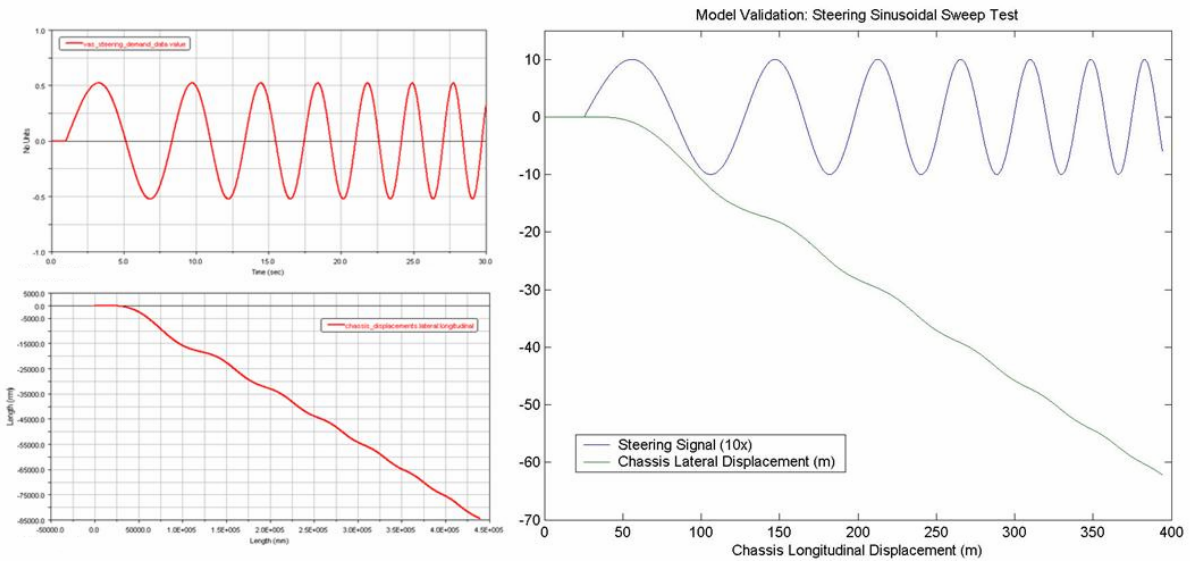

Figure 3.36 Adams Car (left) and Simulation (right) swept sinusoidal steering response.

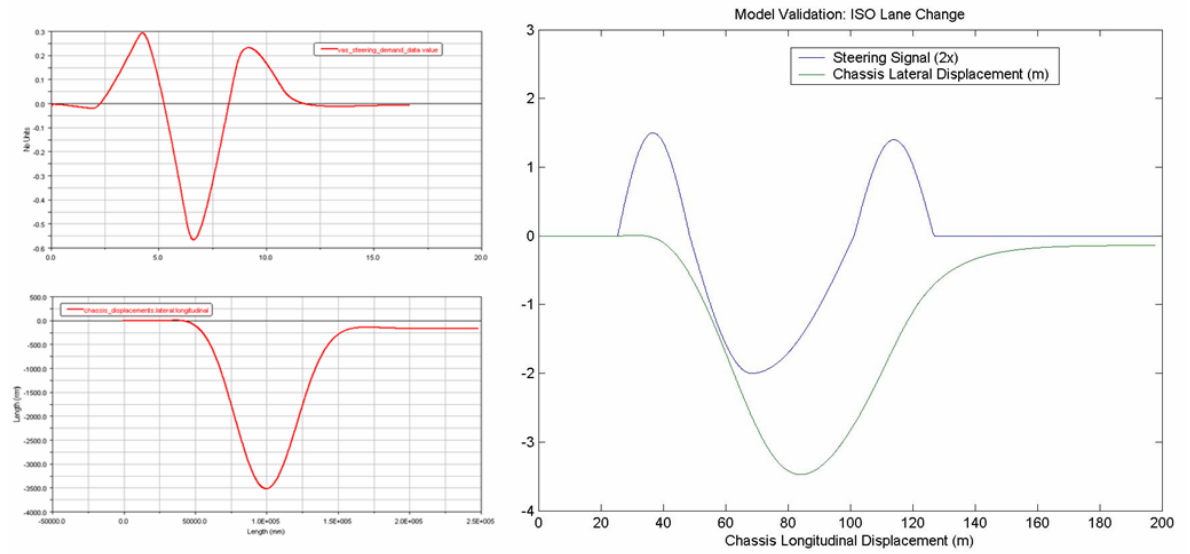

Figure 3.37 Adams Car (left) and Simulation (right) ISO lane change steering response.

Chapter 4

Design

The design of the control system for a decentralized dynamic collaborative driving system is explained in this chapter. The goal of this control system is to achieve automated driving within a group of vehicles. This thesis investigates the use of a class of machine learning techniques called *Reinforcement Learning* for the design of a decentralized automated driving control system. This chapter begins with an overview of the decentralized dynamic collaborative driving problem and follows with a bottom-up description of the control system focusing on the details of implementation.

4.1 Dynamic Collaborative Driving

Dynamic Collaborative Driving is an automated driving concept which has multiple intelligent vehicles equipped with sensors building dynamic local area networks. By sharing their sensory information as a group, they can build up a much larger shared dynamic data representation of their environment, thus allowing the group to coordinate their movement so as to drive collaboratively. The vehicle group not only shares information but space as well. This collaboration can potentially lead to improved safety and traffic control.

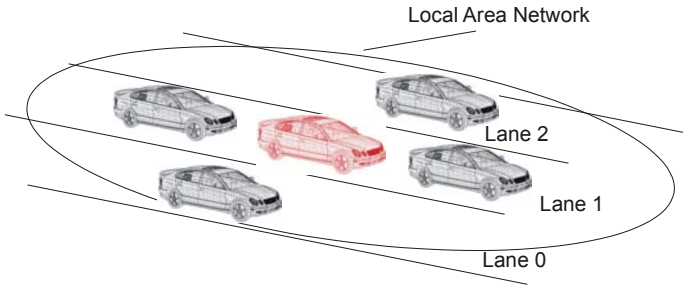

Figure 4.1 Dynamic Collaborative Driving

As the formation of local area networks is dynamic and dependent upon spatial proximity, it is natural to pursue a decentralized control approach to dynamic collaborative driving. While each vehicle should have the intelligence to control itself within the group, the achievement of dynamic collaborative driving is an emergent behavior of the decentralized system.

One design approach for this individual vehicle controller would be to build a single monolithic controller which would include all the logic necessary to complete the task of dynamic collaborative driving. However this task would be daunting, a more manageable approach is to break down the problem of dynamic collaborative driving into smaller modular tasks. In mobile robotics, this division of labor is typically used in control architectures (e.g. in Behavior-Based (BB) architectures [Arkin 1998]). In BB robotics, each modular control task is called a *behavior* which is executed based on sensory input via some control logic. Brooks [1986] popularized this approach by building autonomous robots with rich sensory arrays with modular reactive controllers arranged in

parallel. The robot's composite actions in response to its sensory inputs results in emergent autonomous behavior; Brooks called this a *Subsumption Architecture*.

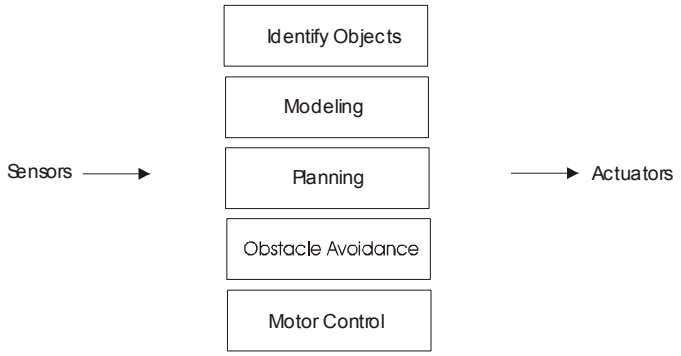

Figure 4.2 Brooks' *Subsumption Architecture*

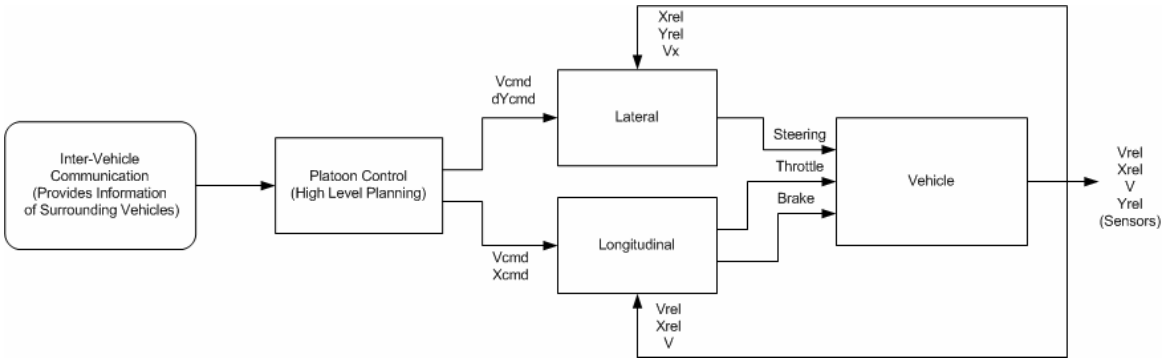

Figure 4.3 Overview of Dynamic Collaborative Driving Control

Similarly, the task of decentralized dynamic collaborative driving can be broken into modular behaviors or individual controllers arranged in a network. Figure 4.3 shows the overall block diagram and information flow of the decentralized dynamic collaborative driving control system. The most basic behavior is the ability to follow another vehicle in the longitudinal axis of the vehicle. This behavior drives the throttle and brake commands in such a way that its speed matches that of the vehicle ahead of it while maintaining a fixed predetermined safety range to it. Once the vehicle's speed can be maintained, lateral control of the vehicle must be achieved. This is performed by the *lateral* behavior which runs parallel to the *longitudinal* control behavior. It drives the steering command so as to minimize any lateral deviation between itself and the vehicle ahead. Higher level planning is controlled by the Platoon Control module which provides equivalent *lateral* and *longitudinal* commands for a given maneuver such as a lane change or when entering or exiting a platoon. These higher-level maneuvers are delivered to the control system via the Inter-Vehicle Communication system.

Although the Platoon Control module and Inter-Vehicle Communication system are shown, they can be considered the beginning of decision making. This thesis focuses specifically on vehicle control thus ending our investigation of dynamic collaborative driving with the *lateral* and

longitudinal behaviors. However, it is touched upon to illustrate where this thesis contributes to solving the overall problem of decentralized dynamic collaborative driving.

4.2 Implementing Reinforcement Learning

Mataric [1997] used reinforcement learning to optimize the process of decentralized control for a foraging task with limited success. Each robot controller was behavior based but the *behaviors* which the optimal controller learned to execute were fixed. Reinforcement learning was used to determine the order of execution of the individual behaviors so as to perform the foraging task while maximizing the received reward. This design takes the complementary approach, whereby the logic which executes behaviors is fixed while reinforcement learning is applied to each of the behaviors (i.e. Longitudinal Control, Lateral Control, Motion Planning and Merging) to optimize and adapt to each behavior.

In this thesis, reinforcement learning is used to develop an optimal control system for various aspects of vehicle control. From the previous chapter, the complexities of vehicle modeling were explained. That is the vehicle exhibits delays and nonlinearities which make it difficult to control using conventional control techniques. These delays also make the processes which we need to control non Markov. As stated in Chapter 2 in order for reinforcement learning to be applied the process needs to be Markov; that is the current state must not be dependent on previous states. In order to make a process with delays Markov, the process can only be considered in the context of a time frame greater than the delay. We consider this time frame an episode and therefore only apply episodic reinforcement learning also known as Monte Carlo Reinforcement Learning to learn each optimized behavior. The use of Monte Carlo Reinforcement Learning has its most recent success by Ng et al [2004], where hovering control of a model helicopter was performed using a control system whose gains were optimized using a recurrent neural network in conjunction with Monte Carlo reinforcement learning. This thesis deviates from this approach by using Monte Carlo reinforcement learning alone to learn adaptive control to deal with the nonlinearities of the longitudinal and lateral vehicle dynamics.

4.2.1 Software Tools

Reinforcement learning software has not made its way into mainstream engineering. Modern Computer Aided Engineering (CAE) tools such as Mathworks Matlab or MapleSoft Maple 11 do not yet have packages for reinforcement learning, however, more established artificial intelligence approaches do have packages (i.e. Neural Networks and Fuzzy Logic). In the academic community, only recently have some researchers agreed upon a limited specification so that future tools could be shared. As a result, highly customized software is developed by each researcher with very limited capabilities of being reused or shared. Therefore, due to the infancy of standardized reinforcement learning software, a custom software package called was also developed for this investigation.

For this thesis, I wrote RLTools, an object library written in C++ for Linux x86 for reinforcement learning. Its only dependency is the standard C library shipped with the GNU C++ 3.2 compiler available on the Linux operating system. The package contains a standard Unix Makefile

which compiles the source code into object files which can be linked to other object files to become a stand-alone executable. The "math2" files are advanced mathematics functions, most importantly, enhanced random number generation, written in ANSI C. The remaining source files are the C++ Objects for reinforcement learning which are explained in detail in their respective sections.

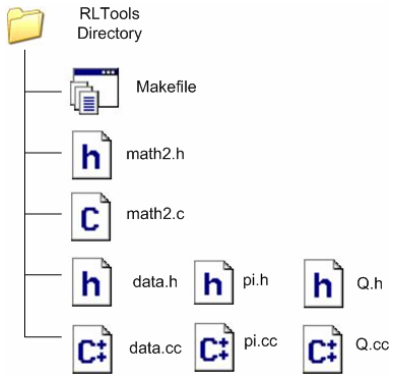

Figure 4.4 Files structure of RLTools

4.2.1.1 The "Data" Object

The *Data* object represents the structure of input or output data in a Markov Decision Process (MDP). In the context of a finite MDP data exists in discrete form. Thus, for control applications, continuous values must be converted into their discrete equivalents in order to be used. This process of digitization is handled by the *Data* object.

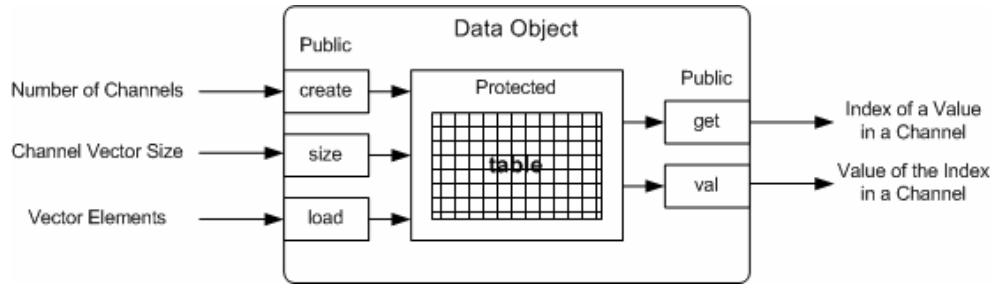

Figure 4.5 Schematic of the *Data* object

Typically, the state signals are represented by a *Data* object, while the action signals are represented by another *Data* object. Within the states or actions, there are *n* channels or individual signals which make up the group. For each channel, there must be a channel vector which describes how the signal will be digitized. This channel vector is an array of *ns* floating point numbers which partition an interval into (*ns-1*) regions. For example, a channel vector [1, 2, 3, 4, 5] of 6 elements represents the interval [1, 5] with 4 intervals. When a continuous value is digitized, the value is compared to the elements of the channel vector. It is assigned the index value of the element in this vector that is closest to and greater than the continuous value. To digitize the continuous value 2.5, we would say that the 2.5 is between 2 and 3. The digitized value would be the index to the element

3 and would be stored as the integer 2. Within the MDP only integer values are used, however to translate the information into continuous values a translation *table* must be maintained.

The *table* at the heart of the *Data* object is a protected data structure, it is created once the number of channels has been specified using the public *create* method. Each channel's vector size must then be specified using the public *size* method. Finally one can load the vector elements of the channel vector into the translation table using the public method *load*. Translation between index values and continuous values are accomplished using the *get* and *val* methods, however the channel must be specified. Figure 4.5 illustrates the *Data* object for further clarification.

4.2.1.2 The "Pi" Object

The *Pi* object represents the policy for a Markov Decision Process (MDP). It is simply a mapping from states to actions. For the purpose of storage efficiency, it is stored as a protected single dynamically linked-list. This allows nodes which contain the state-action pairs to be added or removed as needed, via the public methods *add* and *remove*. To retrieve state-action pairs, a public *search* method is used where the state must be specified. The *search* method performs a linear search; therefore its search time is dependent on the length of the dynamic linked-list. Public methods such as *save* and *load* are available to store or retrieve a policy file. The policy is the end result of reinforcement learning and it is this object which will be used for vehicle control. Figure 4.6 illustrates the *Pi* object for further clarification.

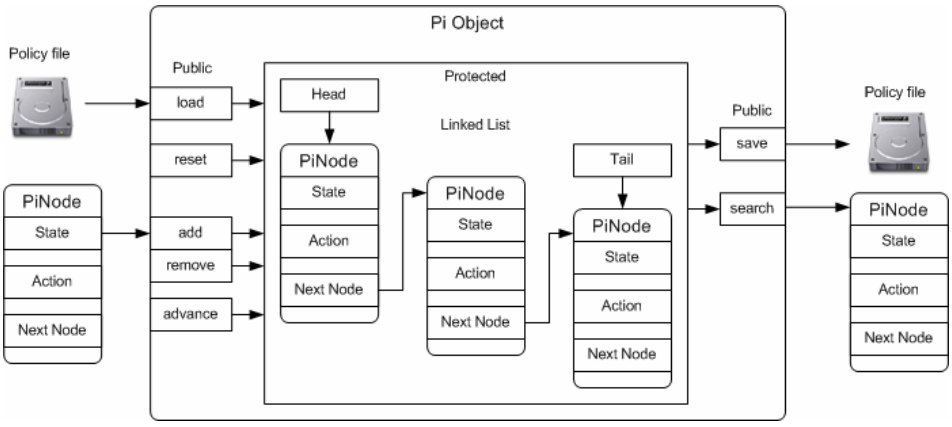

Figure 4.6 Schematic of the *Pi* object

4.2.1.3 The "Q" Object

The *Q* object represents the Q value function of the Markov Decision Process (MDP). The *Q*-value represents the favorability of performing an action while being at a given state, *Q(s, a)*. The optimal policy which results from reinforcement learning should provide actions for every state such that the maximum amount of reward can be received. A single *Q*-value entry consists of its *Q*-value, the state and the action.

Typically for the sake of simplicity, the Q-value function is stored as a Q-table where the state and actions are indices of a fixed multi-dimensional array and the entries are the Q-values. When using a Q-table, all possible states and actions are considered at compile time. This is fine for discrete states and actions and small scale problems, however, with continuous states and actions that require higher resolution, this table can easily grow to the size of terabytes. Therefore it is not scalable or feasible for our purposes.

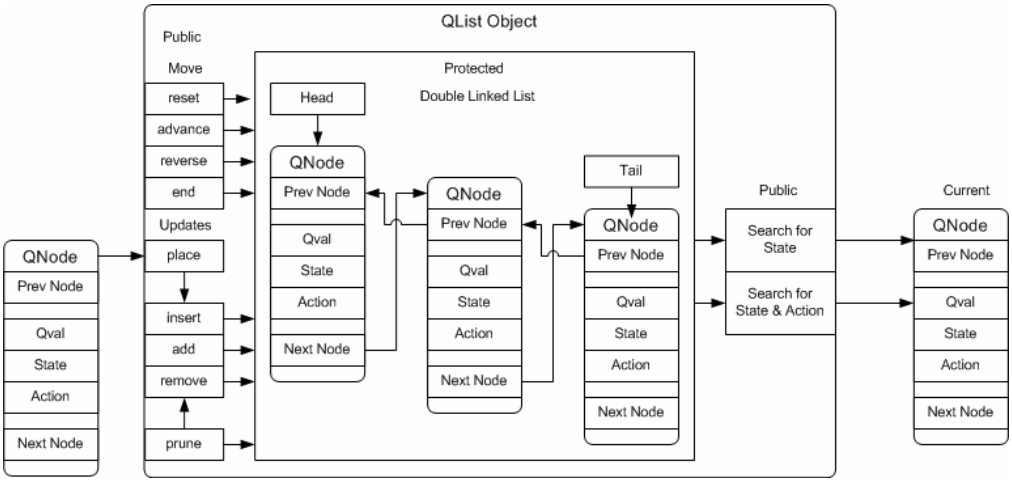

Figure 4.7 Schematic of the *QList* object

At this point, the *QList* object is introduced. The *QList* object is a protected double linked list which represents the Q-value function only (See Figure 4.7). It is a double linked list because it can be traversed in the forward and reverse direction which facilitates insertion and deletions of nodes within the list. By having the Q-value function represented as a linked list, only the visited state-action pairs are stored in memory. Therefore, high resolution states and actions can be used without exceeding memory requirements. This is assuming that the optimal policy can be determined without having to visit every possible state and action.

A key feature of *QList* is that it self organizes, that is it automatically sorts itself upon every update. This is accomplished via the *place* method which places or replaces a new *QNode* into the linked list. The process of placing a *QNode* is that it first looks for a *QNode* with the same existing state-action pairs and deletes the existing one. The new *QNode* is placed with other *QNodes* that match it state, however the *QNode* with the highest Q value is at the top of its state subsection. This facilitates determining the most favorable action for a given state; it is simply the *QNode* at the top of the list with the matching state. To facilitate this, two search methods are available one that searches based on the state provided, and another which searches based on both the state and action provided. The *search* methods perform a linear search; therefore its search time is dependent on the length of the dynamic linked-list.

Another key method is the prune method; this method is used to reduce the size of the linked list. A minimum number of *QNodes* must be specified, the prune method traverses the entire linked list and removes *QNodes* in excess of the number for each state. In fact, the linked list can be reduced

to the optimal policy if a minimum number of 1 is specified when activating the *prune* method (only the nodes with the highest Q value are kept for every state).

The Q object is responsible for the higher functionality of the Q-value function. Primarily it updates the protected *QList* linked list object via the public methods: *set*, *updateSarsa* and *updateQ*. Depending on the reinforcement learning algorithm one needs to employ a particular method will be used. For Temporal-Difference reinforcement learning using SARSA [Rummery &Niranjan 1994] or Q-Learning [Watkins 1989], use the methods called *updateSarsa* and *updateQ* respectively. In this thesis, Monte Carlo reinforcement learning (See Figure 2.6) is used, so the *set* method is sufficient for updating the linked list. It simply sets the Q value for a given state-action pair and uses the *QList::place* method to place this *QNode* into the linked list.

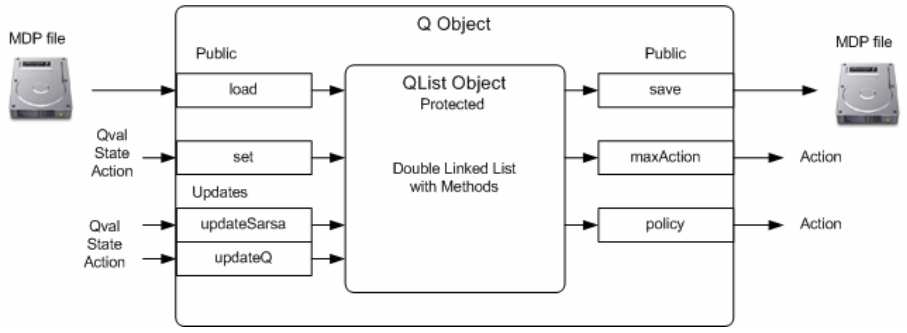

Figure 4.8 Schematic of the *Q* object

The current policy represented by the current Q-value function can be accessed using the two policy functions. The *maxAction* method which provides the action for the given state that will receive the maximum reward. The *policy* method requires a ε value which represents the probability of exploration. Upon calling the policy function a random number is generated for each action, if the random number exceeds the ε value, it chooses the action corresponding to *maxAction* policy, if it is below ε; it chooses a random action for that particular action. This facility allows new actions to be explored but to still remain in the favorable solution space. Figure 4.8 illustrates the *Q* object for further clarification. Finally, *load* and *save* methods are available to either load an existing Q-value function stored in a MDP file into the linked list or to write the existing linked list into an MDP file on local storage.

4.2.2 Implementing Reinforcement Learning using RLTools

This section explains how the above objects are used to obtain optimal policies for vehicle control using reinforcement learning algorithms. In this thesis, a separate standalone executable is built for deriving each individual control system. Each of these executables is referred to as an experiment. Building of an experiment comprises of writing a C++ main program which instantiates and calls these objects. Figure 4.9 illustrates in flow chart form a generalized Monte Carlo reinforcement learning experiment. This represents the general form that all reinforcement learning experiments take, however depending on the class of algorithm, variations exist.

The experiment begins by defining the number of states and actions for the Markov Decision Process (MDP). This includes determining the channel vectors which will dictate how the information will be translated between the discrete space and the continuous space (see section 4.2.1.1 for details on the *Data* object). From the definition of states and actions, a *Data* object called *State* and a *Data* object called *Action* will be instantiated (or created). Subsequently, the contents of the channel vectors will be loaded into the translation table for *State* and *Action*.

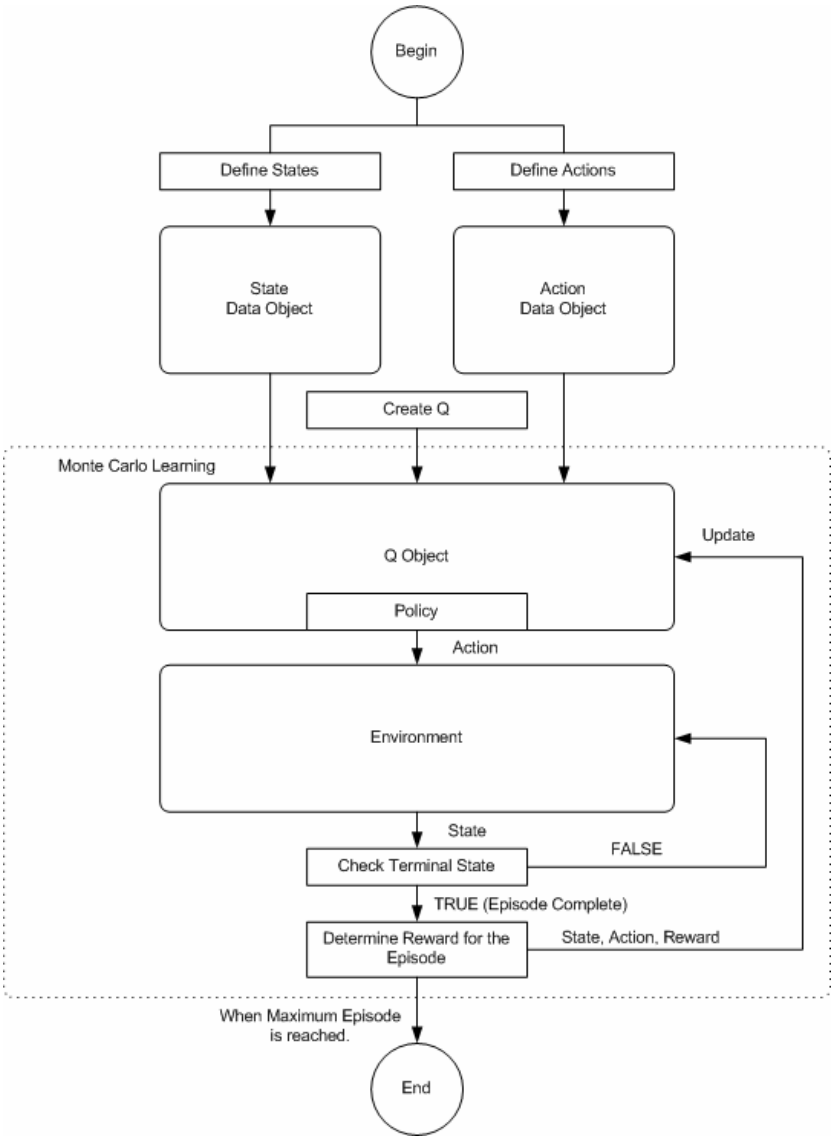

Figure 4.9 Flow chart for Monte Carlo reinforcement learning using RLTools

Once *State* and *Action* are available, the *Q* object called *Q* can be instantiated (or created). This builds the basic structure of the *Q* object but does not add any *QNodes* to the linked list yet. At

this point an *Environment* is required. The *Environment* is what the MDP will be acting upon, that is it will provide states for a given action. For example, for the Monte Carlo reinforcement learning of longitudinal vehicle control, the *Environment* is the vehicle model described in Chapter 3. Therefore, the *Environment* is initialized and provides an initial state. Through the *Q::policy* method an action is selected, because the *Q* linked list is initially empty; a random action is chosen for this initial state.

The environment is repeatedly experienced for the course of the episode; that is until the terminal state is reached. For instance, in the case of learning longitudinal control, the vehicle must travel through x_{max} *m*, therefore, the terminal state is when the $x_{cur} = x_{max}$. During the course of the episode, the rewards are being collected. The accumulated *reward* is associated with this given visit to this state and action pair. At the end of the episode, this reward is updated to the existing *Q(s,a)* in the linked list according to the *Monte Carlo ES* reinforcement learning update rule (see Figure 2.8) which is to average the existing *Q(s,a)* with the new *Q(s,a)*. This process is repeated for a fixed number of episodes or when a learning margin has been reached.

4.3 Longitudinal Control

In this thesis, an adaptive longitudinal vehicle control system is introduced whereby the controller is learned through reinforcement learning using a complex nonlinear vehicle dynamics model. The outputs of the longitudinal control problem are i) the throttle angle, which controls the fuel/air mixture for the combustion process within the engine and ii) the brake pedal position, which applies a braking torque to each wheel. In Figure 4.10, the vehicle model's velocity responses to 100% throttle step input and 50% throttle step input are charted. The responses can be characterized as second order over-damped with a slight delay. By comparing the 50% response multiplied by a factor of two with the 100% response we see that the vehicle model's response with respect to the throttle is clearly non-linear. In Figure 4.11 the vehicle model's velocity response to 100% brake step input and 50% brake step input are shown. The responses show that during braking, Coulomb friction dominates. It is clear that the vehicle response to a 50% brake step input is not half of the 100% signal indicating that the modeled braking system is non-linear. Figure 4.12 shows the vehicle model's response to disengaging the throttle or power-off. The throttle power off resembles the brake system's response although more gradual and can be considered a nonlinear response.

To address each of these nonlinear responses, different control systems are required depending on the operating conditions. Our approach is to divide the control space into regions within which the behavior of the plant approximates linearity. A patch-work of linear controllers would then be able to address the entire operating envelope. These linear controllers would all have the same form, but their gains would differ depending on the operating conditions. This common linear controller along with its collection of gains is considered a form of adaptive control referred to as gain scheduling [Aström & Wittenmark 1994]. The difference in our implementation of gain scheduling, is that the tedious task of determining each gain is accomplished using a machine learning algorithm called *Monte Carlo ES* reinforcement learning.

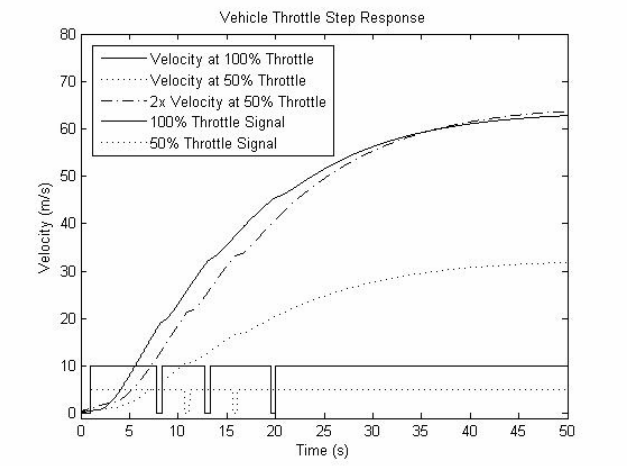

Figure 4.10 Vehicle model velocity responses to throttle step inputs

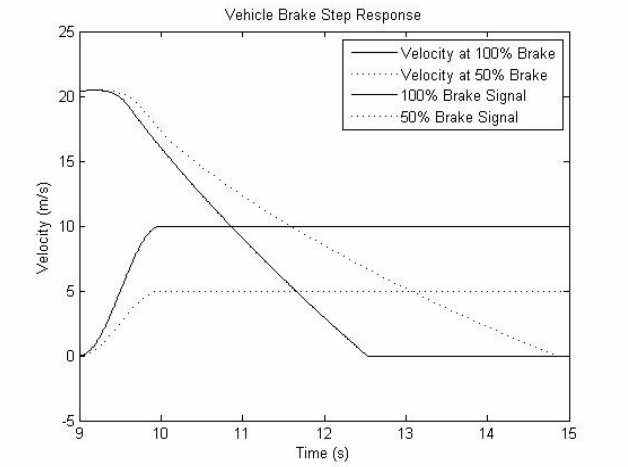

Figure 4.11 Vehicle model velocity responses to brake step inputs

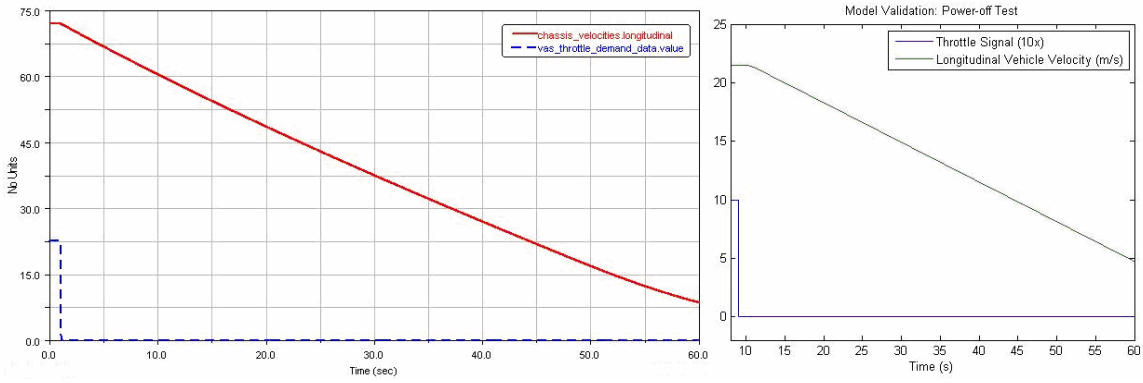

Figure 4.12 Adams Car (left) and Simulation (right) power-off response.

Simply stated, longitudinal control of a vehicle is to be able to follow another vehicle in traffic without colliding into it. That is, the controller must maintain a relative speed of zero with the vehicle ahead while maintaining a fixed distance behind the forward vehicle; this fixed distance will be referred to as Δx_i. During the process of control, the vehicle's relative speed, $V_{rel} = Vx_{i-1} - Vx_i$ and range, $X_{rel} = x_{i-1} - x_i$, to the vehicle ahead will provide feedback to the control system. Figure 4.13 shows how multiple vehicle's are linked to provide longitudinal control for multiple vehicles.

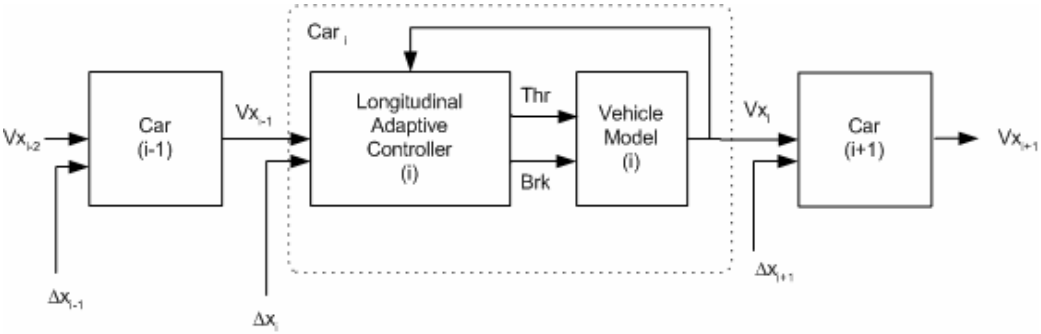

Figure 4.13 Overview of longitudinal control system

Figure 4.14 shows the design of the control system, two parallel control systems are used, one for throttle control, and one for brake control. These two throttle and brake controllers are a combination of a discrete Proportional-Derivative (PD) controller for the relative velocity V_{rel}, and a discrete Proportional-Integral (PI) controller for the relative distance X_{rel} also known as range.

The choice of controller structure was based on the requirement to regulate both relative speed and relative distance with respect to the lead vehicle. From a relative speed perspective, it is desireable to match the lead vehicle speed without overshoot, and a PD controller is therefore appropriate. From a relative distance perspective, the objective is to end up at the prescribed following distance without steady state error, and a PI controller is therefore suitable. This four-term controller structure is appropriate for both throttle and braking since the relative speed and distance objectives are the same, although the controller gains will be different.

The difference equation which provides the throttle/brake command m_n is shown below

$$m_n = m_{n-1} + k_{pv}(v_n - v_{n-1}) + \frac{k_{dv}}{\Delta T}(v_n - 2v_{n-1} + v_{n-2}) + k_{px}(x_n - x_{n-1}) + k_{ix}\Delta T\, x_n \quad (4.1)$$

where n is the current iteration of the control cycle, v is V_{rel}, x is X_{rel}, and ΔT is the period of the control cycle. Moreover, k_{pv}, k_{dv}, k_{px}, and k_{ix} are gains that are functions of MDP state variables s_1, s_2, and s_3 as described in Table 4.1. The results of both the throttle and brake controllers are fed into a logic element controlled by the gain K_{coast} which decides whether throttle control or brake control is to be used. In this paper, K_{coast} is set to 0.25; that is throttle values less than 0.25 utilize the braking system rather than coasting. The logic for this element is shown below

$$
\begin{aligned}
&\text{if } (throttle > 0) \\
&\quad cmd_{throttle} = throttle, cmd_{brake} = 0 \\
&\text{else if } (throttle < -K_{coast}) \\
&\quad cmd_{throttle} = 0, cmd_{brake} = (-brake) - K_{coast} \\
&\text{else} \\
&\quad cmd_{throttle} = 0, cmd_{brake} = 0
\end{aligned}
\tag{4.3}
$$

For a given operating point, there are eight parameters or gains which must be provided in a lookup table or schedule. By formulating the control problem into a MDP, the gain schedule can be learned using reinforcement learning. The episode is defined as starting at the onset of a change in Vx_{i-1} and ending when $Vx_i = Vx_{i-1}$ or when Vx_{i-1} has been changed. This follows the logic that when a new velocity is required, a set of gains should be selected from the gain schedule and applied for the duration of that command. The goodness of a set of gains can therefore only be assessed once the command is complete, thus the MDP is episodic in nature and the *Monte Carlo ES* reinforcement learning algorithm described in Figure 2.8 is used to learn the gain schedule.

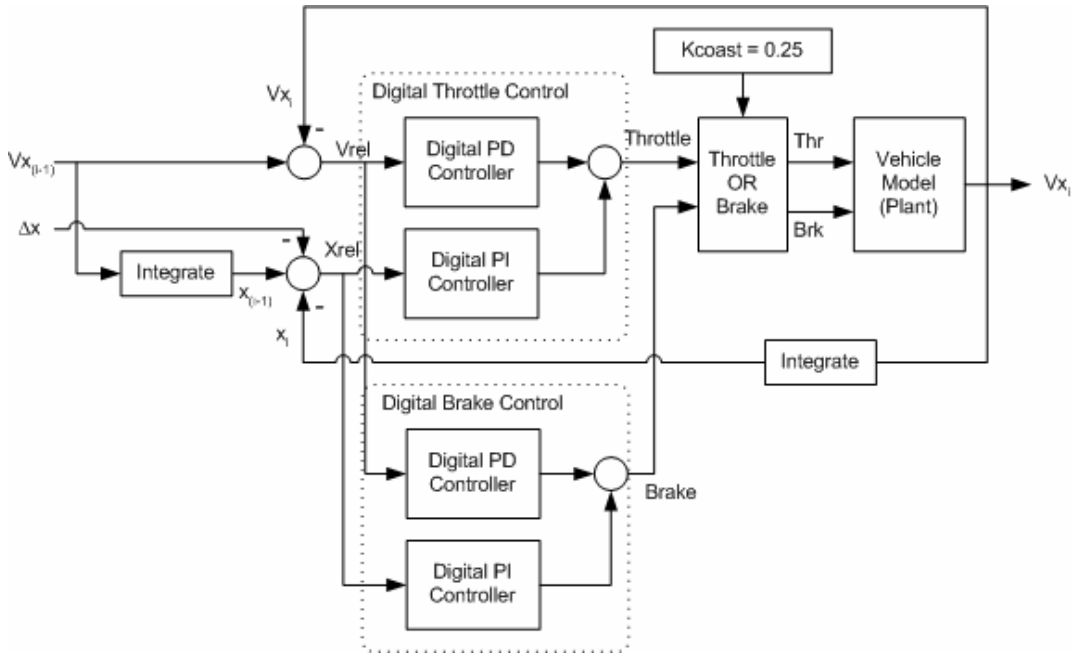

Figure 4.14 Block diagram of longitudinal controller

The choice in the selection of states lies in the nonlinear nature of the throttle response. At different initial speeds the throttle responds differently. Therefore, the controller gains will differ from a given initial speed to a final speed. In addition, the distance required to achieve this acceleration/deceleration which is reflected in the change in vehicle spacing is also an independent variable for the gain schedule. These three parameters are used as states (Table 4.1). The actions are the eight values which represent the gains used in the digital control system (Table 4.2).

Table 4.1 States of the longitudinal MDP

State	*Description*	*Digitization Sets*
s_1	Vx_0: initial vehicle speed	{ 5, 10, 15, 20, 25, 30, 35, 40} m/s
s_2	Vx_{i-1}: target vehicle speed	{ 5, 10, 15, 20, 25, 30, 35, 40} m/s
s_3	$\Delta x_f - \Delta x_i$: change in vehicle spacing	{-100, -90, -80, …, 80, 90, 100} m

Table 4.2 Actions of the longitudinal MDP

Action	*Description*	*Digitization Sets*
a_1	K_{px}: Throttle Proportional Gain (x)	{0.1, 0.2, 0.3, … 99.9} n_s = 1000
a_2	K_{ix}: Throttle Integral Gain (x)	{0.01, 0.02, 0.03, … 9.99} n_s = 1000
a_3	K_{pv}: Throttle Proportional Gain(V)	{0.1, 0.2, 0.3, … 99.9} n_s = 1000
a_4	K_{dv}: Throttle Derivative Gain (V)	{0.1, 0.2, 0.3, … 99.9} n_s = 1000
a_5	K_{px}: Brake Proportional Gain (x)	{0.1, 0.2, 0.3, … 99.9} n_s = 1000
a_6	K_{ix}: Brake Integral Gain (x)	{0.01, 0.02, 0.03, … 9.99} n_s = 1000
a_7	K_{pv}: Brake Proportional Gain (V)	{0.1, 0.2, 0.3, … 99.9} n_s = 1000
a_8	K_{dv}: Brake Derivative Gain (V)	{0.1, 0.2, 0.3, … 99.99} n_s = 1000

The reward function which reflects the specification of the control problem is a discrete function of the feedback variables, the current normalized relative speed and normalized relative velocity of the vehicle and is expressed below.

$$R_{Total} = R_V(V_{rel}) + R_X(X_{rel}) \tag{4.3}$$

$$R_X(X_{rel1}) = \begin{cases} 1 & if\ X_{rel} \le 0.1 \\ -1 & if\ X_{rel} < 0 \end{cases} \qquad R_V(V_{rel1}) = 1 \quad if\ |V_{rel}| < 0.1$$

For a given episode, the solution which maximizes the reward, or minimizes the X_{rel} and V_{rel} without colliding with the vehicle ahead ($X_{rel} < 0$) will be favored. These favored solutions will be explored to determine the optimal solution.

4.4 Lateral Control

In this thesis, an adaptive lateral vehicle control system is introduced whereby the controller is learned through reinforcement learning using a complex nonlinear vehicle dynamics model. The output of the lateral control problem is a normalized steering angle of the front wheels while the

inputs are i) lateral displacement and ii) the vehicle speed. The control problem therefore is to determine the correct steering angle trajectory to minimize the lateral displacement error while following the vehicle ahead. Figure 4.15 shows the desired trajectory of the vehicle for a single lane change or a step input in terms of lateral displacement at a constant speed. It shows that in order to achieve a smooth transition from one lateral position to another, the required steering signal trajectory is a specific delayed single sinusoidal cycle. Therefore, lateral vehicle movement can be considered a nonlinear control problem.

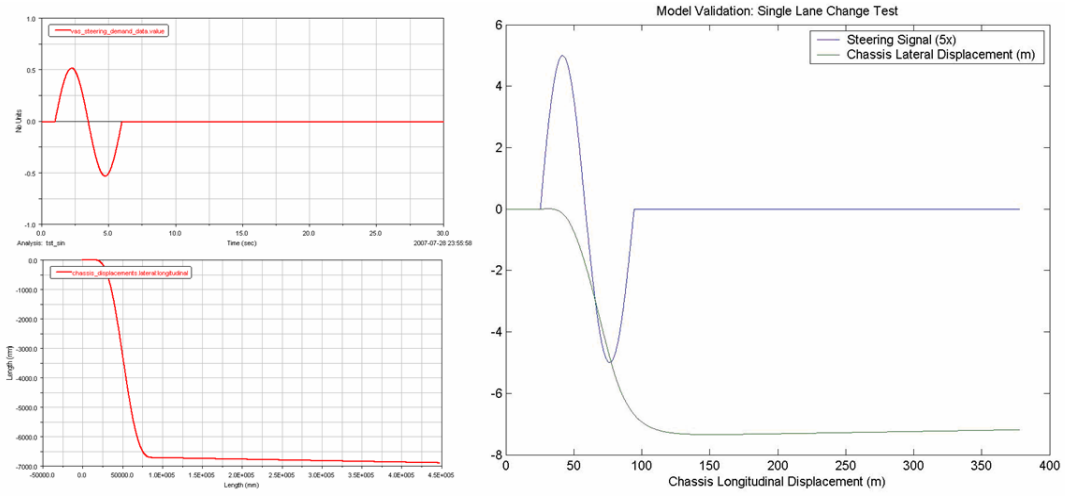

Figure 4.15 Adams Car and simulation of single lane change

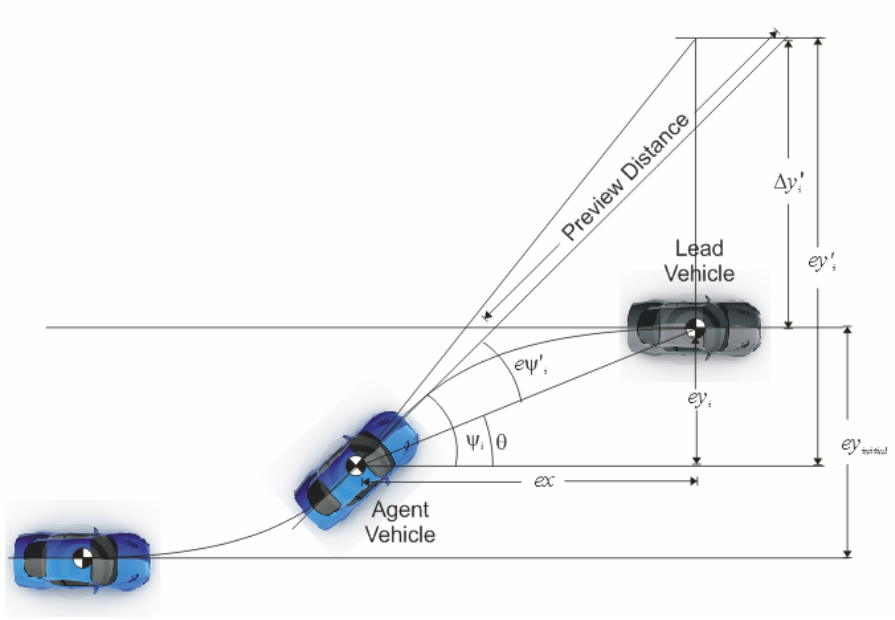

Figure 4.16 Schematic of lateral control

Our approach is to transform the control problem such that the operating envelope can be subdivided into regions within which the behaviour of the plant approximates linearity. A common linear control law is formed where the gains would differ depending on the operating conditions. The control law minimizes a predicted (preview) angular error which gives this control system an anticipatory element. The common linear controller along with its collection of gains is considered a form of adaptive control referred to as gain scheduling [Aström & Wittenmark 1994]. The difference in our implementation of gain scheduling, is that the tedious task of determining each gain is achieved using a form of machine learning called *Monte Carlo ES* reinforcement learning. In addition, the preview length used to determine the predicted angular error is also determined using *Monte Carlo ES*.

The problem of lateral control can be simply stated as the ability to follow another vehicle directly in front of it, by minimizing the relative lateral distance. It is assumed that the vehicle ahead is within sensing range and traveling at a constant speed so as to decouple the problem from longitudinal control. Therefore, the lateral controller must maintain a relative lateral error of zero with the vehicle ahead while maintaining the fixed distance behind the forward vehicle using a separate longitudinal controller. Figure 4.17 shows the overall structure of the vehicle control system and how multiple vehicle's are linked in terms of data to provide automated control for multiple vehicles.

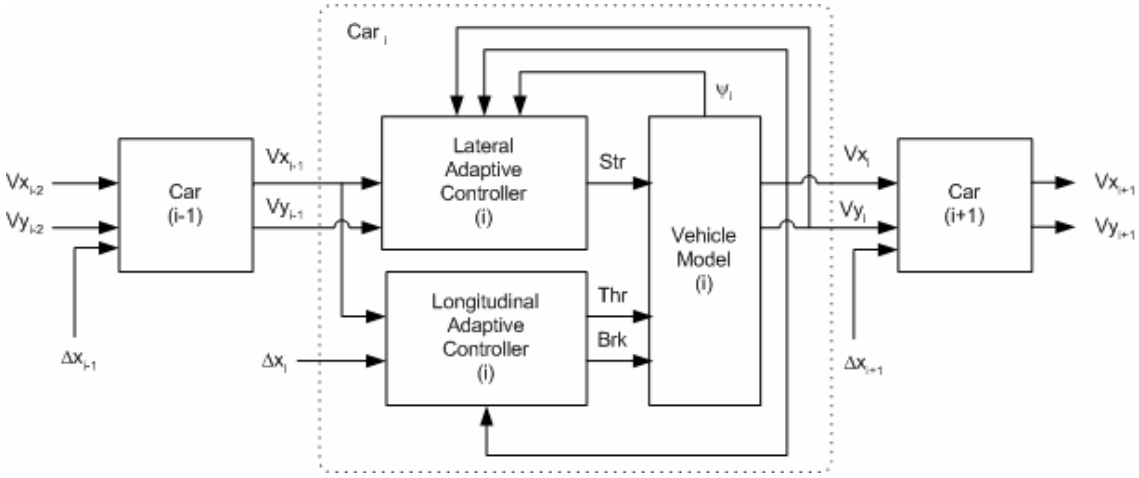

Figure 4.17 Overview of lateral control system

Figure 4.18 shows the design of the lateral adaptive control. Central to the control system is the common linear control law in the form of a discrete Proportional-Derivative (PD) controller which controls $e\psi'_i$ the angular error between the current vehicle and the vehicle ahead. The difference equation of this controller which produces the final steering command m_n is shown below

$$m_n = m_{n-1} + k_p (e_n - e_{n-1}) + \frac{k_d}{\Delta T}(e_n - 2\,e_{n-1} + e_{n-2}) \tag{4.4}$$

where n is the current iteration of the control cycle, e is $e\psi'_i$ and ΔT is the period of the control cycle; k_p and k_d are provided by the learned optimal policy and are functions of MDP state variables $s_1 = Vx$,

the longitudinal vehicle velocity as described in Table 4.3. The angular error $e\psi'_i$ is determined within the *Polar Transform* block using the following equation

$$e\psi'_i = \arctan\left(\frac{ey'_i}{ex}\right) - \psi_i \tag{4.5}$$

where ψ_i is the current yaw angle or heading angle of the vehicle, ex is the longitudinal following error between the vehicle and the vehicle ahead and $ey'_i = y_{i-1} - y'_i$ is the lateral previewed error. The lateral previewed displacement $y'_i = y_i + \Delta y'_i$ where the previewed distance Δy_i is calculated in the *Preview* block using the following equation

$$\Delta y'_i = k_{preview} Vx_i \sin(\psi_i) \tag{4.6}$$

where $k_{preview}$ is a learned gain provided by the optimal policy and Vx_i is the vehicle speed.

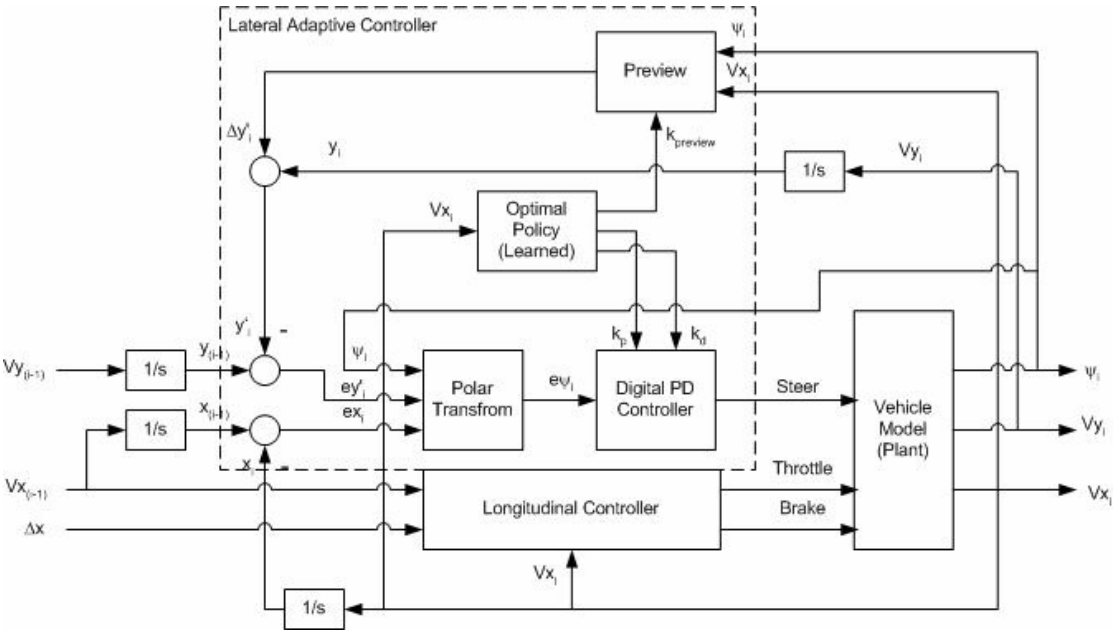

Figure 4.18 Block diagram of lateral control system

For a given operating point, there are three parameters or gains which must be provided in a lookup table or schedule. One could obtain each value in the gain schedule for k_p and k_d using classical control techniques or state-space techniques. In this thesis, it is proposed that all gains can be learned using machine learning if the optimization problem can be formulated into a Markov Decision Process (MDP).

The nature of this optimization problem is episodic, that is, feedback as to the desirability of a given solution can only be provided at the end of an episode. The episode is defined as starting at the onset of a change in lateral position such as a commanded lane change. This follows the logic that when a new lateral command is required, a set of gains should be selected from the gain schedule and applied until the lateral error is eliminated. The goodness of a set of gains can therefore only be

assessed once the command is complete. Since the MDP is episodic in nature, the *Monte Carlo ES* reinforcement learning algorithm described in Figure 2.8 is used to learn the gain schedule.

The MDP that describes this optimization problem requires: states, actions, a reward function and a transition model. The transitions from actions to states are provided by the vehicle. Since a detailed vehicle model was developed, the gain schedule can be obtained by offline Monte Carlo reinforcement learning using simulated experiences provided by the vehicle model.

The choice in the selection of states lies in the nonlinear nature of the steering plant. At different speeds the lateral dynamics respond differently, therefore, the controller gains will differ from a given speed. The actions are the preview gain and the two gains used in the digital control system. The states and actions along with their associated digitization sets are shown in Table 4.3 and Table 4.4.

Table 4.3 States of the lateral MDP

State	*Description*	*Digitization Sets*
s_1	Vx: vehicle speed	{ 5, 10, 15, 20, 25, 30, 35, 40} m/s

Table 4.4 Actions of the lateral MDP

Action	*Description*	*Digitization Sets*
a_1	k_{preview}: Preview Length Gain	{0.1, 0.2, 0.3, … 9.9} $n\_s = 100$
a_2	k_{p}: Proportional Gain	{0.01, 0.02, 0.03, … 0.99} $n\_s = 100$
a_3	k_{d}: Derivative Gain	{0.01, 0.02, 0.03, … 0.99} $n\_s = 100$

The reward function reflects the specification of the control problem. The reward is a piecewise continuous function of the normalized predicted relative angular error variable $e\psi'_i$ and is expressed below.

$$R(e\psi'_i) = \begin{cases} 10 & |e\psi'_i| \le 0.01 \\ 1 - e\psi'_i & 0.01 > |e\psi'_i| \ge 1 \end{cases} \tag{4.7}$$

For a given episode, the solution which maximizes the reward, or minimizes the $e\psi'_i$ will be favored. These favored solutions will be explored to determine the optimal solution.

Chapter 5
Experimentation

5.1 Longitudinal Control

5.1.1 Reinforcement Learning

The *Reinforcement Learning* experiments obtain an optimal policy π^* for the longitudinal control of the vehicle. An experiment consists of 1000 episodes where the probability of exploration of the ε-soft greedy policy is set to $\varepsilon = 0.25$ for a particular combination of the three states. For each episode, the agent must follow another vehicle placed ahead of it which is traveling at a constant speed. Once the leading vehicle has reached the end of the test track, the episode is complete. The length of the test track is dependent on the speed of the lead vehicle using the following equation.

$$x_{\max} = (1 + 0.2\, v_{lead}) \times 1000 \qquad m \qquad (5.1)$$

During each step of an episode, a reward is generated (4.3); this reward is accumulated during the course of an episode to measure the controller's tracking performance using a particular set of actions. In these experiments, each step of every episode is accomplished in 100 *ms* providing a learning cycle of 10 *Hz*. Since it is possible to collide with the vehicle ahead during an episode, it is beneficial if the reward is averaged to reflect the vehicle's progress during the course of the episode. Therefore, the average reward for the course of the entire episode is provided by the following equation.

$$R_{avg} = \frac{\sum_{i=0}^{final} R_i}{x_{\max} - x_{final}} \qquad (5.2)$$

This averaging allows episodes resulting in collisions (i.e. small x_{final} values) to have a large denominator or small average reward, thereby eliminating them from being repeated.

Figure 5.1 shows the average reward as the agent progresses through the learning experiment for a particular state combination. The learning performance is similar for all combinations. One can observe the steady increase in the average reward which eventually reaches a plateau. Due to the exploration rate of $\varepsilon = 0.25$, the reward fluctuates as new combinations of actions are explored. Initially, the average reward is fairly low but rises quickly in the first 100 *episodes*. After 200 *episodes*, the agent converges upon the solution, gradually increasing the average reward.

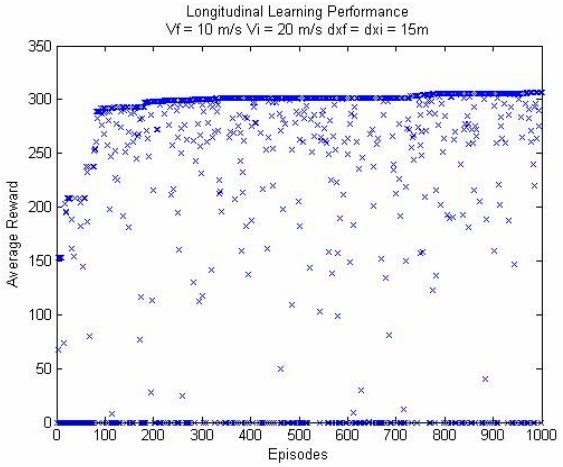

Figure 5.1 Performance of *Longitudinal Reinforcement Learning* experiments

The learned optimal policy is a collection of eight four-dimensional discrete hyperspaces, one for each gain of the longitudinal controller; that is four for the throttle controller and four for the brake controller.

$$\pi^* = \begin{cases} \overset{Throttle}{k_{pv}(v_f, v_0, \Delta x_f - \Delta x_0)} & \overset{Brake}{k_{pv}(v_f, v_0, \Delta x_f - \Delta x_0)} \\ k_{dv}(v_f, v_0, \Delta x_f - \Delta x_0) & k_{dv}(v_f, v_0, \Delta x_f - \Delta x_0) \\ k_{px}(v_f, v_0, \Delta x_f - \Delta x_0) & k_{px}(v_f, v_0, \Delta x_f - \Delta x_0) \\ k_{ix}(v_f, v_0, \Delta x_f - \Delta x_0) & k_{ix}(v_f, v_0, \Delta x_f - \Delta x_0) \end{cases} \tag{5.3}$$

The complete optimal policy is included in Appendix C: Optimal Policy for Longitudinal Control showing all 1344 operating points.

5.1.2 Controller Performance

This section demonstrates the tracking performance of the adaptive longitudinal controller using the optimal policy for gain scheduling at various operating points. The advantage of employing an adaptive control approach (gain scheduling) as opposed to using a fixed gain linear controller for the system is shown in Figure 4.14 is illustrated with the following plots.

Figure 5.2 shows the relative velocity and range tracking performance of the controller with fixed gains that are optimal for an initial V_i and final velocity V_f of 20 *m*/*s* for varying final velocities. The performance degradation is not noticeable at the lower final velocity of V_f = 10 *m*/*s*, however at V_f = 30 *m*/*s* we see a large disturbance in relative velocity as well as a very large change in range with a maximum range of almost 150 *m* as the controller attempts to achieve control. Figure 5.3 shows the tracking performance for varying initial velocity. With an initial velocity of V_i = 10 *m*/*s*, the range tracking performance is poor with a maximum range of almost 80 *m* during the maneuver. At an initial speed of V_i = 30 *m*/*s*, the braking maneuver to 20 *m*/*s* results in a maximum range of almost 15 *m*.

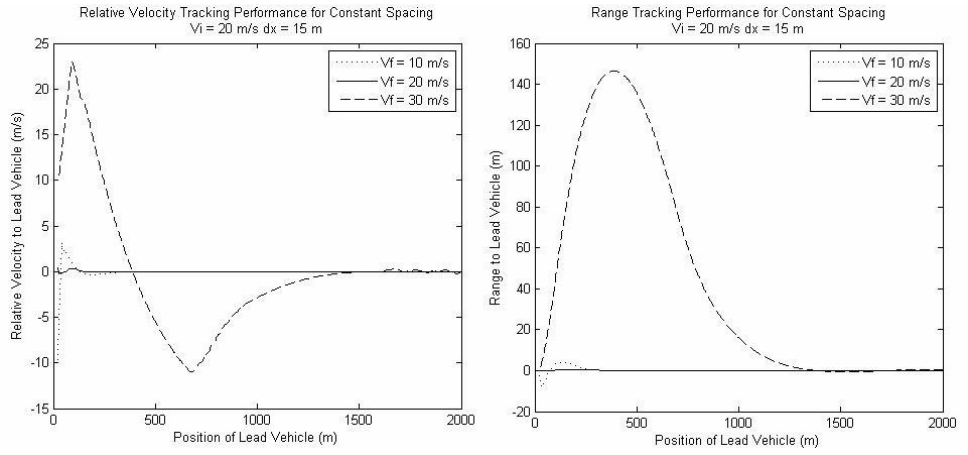

Figure 5.2 Fixed gain controller performance with varying final velocity

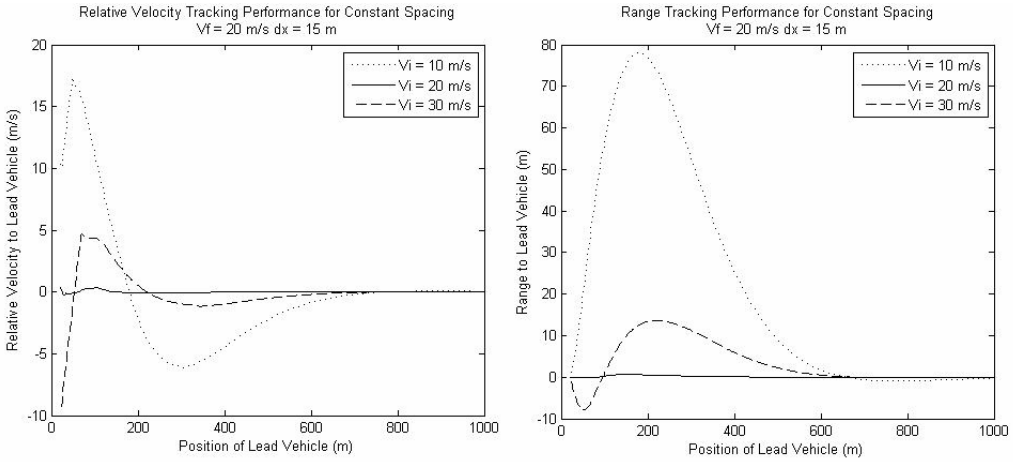

Figure 5.3 Fixed gain controller performance for various initial velocity

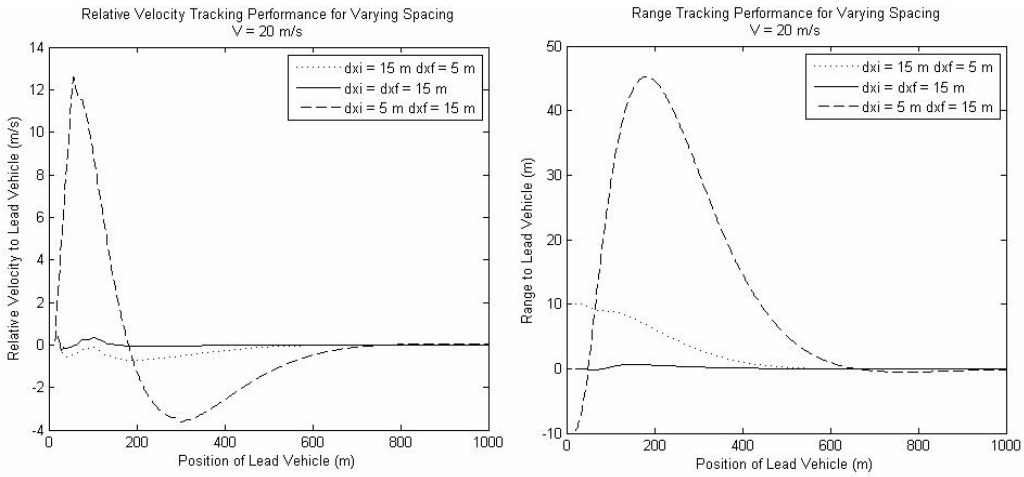

Figure 5.4 Fixed gain controller performance with varying inter-vehicle spacing

Figure 5.4 shows the relative velocity and range tracking performance of the controller with fixed gains which are optimal for an initial velocity V_i = 20 *m*/*s*, final velocity V_f of 20 *m*/*s*, initial inter-vehicle spacing Δx_f = 15 *m*, and final inter-vehicle spacing Δx_f = 15 *m* with varying inter-vehicle spacing. The performance is sluggish when the inter-vehicle spacing changes from 15 *m* to 5 *m*, this is evident in range tracking performance plot. With the inter-vehicle spacing change from 5 *m* to 15 *m*, braking causes the maximum range to reach 45 *m*.

Figures 5.2 to 5.4 show that a single set of gains is not sufficient to address the problem of longitudinal control for the automobile. The controller requires learned optimal gains at various operating conditions patched together to form an adaptive control system. The performance of this adaptive controller is demonstrated in the following experiments.

Three control situations (or sets of experiments) are shown which form the basis of platoon maneuvers which allow vehicles to enter or exit formations. The first of these experiments the results of which are shown in Figure 5.5 are *constant spacing* experiments. In the 10 *m*/*s* experiment, the vehicle begins at 20 *m*/*s* and must decrease its speed to 10 *m*/*s* while maintaining a separation distance to the vehicle ahead of 15 *m*. Note that the plot shows the relative range with respect to the final desired range of 15 *m*. As the vehicle undergoes its initial deceleration, the range becomes negative. A negative range means the vehicle has moved beyond its desired point; that is the range to the vehicle ahead is less than 15 *m*. The deceleration overshoots by 2 *m*/*s* and is a straight line indicating that braking is occurring. Throttle action is then used to bring the vehicle to the desired speed and range. To maintain a speed of 20 *m*/*s* and a spacing of 15 *m*, braking is not required, but coasting and slight throttle action is employed as seen in the 20 *m*/*s* plots. In the 30 *m*/*s* experiment, the vehicle begins at 20 *m*/*s* and must increase its speed to 30 *m*/*s* while maintaining a separation distance to the vehicle ahead of 15 *m*. As the vehicle attempts to accelerate, we see a slight delay due to an interruption in throttle activity which accompanies a gear change. The range increases to a maximum of 40 *m* as the vehicle attempts to catch up with the vehicle ahead. The speed increase overshoots the target by about 4 *m*/*s* and modulates its throttle action to reach the target speed and spacing. The vehicle tracking learned by the agent for each case is very smooth as it reaches steady-state.

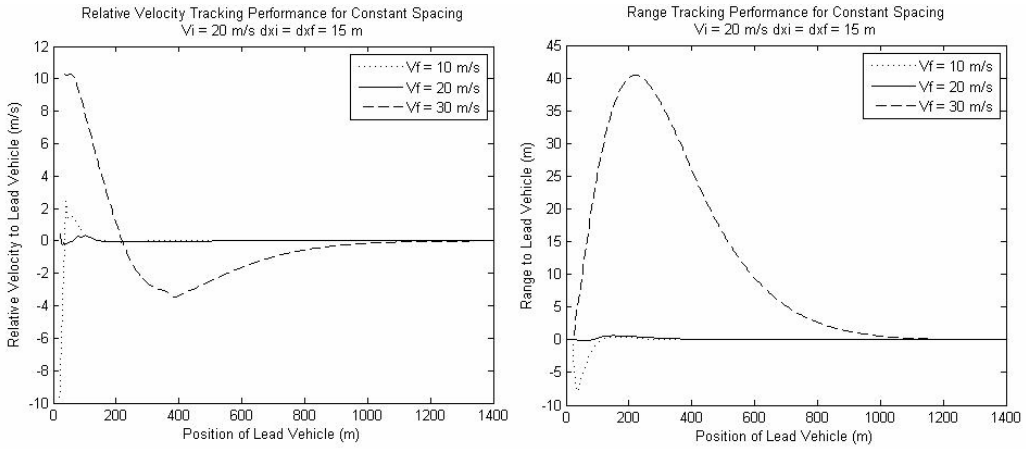

Figure 5.5 Adaptive Controller for constant spacing experiments

The second control situation or experiment set (shown in Figure 5.6) consists of the *constant velocity experiments (close)*. The vehicle must move from an inter-vehicle space of 15 *m* to 5 *m* while maintaining a speed of 10, 20, and 30 *m*/*s*. Note that the plot shows the relative range with respect to the final desired range of 5 *m*. Also, the variation in speed for each experiment is small with a maximum absolute relative speed of 1.5 *m*/*s* for the 10 *m*/*s* and 20 *m*/*s* experiments. For the 30 *m*/*s* experiment the maximum absolute relative speed is half of that at 0.75 *m*/*s*. This is due to the modulating of the throttle action. In each case, the throttle action is increased which results in a more negative relative speed and a smooth reduction in range as the vehicle moves to the desired spacing of 5 *m*. For the 10 *m*/*s* and 30 *m*/*s* case a slight oscillation in relative speed occurs as the vehicle attempts to maintain its speed as it closes the gap, which shows up in the plots as a smaller bump. Again, the tracking learned by the agent for each case is smooth. This maneuver is completed within 300, 500 and 1000 *m* for 10, 20 and 30 *m*/*s* respectively.

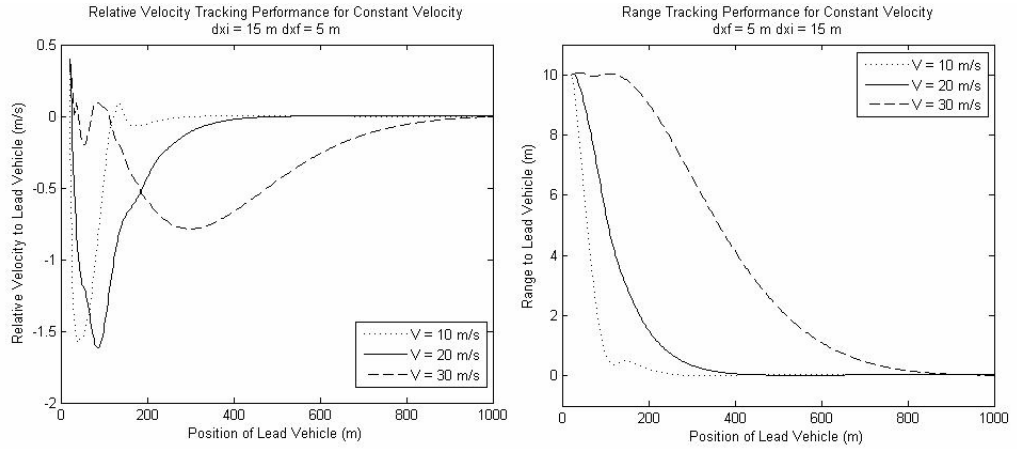

Figure 5.6 Adaptive controller for constant velocity experiments (close)

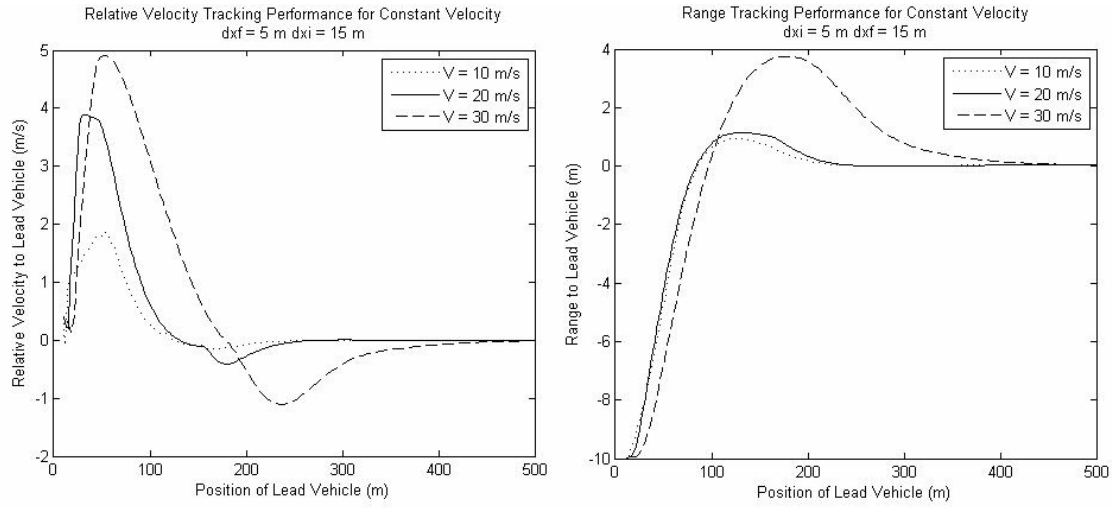

Figure 5.7 Adaptive controller for constant velocity experiments (open)

Figure 5.7 shows the third control situation or experiment set, the *constant velocity experiments (open)*. The vehicle must move from an inter-vehicle space of 5 *m* to 15 *m* while maintaining a speed of 10, 20, and 30 *m*/*s*. Note that the plot shows the relative range with respect to the final desired range of 15 *m*. In all three cases, the experiments begin with the vehicle applying some braking action which slows the vehicle down thereby increasing the range to the vehicle ahead. In the 10 *m*/*s* case, power-off or coasting occurs to reduce the amount of braking. The throttle action is then applied to get back to the target speed. In all three cases, the vehicle reduces its throttle slightly before it overshoots the target velocity. The vehicle also overshoots its target range. An interesting note is that the vehicle has *learned* a similar range response for both 10 and 20 *m*/*s* cases. Again, the tracking learned by the agent for each case is smooth. This maneuver is completed within 250 *m* for the 10 and 20 *m*/*s* case, and 1000 *m* for the 30 *m*/*s* case. These experiments represent the basis for platoon maneuvers which allow vehicles to enter into the new open space or to close the formation when a vehicle has left.

5.1.3 Multi-Vehicle Controller Performance

This section demonstrates the performance of the adaptive longitudinal controller in a multi-vehicle setting. It is possible to compare the performance of the adaptive lateral controller using the optimal policy for gain scheduling with previous results in the literature. Ioannou and Chien [1993] introduced an Autonomous Intelligent Cruise Control (AICC) system. The AICC controller is based on a linear state-space model and demonstrates superior performance compared to various human driver models. The vehicle following performance of a 20 car platoon is shown in Figures 5.8, 5.9 and 5.10 for an acceleration maneuver. The vehicles begin at rest separated by a distance of 4.5 *m*, the vehicles accelerate to 30 *miles*/*h* or 13.41 *m*/*s* in 10 *s*. Figure 5.8 shows the linear follow-the-leader human driver model based on linear proportional control of the relative velocity. Notice the under-damped characteristic of the response which amplifies as one proceeds farther down the platoon. Figure 5.9 shows a linear optimal control human driver model based on a quadratic cost function on the relative velocity. Notice the over-damped response. As one proceeds farther down the platoon, the response slows but not very much. Figure 5.10 shows a look-ahead driver model, the system uses switching logic based on observations of the 3 preceding vehicles. The response is over-damped and is slower as one proceeds down the platoon.

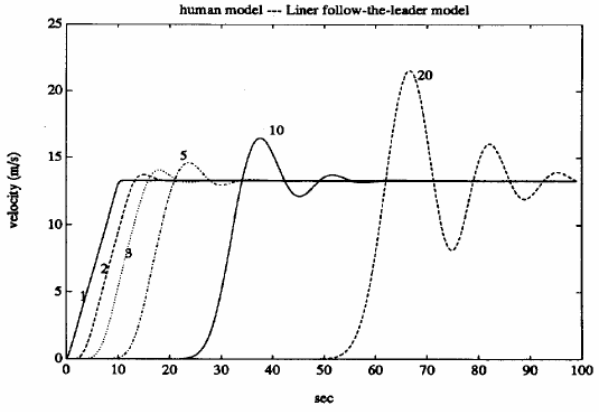

Figure 5.8 Human model – linear follow the leader [Ioannou & Chien 1994]

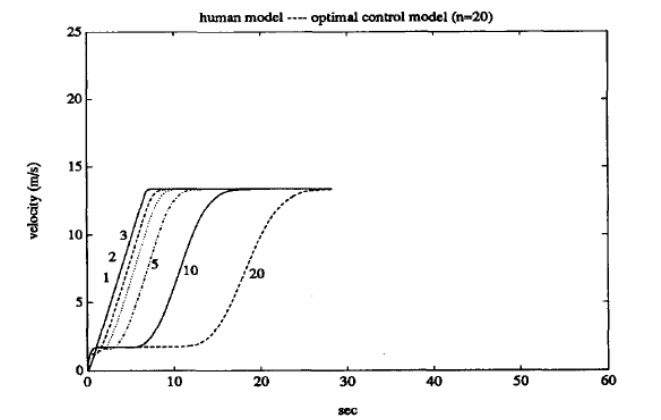

Figure 5.9 Human model – mimicking optimal control [Ioannou & Chien 1994]

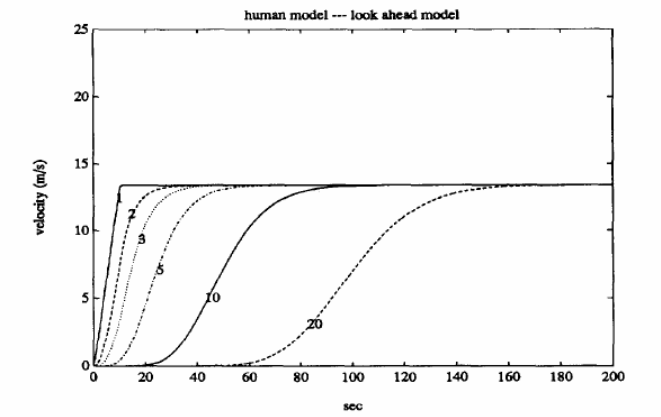

Figure 5.10 Human model – look-ahead [Ioannou & Chien 1994]

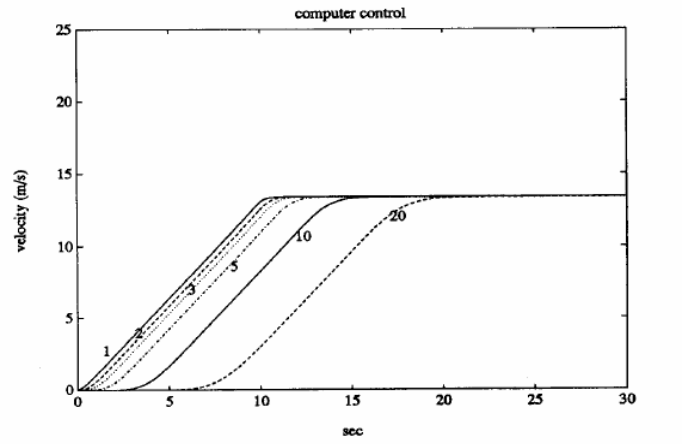

Figure 5.11 AICC linear controller by Ioannou & Chien [1994]

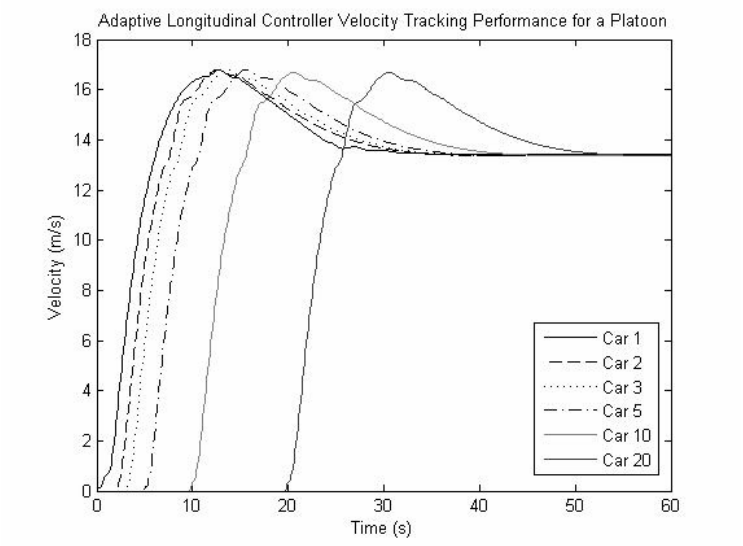

Figure 5.12 Adaptive longitudinal controller velocity tracking performance

Figure 5.11 shows the performance of the AICC controller, its response is similar to that of the linear optimal control human model. The response is critically damped, displays no overshoot and its response does not slow down as one proceeds down the formation. The response of vehicle 20 reaches steady state in 20 *s* compared to 30 *s* of the optimal control human model. Figure 5.12 shows the velocity tracking performance of the *adaptive longitudinal controller*. The response is under-damped and has an overshoot of 3 *m*/*s*. The responses are very similar as we proceed down the platoon offset by approximately 1 *s* each.

Ioannou and Chien [1993] provide velocity and inter-vehicle spacing tracking performance results for a 5 car platoon undergoing acceleration and deceleration (see Figure 5.14). In the experiment, the vehicles start at rest with a 4.5 *m* inter-vehicle spacing. They proceed to accelerate to 60 *miles*/*h* or 26.82 *m*/*s* in 15 *s*, the speed remains constant for 5 *s*, the formation then decelerates to a full stop in 15 *s*. Note that the emergency stop begins with an inter-vehicle spacing of about 15 *m*. Figure 5.15 shows the adaptive longitudinal controller performance under similar conditions. The response for the acceleration portion is much slower requiring about 50 *s* to reach steady-state; however, the inter-vehicle spacing is maintained at a 4.5 *m* which does not occur in the case of the AICC controller in Figure 5.14. The braking response for the *adaptive longitudinal controller* is quicker, as it completes the emergency stop in 5 *s* with a starting inter-vehicle spacing of 4.5 *m*. However the plot showing the inter-vehicle spacing indicates that *Car 2* and *Car 3* do not have sufficient space to complete the emergency stop successfully, as indicated by the negative inter-vehicle spacing of -1.8 *m* and -0.8 *m* respectively.

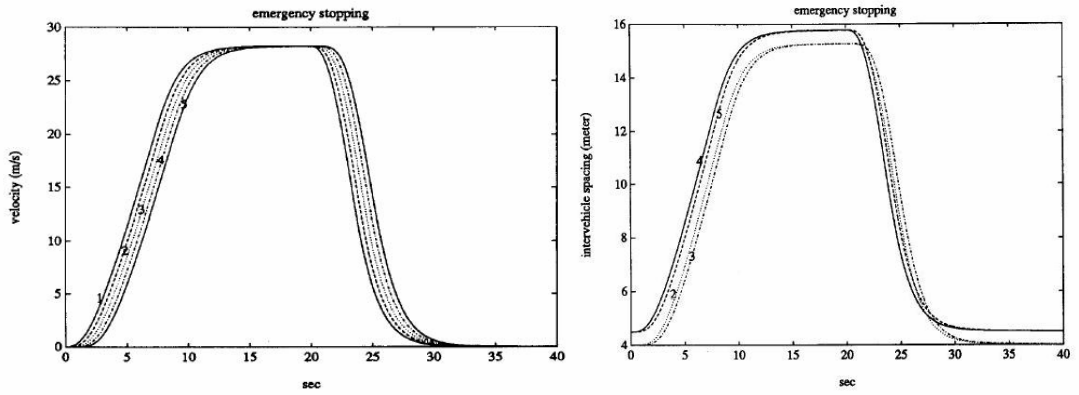

Figure 5.14 AICC optimal linear controller for 5-car platoon by Ioannou & Chien [1994]

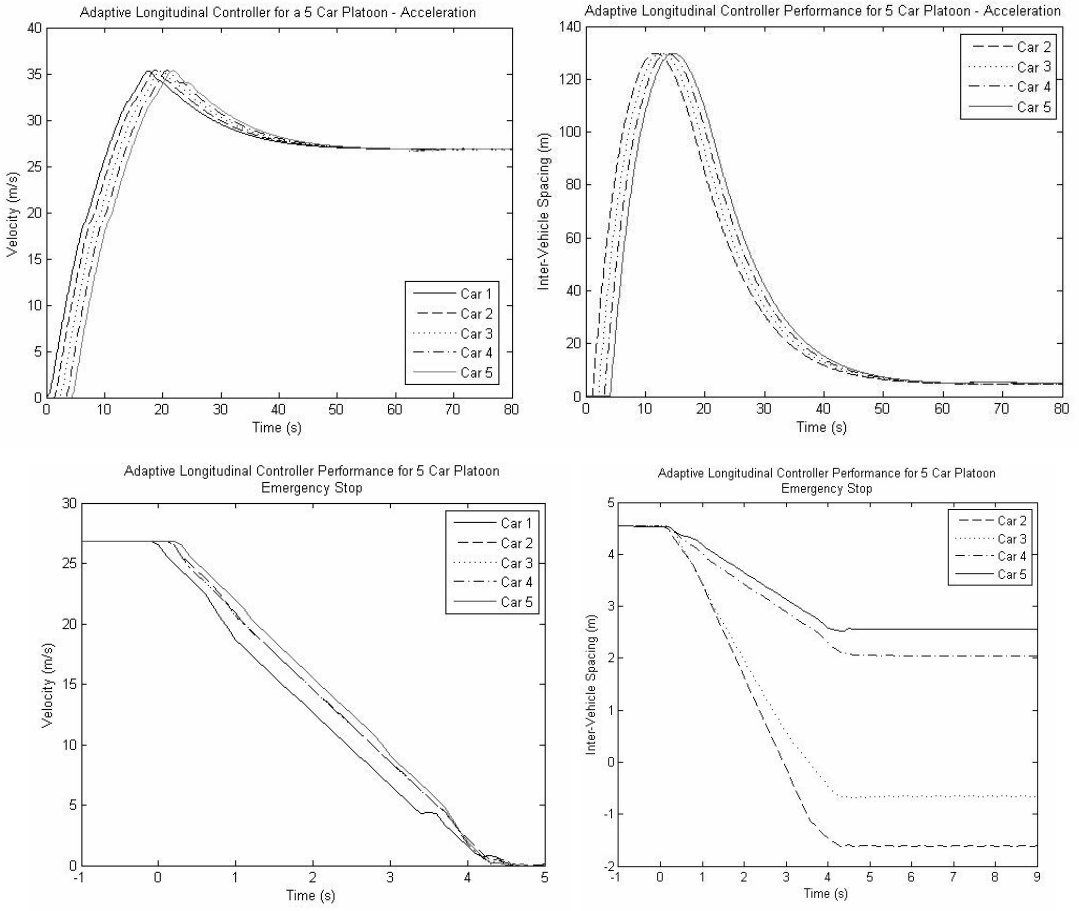

Figure 5.15 Adaptive lateral controller for 5-car platoon for acceleration and braking

Further experiments are shown to demonstrate the operation of the control system within a five car formation or platoon. Five control situations have been chosen to demonstrate the range tracking performance of the optimal policy for each of the four following vehicles. Figure 5.16

shows the responses of a five car formation moving at a constant speed of 20 *m*/*s* undergoing a range disturbance. The first car, *Car 0* is assumed to be the leader; the plots depict the velocity and range response with respect to time for the 4 following vehicles. In the first experiment, all vehicles are under longitudinal control with the inter-vehicle spacing set to 15 *m* between each car at a speed of 20 *m*/*s*. At time $t = 0$ *s*, *Car 1* is instructed to close the space in front to 5 *m*. The *Car 1* velocity response shows an initial reduction of speed as the automatic transmission downshifts in order to obtain the power required to accelerate. The effect is an initial gain of 2 *m* in range by *Car 1*; a sharp acceleration follows and gradually reduces to track the new range of 5 *m* without overshooting. *Car 2*, *Car 3* and *Car 4* must maintain their inter-vehicle spacing at 15 *m* and show a maximum deviation from their target range of 4.5, 4 and 4 *m* respectively, showing slight oscillation as they reach steady state. The velocities of *Car 2*, *Car 3* and *Car 4* have a maximum deviation from the target speed 20 *m*/*s* by 1.3, 1.3 and 1.5 *m*/*s* respectively, showing slight oscillations as they reach steady state. As we move farther down the formation, the settling time is longer. Overall, the response of the formation appears to be stable for this disturbance.

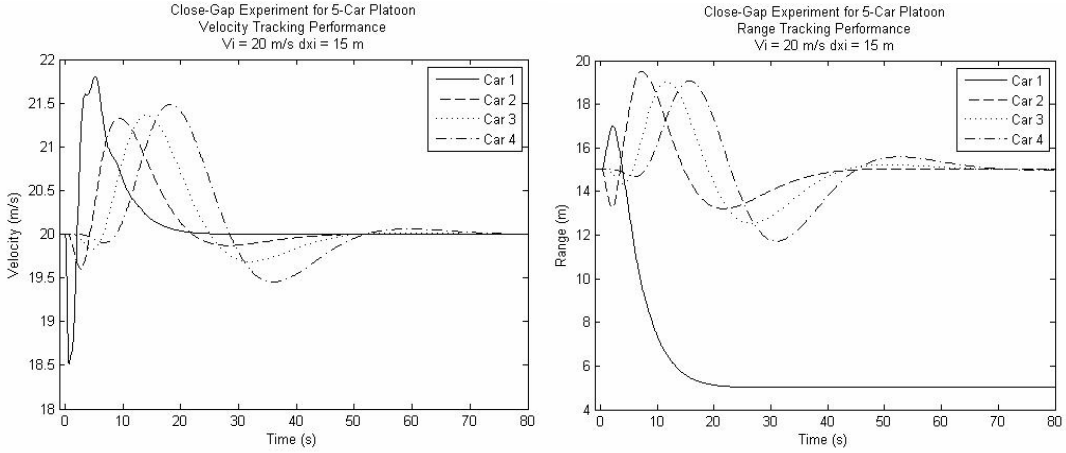

Figure 5.16 Multi-vehicle range control experiment: close

Figure 5.17 shows the responses of a five car formation moving at a constant speed of 20 *m*/*s* undergoing a different range disturbance. In this experiment, all vehicles are under longitudinal control with the inter-vehicle spacing set to 5 *m* between each car at a speed of 20 *m*/*s*. At time $t = 0$ *s*, *Car 1* is instructed to open the space in front to 15 *m*. The *Car 1* velocity response shows an immediate braking action which reduces the speed by over 2 *m*/*s* in 10 *s* which effectively opens the space to a range of 17.5 *m* overshooting the target range. The overshoot is compensated for by a sharp acceleration to 20 *m*/*s* in 5 *s* with a slight overshoot which smoothly brings the range to a steady-state value of 15 *m*. *Car 2*, *Car 3* and *Car 4* must maintain their inter-vehicle spacing at 5 *m* while *Car 1* is changing its spacing. The range responses for *Car 2*, *Car 3* and *Car 4* shows the range being reduced to almost zero for this disturbance indicating that a following distance of 5 *m* (approximately one car length) is at the limit of the control system for such a disturbance. The responses for *Car 2*, *Car 3* and Car *4* are similar in shape. They show slight oscillations as they reach steady state. As we move farther down the formation the maximum range grows as well as the maximum speed which is needed to compensate for this increase in range. However, by time $t = 70$ *s*

all oscillations have settled and all cars have reached steady state. Overall, the response of the formation appears to be stable for this disturbance.

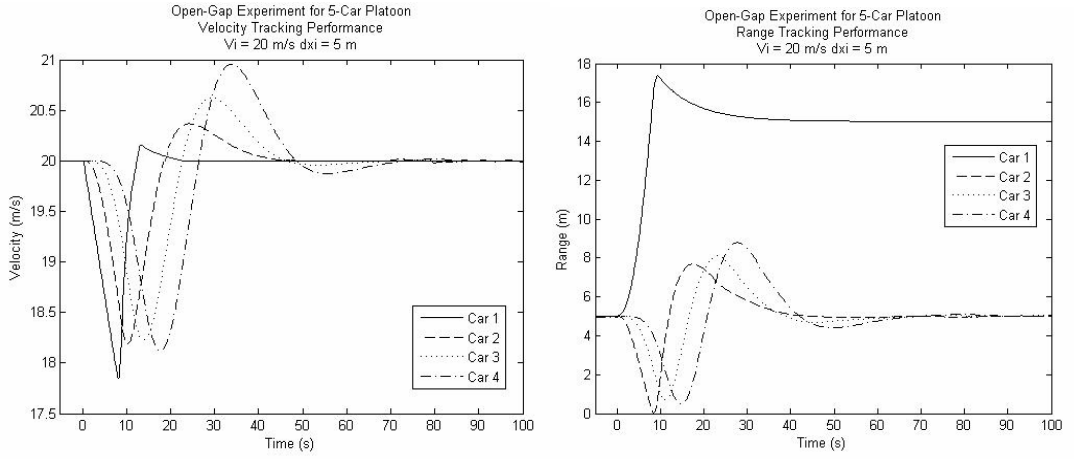

Figure 5.17 Multi-vehicle range control experiment: open

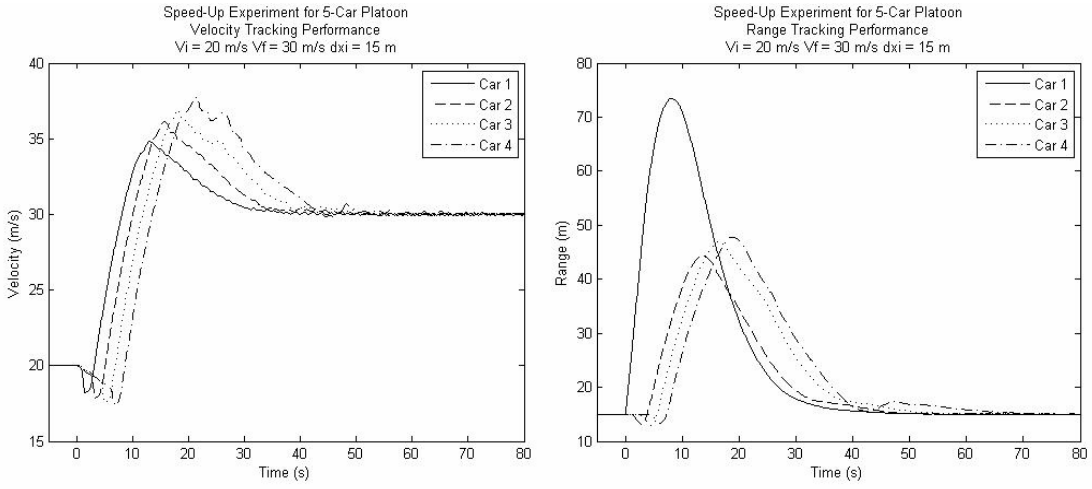

Figure 5.18 Multi-vehicle velocity control experiment: acceleration

Figure 5.18 shows the responses of a five car formation with a constant spacing of 15 *m* undergoing a speed disturbance. In this experiment, all vehicles are under longitudinal control with the inter-vehicle spacing set to 15 *m* between each car at an initial speed of 20 *m*/*s*. At time $t = 0$ *s*, all cars are instructed to speed up to 30 *m*/*s* while maintaining the 15 *m* spacing. The velocity responses of all the cars in the formation show a similar shape but are shifted by about 2 *s*. The response begins with a decrease in speed as the vehicle's automatic transmission shifts gears to meet the required torque needed for acceleration. A smooth acceleration for about 10 *s* results in overshooting 30 *m*/*s*. As we move farther down the formation, the overshoot gets larger. However, by 50 *s*, all cars reach their approximate steady state. In this experiment, *Car 0*, the leader is assumed to have instantaneously increased its speed to 30 *m*/*s*, therefore the maximum range for *Car 1*, the car

following it, is significantly larger. The range responses of *Car 2*, *Car 3*, and *Car 4* have a similar shape. They are also shifted by approximately 2 *s* with an increasing maximum range as we move farther down the formation; however by 70 *s* the range responses have reached steady state. Overall, the response of the formation appears to be stable for this disturbance.

Figure 5.19 shows the responses of a five car formation with a constant spacing of 15 *m* undergoing a speed disturbance. In this experiment, all vehicles are under longitudinal control with the inter-vehicle spacing set to 15 *m* between each car at an initial speed of 20 *m*/*s*. At time $t = 0$ s, all cars are instructed to slow down to 10 *m*/*s* while maintaining the 15 *m* spacing. In this experiment, *Car 0*, the leader is assumed to have instantaneously decreased its speed to 10 *m*/*s*. The responses of all the cars in the formation show a similar shape but the amount of braking effort affects the size of the response. All vehicles begin by applying braking. In the velocity responses we can see that the braking force is the same for all vehicles as all 4 responses are coincident. The only difference is how long the brake is being applied for. All 4 cars overshoot the target of 10 *m*/*s*, as we move farther down the formation, the amount of overshoot increases with *Car 3* and *Car 4* almost stopping. The cars then accelerate to reach the target speed of 10 *m*/*s*. In the range response, we see that the shape is also the same for all cars. *Car 1* gets the closest to the vehicle ahead and reaches 15 *m* in the shortest amount of time. As we move farther down the formation, the maximum range increases as well as the settling time, however, all cars reach steady state by 40 *s*. Overall, the response of the formation appears to be stable for this disturbance.

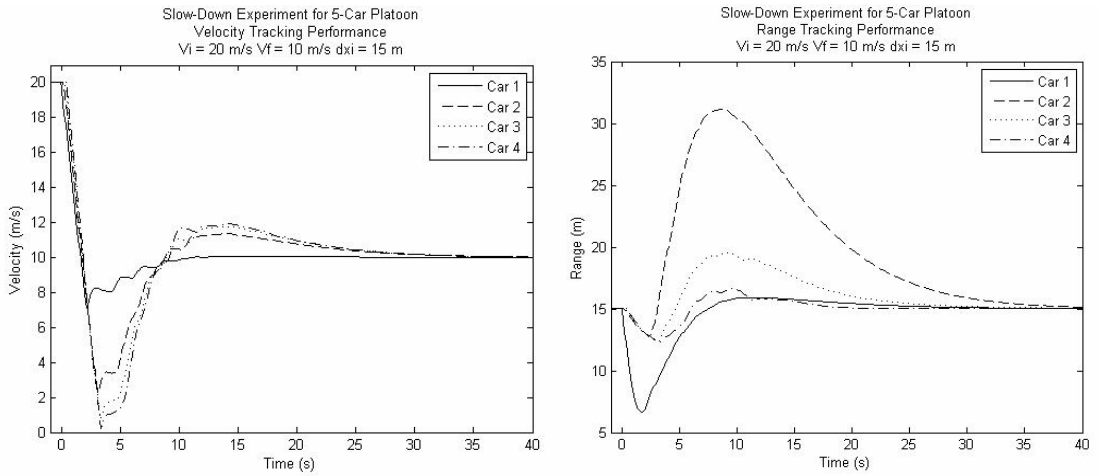

Figure 5.19 Multi-vehicle velocity control experiment: deceleration

Figure 5.20 shows the responses of a five car formation with a constant spacing of 15 *m* undergoing an emergency stop. In this experiment, all vehicles are under longitudinal control at an initial speed of 20 *m*/*s* with the inter-vehicle spacing set to 15 *m* between each car except between *Car 0* and *Car 1* which is set to 28 *m*. At time $t = 0$ *s*, all cars are instructed to slow down to 0 *m*/*s*. In this experiment, *Car 0*, the leader is assumed to have instantaneously decreased its speed to 0 *m*/*s*, thereby simulating a collision. The velocity responses of the vehicles are the same except that they are shifted by fractions of seconds. We observe that all cars have the same braking capability; however, *Car 1*'s response occurs slightly before *Car 2* and so forth. It takes approximately 2.5 *s* for

all cars to stop from 20 *m*/*s*. *Car 1* requires 28 *m* to come to a full stop in 2.5 *s* with a parabolic range response. The range response for *Car 2*, *Car 3*, and *Car 4* are linear as the car ahead is still moving, therefore the final spacing is slightly less than 15 *m*.

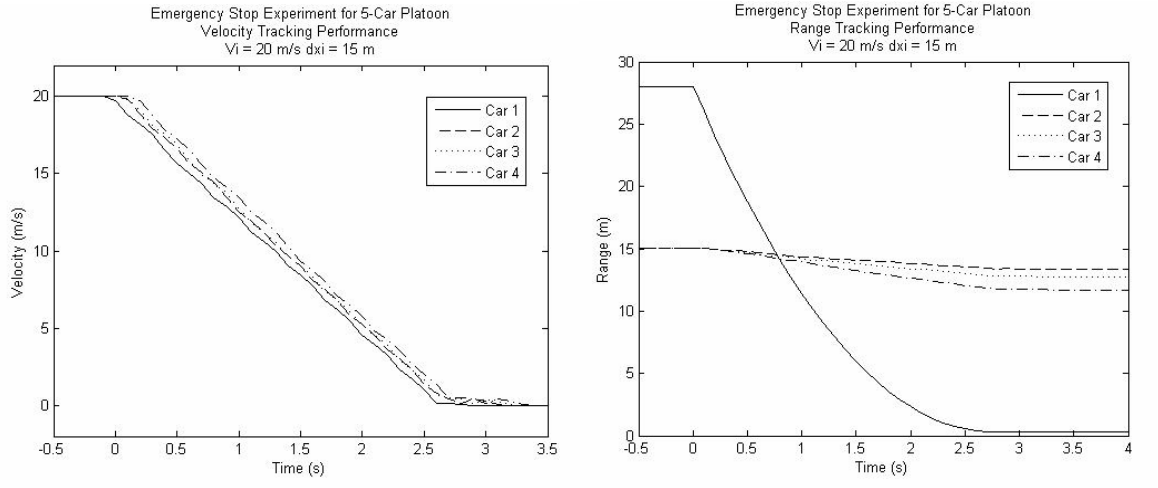

Figure 5.20 Multi-vehicle velocity control experiment (emergency stop)

5.2 Lateral Control

5.2.1 Reinforcement Learning

The RL experiments obtain an optimal policy π^* for the lateral control of the vehicle. An experiment consists of 10000 episodes where the exploration probability of the ε-soft greedy policy is set to $\varepsilon = 0.25$ for a particular combination of the three states. For each episode, the agent must follow another vehicle placed ahead of it which is traveling at a constant speed. Once the leading vehicle has reached the end of the test track, the episode is complete. The distance of the test track is dependent on the speed of the lead vehicle using the following equation.

$$x_{\max} = (1 + 0.2 v_{lead}) \times 1000 \qquad m \qquad (5.4)$$

During each step of an episode, a reward is generated (4.7); this reward is accumulated during the course of an episode to measure the controller's tracking performance using a particular set of actions. In these experiments, each step of every episode is accomplished in 100 *ms* providing a learning cycle of 10 *Hz*. Since it is possible to collide with the vehicle ahead during an episode, it would be beneficial if the reward were averaged to reflect the vehicle's progress during the course of the episode. Therefore, the average reward for the course of the entire episode is provided by the following equation.

$$R_{avg} = \frac{\sum_{i=0}^{final} R_i}{x_{\max} - x_{final}} \qquad (5.5)$$

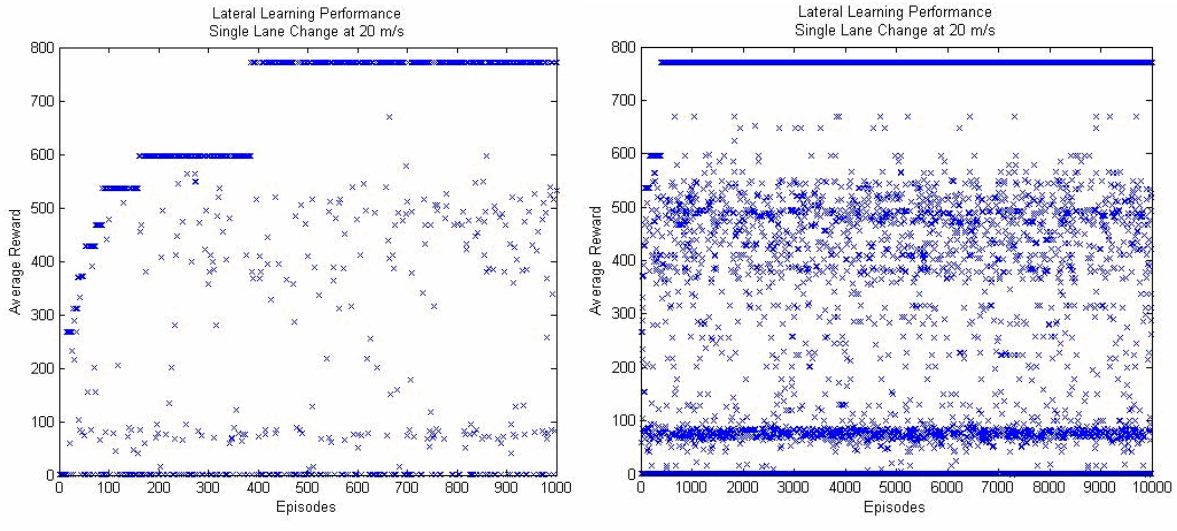

Figure 5.21 Performance of *Lateral Reinforcement Learning* experiments

Figure 5.21 shows the average reward as the agent progresses through the learning experiment for a particular state combination. The learning performance is similar for all combinations. One can observe the steady increase in the average reward which eventually reaches a plateau.

The learned optimal policy is a collection of three functions of vehicle speed which represents each of the gains used in the adaptive controller.

$$\pi^* = \begin{cases} k_{preview}(v_i) \\ k_p(v_i) \\ k_d(v_i) \end{cases} \tag{10}$$

Figure 5.22 shows a set of 3 plots which represents the optimal policy. In the plot for the preview gain (a_1) there is an upward trend with increasing speed with the exception of the value at 10 *m/s*. For the proportional gain (a_2) we see a downward trend with increasing speed. For the derivative gain (a_3) an upward trend is seen but a plateau of 0.070 is reached at 15 *m/s*. The value at 10 *m/s* is very low and corresponds to the high preview gain value at the same speed, indicating that these gains are compensating for each other. For a complete tabulation of the optimal policy for lateral control refer to Appendix E: Optimal Policy for Lateral Control.

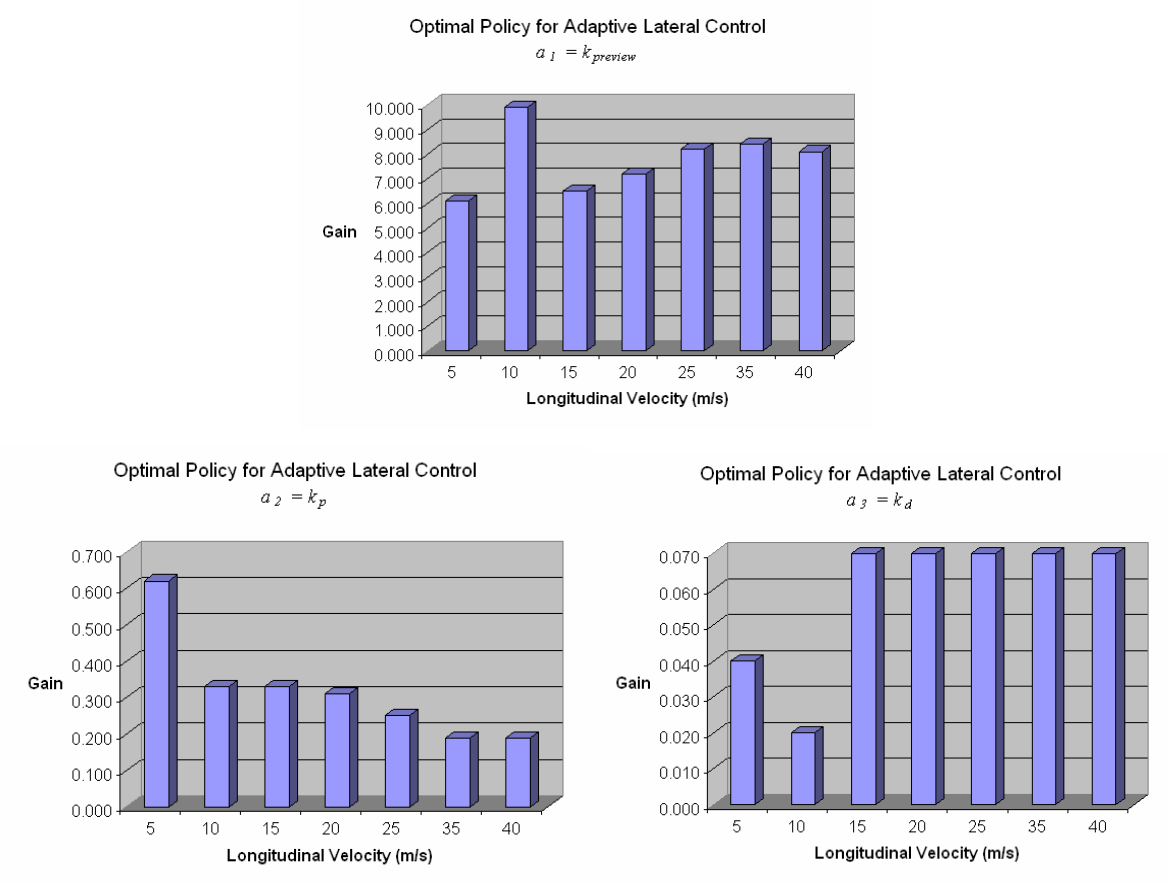

Figure 5.22 Optimal Policy for lateral control.

5.2.2 Controller Performance

This section demonstrates the tracking performance of the adaptive lateral controller using the optimal policy for gain scheduling at various operating points. We begin by illustrating the advantage of employing an adaptive control approach (gain scheduling) as opposed to using the preview control system shown in Figure 4.18 with a fixed gain, the following plots are shown. In these experiments, the vehicle is driven using the longitudinal controller at a constant initial speed. At time $t = 50\ s$, a step input is fed to the lateral control system and the vehicle begins lateral tracking to reach its new lateral position. Figure 5.23 shows the path of the vehicle during a single lane change with a controller with gains fixed which are optimal for a velocity of 20 m/s but applied to various velocities. At the lower speed of $V = 10\ m/s$ a noticeable oscillation can be seen once steady state has been reached, the speed of the response is similar to $V = 20\ m/s$. At the higher speed of $V = 30\ m/s$, the response is slower but the oscillations at steady state are not present.

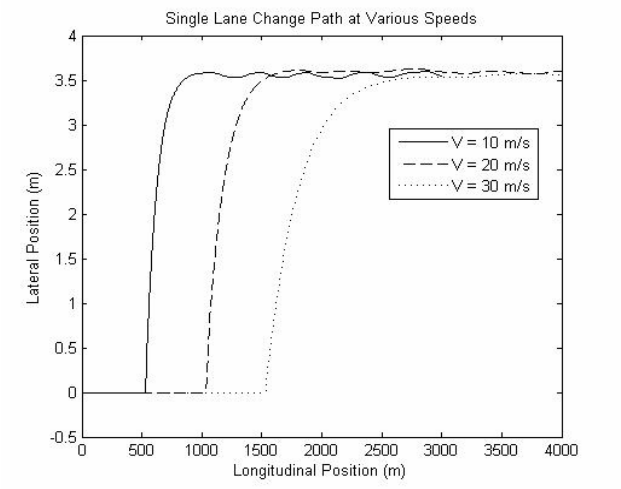

Figure 5.23 Fixed gain controller single lane change performance

Figure 5.24 shows the vehicle paths for executing a single lane change ($y_f = 3.6\ m$) at various speeds (10, 20, and 30 *m*/*s*). Due to the different vehicle speeds, the position where the lane change occurs varies. The vehicle path using the optimal policy gains for each velocity is fairly smooth. At 10 *m*/*s*, the path shows slight under-damping in the lateral axis with a very minimal overshoot. At 20 and 30 *m*/*s*, the path is critically damped with no overshoot. Despite increasing speed the paths remain very similar and the lane change is accomplished within 500 *m* indicating that lateral acceleration is increasing with velocity.

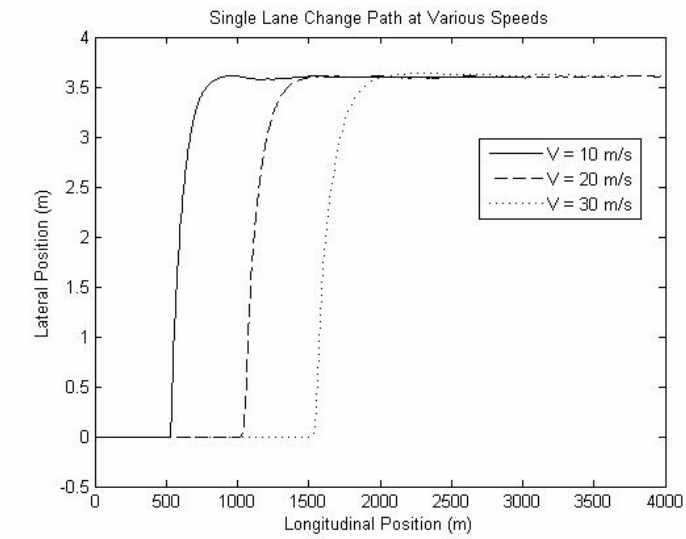

Figure 5.24 Single lane change performance with RL-based adaptive control

By comparing Figure 5.23 with 5.24 it can be observed that the fixed gain controller induces a larger overshoot and longer settling time. Therefore, the performance of the controller with learned gains for each velocity is superior to the fixed gain controller for the problem of lateral control of an

automobile. The variable gain controller with gains learned at various operating conditions when patched together form an adaptive control system.

Next, let us compare the performance of the adaptive lateral controller using the optimal policy for gain scheduling with results from previous studies in the literature. Mammar [1997] provides a plot demonstrating the lateral response of a gain scheduled H∞, controller for a 3 *m* lateral displacement. The vehicle traveling at 20 *m*/*s* completes the maneuver in under 10 *s*, this can be considered an extremely fast lateral response. However, the controller is both designed and simulated using a simplified linear single track model of a bus. Mass and cornering stiffness is modeled, however, there are no component dynamics included in the model (i.e. engine, tire, suspension, etc).

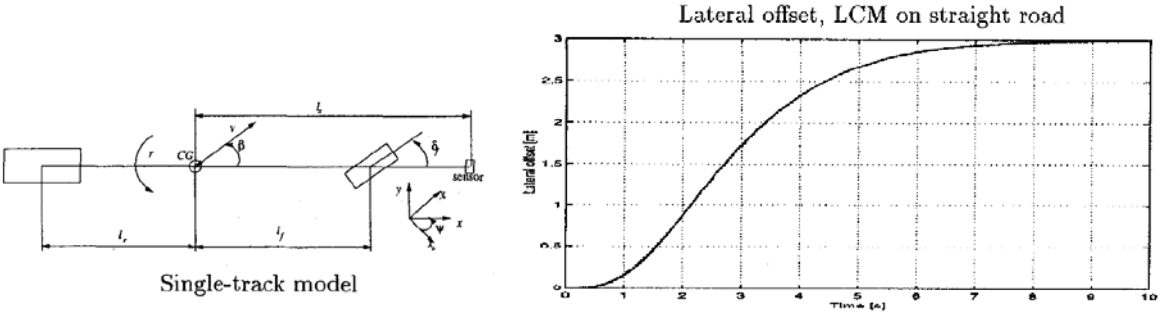

Figure 5.25 H∞, controller by Mammar [1997] for 20 m/s

Meier et al [2004] provides a plot demonstrating the tracking control for a vision based *look-ahead* system for a 2 *m* lateral displacement. The tracking control system uses vision to *track* the lateral displacement of the vehicle as it moves according to a preprocessed path. The vehicle traveling at 30 *km*/*h* or 8.333 *m*/*s* completes the maneuver in 20 *s*, and is slow compared to Figure 5.25 [Mammar 1997]. However, this system is designed using an actual automobile and demonstrated in hardware on a test vehicle provided by Audi AG.

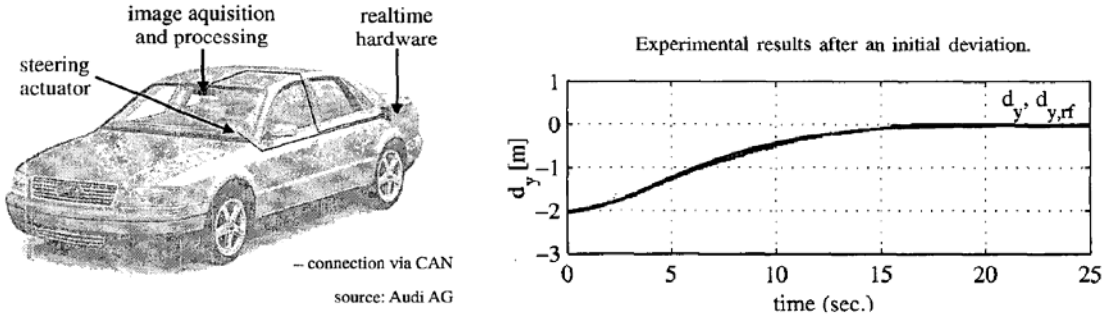

Figure 5.26 Tracking control by Meier et al [2004] at 8.33 m/s (30 km/h)

To compare our results to these two former studies, the adaptive lateral controller along with our high fidelity vehicle dynamics model is subjected to the same test conditions as the Mammar [1997] study and the Meier study [Meier et al 2004]. Figure 5.27 shows the plots for the lateral

response of the adaptive lateral controller and vehicle model. The plot shows that the maneuver requires 30 *s* to complete, hence it is much slower than Mammar's H∞ controller and is comparable in response time to Meier's vision based tracking control system.

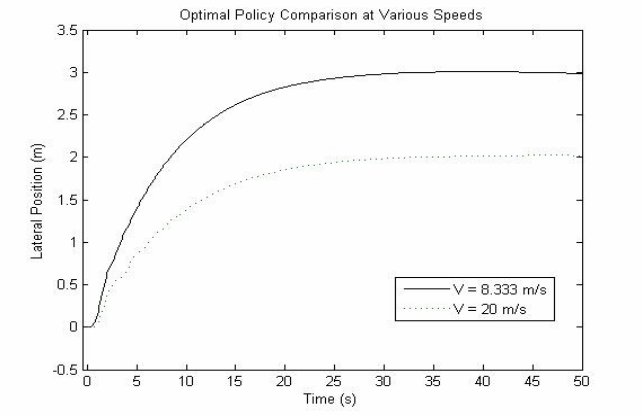

Figure 5.27 Reinforcement learning optimal policy performance

Finally, the following experiments demonstrate the lateral tracking performance of the optimal policy for different speeds and for varying lateral positions. In Figures 5.28, 5.29 and 5.30 the vehicle paths are shown with respect to changing lateral position under a constant speed. The vehicle paths shown correspond to 1 *m*, 1.8 *m* (½ lane), 3.6 *m* (single lane) and 7.2 *m* (double lane). At 10 *m*/*s* (Figure 5.28) all paths reach the steady-state lateral position within 300 *m*. Figure 5.29 and 5.30 show the paths for 20 *m*/*s* and 30 *m*/*s* respectively, despite the different vehicle speeds the vehicle paths remain similar for a given lateral displacement. Therefore with higher speeds, the maneuvers are being accomplished under higher lateral accelerations. All vehicle paths are shown to be critically damped and smooth.

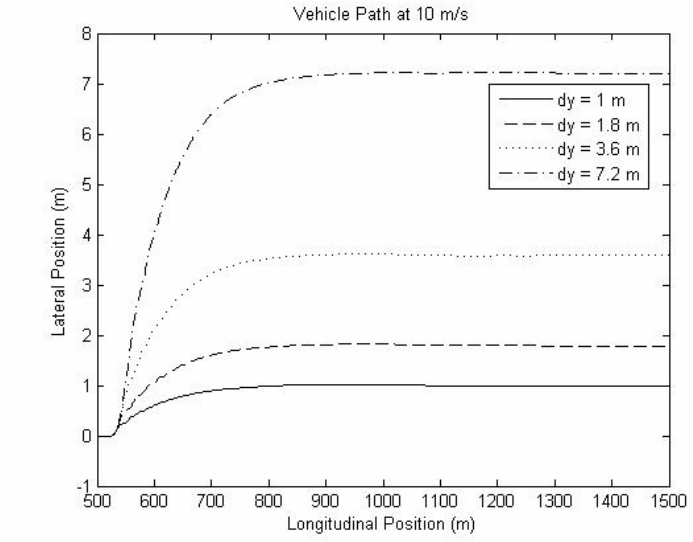

Figure 5.28 Lateral performance at 10 *m*/*s*

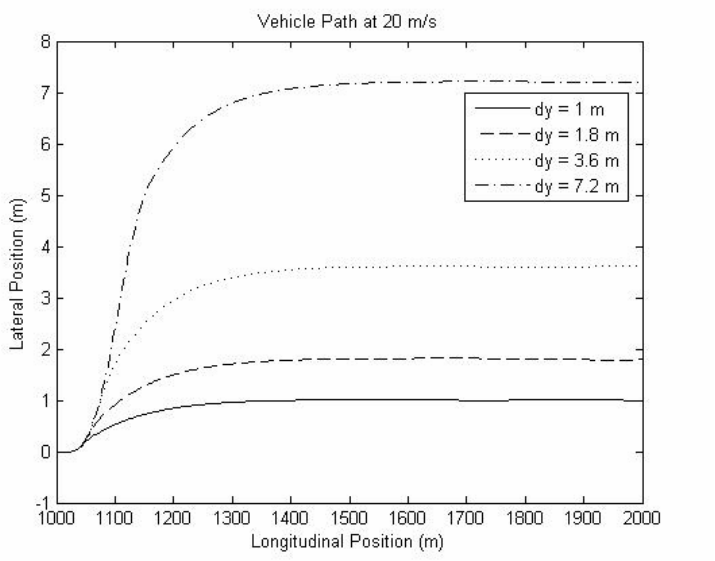

Figure 5.29 Lateral performance at 20 *m/s*

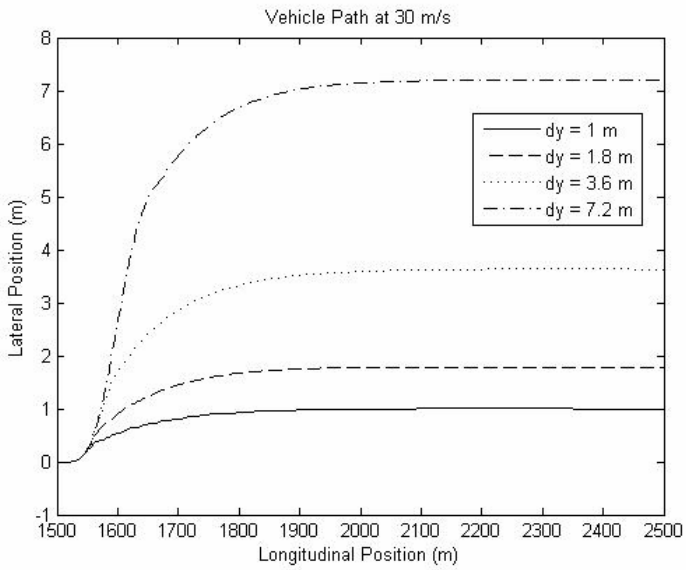

Figure 5.30 Lateral performance at 30 *m/s*

These experiments are important because they demonstrate that the lateral adaptive control system is capable of relatively quick and accurate lateral tracking. This tracking capability forms the basis for platoon maneuvers which allow vehicles to enter or exit its current platoon for decentralized dynamic collaborative driving control.

5.2.3 Multi-Vehicle Controller Performance

These experiments demonstrate the performance of the lateral control system within a five car formation or platoon. Each car is equipped with the longitudinal control system described in this thesis which controls the throttle and brake so as to maintain a constant speed and a constant inter-vehicle spacing. In these experiments, the initial speed is set to 20 *m*/*s* (72 *km*/*h*) and inter-vehicle spacing is set to 20 *m*. At $t = 0$ *s* or at $x = 2.1$ *km*, the lead vehicle is placed at a specific lateral distance, each subsequent vehicle responds by following the vehicle ahead. The vehicle path for each of the five vehicles is recorded for the next 2 *km*. Four experiments are shown to illustrate the lateral controller performance, they are conducted at $y = 1$ *m*, 1.8 *m* (½ lane), 3.6 *m* (single lane) and 7.2 *m* (double lane). Figure 5.31 shows the 5 car formation for a lateral change in position of $y = 1$ *m*. The response is slightly under-damped and the overshoot is propagated and increases with each subsequent vehicle. The resulting oscillations in the vehicle path decrease as it progresses through the experiment. The response remains under-damped at a lateral position change of $y = 1.8$ *m* ((½ lane) as seen in Figure 5.32, the overshoot is smaller than at $y = 1$ *m*. This trend continues as the lateral position change increases to $y = 3.6$ *m* (single lane) in Figure 5.33. At $y = 7.2$ *m* (double lane), the responses is considered critically damped (Figure 5.34). These experiments demonstrate that the lateral controller can be deployed effectively in a multi-vehicle platoon with minimal overshoot and oscillation for varying degrees of lateral tracking.

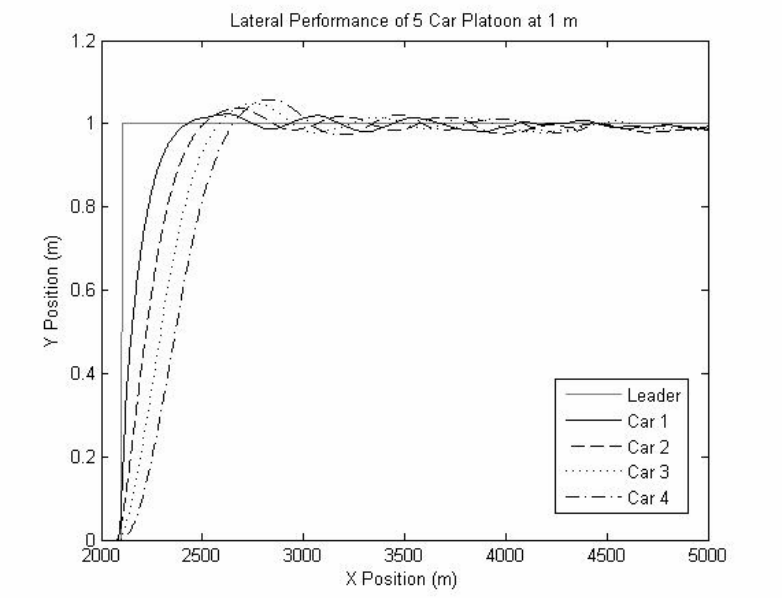

Figure 5.31 Lateral performance for 5 car platoon at 1 *m*

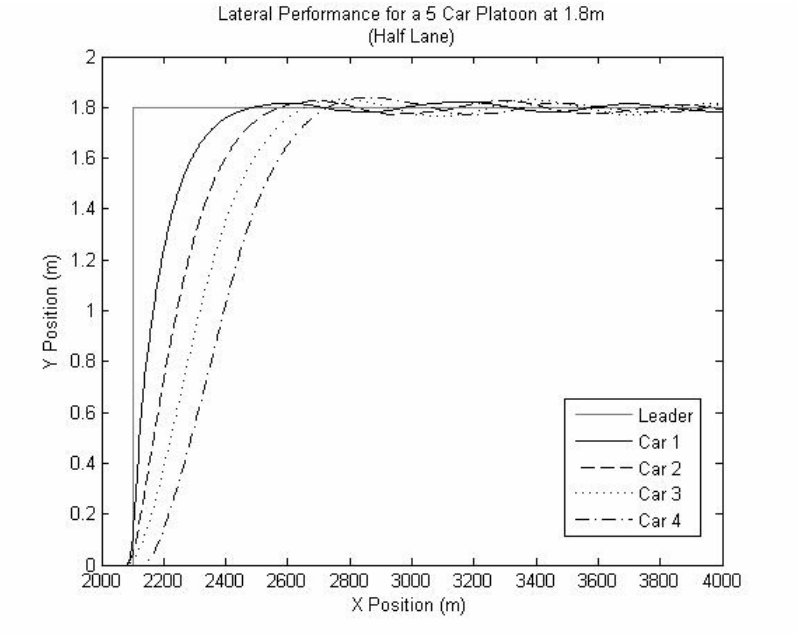

Figure 5.32 Lateral performance for 5 car platoon at 1.8 *m*

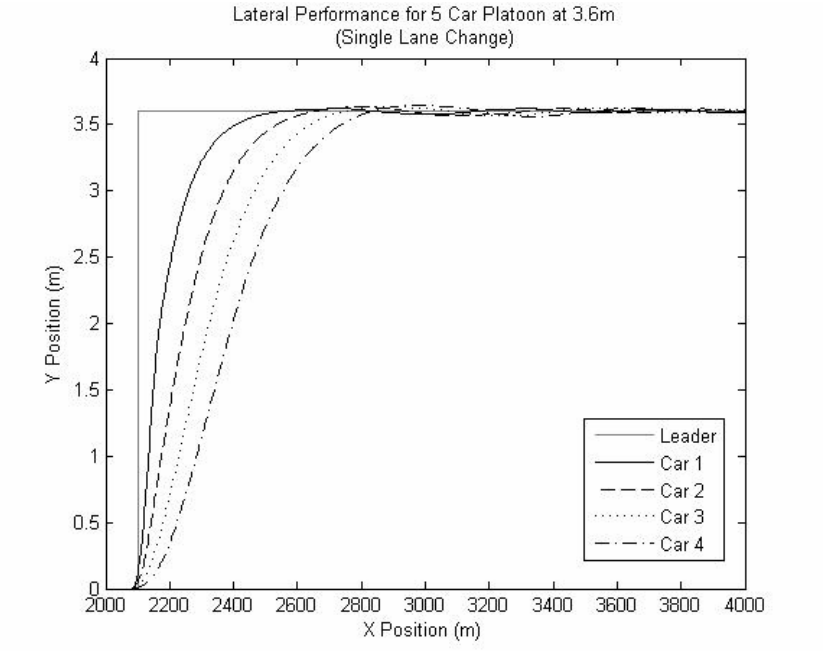

Figure 5.33 Lateral performance for 5 car platoon at 3.6 *m*

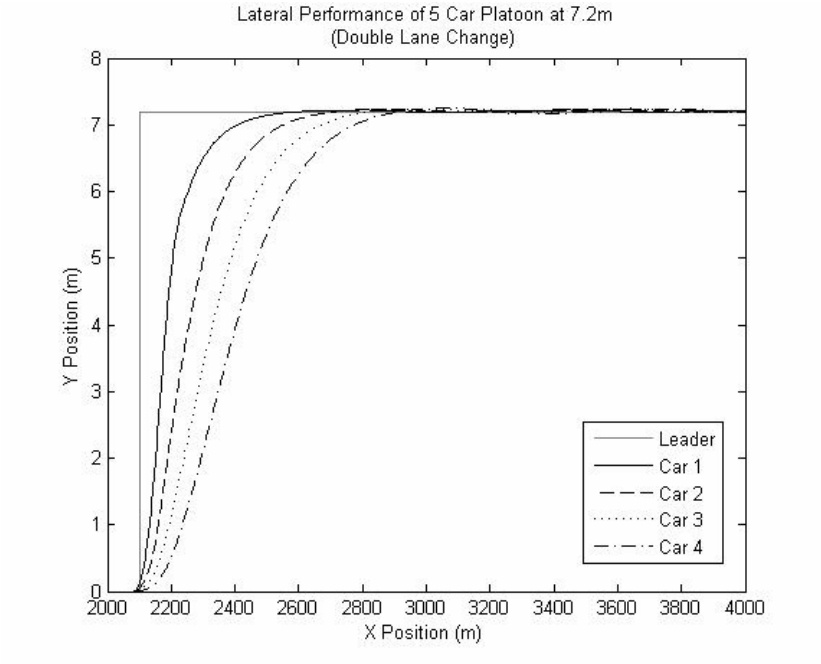

Figure 5.34 Lateral performance for 5 car platoon at 7.2 *m*

Chapter 6

Conclusion

Although automated driving dates back to the 1950s, it is still not yet a reality. Many issues such as safety, fault-tolerance, and the coexistence of automated vehicles with human driven vehicles must be solved first. New approaches to automated driving such as decentralized control may increase fault tolerance and reliability. Scalable decentralized controllers built using the latest artificial intelligence approaches, sensor fusion and inter-vehicle communication promise smarter vehicles that can accommodate human driven vehicles and offer the potential of increased reliability.

This thesis has investigated the implementation of an advanced artificial intelligence approach called Reinforcement Learning to the problem of Dynamic Collaborative Driving, a multi-vehicle automated driving concept. Specifically, this thesis introduces the idea of formulating the basic skills required in dynamic collaborative driving into finite Markov Decision Processes (MDP) which can be solved using reinforcement learning algorithms so as to produce decentralized controllers which have the potential to continually adapt and learn to optimize its performance based on experience. This methodology allows the nonlinear nature of the vehicle dynamics to be incorporated into the design of the controller without having to first linearize the model as in conventional state-space methods. The basic skills are i) longitudinal control sometimes referred to as Adaptive Intelligent Cruise Control (AICC) and ii) lateral control sometimes referred to as automated steering. These two skills form the basis of higher level multi-vehicle coordination maneuvers (platoon maneuvers).

To gain an understanding of the complexities of controlling a vehicle in both the longitudinal and lateral sense, a detailed vehicle dynamics model was created. This model demonstrates the nonlinear nature of the vehicle dynamics involved and provides a simulation platform for controller development and testing. Due to the nonlinearities present in the engine model, the transmission model, the tire model suspension and the rigid body dynamics of the modeled vehicle, a complex nonlinear model results. For the longitudinal vehicle dynamics, there are in fact 3 distinct nonlinear regions. There is the throttle response, in the presence of automatic gear shifting. There is the power off portion cause by the engine braking. There is the braking portion due to the tires. Each of these regions requires a specific nonlinear controller. For the lateral vehicle dynamics, the tire dynamics and delays in steering actuation give rise to the nonlinearities.

From this, it can be concluded that linearization of the model used in developing past vehicle control solutions may not be suitable for the entire operating range of the vehicle. In other words, the linear controllers resulting from using a simplified linear model of the vehicle dynamics in the design process may only be adequate for a particular operating point. The use of a more accurate nonlinear vehicle dynamics model in the design process should result in better nonlinear control systems for both longitudinal and lateral control.

For longitudinal control, an adaptive control system using gain scheduling is introduced whereby the gains are learned using reinforcement learning. Even with a simple reward function, it is

possible for Monte Carlo reinforcement learning to converge upon an optimal policy within a thousand episodes for a particular operating regime; therefore, the MDP properly describes the task to be learned.

For lateral control, an adaptive control system using gain scheduling is introduced whereby the gains are learned using reinforcement learning. It was observed that in order to achieve a smooth transition from one lateral position to another, a steering trajectory had to be provided. To produce this trajectory in a close-loop form, an element of anticipatory control is incorporated into a common PD control system. A learned preview or look-ahead distance is used to calculate a predicted lateral error feedback which is controlled using the adaptive PD controller. Even with a simple reward function, it is possible for Monte Carlo ES reinforcement learning to converge upon an optimal policy within a thousand episodes for a particular operating regime; therefore, the MDP properly describes the task to be learned.

When the learned optimal policies are combined to provide an adaptive control surface or a gain schedule, nonlinear control is achieved throughout the operating range in both the longitudinal and lateral case. For longitudinal control, the performance of the controller at specific operating points shows accurate tracking of both velocity and position in most cases. When the adaptive controller is deployed in a multi-vehicle convoy or platoon, the tracking performance is smooth but under-damped. As the second car attempts to track the leader, it overshoots and slight oscillations are passed down the formation. However, as we move farther in the formation, the oscillations decrease, implying that although under-damped, the overall system appears stable. For lateral control, the performance of the controller at specific operating points shows accurate and smooth tracking. In a multi-vehicle convoy or platoon, the lateral tracking performance is also accurate and smooth with minimal overshoot and oscillation. The oscillations, although small do decrease as the tracking progresses demonstrating stability in the cases presented.

Currently, advanced driving automation is only available among flagship luxury automobiles such as the Lexus LS460 (Figure 6.1) or the 2009 Opel Insignia (Figure 6.2) due to the large product development costs required to ensure that this automation is both safe and reliable. This automation currently exists in the form of separate modules for adaptive cruise control, adaptive braking, and lane keeping assist. The implication of this work to the current state of the art in automotive research is that reinforcement learning is a viable alternative means of creating generic adaptive control systems that provide a universal solution which continuously tunes itself to a specific car and perhaps will cut down on development time. In addition, with reinforcement learning, these automation modules need not be separate modules, but can exist as an integrated driving solution. Future work will attempt to take this concept and deploy it on a real automobile.

In order to deploy the control system on a real automobile, reinforcement learning training must be completed on a more accurate vehicle model which would require more data. The data required would be in the form of engineering vehicle data from the automobile manufacturers which would allow the model's response to be closer to that of an actual vehicle. Empirical tire data from the tire manufacturers would allow for accurate environments and different driving conditions to be modeled. In addition long-term vehicle failure data would allow the degradation of the vehicle to be modeled over time.

Figure 6.1 2008 Lexus LS 460 featuring *adaptive cruise control*, adaptive braking and lane keeping assist

Figure 6.2 2009 Opel Insignia featuring *Traffic Assist*

Other issues for potential future studies include, the controller performance variation from vehicle to vehicle, the controller performance variation with respect to the environment and driving conditions, as well as the affect on controller performance by existing basic electronic driving enhancements such as anti-lock braking systems (ABS), all-wheel-drive (AWD), traction control systems (TCS), electronic stability control (ESC) and dynamic steering response (DRS) systems.

Another interesting potential study from an artificial intelligence persepective would be use of human driving data for offline reinforcement learning. This could allow human experience to improve the machine's optimal policy. The use of reinforcement learning as an approach to controller design has potential for success demonstrated in this thesis. Its applicability is only limited by our imagination and perhaps by our perseverance

Appendix A: Discrete PID Control

The following is the derivation of the difference equation for PID control [Bollinger & Duffie 1988]. Assume that a discrete process is to be controlled whose output c_n can be sampled at a period of T seconds and a desired output is r_n. The error in the processes output is determined using

$$e_n = r_n - c_n \tag{A.1}$$

and the discrete output of the controller is m_n where n is the current time step. The output of proportional control action for continuous time is expressed as

$$m(t) = K_p e(t) \tag{A.2}$$

while the discrete form is

$$m_n = K_p e_n . \tag{A.3}$$

Shifting this equation backward one sample period yields

$$m_{n-1} = K_p e_{n-1} \quad . \tag{A.4}$$

Subtracting Equation (2.8) from Equation (2.7) yields the incremental approximation of proportional control which is

$$\Delta m_n = m_n - m_{n-1} = K_p (e_n - e_{n-1}) \tag{A.5}$$

The output of integral control action for continuous time is expressed as

$$m(t) = K_i \int_0^t e(\tau) d\tau \tag{A.6}$$

while the discrete form is

$$m_n = K_i \sum_{j=1}^{n} T e_j . \tag{A.8}$$

This can be rewritten as

$$m_n = K_i \sum_{j=1}^{n-1} T e_j + K_i T e_n . \tag{A.9}$$

Also note that

$$m_{n-1} = K_i \sum_{j=1}^{n-1} T e_j . \tag{A.10}$$

Subtracting Equation (2.13) from Equation (2.12) yields the incremental of proportional control which is

$$\Delta m_n = m_n - m_{n-1} = K_i T e_n \tag{A.11}$$

which is the incremental discrete approximation of integral control action.

The output of derivative control action for continuous time is expressed as

$$m(t) = K_p \frac{de(t)}{dt}. \tag{A.12}$$

The backward difference approximation can be used to obtain the associated discrete equation

$$m_n = K_d \left(\frac{e_n - e_{n-1}}{T} \right). \tag{A.13}$$

Shifting this equation backward one sample period yields

$$m_{n-1} = K_d \left(\frac{e_{n-1} - e_{n-2}}{T} \right). \tag{A.14}$$

Subtracting Equation (2.17) from Equation (2.16) yields the incremental discrete approximation of derivative control which is

$$\Delta m_n = m_n - m_{n-1} = \frac{K_d}{T}(e_n - 2e_{n-1} + e_{n-2}). \tag{A.15}$$

Combining the three elements into a cascade PID controller

$$\Delta m_n = (\Delta m_n)_P + (\Delta m_n)_I + (\Delta m_n)_D \tag{A.16}$$

$$\Delta m_n = m_n - m_{n-1} = K_p(e_n - e_{n-1}) + K_i T e_n + \frac{K_d}{T}(e_n - 2e_{n-1} + e_{n-2}) \tag{A.18}$$

$$m_n = m_{n-1} + K_p(e_n - e_{n-1}) + K_i T e_n + \frac{K_d}{T}(e_n - 2e_{n-1} + e_{n-2}) \tag{A.19}$$

and simplifying to yield the difference equation for the discrete PID control

$$m_n = m_{n-1} + K_0 e_n + K_1 e_{n-1} + K_2 e_{n-2} \tag{A.20}$$

where

$$K_0 = K_p + K_i T + \frac{K_d}{T} \qquad K_1 = -K_p - 2\frac{K_d}{T} \qquad K_2 = \frac{K_d}{T}.$$

Appendix B: Equations of Motion

The following is the derivation of the equations of motions for a vehicle based on the Pham et al [1997]. Given a four-wheeled vehicle steered via the front two wheels where the external forces enter this vehicle through the tires, two moving reference frames are defined. The first frame (O_u in Figure B.1) is with respect to the *unsprung mass* (i.e. the tires and wheels separated by a frame), the second frame (O_s in Figure B.1) with respect to the *sprung mass* which is the mass which rests upon the suspension system. The equations of motions will be expressed with respect to the *unsprung mass reference frame* to facilitate implementation in a numerical vehicle simulation [Ellis 1969].

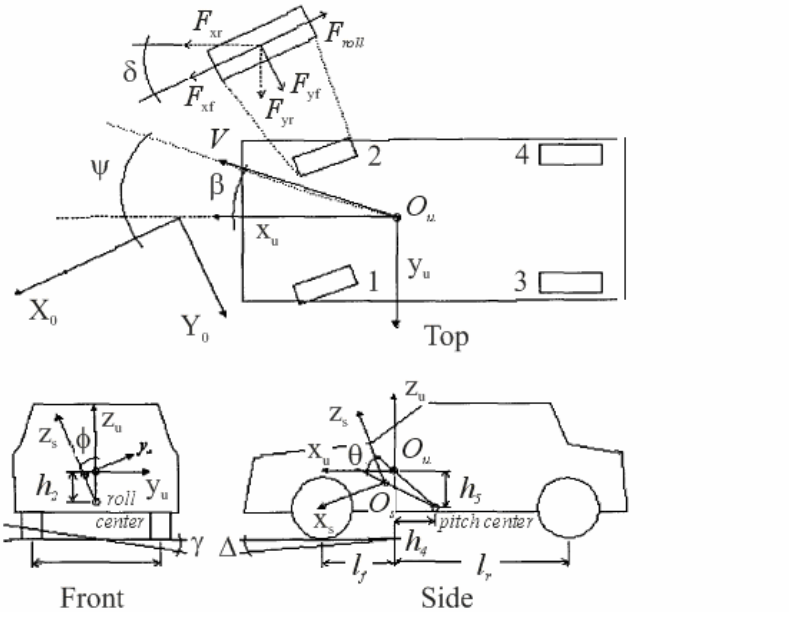

Figure B.1 Schematic of vehicle reference frames

The equations of motions are based on the summation of the external forces and moments.

$$\begin{bmatrix} \sum F_x \\ \sum F_y \\ \sum F_z \end{bmatrix} = m \begin{bmatrix} a_x \\ a_y \\ a_z \end{bmatrix} \tag{B.1}$$

where $[a_x, a_y, a_z,]^T = [\dot{V}_x, \dot{V}_y, \dot{V}_z]^T$ and

$$\begin{bmatrix} \sum M_x \\ \sum M_y \\ \sum M_z \end{bmatrix} = [I] \begin{bmatrix} \alpha_x \\ \alpha_y \\ \alpha_z \end{bmatrix} + \begin{bmatrix} 0 & -\omega_z & \omega_y \\ \omega_z & 0 & -\omega_x \\ -\omega_y & \omega_x & 0 \end{bmatrix} [I] \begin{bmatrix} \omega_x \\ \omega_y \\ \omega_z \end{bmatrix} \tag{B.2}$$

where $[\alpha_x, \alpha_y, \alpha_z,]^T = [\dot{\omega}_x, \dot{\omega}_y, \dot{\omega}_z]^T$. The special case where *xyz* are principal axes leads to the Euler's equations of rotational motion, which explicitly express the dependence on the angular velocity and acceleration (see equations 5.72-5.74 in [Ginsberg 1995]).

$$\begin{aligned} \sum M_x &= I_{xx}\alpha_x - (I_{yy} - I_{zz})\omega_y\omega_z \\ \sum M_y &= I_{yy}\alpha_y - (I_{zz} - I_{xx})\omega_x\omega_z \\ \sum M_z &= I_{zz}\alpha_z - (I_{xx} - I_{yy})\omega_x\omega_y \end{aligned} \tag{B.3}$$

Figure B.2 illustrates the relationship between the different reference frames. Point *P* lies on the path of the road *C*(*s*), point *U* is the origin of the unsprung mass O_u and point *S* is the origin of the *sprung mass* O_s. The challenge is to determine the translational/rotational velocities and accelerations required in equations B.1-3.

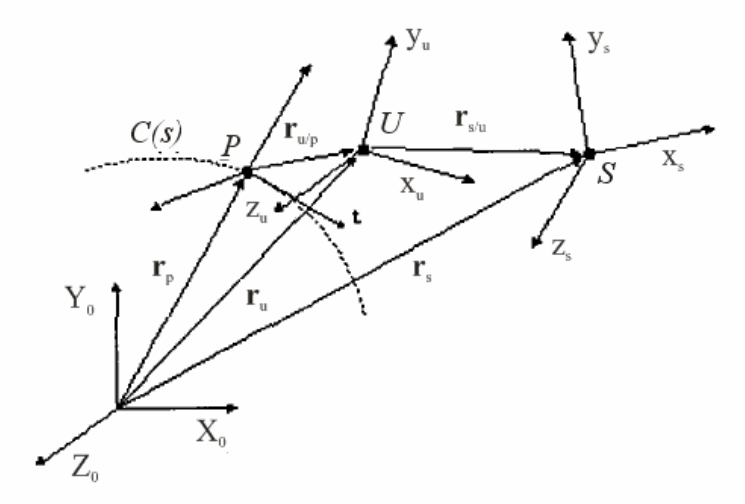

Figure B.2 Vector Diagram of Reference Frames

Let $\mathbf{r}_U$ be the vector from the origin of the inertial reference frame to *U* and let $\mathbf{r}_{S/U}$ be the vector from *U* to *S*. The acceleration of the *sprung mass* with respect to the unsprung coordinates can be determined from

$$\begin{bmatrix} a_x \\ a_y \\ a_z \end{bmatrix} = {}_u\ddot{\mathbf{r}}_S = {}_u\ddot{\mathbf{r}}_U + {}_u\ddot{\mathbf{r}}_{S/U} \tag{B.4}$$

where the left subscript *u* denotes the vector with respect to the rotating unsprung frame fixed to *U*. As the vehicle or *unsprung mass* travels along path *C*(*s*) it is undergoing planar motion, the angular velocity of the vehicle can be expressed as

$$ {}_i\omega_O = \begin{bmatrix} 0 \\ 0 \\ \dot{\psi} \end{bmatrix} \tag{B.5} $$

with respect to the inertial reference frame (the *i* subscript on the lower left indicates this) where $\dot{\psi}$ is the yaw rotation rate of the vehicle about the *z* axis. For a non-flat road, the angular velocity of the *unsprung mass* is perturbed by following the angular velocities due to the road

$$ {}_i\omega_{O_u/O} = \begin{bmatrix} \dot{\gamma} \\ \dot{\Delta} \\ -\dot{\beta} \end{bmatrix} \tag{B.6} $$

where γ is the superelevation, Δ is the gradient, and β is the sideslip angles as seen in Figure B.1. For small angles of γ, Δ and β the rotation matrix required to go from the inertial reference frame to the *unsprung mass* frame fixed to *U* is approximated as

$$ {}_u\Theta_i \approx \begin{bmatrix} 1 & \beta & -\Delta \\ -\beta & 1 & \gamma \\ \Delta & -\gamma & 1 \end{bmatrix} \tag{B.7} $$

(see equation 3.31 in [Ginsberg 1995]). The angular velocity of the unsprung mass with respect to moving frame *U* can be determined using the following equation and equations B.5, B.6, B.7.

$$ {}_u\omega_{O_u} = {}_u\Theta_i \left\{ {}_i\omega_{O_u/O} + {}_i\omega_{O_i} \right\} = \begin{bmatrix} 1 & \beta & -\Delta \\ -\beta & 1 & \gamma \\ \Delta & -\gamma & 1 \end{bmatrix} \left(\begin{bmatrix} \dot{\gamma} \\ \dot{\Delta} \\ -\dot{\beta} \end{bmatrix} + \begin{bmatrix} 0 \\ 0 \\ \dot{\psi} \end{bmatrix} \right) = \begin{bmatrix} \dot{\gamma} + \beta\dot{\Delta} - \Delta\dot{\psi} \\ -\beta\dot{\gamma} + \dot{\Delta} + \gamma\dot{\psi} \\ \dot{\psi} \end{bmatrix}. \tag{B.8} $$

Differentiating with respect to time will provide

$$ {}_u\dot{\omega}_{O_u} = \frac{d}{dt}\left({}_u\omega_{O_u} \right) = \begin{bmatrix} \ddot{\gamma} + \dot{\beta}\dot{\Delta} + \beta\ddot{\Delta} - \dot{\Delta}\dot{\psi} - \Delta\ddot{\psi} \\ -\dot{\beta}\dot{\gamma} - \beta\ddot{\gamma} + \ddot{\Delta} + \dot{\gamma}\dot{\psi} + \gamma\ddot{\psi} \\ \ddot{\psi} \end{bmatrix}. \tag{B.9} $$

The velocity of the *unsprung mass* with respect to moving frame *U* is described as

$$ {}_u\dot{\mathbf{r}}_U = \begin{bmatrix} V_x \\ V_y \\ 0 \end{bmatrix} \tag{B.10} $$

where the z^{th} component of velocity due to the tire deflection is assumed to be negligible. The acceleration of the *unsprung mass* in moving frame *U* is determined using equations B.8 and B.10.

$$ {}_u\ddot{\mathbf{r}}_U = \frac{d}{dt}\left({}_u\dot{\mathbf{r}}_U\right) = \frac{\partial}{\partial t}\left({}_u\dot{\mathbf{r}}_U\right) + {}_u\omega_{O_u} \times {}_u\dot{\mathbf{r}}_U = \begin{bmatrix} \dot{V}_x \\ \dot{V}_y \\ 0 \end{bmatrix} + \begin{bmatrix} -V_y\dot{\psi} \\ V_x\dot{\psi} \\ V_y\left\{\dot{\gamma} + \beta\dot{\Delta} - \Delta\dot{\psi}\right\} - V_x\left\{-\beta\dot{\gamma} + \dot{\Delta} + \gamma\dot{\psi}\right\} \end{bmatrix} $$

$$ = \begin{bmatrix} \dot{V}_x - V_y\dot{\psi} \\ \dot{V}_y + V_x\dot{\psi} \\ V_y\left\{\dot{\gamma} + \beta\dot{\Delta} - \Delta\dot{\psi}\right\} - V_x\left\{-\beta\dot{\gamma} + \dot{\Delta} + \gamma\dot{\psi}\right\} \end{bmatrix} \tag{B.11} $$

Due to the presence of the suspension, the *sprung mass* undergoes roll ϕ, pitch θ and vertical motion z, relative to the *unsprung mass* frame U. From simple geometry (Figure B.1) the relative position vector from frame U to S is given by

$$ {}_u\mathbf{r}_{S/U} = \begin{bmatrix} h_4\,\theta \\ -h_2\,\phi \\ z - h_5\,\theta \end{bmatrix}. \tag{B.12} $$

Differentiating the vector with respect to time will provide the relative velocity of the *unsprung mass* with respect to frame U.

$$ {}_u\dot{\mathbf{r}}_{S/U} = \frac{\partial}{\partial t}\left({}_u\mathbf{r}_{S/U}\right) = \begin{bmatrix} h_4\,\dot{\theta} \\ -h_2\,\dot{\phi} \\ \dot{z} - h_5\,\dot{\theta} \end{bmatrix} \tag{B.13} $$

Further differentiation of the vector gives

$$ \frac{\partial^2}{\partial t^2}\left({}_u\mathbf{r}_{S/U}\right) = \begin{bmatrix} h_4\,\ddot{\theta} \\ -h_2\,\ddot{\phi} \\ \ddot{z} - h_5\,\ddot{\theta} \end{bmatrix}. \tag{B.14} $$

The relative *sprung mass* acceleration with respect to frame U can be determined using equations B.8-B.14.

$$
{}_u\ddot{\mathbf{r}}_{S/U} = \begin{bmatrix} ({}_u\ddot{\mathbf{r}}_{S/U})_x \\ ({}_u\ddot{\mathbf{r}}_{S/U})_x \\ ({}_u\ddot{\mathbf{r}}_{S/U})_z \end{bmatrix} = \frac{\partial^2}{\partial t^2}({}_u\mathbf{r}_{S/U}) + {}_u\dot{\omega}_{O_u} \times {}_u\mathbf{r}_{S/U} + {}_u\omega_{O_u} \times (\omega_{O_u} \times {}_u\mathbf{r}_{S/U}) + 2\ {}_u\omega_{O_u} \times \frac{\partial}{\partial t}({}_u\mathbf{r}_{S/U})
$$

$$
= \begin{bmatrix} h_4\ddot{\theta} \\ -h_2\ddot{\phi} \\ \ddot{z} - h_5\ddot{\theta} \end{bmatrix} + \begin{bmatrix} (-\dot{\beta}\dot{\gamma} - \beta\ddot{\gamma} + \ddot{\Delta} + \dot{\gamma}\dot{\psi} + \gamma\ddot{\psi})(z - h_5\theta) + h_2\phi\ddot{\psi} \\ (\ddot{\gamma} + \dot{\beta}\dot{\Delta} + \beta\ddot{\Delta} - \dot{\Delta}\dot{\gamma} - \Delta\ddot{\gamma})(z - h_5\theta) - h_4\theta\ddot{\psi} \\ (\ddot{\gamma} + \dot{\beta}\dot{\Delta} + \beta\ddot{\Delta} - \dot{\Delta}\dot{\gamma} - \Delta\ddot{\gamma})h_2\phi - (\dot{\beta}\dot{\gamma} + \beta\ddot{\gamma} - \ddot{\Delta} - \dot{\gamma}\dot{\psi} - \gamma\ddot{\psi})h_4\theta \end{bmatrix}
$$

$$
+ \begin{bmatrix} -h_2\phi(-\beta\dot{\psi} + \dot{\Delta} + \gamma\dot{\psi})(\dot{\gamma} + \beta\dot{\Delta} + \Delta\dot{\psi}) - h_4\theta(-\beta\dot{\psi} + \dot{\Delta} + \gamma\dot{\psi})^2 - \dot{\psi}(\dot{\gamma} + \beta\dot{\Delta} + \Delta\dot{\psi})(z - h_5\theta) \\ +\dot{\psi}^2 h_4\theta \\ \\ -h_2\phi(\dot{\gamma} + \beta\dot{\Delta} + \Delta\dot{\psi}) - h_4\theta(\dot{\gamma} + \beta\dot{\Delta} + \Delta\dot{\psi})(-\beta\dot{\psi} + \dot{\Delta} + \gamma\dot{\psi}) - \dot{\psi}(-\beta\dot{\psi} + \dot{\Delta} + \gamma\dot{\psi})^2(z - h_5\theta) \\ +\dot{\psi}^2(-\beta\dot{\psi} + \dot{\Delta} + \gamma\dot{\psi}) \\ \\ (\dot{\gamma} + \beta\dot{\Delta} + \Delta\dot{\psi})^2(z - h_5\theta) - \dot{\psi}\, h_4\theta(\dot{\gamma} + \beta\dot{\Delta} + \Delta\dot{\psi}) - (-\beta\dot{\psi} + \dot{\Delta} + \gamma\dot{\psi})^2(z - h_5\theta) \\ -\dot{\psi}\, h_2\phi(-\beta\dot{\psi} + \dot{\Delta} + \gamma\dot{\psi}) \end{bmatrix}
$$

$$
+ 2\begin{bmatrix} h_4\dot{\theta}(-\beta\dot{\psi} + \dot{\Delta} + \gamma\dot{\psi}) + \dot{\psi}\, h_2\dot{\phi} \\ (\dot{\gamma} + \beta\dot{\Delta} + \Delta\dot{\psi})(z - h_5\theta) - \dot{\psi}\, h_4\dot{\theta} \\ h_2\dot{\phi}(\dot{\gamma} + \beta\dot{\Delta} + \Delta\dot{\psi}) - (-\beta\dot{\psi} + \dot{\Delta} + \gamma\dot{\psi})h_4\dot{\theta} \end{bmatrix}
$$

(B.15)

where the last term $2\ {}_u\omega_{O_u} \times \frac{\partial}{\partial t}({}_u\mathbf{r}_{S/U})$ is the Coriolis term. Equations B.1, B.4, B.11 and B.15 are then combined to form the translational equations of motion expressed below as

$$
m\left[\dot{V}_x - V_y\dot{\psi} + ({}_u\ddot{\mathbf{r}}_{S/U})_x\right] = \sum_{i=1}^{4} F_{X_i} - C_x V_x{}^2 - F_{roll} + \Delta mg \tag{B.16}
$$

$$
m\left[\dot{V}_y + V_x\dot{\psi} + ({}_u\ddot{\mathbf{r}}_{S/U})_y\right] = \sum_{i=1}^{4} F_{Y_i} - C_y V_y{}^2 - \gamma mg \tag{B.17}
$$

$$
m\left[V_y(\dot{\gamma} + \beta\dot{\Delta} - \Delta\dot{\psi}) - V_x(-\beta\dot{\gamma} + \dot{\Delta} + \gamma\dot{\psi}) + ({}_u\ddot{\mathbf{r}}_{S/U})_z\right] = \sum_{i=1}^{4} F_{Z_i} - mg \tag{B.18}
$$

where C_x = 0.45 and C_y = 2.1 are the aerodynamic coefficients of drag. The rolling resistance due to tire deformation F_{roll} = 274.7 N is specific to tire and the tire pressure, it is considered a constant for this simulation as it is independent of velocity [Gillespie 1992].

The angular velocity of the *sprung mass* is the sum of the *unsprung mass* angular velocity and the relative angular velocity between the two masses.

$$ {}_s\omega_{O_s} = {}_s\Theta_u \left\{ {}_u\omega_{O_u} + {}_u\omega_{O_s/O_u} \right\} \tag{B.19} $$

Due to the physical contraints of the suspension system, the *sprung mass* is not allowed to rotate about the *z* axis. The transformation matrix required to go from the *unsprung mass* frame *U* to the *sprung mass* frame *S* for small pitch θ and roll ϕ angles is expressed as

$$ {}_s\Theta_u \approx \begin{bmatrix} 1 & 0 & -\theta \\ 0 & 1 & \phi \\ \theta & -\phi & 1 \end{bmatrix} \tag{B.21} $$

The relative angular velocity of the *sprung mass* due the above constraints is

$$ {}_u\omega_{O_s/O_u} = \begin{bmatrix} \dot{\phi} \\ \dot{\theta} \\ 0 \end{bmatrix}. \tag{B.22} $$

By combining equations B.8, B.21 and B.22 into equation B.19 the angular velocity of the *sprung mass* can be determined as

$$ {}_s\omega_{O_s} = {}_s\Theta_u \left\{ {}_u\omega_{O_s/O_u} + {}_u\omega_{O_{ui}} \right\} = \begin{bmatrix} 1 & 0 & -\theta \\ 0 & 1 & \phi \\ \theta & -\phi & 1 \end{bmatrix} \left(\begin{bmatrix} \dot{\phi} \\ \dot{\theta} \\ 0 \end{bmatrix} + \begin{bmatrix} \dot{\gamma} + \beta\dot{\Delta} - \Delta\dot{\psi} \\ -\beta\dot{\gamma} + \dot{\Delta} + \gamma\dot{\psi} \\ \dot{\psi} \end{bmatrix} \right) = \begin{bmatrix} \dot{\phi} + \dot{\gamma} + \beta\dot{\Delta} - \{\Delta + \theta\}\dot{\psi} \\ \dot{\theta} + \beta\dot{\gamma} + \dot{\Delta} - \{\gamma + \phi\}\dot{\psi} \\ \theta\{\dot{\phi} + \dot{\gamma}\} - \phi\{\dot{\theta} + \dot{\Delta}\} + \dot{\psi} \end{bmatrix} \tag{B.23} $$

Taking the derivative with respect to time provides the angular acceleration of the *sprung mass*

$$ {}_s\dot{\omega}_{O_s} = \frac{d}{dt}\left({}_s\omega_{O_s} \right) = \begin{bmatrix} \ddot{\phi} + \ddot{\gamma} + \dot{\beta}\dot{\Delta} + \beta\ddot{\Delta} - (\Delta + \theta)\dot{\psi} + (\dot{\Delta} + \dot{\theta})\dot{\psi} \\ \ddot{\theta} + \dot{\beta}\dot{\gamma} + \beta\ddot{\gamma} + \ddot{\Delta} - (\gamma + \phi)\ddot{\psi} - (\dot{\gamma} + \dot{\phi})\dot{\psi} \\ \dot{\theta}(\dot{\gamma} + \dot{\phi}) + \theta(\ddot{\gamma} + \ddot{\phi}) - \dot{\phi}(\dot{\Delta} + \dot{\theta}) - \phi(\ddot{\Delta} + \ddot{\theta}) + \ddot{\psi} \end{bmatrix}. \tag{B.24} $$

The Euler Equations in B.3 along the transformed moments using the rotation matrix in B.21

$$ \begin{bmatrix} I_x\dot{\omega}_x - (I_y - I_z)\omega_y\omega_z \\ I_y\dot{\omega}_y - (I_z - I_x)\omega_x\omega_z \\ I_z\dot{\omega}_z - (I_x - I_y)\omega_x\omega_y \end{bmatrix} = \begin{bmatrix} 1 & 0 & -\theta \\ 0 & 1 & \phi \\ \theta & -\phi & 1 \end{bmatrix} \begin{bmatrix} M_x \\ M_y \\ M_z \end{bmatrix} \tag{B.25} $$

where M_x refers to ΣM_x, M_y refers to ΣM_y, and M_z refers to ΣM_z. Equation B.25 is combined with equations B.23 and B.24 to form the rotational equations of motion and expressed below as

$$ \begin{aligned} & I_x\left[\ddot{\phi} + \ddot{\gamma} + \dot{\beta}\dot{\Delta} + \beta\ddot{\Delta} - (\Delta + \theta)\ddot{\psi} - (\dot{\Delta} + \dot{\theta})\dot{\psi}\right] \\ & -(I_y - I_z)\cdot\left(\dot{\theta} + \dot{\gamma} + \beta\dot{\Delta} - \{\Delta + \theta\}\dot{\psi}\right)\cdot\left(\theta\{\dot{\phi} + \dot{\gamma}\} - \phi\{\dot{\theta} + \dot{\Delta}\} + \dot{\psi}\right) = M_x - \theta M_z \end{aligned} \tag{B.26} $$

$$ \begin{aligned} & I_y\left[\ddot{\phi} - \dot{\beta}\dot{\gamma} + \beta\ddot{\gamma} + \ddot{\Delta} + (\gamma + \phi)\ddot{\psi} - (\dot{\gamma} + \dot{\phi})\dot{\psi}\right] \\ & -(I_z - I_x)\cdot\left(\dot{\phi} + \dot{\gamma} + \beta\dot{\Delta} - \{\Delta + \theta\}\dot{\psi}\right)\cdot\left(\theta\{\dot{\phi} + \dot{\gamma}\} - \phi\{\dot{\theta} + \dot{\Delta}\} + \dot{\psi}\right) = M_y + \phi M_z \end{aligned} \tag{B.27} $$

$$I_z\left[\dot{\theta}(\dot{\gamma}+\dot{\phi})+\theta(\ddot{\gamma}+\ddot{\phi})-\dot{\phi}(\dot{\Delta}+\dot{\theta})-\phi(\ddot{\Delta}+\ddot{\theta})+\ddot{\psi}\right]$$
$$-(I_x-I_y)\cdot\left(\dot{\phi}+\dot{\gamma}+\beta\dot{\Delta}-\{\Delta+\theta\}\dot{\psi}\right)\cdot\left(\dot{\theta}+\beta\dot{\gamma}+\dot{\Delta}-\{\gamma+\phi\}\dot{\psi}\right)=M_x-\theta M_y+M_z \tag{B.28}$$

where $I_x =$ 479.6 $kg{\cdot}m^2$, $I_y =$ 2549.3 $kg{\cdot}m^2$, $I_z =$ 2782.1 $kg{\cdot}m^2$ are the moments of inertia about each axis, Δ is the gradient angle of the road, β is the slip angle and γ is the super-elevation angle of the road in radians.

For a flat and straight road, the gradient angle and rates are $\Delta=\dot{\Delta}=\ddot{\Delta}=0$, the slip angle and rates are $\beta=\dot{\beta}=\ddot{\beta}=0$ and super-elevation angles and rates are $\gamma=\dot{\gamma}=\ddot{\gamma}=0$. Therefore, the *sprung mass* acceleration becomes

$${}_u\ddot{\mathbf{r}}_{S/U}=\begin{bmatrix} h_4\ddot{\theta} \\ -h_2\ddot{\phi} \\ \ddot{z}-h_5\ddot{\theta}\end{bmatrix}+\begin{bmatrix} h_2\phi\ddot{\psi} \\ -h_4\theta\ddot{\psi} \\ 0\end{bmatrix}+\begin{bmatrix} \dot{\psi}^2h_4\theta \\ 0 \\ 0\end{bmatrix}+2\begin{bmatrix} \dot{\psi}\,h_2\dot{\phi} \\ -\dot{\psi}\,h_4\dot{\theta} \\ 0\end{bmatrix} \tag{B.29}$$

and the equations of motion become

$$m\left[\dot{V}_x-V_y\dot{\psi}+h_4\ddot{\theta}+h_2\phi\ddot{\psi}+\dot{\psi}^2h_4\theta\right]=\sum_{i=1}^{4}F_{X_i}-C_xV_x{}^2-F_{roll} \tag{B.30}$$

$$m\left[\dot{V}_y+V_x\dot{\psi}+-h_2\ddot{\phi}-h_4\theta\ddot{\psi}-2\dot{\psi}h_4\dot{\theta}\right]=\sum_{i=1}^{4}F_{Y_i}-C_yV_y{}^2 \tag{B.31}$$

$$m\left[\ddot{z}-h_5\ddot{\theta}\right]=\sum_{i=1}^{4}F_{Z_i}-mg \tag{B.32}$$

$$I_x\left[\ddot{\phi}-\theta\ddot{\psi}-\dot{\theta}\dot{\psi}\right]-(I_y-I_z)\cdot\left(\dot{\theta}-\theta\dot{\psi}\right)\cdot\left(\theta\dot{\phi}-\phi\dot{\theta}+\dot{\psi}\right)=M_x-\theta M_z \tag{B.33}$$

$$I_y\left[\ddot{\phi}+\phi\ddot{\psi}-\dot{\phi}\dot{\psi}\right]-(I_z-I_x)\cdot\left(\dot{\phi}-\theta\dot{\psi}\right)\cdot\left(\theta\dot{\phi}-\phi\dot{\theta}+\dot{\psi}\right)=M_y+\phi M_z \tag{B.34}$$

$$I_z\left[\dot{\theta}\dot{\phi}+\theta\ddot{\phi}-\dot{\phi}\dot{\theta}-\phi\ddot{\theta}+\ddot{\psi}\right]-(I_x-I_y)\cdot\left(\dot{\phi}-\theta\dot{\psi}\right)\cdot\left(\dot{\theta}-\phi\dot{\psi}\right)=M_x-\theta M_y+M_z \tag{B.35}$$

where $\begin{bmatrix}\dot{\omega}_x\\ \dot{\omega}_y\\ \dot{\omega}_z\end{bmatrix}=\begin{bmatrix}\ddot{\phi}+\theta\ddot{\psi}-\dot{\theta}\dot{\psi}\\ \ddot{\phi}+\phi\ddot{\psi}-\dot{\phi}\dot{\psi}\\ \dot{\theta}\dot{\phi}+\theta\ddot{\phi}-\dot{\phi}\dot{\theta}-\phi\ddot{\theta}+\ddot{\psi}\end{bmatrix}$ and $\begin{bmatrix}\omega_x\\ \omega_y\\ \omega_z\end{bmatrix}=\begin{bmatrix}\dot{\phi}-\theta\dot{\psi}\\ \dot{\theta}-\phi\dot{\psi}\\ \theta\dot{\phi}-\phi\dot{\theta}+\dot{\psi}\end{bmatrix}$.

Appendix C: Optimal Policy for Adaptive Longitudinal Control

Table C.1: Optimal Policy for Adaptive Longitudinal Control

					Throttle				*Brake*			
s_1	s_2			s_3	a_1	a_2	a_3	a_4	a_5	a_6	a_7	a_8
Vx_f (m/s)	Vx_i (m/s)	$range_f$ (m)	$range_i$ (m)	$\Delta range$ (m)	Kp_x	Ki_x	Kp_v	Kd_v	Kp_x	Ki_x	Kp_v	Kd_v
5.00	5.00	15.00	115.00	-100.00	22.100	2.180	14.300	7.500	17.700	2.080	2.500	4.300
5.00	10.00	15.00	115.00	-100.00	22.100	1.290	20.800	4.900	5.800	1.020	2.500	22.800
5.00	15.00	15.00	115.00	-100.00	22.100	1.520	18.200	4.900	17.700	0.840	19.600	0.100
5.00	20.00	15.00	115.00	-100.00	18.400	1.520	14.300	7.400	5.800	0.840	2.500	0.100
5.00	25.00	15.00	115.00	-100.00	12.700	0.560	4.200	6.400	8.900	1.990	11.500	22.800
5.00	30.00	15.00	115.00	-100.00	12.700	0.560	4.200	6.400	8.900	1.990	11.500	22.800
5.00	35.00	15.00	115.00	-100.00	12.700	0.560	4.200	6.400	8.900	1.990	11.500	22.800
5.00	40.00	15.00	115.00	-100.00	12.700	0.560	4.200	6.400	8.900	1.990	11.500	22.800
10.00	5.00	15.00	115.00	-100.00	12.200	0.700	4.200	4.600	14.900	2.310	6.800	5.700
10.00	10.00	15.00	115.00	-100.00	13.700	0.160	4.200	7.300	20.700	1.730	22.000	5.700
10.00	15.00	15.00	115.00	-100.00	17.900	1.070	18.500	9.300	23.000	2.080	2.500	9.200
10.00	20.00	15.00	115.00	-100.00	18.400	1.520	14.300	7.500	19.100	0.840	2.500	0.100
10.00	25.00	15.00	115.00	-100.00	22.100	1.310	17.100	16.600	5.800	1.020	2.500	22.800
10.00	30.00	15.00	115.00	-100.00	22.100	1.310	17.100	16.600	5.800	1.020	2.500	22.800
10.00	35.00	15.00	115.00	-100.00	22.100	1.310	17.100	16.600	5.800	1.020	2.500	22.800
10.00	40.00	15.00	115.00	-100.00	22.100	1.310	17.100	16.600	5.800	1.020	2.500	22.800
15.00	5.00	15.00	115.00	-100.00	14.400	0.700	4.200	6.200	7.900	1.150	6.800	5.700
15.00	10.00	15.00	115.00	-100.00	15.400	1.520	10.700	7.400	11.500	0.840	19.600	0.100
15.00	15.00	15.00	115.00	-100.00	12.700	0.560	17.100	4.600	14.900	2.080	2.500	22.800
15.00	20.00	15.00	115.00	-100.00	19.100	1.290	17.100	4.600	14.900	1.020	2.500	22.800
15.00	25.00	15.00	115.00	-100.00	18.400	1.520	14.300	7.400	14.900	0.840	2.500	0.100
15.00	30.00	15.00	115.00	-100.00	18.400	1.520	14.300	7.400	14.900	0.840	2.500	0.100
15.00	35.00	15.00	115.00	-100.00	18.400	1.520	14.300	7.400	14.900	0.840	2.500	0.100
15.00	40.00	15.00	115.00	-100.00	18.400	1.520	14.300	7.400	14.900	0.840	2.500	0.100
20.00	5.00	15.00	115.00	-100.00	2.600	0.100	1.800	6.300	17.700	2.200	18.800	5.700
20.00	10.00	15.00	115.00	-100.00	18.400	1.520	14.300	7.500	5.800	0.840	2.500	0.100
20.00	15.00	15.00	115.00	-100.00	14.900	1.310	10.300	4.100	8.900	1.990	2.500	10.200
20.00	20.00	15.00	115.00	-100.00	12.200	1.310	7.300	4.600	14.900	1.020	2.500	22.800
20.00	25.00	15.00	115.00	-100.00	18.400	0.160	1.800	6.300	16.100	2.200	17.600	9.200
20.00	30.00	15.00	115.00	-100.00	18.400	0.160	1.800	6.300	16.100	2.200	17.600	9.200
20.00	35.00	15.00	115.00	-100.00	18.400	0.160	1.800	6.300	16.100	2.200	17.600	9.200
20.00	40.00	15.00	115.00	-100.00	18.400	0.160	1.800	6.300	16.100	2.200	17.600	9.200
25.00	5.00	15.00	115.00	-100.00	15.400	0.700	14.300	7.500	11.500	1.990	6.800	5.700
25.00	10.00	15.00	115.00	-100.00	14.900	1.520	7.300	4.100	5.800	0.840	2.500	0.100
25.00	15.00	15.00	115.00	-100.00	14.900	0.160	1.800	4.100	14.900	1.730	17.200	8.300
25.00	20.00	15.00	115.00	-100.00	14.900	1.520	7.300	4.100	14.900	0.840	2.500	0.100
25.00	25.00	15.00	115.00	-100.00	17.600	0.700	4.200	6.200	20.700	2.080	18.800	5.700
25.00	30.00	15.00	115.00	-100.00	12.700	0.700	10.300	6.200	4.300	0.370	17.200	20.700
25.00	35.00	15.00	115.00	-100.00	12.700	0.700	10.300	6.200	4.300	0.370	17.200	20.700

25.00	40.00	15.00	115.00	-100.00	12.700	0.700	10.300	6.200	4.300	0.370	17.200	20.700
30.00	5.00	15.00	115.00	-100.00	18.400	1.520	14.300	13.200	11.500	0.840	17.600	0.100
30.00	10.00	15.00	115.00	-100.00	12.200	1.520	4.200	4.600	14.900	0.840	19.600	0.100
30.00	15.00	15.00	115.00	-100.00	17.600	1.570	7.300	6.200	17.200	1.730	18.800	10.200
30.00	20.00	15.00	115.00	-100.00	14.900	1.520	14.300	4.100	5.800	0.840	17.600	0.100
30.00	25.00	15.00	115.00	-100.00	12.200	0.700	4.200	4.600	14.900	2.080	17.200	10.200
30.00	30.00	15.00	115.00	-100.00	9.000	0.700	4.200	6.400	17.200	1.990	2.500	11.500
30.00	35.00	15.00	115.00	-100.00	12.200	0.700	4.200	4.600	14.900	2.080	17.200	10.200
30.00	40.00	15.00	115.00	-100.00	12.200	0.700	4.200	4.600	14.900	2.080	17.200	10.200
35.00	5.00	15.00	115.00	-100.00	22.100	1.310	23.100	4.600	14.900	1.020	17.200	10.900
35.00	10.00	15.00	115.00	-100.00	19.100	1.570	14.400	6.300	22.600	2.200	18.800	10.700
35.00	15.00	15.00	115.00	-100.00	19.100	2.180	20.800	6.300	19.100	0.370	2.500	22.800
35.00	20.00	15.00	115.00	-100.00	15.400	1.070	18.500	4.600	14.900	1.990	4.300	10.700
35.00	25.00	15.00	115.00	-100.00	14.900	1.520	13.600	4.100	14.900	0.840	2.500	0.100
35.00	30.00	15.00	115.00	-100.00	14.900	1.520	13.600	4.100	14.900	0.840	2.500	0.100
35.00	35.00	15.00	115.00	-100.00	14.900	1.520	13.600	4.100	14.900	0.840	2.500	0.100
35.00	40.00	15.00	115.00	-100.00	14.900	1.520	13.600	4.100	14.900	0.840	2.500	0.100
40.00	5.00	15.00	115.00	-100.00	14.900	1.570	5.800	4.100	4.300	0.510	17.200	22.800
40.00	10.00	15.00	115.00	-100.00	18.400	2.180	18.500	4.600	14.900	0.750	17.600	22.800
40.00	15.00	15.00	115.00	-100.00	12.200	1.520	7.300	4.900	5.800	1.020	2.500	22.800
40.00	20.00	15.00	115.00	-100.00	22.100	1.520	20.800	4.900	5.800	0.840	2.500	0.100
40.00	25.00	15.00	115.00	-100.00	14.900	2.180	20.800	4.100	5.800	1.020	2.500	22.800
40.00	30.00	15.00	115.00	-100.00	14.900	2.180	20.800	4.100	5.800	1.020	2.500	22.800
40.00	35.00	15.00	115.00	-100.00	14.900	2.180	20.800	4.100	5.800	1.020	2.500	22.800
40.00	40.00	15.00	115.00	-100.00	14.900	2.180	20.800	4.100	5.800	1.020	2.500	22.800
5.00	5.00	15.00	105.00	-90.00	19.100	1.290	17.100	4.900	5.800	1.020	2.500	22.800
5.00	10.00	15.00	105.00	-90.00	12.700	1.520	14.300	7.500	5.800	0.840	19.600	0.100
5.00	15.00	15.00	105.00	-90.00	18.400	1.520	14.300	4.600	14.900	0.840	17.600	0.100
5.00	20.00	15.00	105.00	-90.00	19.100	1.520	18.500	16.600	19.600	0.840	19.600	0.100
5.00	25.00	15.00	105.00	-90.00	18.400	1.290	13.600	13.200	5.800	1.020	2.500	10.900
5.00	30.00	15.00	105.00	-90.00	18.400	1.290	13.600	13.200	5.800	1.020	2.500	10.900
5.00	35.00	15.00	105.00	-90.00	18.400	1.290	13.600	13.200	5.800	1.020	2.500	10.900
5.00	40.00	15.00	105.00	-90.00	18.400	1.290	13.600	13.200	5.800	1.020	2.500	10.900
10.00	5.00	15.00	105.00	-90.00	12.200	0.700	4.200	4.600	14.900	2.200	17.200	5.700
10.00	10.00	15.00	105.00	-90.00	14.900	1.520	10.700	4.100	19.100	0.840	2.500	0.100
10.00	15.00	15.00	105.00	-90.00	14.900	1.310	7.300	4.100	21.600	1.240	3.100	9.800
10.00	20.00	15.00	105.00	-90.00	18.400	1.520	14.300	7.400	19.100	0.840	2.500	0.100
10.00	25.00	15.00	105.00	-90.00	17.900	1.070	18.500	16.600	19.100	1.020	2.500	10.900
10.00	30.00	15.00	105.00	-90.00	17.900	1.070	18.500	16.600	19.100	1.020	2.500	10.900
10.00	35.00	15.00	105.00	-90.00	17.900	1.070	18.500	16.600	19.100	1.020	2.500	10.900
10.00	40.00	15.00	105.00	-90.00	17.900	1.070	18.500	16.600	19.100	1.020	2.500	10.900
15.00	5.00	15.00	105.00	-90.00	18.400	0.560	4.200	6.200	19.100	2.080	17.600	5.700
15.00	10.00	15.00	105.00	-90.00	18.400	0.700	4.200	6.300	17.700	2.200	17.600	5.700
15.00	15.00	15.00	105.00	-90.00	14.900	1.520	14.300	4.100	14.900	0.840	2.500	22.800
15.00	20.00	15.00	105.00	-90.00	22.100	1.520	20.800	13.200	5.800	0.840	2.500	0.100
15.00	25.00	15.00	105.00	-90.00	12.700	0.100	4.200	17.500	8.900	2.200	6.800	5.700
15.00	30.00	15.00	105.00	-90.00	12.700	0.100	4.200	17.500	8.900	2.200	6.800	5.700
15.00	35.00	15.00	105.00	-90.00	12.700	0.100	4.200	17.500	8.900	2.200	6.800	5.700

15.00	40.00	15.00	105.00	-90.00	12.700	0.100	4.200	17.500	8.900	2.200	6.800	5.700
20.00	5.00	15.00	105.00	-90.00	9.000	0.700	4.200	4.600	14.900	0.370	18.100	22.800
20.00	10.00	15.00	105.00	-90.00	14.900	0.160	1.800	4.100	14.900	1.990	3.100	8.300
20.00	15.00	15.00	105.00	-90.00	14.900	0.100	10.700	4.100	8.900	2.310	1.900	11.100
20.00	20.00	15.00	105.00	-90.00	17.900	1.310	14.400	4.600	14.900	1.020	2.500	22.800
20.00	25.00	15.00	105.00	-90.00	14.400	1.520	7.300	13.200	7.900	0.840	19.600	0.100
20.00	30.00	15.00	105.00	-90.00	14.400	1.520	7.300	13.200	7.900	0.840	19.600	0.100
20.00	35.00	15.00	105.00	-90.00	14.400	1.520	7.300	13.200	7.900	0.840	19.600	0.100
20.00	40.00	15.00	105.00	-90.00	14.400	1.520	7.300	13.200	7.900	0.840	19.600	0.100
25.00	5.00	15.00	105.00	-90.00	15.400	1.520	10.700	7.400	5.800	0.840	2.500	0.100
25.00	10.00	15.00	105.00	-90.00	9.000	1.310	4.200	4.600	14.900	2.080	17.200	22.800
25.00	15.00	15.00	105.00	-90.00	15.400	0.700	4.200	7.400	11.500	2.080	6.800	5.700
25.00	20.00	15.00	105.00	-90.00	9.000	1.310	4.200	4.600	14.900	2.080	18.100	22.800
25.00	25.00	15.00	105.00	-90.00	18.400	0.560	4.200	6.200	17.200	1.730	17.600	5.700
25.00	30.00	15.00	105.00	-90.00	9.000	1.310	4.200	4.600	14.900	1.170	17.200	22.800
25.00	35.00	15.00	105.00	-90.00	9.000	1.310	4.200	4.600	14.900	1.170	17.200	22.800
25.00	40.00	15.00	105.00	-90.00	9.000	1.310	4.200	4.600	14.900	1.170	17.200	22.800
30.00	5.00	15.00	105.00	-90.00	17.900	1.070	18.200	4.900	20.700	0.500	17.200	22.800
30.00	10.00	15.00	105.00	-90.00	14.900	1.520	14.300	4.100	11.500	0.840	19.600	0.100
30.00	15.00	15.00	105.00	-90.00	15.400	1.520	14.300	7.500	5.800	0.840	19.600	0.100
30.00	20.00	15.00	105.00	-90.00	14.900	0.700	14.300	4.100	19.100	2.080	2.500	5.700
30.00	25.00	15.00	105.00	-90.00	12.200	0.700	4.200	4.600	14.900	2.080	17.200	22.800
30.00	30.00	15.00	105.00	-90.00	17.600	0.700	20.800	6.200	22.600	2.080	11.500	9.200
30.00	35.00	15.00	105.00	-90.00	12.200	0.700	4.200	4.600	14.900	2.080	17.200	22.800
30.00	40.00	15.00	105.00	-90.00	12.200	0.700	4.200	4.600	14.900	2.080	17.200	22.800
35.00	5.00	15.00	105.00	-90.00	17.900	1.310	14.400	4.900	22.600	1.730	2.500	9.800
35.00	10.00	15.00	105.00	-90.00	13.700	1.070	13.600	4.600	14.900	2.200	17.200	10.200
35.00	15.00	15.00	105.00	-90.00	22.100	2.180	18.200	6.300	22.600	1.170	2.500	22.800
35.00	20.00	15.00	105.00	-90.00	18.400	1.520	14.400	4.600	14.900	0.840	2.500	0.100
35.00	25.00	15.00	105.00	-90.00	17.900	1.570	18.200	4.900	20.700	2.200	3.100	10.700
35.00	30.00	15.00	105.00	-90.00	17.900	1.570	18.200	4.900	20.700	2.200	3.100	10.700
35.00	35.00	15.00	105.00	-90.00	17.900	1.570	18.200	4.900	20.700	2.200	3.100	10.700
35.00	40.00	15.00	105.00	-90.00	17.900	1.570	18.200	4.900	20.700	2.200	3.100	10.700
40.00	5.00	15.00	105.00	-90.00	17.900	2.180	10.300	6.200	10.400	2.080	2.500	22.800
40.00	10.00	15.00	105.00	-90.00	12.700	2.180	20.800	4.900	8.900	1.730	2.500	22.800
40.00	15.00	15.00	105.00	-90.00	22.100	1.310	18.200	4.900	4.300	1.730	11.500	20.700
40.00	20.00	15.00	105.00	-90.00	14.900	1.520	20.800	4.100	14.900	0.840	2.500	0.100
40.00	25.00	15.00	105.00	-90.00	14.900	1.520	20.800	4.100	5.800	0.840	2.500	0.100
40.00	30.00	15.00	105.00	-90.00	14.900	1.520	20.800	4.100	5.800	0.840	2.500	0.100
40.00	35.00	15.00	105.00	-90.00	14.900	1.520	20.800	4.100	5.800	0.840	2.500	0.100
40.00	40.00	15.00	105.00	-90.00	14.900	1.520	20.800	4.100	5.800	0.840	2.500	0.100
5.00	5.00	15.00	95.00	-80.00	14.900	1.520	10.700	4.100	14.900	0.840	19.600	0.100
5.00	10.00	15.00	95.00	-80.00	12.200	0.700	13.600	4.600	14.900	0.370	2.500	8.300
5.00	15.00	15.00	95.00	-80.00	19.100	1.520	14.300	7.400	5.800	0.840	19.600	0.100
5.00	20.00	15.00	95.00	-80.00	18.400	1.070	20.800	17.500	22.600	1.170	17.600	4.300
5.00	25.00	15.00	95.00	-80.00	19.100	0.700	10.700	7.400	5.800	2.200	2.500	11.100
5.00	30.00	15.00	95.00	-80.00	19.100	0.700	10.700	7.400	5.800	2.200	2.500	11.100
5.00	35.00	15.00	95.00	-80.00	19.100	0.700	10.700	7.400	5.800	2.200	2.500	11.100

5.00	40.00	15.00	95.00	-80.00	19.100	0.700	10.700	7.400	5.800	2.200	2.500	11.100
10.00	5.00	15.00	95.00	-80.00	18.400	1.520	14.300	4.600	14.900	0.840	2.500	0.100
10.00	10.00	15.00	95.00	-80.00	17.900	1.310	14.400	4.600	14.900	1.020	2.500	22.800
10.00	15.00	15.00	95.00	-80.00	19.100	1.310	17.100	4.600	14.900	1.020	2.500	22.800
10.00	20.00	15.00	95.00	-80.00	19.100	1.520	14.400	4.600	14.900	0.840	19.600	0.100
10.00	25.00	15.00	95.00	-80.00	22.200	1.070	5.800	7.400	14.900	1.020	2.500	22.800
10.00	30.00	15.00	95.00	-80.00	22.200	1.070	5.800	7.400	14.900	1.020	2.500	22.800
10.00	35.00	15.00	95.00	-80.00	22.200	1.070	5.800	7.400	14.900	1.020	2.500	22.800
10.00	40.00	15.00	95.00	-80.00	22.200	1.070	5.800	7.400	14.900	1.020	2.500	22.800
15.00	5.00	15.00	95.00	-80.00	12.200	0.560	14.300	7.500	17.700	2.080	18.100	5.700
15.00	10.00	15.00	95.00	-80.00	14.900	1.290	10.300	4.100	8.900	1.730	3.100	10.200
15.00	15.00	15.00	95.00	-80.00	18.400	1.520	14.300	7.400	5.800	0.840	2.500	0.100
15.00	20.00	15.00	95.00	-80.00	18.400	1.520	14.300	7.500	5.800	0.840	17.600	0.100
15.00	25.00	15.00	95.00	-80.00	18.400	1.520	14.300	7.500	5.800	0.840	2.500	0.100
15.00	30.00	15.00	95.00	-80.00	18.400	1.520	14.300	7.500	5.800	0.840	2.500	0.100
15.00	35.00	15.00	95.00	-80.00	18.400	1.520	14.300	7.500	5.800	0.840	2.500	0.100
15.00	40.00	15.00	95.00	-80.00	18.400	1.520	14.300	7.500	5.800	0.840	2.500	0.100
20.00	5.00	15.00	95.00	-80.00	1.400	0.100	13.600	16.500	17.700	2.310	3.100	8.300
20.00	10.00	15.00	95.00	-80.00	2.600	0.100	10.700	6.200	4.300	1.020	11.500	10.900
20.00	15.00	15.00	95.00	-80.00	18.400	1.310	13.600	4.900	8.900	1.150	2.500	9.200
20.00	20.00	15.00	95.00	-80.00	17.900	1.310	14.400	4.600	14.900	1.020	2.500	22.800
20.00	25.00	15.00	95.00	-80.00	14.900	0.700	4.200	4.100	19.100	1.150	17.200	5.700
20.00	30.00	15.00	95.00	-80.00	14.900	0.700	4.200	4.100	19.100	1.150	17.200	5.700
20.00	35.00	15.00	95.00	-80.00	14.900	0.700	4.200	4.100	19.100	1.150	17.200	5.700
20.00	40.00	15.00	95.00	-80.00	14.900	0.700	4.200	4.100	19.100	1.150	17.200	5.700
25.00	5.00	15.00	95.00	-80.00	17.600	1.290	7.300	7.300	17.200	1.730	22.000	8.300
25.00	10.00	15.00	95.00	-80.00	9.000	1.310	4.200	4.600	14.900	2.080	17.200	22.800
25.00	15.00	15.00	95.00	-80.00	14.900	1.520	14.300	4.100	5.800	0.840	19.600	0.100
25.00	20.00	15.00	95.00	-80.00	7.800	0.160	1.800	7.300	17.200	2.200	23.200	10.700
25.00	25.00	15.00	95.00	-80.00	15.400	0.700	4.200	6.400	11.500	2.080	2.500	5.700
25.00	30.00	15.00	95.00	-80.00	15.400	0.700	4.200	6.400	11.500	2.080	2.500	5.700
25.00	35.00	15.00	95.00	-80.00	15.400	0.700	4.200	6.400	11.500	2.080	2.500	5.700
25.00	40.00	15.00	95.00	-80.00	15.400	0.700	4.200	6.400	11.500	2.080	2.500	5.700
30.00	5.00	15.00	95.00	-80.00	14.900	1.520	7.300	4.100	11.500	0.840	19.600	0.100
30.00	10.00	15.00	95.00	-80.00	14.900	0.160	13.600	4.100	14.900	1.240	13.700	22.800
30.00	15.00	15.00	95.00	-80.00	14.900	1.520	14.300	4.100	5.800	0.840	19.600	0.100
30.00	20.00	15.00	95.00	-80.00	12.200	0.700	4.200	4.600	14.900	2.200	18.800	10.200
30.00	25.00	15.00	95.00	-80.00	12.200	0.700	4.200	4.600	14.900	2.200	2.500	5.700
30.00	30.00	15.00	95.00	-80.00	17.600	2.180	10.300	6.300	19.100	1.020	17.200	22.800
30.00	35.00	15.00	95.00	-80.00	12.200	0.700	4.200	4.600	14.900	2.200	2.500	5.700
30.00	40.00	15.00	95.00	-80.00	12.200	0.700	4.200	4.600	14.900	2.200	2.500	5.700
35.00	5.00	15.00	95.00	-80.00	22.100	1.570	23.100	4.900	19.600	1.170	18.100	22.800
35.00	10.00	15.00	95.00	-80.00	17.600	2.180	10.300	7.400	17.700	2.080	2.500	22.800
35.00	15.00	15.00	95.00	-80.00	17.600	0.560	14.300	4.600	14.900	0.510	2.500	5.700
35.00	20.00	15.00	95.00	-80.00	18.400	1.520	14.400	6.400	5.800	0.840	2.500	0.100
35.00	25.00	15.00	95.00	-80.00	17.900	1.570	20.800	4.900	17.700	1.730	3.100	4.300
35.00	30.00	15.00	95.00	-80.00	17.900	1.570	20.800	4.900	17.700	1.730	3.100	4.300
35.00	35.00	15.00	95.00	-80.00	17.900	1.570	20.800	4.900	17.700	1.730	3.100	4.300

35.00	40.00	15.00	95.00	-80.00	17.900	1.570	20.800	4.900	17.700	1.730	3.100	4.300
40.00	5.00	15.00	95.00	-80.00	14.900	2.180	18.200	4.100	3.800	0.500	11.500	9.200
40.00	10.00	15.00	95.00	-80.00	22.200	1.570	5.800	6.200	6.700	1.730	16.300	22.200
40.00	15.00	15.00	95.00	-80.00	22.100	2.180	10.700	6.200	17.200	1.730	2.500	22.800
40.00	20.00	15.00	95.00	-80.00	14.900	2.180	18.200	4.100	7.200	1.020	2.500	22.800
40.00	25.00	15.00	95.00	-80.00	14.900	1.520	20.800	4.100	5.800	0.840	2.500	0.100
40.00	30.00	15.00	95.00	-80.00	14.900	1.520	20.800	4.100	5.800	0.840	2.500	0.100
40.00	35.00	15.00	95.00	-80.00	14.900	1.520	20.800	4.100	5.800	0.840	2.500	0.100
40.00	40.00	15.00	95.00	-80.00	14.900	1.520	20.800	4.100	5.800	0.840	2.500	0.100
5.00	5.00	15.00	85.00	-70.00	14.900	0.700	14.400	4.100	14.900	2.080	2.500	8.300
5.00	10.00	15.00	85.00	-70.00	18.400	1.520	17.100	4.600	14.900	1.020	2.500	22.800
5.00	15.00	15.00	85.00	-70.00	17.900	1.520	13.600	4.600	14.900	0.840	19.600	0.100
5.00	20.00	15.00	85.00	-70.00	14.900	1.520	13.600	4.100	14.900	0.840	19.600	0.100
5.00	25.00	15.00	85.00	-70.00	17.900	1.520	10.300	12.200	17.700	0.840	19.600	0.100
5.00	30.00	15.00	85.00	-70.00	17.900	1.520	10.300	12.200	17.700	0.840	19.600	0.100
5.00	35.00	15.00	85.00	-70.00	17.900	1.520	10.300	12.200	17.700	0.840	19.600	0.100
5.00	40.00	15.00	85.00	-70.00	17.900	1.520	10.300	12.200	17.700	0.840	19.600	0.100
10.00	5.00	15.00	85.00	-70.00	19.100	1.310	17.100	4.600	14.900	1.020	2.500	22.800
10.00	10.00	15.00	85.00	-70.00	17.900	1.310	14.400	4.600	14.900	1.020	2.500	22.800
10.00	15.00	15.00	85.00	-70.00	18.400	1.520	14.300	7.400	5.800	0.840	2.500	0.100
10.00	20.00	15.00	85.00	-70.00	17.900	1.310	14.400	4.600	14.900	1.020	2.500	22.800
10.00	25.00	15.00	85.00	-70.00	17.900	1.070	18.500	16.600	19.100	1.020	2.500	10.900
10.00	30.00	15.00	85.00	-70.00	17.900	1.070	18.500	16.600	19.100	1.020	2.500	10.900
10.00	35.00	15.00	85.00	-70.00	17.900	1.070	18.500	16.600	19.100	1.020	2.500	10.900
10.00	40.00	15.00	85.00	-70.00	17.900	1.070	18.500	16.600	19.100	1.020	2.500	10.900
15.00	5.00	15.00	85.00	-70.00	14.900	0.560	4.200	4.100	11.500	1.990	6.800	5.700
15.00	10.00	15.00	85.00	-70.00	14.900	1.310	7.300	4.100	19.100	2.080	17.200	11.500
15.00	15.00	15.00	85.00	-70.00	12.700	0.700	14.300	4.600	14.900	2.080	2.500	22.800
15.00	20.00	15.00	85.00	-70.00	14.400	1.520	14.400	4.600	14.900	0.840	19.600	0.100
15.00	25.00	15.00	85.00	-70.00	12.700	0.560	10.300	13.700	5.800	1.150	3.100	4.300
15.00	30.00	15.00	85.00	-70.00	12.700	0.560	10.300	13.700	5.800	1.150	3.100	4.300
15.00	35.00	15.00	85.00	-70.00	12.700	0.560	10.300	13.700	5.800	1.150	3.100	4.300
15.00	40.00	15.00	85.00	-70.00	12.700	0.560	10.300	13.700	5.800	1.150	3.100	4.300
20.00	5.00	15.00	85.00	-70.00	17.600	0.700	4.200	6.300	19.100	2.200	18.800	5.700
20.00	10.00	15.00	85.00	-70.00	1.400	0.100	10.700	7.300	17.700	0.370	17.200	11.100
20.00	15.00	15.00	85.00	-70.00	18.400	1.310	14.300	7.400	8.900	1.170	2.500	4.300
20.00	20.00	15.00	85.00	-70.00	17.900	1.310	13.600	4.600	14.900	1.020	2.500	22.800
20.00	25.00	15.00	85.00	-70.00	14.900	0.160	17.100	4.100	5.800	0.370	23.200	8.300
20.00	30.00	15.00	85.00	-70.00	14.900	0.160	17.100	4.100	5.800	0.370	23.200	8.300
20.00	35.00	15.00	85.00	-70.00	14.900	0.160	17.100	4.100	5.800	0.370	23.200	8.300
20.00	40.00	15.00	85.00	-70.00	14.900	0.160	17.100	4.100	5.800	0.370	23.200	8.300
25.00	5.00	15.00	85.00	-70.00	9.000	1.310	4.200	4.600	14.900	0.370	17.200	22.800
25.00	10.00	15.00	85.00	-70.00	15.400	0.700	4.200	6.200	11.500	2.080	6.800	5.700
25.00	15.00	15.00	85.00	-70.00	9.000	1.310	4.200	4.600	14.900	1.990	6.800	5.700
25.00	20.00	15.00	85.00	-70.00	14.900	0.700	14.300	4.100	17.700	1.170	17.600	4.300
25.00	25.00	15.00	85.00	-70.00	17.600	0.700	4.200	6.200	19.600	2.310	18.800	5.700
25.00	30.00	15.00	85.00	-70.00	12.200	0.100	4.200	6.300	17.200	2.310	18.800	5.700
25.00	35.00	15.00	85.00	-70.00	12.200	0.100	4.200	6.300	17.200	2.310	18.800	5.700

25.00	40.00	15.00	85.00	-70.00	12.200	0.100	4.200	6.300	17.200	2.310	18.800	5.700
30.00	5.00	15.00	85.00	-70.00	15.400	1.290	14.400	6.200	11.500	1.990	10.400	8.300
30.00	10.00	15.00	85.00	-70.00	15.400	1.520	14.300	7.400	11.500	0.840	19.600	0.100
30.00	15.00	15.00	85.00	-70.00	2.000	0.100	10.600	22.200	17.700	1.290	10.400	10.200
30.00	20.00	15.00	85.00	-70.00	2.600	0.160	13.600	9.300	2.400	1.150	10.400	8.300
30.00	25.00	15.00	85.00	-70.00	12.200	0.700	4.200	4.600	14.900	2.080	11.500	9.200
30.00	30.00	15.00	85.00	-70.00	14.900	1.310	7.300	4.100	5.800	1.020	2.500	22.800
30.00	35.00	15.00	85.00	-70.00	12.200	0.700	4.200	4.600	14.900	2.080	11.500	9.200
30.00	40.00	15.00	85.00	-70.00	12.200	0.700	4.200	4.600	14.900	2.080	11.500	9.200
35.00	5.00	15.00	85.00	-70.00	22.100	1.520	23.100	4.900	17.700	0.840	2.500	0.100
35.00	10.00	15.00	85.00	-70.00	17.900	1.520	13.600	4.900	20.700	0.840	2.500	0.100
35.00	15.00	15.00	85.00	-70.00	12.200	0.700	13.600	4.900	16.100	2.200	2.500	10.200
35.00	20.00	15.00	85.00	-70.00	22.100	2.180	23.100	4.900	19.100	2.200	10.400	10.700
35.00	25.00	15.00	85.00	-70.00	14.900	1.570	7.300	4.100	14.900	2.080	2.500	22.800
35.00	30.00	15.00	85.00	-70.00	14.900	1.570	7.300	4.100	14.900	2.080	2.500	22.800
35.00	35.00	15.00	85.00	-70.00	14.900	1.570	7.300	4.100	14.900	2.080	2.500	22.800
35.00	40.00	15.00	85.00	-70.00	14.900	1.570	7.300	4.100	14.900	2.080	2.500	22.800
40.00	5.00	15.00	85.00	-70.00	12.200	1.520	7.300	4.900	17.200	0.840	2.500	0.100
40.00	10.00	15.00	85.00	-70.00	22.100	1.290	17.100	4.900	2.400	0.500	17.200	4.300
40.00	15.00	15.00	85.00	-70.00	22.100	2.180	20.800	4.900	4.300	1.170	17.200	20.700
40.00	20.00	15.00	85.00	-70.00	22.100	1.520	18.200	4.900	5.800	0.840	2.500	0.100
40.00	25.00	15.00	85.00	-70.00	14.900	2.180	20.800	4.100	2.400	1.020	2.500	22.800
40.00	30.00	15.00	85.00	-70.00	14.900	2.180	20.800	4.100	2.400	1.020	2.500	22.800
40.00	35.00	15.00	85.00	-70.00	14.900	2.180	20.800	4.100	2.400	1.020	2.500	22.800
40.00	40.00	15.00	85.00	-70.00	14.900	2.180	20.800	4.100	2.400	1.020	2.500	22.800
5.00	5.00	15.00	75.00	-60.00	12.200	0.560	17.100	4.900	5.800	2.080	2.500	22.800
5.00	10.00	15.00	75.00	-60.00	19.100	1.310	17.100	4.600	14.900	1.020	2.500	22.800
5.00	15.00	15.00	75.00	-60.00	12.700	1.520	10.300	4.900	19.100	0.840	19.600	0.100
5.00	20.00	15.00	75.00	-60.00	17.900	1.310	14.400	21.500	17.700	2.200	10.400	10.700
5.00	25.00	15.00	75.00	-60.00	22.200	1.310	5.800	4.900	5.800	1.020	2.500	22.800
5.00	30.00	15.00	75.00	-60.00	22.200	1.310	5.800	4.900	5.800	1.020	2.500	22.800
5.00	35.00	15.00	75.00	-60.00	22.200	1.310	5.800	4.900	5.800	1.020	2.500	22.800
5.00	40.00	15.00	75.00	-60.00	22.200	1.310	5.800	4.900	5.800	1.020	2.500	22.800
10.00	5.00	15.00	95.00	-80.00	18.400	1.520	14.300	4.600	14.900	0.840	2.500	0.100
10.00	10.00	15.00	95.00	-80.00	17.900	1.310	14.400	4.600	14.900	1.020	2.500	22.800
10.00	15.00	15.00	95.00	-80.00	19.100	1.310	17.100	4.600	14.900	1.020	2.500	22.800
10.00	20.00	15.00	95.00	-80.00	19.100	1.520	14.400	4.600	14.900	0.840	19.600	0.100
10.00	25.00	15.00	95.00	-80.00	22.200	1.070	5.800	7.400	14.900	1.020	2.500	22.800
10.00	30.00	15.00	95.00	-80.00	22.200	1.070	5.800	7.400	14.900	1.020	2.500	22.800
10.00	35.00	15.00	95.00	-80.00	22.200	1.070	5.800	7.400	14.900	1.020	2.500	22.800
10.00	40.00	15.00	95.00	-80.00	22.200	1.070	5.800	7.400	14.900	1.020	2.500	22.800
15.00	5.00	15.00	75.00	-60.00	9.000	1.310	4.200	6.400	8.900	1.990	6.800	5.700
15.00	10.00	15.00	75.00	-60.00	18.400	1.520	14.300	7.400	5.800	0.840	2.500	0.100
15.00	15.00	15.00	75.00	-60.00	17.900	1.520	14.400	4.900	5.800	1.020	2.500	22.800
15.00	20.00	15.00	75.00	-60.00	22.200	1.290	5.800	4.900	5.800	1.020	17.200	22.800
15.00	25.00	15.00	75.00	-60.00	14.400	0.550	4.200	23.200	7.900	1.150	6.800	5.700
15.00	30.00	15.00	75.00	-60.00	14.400	0.550	4.200	23.200	7.900	1.150	6.800	5.700
15.00	35.00	15.00	75.00	-60.00	14.400	0.550	4.200	23.200	7.900	1.150	6.800	5.700

15.00	40.00	15.00	75.00	-60.00	14.400	0.550	4.200	23.200	7.900	1.150	6.800	5.700
20.00	5.00	15.00	75.00	-60.00	7.800	0.160	13.600	17.500	17.700	2.310	23.200	8.300
20.00	10.00	15.00	75.00	-60.00	18.400	1.520	14.300	13.200	5.800	0.840	2.500	0.100
20.00	15.00	15.00	75.00	-60.00	14.400	0.160	0.700	7.300	7.900	1.150	20.200	8.300
20.00	20.00	15.00	75.00	-60.00	14.900	1.520	10.300	4.100	5.800	0.840	2.500	0.100
20.00	25.00	15.00	75.00	-60.00	14.900	0.560	4.200	4.100	11.500	1.990	6.800	5.700
20.00	30.00	15.00	75.00	-60.00	14.900	0.560	4.200	4.100	11.500	1.990	6.800	5.700
20.00	35.00	15.00	75.00	-60.00	14.900	0.560	4.200	4.100	11.500	1.990	6.800	5.700
20.00	40.00	15.00	75.00	-60.00	14.900	0.560	4.200	4.100	11.500	1.990	6.800	5.700
25.00	5.00	15.00	75.00	-60.00	9.000	1.310	4.200	4.600	14.900	2.080	6.800	5.700
25.00	10.00	15.00	75.00	-60.00	9.000	0.700	4.200	6.200	8.900	2.080	6.800	5.700
25.00	15.00	15.00	75.00	-60.00	14.900	0.700	4.200	4.100	17.200	2.310	18.800	5.700
25.00	20.00	15.00	75.00	-60.00	17.600	0.700	4.200	6.300	19.100	2.310	18.800	5.700
25.00	25.00	15.00	75.00	-60.00	15.400	0.560	4.200	6.200	11.500	1.990	6.800	5.700
25.00	30.00	15.00	75.00	-60.00	18.400	0.700	4.200	6.200	22.600	2.310	17.600	5.700
25.00	35.00	15.00	75.00	-60.00	18.400	0.700	4.200	6.200	22.600	2.310	17.600	5.700
25.00	40.00	15.00	75.00	-60.00	18.400	0.700	4.200	6.200	22.600	2.310	17.600	5.700
30.00	5.00	15.00	75.00	-60.00	17.900	1.070	18.500	6.300	17.700	0.370	17.200	22.800
30.00	10.00	15.00	75.00	-60.00	12.200	1.520	4.200	6.200	5.800	0.840	19.600	0.100
30.00	15.00	15.00	75.00	-60.00	15.400	0.700	14.300	7.500	11.500	2.080	6.800	5.700
30.00	20.00	15.00	75.00	-60.00	14.900	1.520	7.300	4.100	14.900	0.840	2.500	0.100
30.00	25.00	15.00	75.00	-60.00	12.200	0.700	4.200	4.600	14.900	2.200	2.500	5.700
30.00	30.00	15.00	75.00	-60.00	17.900	2.180	13.600	4.900	5.800	1.020	2.500	22.800
30.00	35.00	15.00	75.00	-60.00	12.200	0.700	4.200	4.600	14.900	2.200	2.500	5.700
30.00	40.00	15.00	75.00	-60.00	12.200	0.700	4.200	4.600	14.900	2.200	2.500	5.700
35.00	5.00	15.00	75.00	-60.00	17.900	1.570	18.200	7.300	20.700	1.730	22.000	8.300
35.00	10.00	15.00	75.00	-60.00	17.900	1.520	13.600	4.900	19.600	0.840	2.500	0.100
35.00	15.00	15.00	75.00	-60.00	12.200	0.560	13.600	4.900	17.700	1.170	18.100	11.500
35.00	20.00	15.00	75.00	-60.00	18.400	1.520	14.400	4.900	5.800	0.840	2.500	0.100
35.00	25.00	15.00	75.00	-60.00	18.400	2.180	23.100	4.900	17.700	2.200	2.500	10.700
35.00	30.00	15.00	75.00	-60.00	18.400	2.180	23.100	4.900	17.700	2.200	2.500	10.700
35.00	35.00	15.00	75.00	-60.00	18.400	2.180	23.100	4.900	17.700	2.200	2.500	10.700
35.00	40.00	15.00	75.00	-60.00	18.400	2.180	23.100	4.900	17.700	2.200	2.500	10.700
40.00	5.00	15.00	75.00	-60.00	18.400	2.180	10.300	6.300	10.400	1.730	2.500	22.800
40.00	10.00	15.00	75.00	-60.00	14.900	1.520	14.300	4.100	14.900	0.840	2.500	0.100
40.00	15.00	15.00	75.00	-60.00	18.400	2.180	18.500	4.600	14.900	0.510	17.600	8.300
40.00	20.00	15.00	75.00	-60.00	22.200	1.520	5.800	4.900	5.800	0.840	2.500	0.100
40.00	25.00	15.00	75.00	-60.00	12.700	1.290	20.800	4.600	14.900	2.200	2.500	22.800
40.00	30.00	15.00	75.00	-60.00	12.700	1.290	20.800	4.600	14.900	2.200	2.500	22.800
40.00	35.00	15.00	75.00	-60.00	12.700	1.290	20.800	4.600	14.900	2.200	2.500	22.800
40.00	40.00	15.00	75.00	-60.00	12.700	1.290	20.800	4.600	14.900	2.200	2.500	22.800
5.00	5.00	15.00	65.00	-50.00	12.200	0.560	10.300	21.500	17.700	1.730	17.200	8.300
5.00	10.00	15.00	65.00	-50.00	19.100	1.070	20.800	4.600	14.900	2.080	17.200	22.800
5.00	15.00	15.00	65.00	-50.00	17.900	1.310	14.400	4.600	14.900	2.200	3.100	22.800
5.00	20.00	15.00	65.00	-50.00	18.400	1.520	14.300	7.400	5.800	0.840	17.600	0.100
5.00	25.00	15.00	65.00	-50.00	19.100	1.520	10.300	13.700	5.800	0.840	19.600	0.100
5.00	30.00	15.00	65.00	-50.00	19.100	1.520	10.300	13.700	5.800	0.840	19.600	0.100
5.00	35.00	15.00	65.00	-50.00	19.100	1.520	10.300	13.700	5.800	0.840	19.600	0.100

5.00	40.00	15.00	65.00	-50.00	19.100	1.520	10.300	13.700	5.800	0.840	19.600	0.100
10.00	5.00	15.00	65.00	-50.00	22.100	1.290	23.100	4.900	5.800	1.020	2.500	22.800
10.00	10.00	15.00	65.00	-50.00	14.900	1.290	10.300	4.100	5.800	1.020	2.500	22.800
10.00	15.00	15.00	65.00	-50.00	12.200	0.700	13.600	8.400	23.000	0.370	18.100	8.300
10.00	20.00	15.00	65.00	-50.00	17.900	1.310	14.400	4.600	14.900	1.020	2.500	22.800
10.00	25.00	15.00	65.00	-50.00	17.900	1.070	18.500	16.600	23.000	1.020	2.500	10.900
10.00	30.00	15.00	65.00	-50.00	17.900	1.070	18.500	16.600	23.000	1.020	2.500	10.900
10.00	35.00	15.00	65.00	-50.00	17.900	1.070	18.500	16.600	23.000	1.020	2.500	10.900
10.00	40.00	15.00	65.00	-50.00	17.900	1.070	18.500	16.600	23.000	1.020	2.500	10.900
15.00	5.00	15.00	65.00	-50.00	12.200	0.100	1.800	13.200	17.200	2.080	18.100	5.700
15.00	10.00	15.00	65.00	-50.00	19.100	1.310	17.100	4.900	2.400	0.030	2.500	11.500
15.00	15.00	15.00	65.00	-50.00	18.400	1.520	14.400	4.900	5.800	1.020	2.500	22.800
15.00	20.00	15.00	65.00	-50.00	18.400	1.310	14.400	4.900	5.800	1.020	2.500	22.800
15.00	25.00	15.00	65.00	-50.00	12.200	0.560	10.300	13.700	10.400	2.200	3.100	10.700
15.00	30.00	15.00	65.00	-50.00	12.200	0.560	10.300	13.700	10.400	2.200	3.100	10.700
15.00	35.00	15.00	65.00	-50.00	12.200	0.560	10.300	13.700	10.400	2.200	3.100	10.700
15.00	40.00	15.00	65.00	-50.00	12.200	0.560	10.300	13.700	10.400	2.200	3.100	10.700
20.00	5.00	15.00	65.00	-50.00	14.900	0.160	13.600	4.100	21.600	2.310	23.200	8.300
20.00	10.00	15.00	65.00	-50.00	12.200	1.520	7.300	7.400	19.100	0.840	2.500	0.100
20.00	15.00	15.00	65.00	-50.00	14.900	1.520	7.300	4.100	8.900	0.840	19.600	0.100
20.00	20.00	15.00	65.00	-50.00	12.700	1.570	7.300	4.600	14.900	1.020	2.500	22.800
20.00	25.00	15.00	65.00	-50.00	18.400	1.310	7.300	4.600	14.900	1.020	17.600	22.800
20.00	30.00	15.00	65.00	-50.00	18.400	1.310	7.300	4.600	14.900	1.020	17.600	22.800
20.00	35.00	15.00	65.00	-50.00	18.400	1.310	7.300	4.600	14.900	1.020	17.600	22.800
20.00	40.00	15.00	65.00	-50.00	18.400	1.310	7.300	4.600	14.900	1.020	17.600	22.800
25.00	5.00	15.00	65.00	-50.00	15.400	0.700	14.300	7.400	11.500	2.080	6.800	5.700
25.00	10.00	15.00	65.00	-50.00	18.400	1.520	13.600	4.600	14.900	0.840	2.500	0.100
25.00	15.00	15.00	65.00	-50.00	14.900	0.100	10.300	4.100	19.100	2.310	2.500	9.800
25.00	20.00	15.00	65.00	-50.00	15.400	0.700	20.800	12.200	17.700	0.780	17.200	4.300
25.00	25.00	15.00	65.00	-50.00	17.900	1.290	14.400	16.500	19.600	1.730	10.400	8.300
25.00	30.00	15.00	65.00	-50.00	22.100	1.520	10.300	17.500	5.800	0.840	2.500	0.100
25.00	35.00	15.00	65.00	-50.00	22.100	1.520	10.300	17.500	5.800	0.840	2.500	0.100
25.00	40.00	15.00	65.00	-50.00	22.100	1.520	10.300	17.500	5.800	0.840	2.500	0.100
30.00	5.00	15.00	65.00	-50.00	12.200	1.520	7.300	7.300	16.100	0.840	2.500	0.100
30.00	10.00	15.00	65.00	-50.00	14.900	1.520	7.300	4.100	5.800	0.840	2.500	0.100
30.00	15.00	15.00	65.00	-50.00	14.900	1.520	10.300	4.100	5.800	0.840	2.500	0.100
30.00	20.00	15.00	65.00	-50.00	12.200	1.520	7.300	4.900	5.800	0.840	2.500	0.100
30.00	25.00	15.00	65.00	-50.00	13.700	1.070	13.600	8.400	5.800	1.730	2.500	8.300
30.00	30.00	15.00	65.00	-50.00	13.700	1.070	13.600	8.400	5.800	1.730	2.500	8.300
30.00	35.00	15.00	65.00	-50.00	13.700	1.070	13.600	8.400	5.800	1.730	2.500	8.300
30.00	40.00	15.00	65.00	-50.00	13.700	1.070	13.600	8.400	5.800	1.730	2.500	8.300
35.00	5.00	15.00	65.00	-50.00	22.100	1.070	23.100	4.900	17.200	1.170	17.200	8.300
35.00	10.00	15.00	65.00	-50.00	13.700	1.070	18.500	7.300	19.100	1.170	2.500	10.200
35.00	15.00	15.00	65.00	-50.00	12.700	1.520	10.300	4.600	14.900	0.840	2.500	0.100
35.00	20.00	15.00	65.00	-50.00	13.700	1.290	14.400	4.900	17.700	2.200	12.700	10.700
35.00	25.00	15.00	65.00	-50.00	14.400	1.570	10.300	4.600	14.900	2.080	2.500	22.800
35.00	30.00	15.00	65.00	-50.00	14.400	1.570	10.300	4.600	14.900	2.080	2.500	22.800
35.00	35.00	15.00	65.00	-50.00	14.400	1.570	10.300	4.600	14.900	2.080	2.500	22.800

35.00	40.00	15.00	65.00	-50.00	14.400	1.570	10.300	4.600	14.900	2.080	2.500	22.800
40.00	5.00	15.00	65.00	-50.00	19.100	1.520	18.500	4.900	19.100	0.840	2.500	0.100
40.00	10.00	15.00	65.00	-50.00	22.100	1.570	20.800	4.900	16.100	1.730	4.300	4.300
40.00	15.00	15.00	65.00	-50.00	18.400	1.570	20.800	4.900	22.600	0.030	2.500	22.800
40.00	20.00	15.00	65.00	-50.00	22.100	1.520	18.200	4.900	5.800	0.840	2.500	0.100
40.00	25.00	15.00	65.00	-50.00	14.900	1.520	20.800	4.100	5.800	0.840	2.500	0.100
40.00	30.00	15.00	65.00	-50.00	14.900	1.520	20.800	4.100	5.800	0.840	2.500	0.100
40.00	35.00	15.00	65.00	-50.00	14.900	1.520	20.800	4.100	5.800	0.840	2.500	0.100
40.00	40.00	15.00	65.00	-50.00	14.900	1.520	20.800	4.100	5.800	0.840	2.500	0.100
5.00	5.00	15.00	55.00	-40.00	19.100	1.290	17.100	4.900	5.800	1.020	2.500	22.800
5.00	10.00	15.00	55.00	-40.00	14.400	1.290	10.300	4.600	14.900	1.020	2.500	22.800
5.00	15.00	15.00	55.00	-40.00	12.700	1.520	10.300	4.600	14.900	0.840	19.600	0.100
5.00	20.00	15.00	55.00	-40.00	13.700	1.290	18.500	4.600	14.900	1.170	17.200	8.300
5.00	25.00	15.00	55.00	-40.00	22.200	1.070	5.800	6.300	5.800	1.020	2.500	22.800
5.00	30.00	15.00	55.00	-40.00	22.200	1.070	5.800	6.300	5.800	1.020	2.500	22.800
5.00	35.00	15.00	55.00	-40.00	22.200	1.070	5.800	6.300	5.800	1.020	2.500	22.800
5.00	40.00	15.00	55.00	-40.00	22.200	1.070	5.800	6.300	5.800	1.020	2.500	22.800
10.00	5.00	15.00	55.00	-40.00	17.900	1.310	14.400	4.600	14.900	1.020	2.500	22.800
10.00	10.00	15.00	55.00	-40.00	12.200	1.290	7.300	4.900	16.100	1.730	2.500	8.300
10.00	15.00	15.00	55.00	-40.00	17.900	1.070	18.500	4.900	3.800	1.170	18.100	10.200
10.00	20.00	15.00	55.00	-40.00	17.900	1.310	14.400	4.600	14.900	1.020	2.500	22.800
10.00	25.00	15.00	55.00	-40.00	17.600	0.560	18.200	6.200	19.100	2.080	2.500	5.700
10.00	30.00	15.00	55.00	-40.00	17.600	0.560	18.200	6.200	19.100	2.080	2.500	5.700
10.00	35.00	15.00	55.00	-40.00	17.600	0.560	18.200	6.200	19.100	2.080	2.500	5.700
10.00	40.00	15.00	55.00	-40.00	17.600	0.560	18.200	6.200	19.100	2.080	2.500	5.700
15.00	5.00	15.00	55.00	-40.00	12.700	0.700	7.300	4.600	14.900	2.080	2.500	22.800
15.00	10.00	15.00	55.00	-40.00	18.400	1.520	14.300	7.400	5.800	0.840	2.500	0.100
15.00	15.00	15.00	55.00	-40.00	19.100	2.180	14.300	13.200	5.800	2.080	2.500	4.300
15.00	20.00	15.00	55.00	-40.00	19.100	1.520	14.400	4.900	5.800	1.020	2.500	22.800
15.00	25.00	15.00	55.00	-40.00	13.700	1.290	10.700	6.300	5.800	1.020	2.500	22.800
15.00	30.00	15.00	55.00	-40.00	13.700	1.290	10.700	6.300	5.800	1.020	2.500	22.800
15.00	35.00	15.00	55.00	-40.00	13.700	1.290	10.700	6.300	5.800	1.020	2.500	22.800
15.00	40.00	15.00	55.00	-40.00	13.700	1.290	10.700	6.300	5.800	1.020	2.500	22.800
20.00	5.00	15.00	55.00	-40.00	14.900	0.160	4.200	4.100	17.200	1.150	22.000	10.200
20.00	10.00	15.00	55.00	-40.00	18.400	1.520	14.300	7.400	5.800	0.840	2.500	0.100
20.00	15.00	15.00	55.00	-40.00	9.000	0.700	7.300	4.900	19.100	0.370	2.500	11.500
20.00	20.00	15.00	55.00	-40.00	12.200	1.520	7.300	4.900	5.800	1.020	2.500	22.800
20.00	25.00	15.00	55.00	-40.00	18.400	1.520	7.300	13.200	7.200	0.840	2.500	0.100
20.00	30.00	15.00	55.00	-40.00	18.400	1.520	7.300	13.200	7.200	0.840	2.500	0.100
20.00	35.00	15.00	55.00	-40.00	18.400	1.520	7.300	13.200	7.200	0.840	2.500	0.100
20.00	40.00	15.00	55.00	-40.00	18.400	1.520	7.300	13.200	7.200	0.840	2.500	0.100
25.00	5.00	15.00	55.00	-40.00	18.400	1.520	13.600	7.400	5.800	0.840	2.500	0.100
25.00	10.00	15.00	55.00	-40.00	14.900	1.520	7.300	4.100	14.900	0.840	2.500	0.100
25.00	15.00	15.00	55.00	-40.00	14.900	0.100	10.300	4.100	23.000	2.080	17.200	11.500
25.00	20.00	15.00	55.00	-40.00	7.800	0.160	1.800	6.200	17.200	2.310	11.500	9.200
25.00	25.00	15.00	55.00	-40.00	12.200	0.560	14.400	16.600	19.100	1.730	12.700	8.300
25.00	30.00	15.00	55.00	-40.00	14.900	0.700	13.600	4.100	17.700	1.990	18.800	8.300
25.00	35.00	15.00	55.00	-40.00	14.900	0.700	13.600	4.100	17.700	1.990	18.800	8.300

25.00	40.00	15.00	55.00	-40.00	14.900	0.700	13.600	4.100	17.700	1.990	18.800	8.300
30.00	5.00	15.00	55.00	-40.00	17.900	1.570	14.400	16.600	22.600	0.500	10.400	8.300
30.00	10.00	15.00	55.00	-40.00	9.000	1.310	4.200	4.600	14.900	1.990	6.800	22.800
30.00	15.00	15.00	55.00	-40.00	14.900	0.560	4.200	4.100	8.900	1.990	6.800	5.700
30.00	20.00	15.00	55.00	-40.00	12.200	1.520	7.300	4.900	5.800	0.840	2.500	0.100
30.00	25.00	15.00	55.00	-40.00	12.200	0.700	4.200	4.600	14.900	2.080	17.200	11.500
30.00	30.00	15.00	55.00	-40.00	12.200	0.560	13.600	4.900	20.700	1.730	17.200	8.300
30.00	35.00	15.00	55.00	-40.00	12.200	0.700	4.200	4.600	14.900	2.080	17.200	11.500
30.00	40.00	15.00	55.00	-40.00	12.200	0.700	4.200	4.600	14.900	2.080	17.200	11.500
35.00	5.00	15.00	55.00	-40.00	22.100	1.310	23.100	4.900	7.200	0.500	3.100	9.800
35.00	10.00	15.00	55.00	-40.00	22.100	1.520	20.800	4.900	17.700	0.840	19.600	0.100
35.00	15.00	15.00	55.00	-40.00	13.700	1.070	13.600	4.900	17.700	1.730	3.100	8.300
35.00	20.00	15.00	55.00	-40.00	22.100	1.520	20.800	4.600	14.900	0.840	2.500	0.100
35.00	25.00	15.00	55.00	-40.00	14.900	2.180	18.500	4.100	14.900	1.150	2.500	22.800
35.00	30.00	15.00	55.00	-40.00	14.900	2.180	18.500	4.100	14.900	1.150	2.500	22.800
35.00	35.00	15.00	55.00	-40.00	14.900	2.180	18.500	4.100	14.900	1.150	2.500	22.800
35.00	40.00	15.00	55.00	-40.00	14.900	2.180	18.500	4.100	14.900	1.150	2.500	22.800
40.00	5.00	15.00	55.00	-40.00	9.100	1.290	18.500	8.400	5.500	0.750	10.400	8.300
40.00	10.00	15.00	55.00	-40.00	17.900	2.180	17.100	16.600	2.400	1.730	2.500	10.200
40.00	15.00	15.00	55.00	-40.00	14.900	1.570	20.800	4.100	20.700	1.020	17.600	22.800
40.00	20.00	15.00	55.00	-40.00	14.900	1.520	18.200	4.100	14.900	0.840	2.500	0.100
40.00	25.00	15.00	55.00	-40.00	14.900	1.520	20.800	4.100	5.800	0.840	2.500	0.100
40.00	30.00	15.00	55.00	-40.00	14.900	1.520	20.800	4.100	5.800	0.840	2.500	0.100
40.00	35.00	15.00	55.00	-40.00	14.900	1.520	20.800	4.100	5.800	0.840	2.500	0.100
40.00	40.00	15.00	55.00	-40.00	14.900	1.520	20.800	4.100	5.800	0.840	2.500	0.100
5.00	5.00	15.00	45.00	-30.00	17.900	1.310	14.400	4.600	14.900	1.020	2.500	10.900
5.00	10.00	15.00	45.00	-30.00	18.400	1.520	14.300	7.300	23.000	0.840	2.500	0.100
5.00	15.00	15.00	45.00	-30.00	18.400	1.520	14.300	7.400	5.800	0.840	17.600	0.100
5.00	20.00	15.00	45.00	-30.00	18.400	1.520	10.700	4.600	14.900	0.840	2.500	22.800
5.00	25.00	15.00	45.00	-30.00	12.200	1.520	7.300	13.200	5.800	0.840	19.600	0.100
5.00	30.00	15.00	45.00	-30.00	12.200	1.520	7.300	13.200	5.800	0.840	19.600	0.100
5.00	35.00	15.00	45.00	-30.00	12.200	1.520	7.300	13.200	5.800	0.840	19.600	0.100
5.00	40.00	15.00	45.00	-30.00	12.200	1.520	7.300	13.200	5.800	0.840	19.600	0.100
10.00	5.00	15.00	45.00	-30.00	17.900	1.310	14.400	4.600	14.900	1.020	2.500	22.800
10.00	10.00	15.00	45.00	-30.00	22.100	1.520	20.800	13.200	5.800	0.840	2.500	0.100
10.00	15.00	15.00	45.00	-30.00	22.100	1.520	20.800	4.900	19.100	0.840	19.600	0.100
10.00	20.00	15.00	45.00	-30.00	18.400	1.520	14.400	4.600	14.900	0.840	17.600	0.100
10.00	25.00	15.00	45.00	-30.00	14.900	0.560	7.300	4.100	14.900	1.020	2.500	22.800
10.00	30.00	15.00	45.00	-30.00	14.900	0.560	7.300	4.100	14.900	1.020	2.500	22.800
10.00	35.00	15.00	45.00	-30.00	14.900	0.560	7.300	4.100	14.900	1.020	2.500	22.800
10.00	40.00	15.00	45.00	-30.00	14.900	0.560	7.300	4.100	14.900	1.020	2.500	22.800
15.00	5.00	15.00	45.00	-30.00	18.400	1.520	14.300	7.400	5.800	0.840	2.500	0.100
15.00	10.00	15.00	45.00	-30.00	17.900	1.570	14.400	16.500	17.200	2.080	2.500	10.200
15.00	15.00	15.00	45.00	-30.00	14.400	1.520	14.300	7.500	5.800	0.840	2.500	0.100
15.00	20.00	15.00	45.00	-30.00	18.400	1.520	14.300	7.400	5.800	0.840	17.600	0.100
15.00	25.00	15.00	45.00	-30.00	12.200	0.560	14.400	4.600	14.900	0.510	3.100	22.800
15.00	30.00	15.00	45.00	-30.00	12.200	0.560	14.400	4.600	14.900	0.510	3.100	22.800
15.00	35.00	15.00	45.00	-30.00	12.200	0.560	14.400	4.600	14.900	0.510	3.100	22.800

15.00	40.00	15.00	45.00	-30.00	12.200	0.560	14.400	4.600	14.900	0.510	3.100	22.800
20.00	5.00	15.00	45.00	-30.00	14.900	0.100	13.600	4.100	21.600	2.310	3.100	8.300
20.00	10.00	15.00	45.00	-30.00	12.200	1.520	7.300	4.600	14.900	0.840	2.500	0.100
20.00	15.00	15.00	45.00	-30.00	9.000	0.700	7.300	4.900	17.200	2.080	11.500	22.800
20.00	20.00	15.00	45.00	-30.00	22.100	1.310	23.100	4.600	14.900	1.020	2.500	22.800
20.00	25.00	15.00	45.00	-30.00	12.700	0.560	10.300	13.700	23.000	2.080	2.500	4.300
20.00	30.00	15.00	45.00	-30.00	12.700	0.560	10.300	13.700	23.000	2.080	2.500	4.300
20.00	35.00	15.00	45.00	-30.00	12.700	0.560	10.300	13.700	23.000	2.080	2.500	4.300
20.00	40.00	15.00	45.00	-30.00	12.700	0.560	10.300	13.700	23.000	2.080	2.500	4.300
25.00	5.00	15.00	45.00	-30.00	18.400	1.520	13.600	4.600	14.900	0.840	2.500	0.100
25.00	10.00	15.00	45.00	-30.00	15.400	1.520	10.700	13.200	5.800	0.840	2.500	0.100
25.00	15.00	15.00	45.00	-30.00	19.100	1.520	14.400	4.600	14.900	0.840	2.500	0.100
25.00	20.00	15.00	45.00	-30.00	18.400	0.100	4.200	17.500	17.200	2.310	17.600	5.700
25.00	25.00	15.00	45.00	-30.00	17.600	1.070	7.300	6.300	19.100	1.020	2.500	10.900
25.00	30.00	15.00	45.00	-30.00	17.600	1.070	7.300	6.300	19.100	1.020	2.500	10.900
25.00	35.00	15.00	45.00	-30.00	17.600	1.070	7.300	6.300	19.100	1.020	2.500	10.900
25.00	40.00	15.00	45.00	-30.00	17.600	1.070	7.300	6.300	19.100	1.020	2.500	10.900
30.00	5.00	15.00	45.00	-30.00	17.900	1.290	14.400	13.200	17.200	1.730	12.700	8.300
30.00	10.00	15.00	45.00	-30.00	17.900	1.520	14.300	7.500	5.800	0.840	2.500	0.100
30.00	15.00	15.00	45.00	-30.00	18.400	1.520	14.300	7.500	5.800	0.840	2.500	0.100
30.00	20.00	15.00	45.00	-30.00	18.400	1.520	14.300	4.600	14.900	0.840	2.500	0.100
30.00	25.00	15.00	45.00	-30.00	13.700	1.290	14.300	21.700	12.400	1.730	2.500	8.300
30.00	30.00	15.00	45.00	-30.00	13.700	1.290	14.300	21.700	12.400	1.730	2.500	8.300
30.00	35.00	15.00	45.00	-30.00	13.700	1.290	14.300	21.700	12.400	1.730	2.500	8.300
30.00	40.00	15.00	45.00	-30.00	13.700	1.290	14.300	21.700	12.400	1.730	2.500	8.300
35.00	5.00	15.00	45.00	-30.00	17.900	1.570	10.700	7.300	20.700	1.730	17.200	11.500
35.00	10.00	15.00	45.00	-30.00	15.400	1.070	7.300	6.400	11.500	1.990	13.700	8.300
35.00	15.00	15.00	45.00	-30.00	13.700	1.520	13.600	4.600	14.900	0.840	2.500	0.100
35.00	20.00	15.00	45.00	-30.00	9.100	1.070	14.400	16.600	2.400	1.150	10.400	8.300
35.00	25.00	15.00	45.00	-30.00	15.400	1.520	10.300	4.600	14.900	0.840	2.500	22.800
35.00	30.00	15.00	45.00	-30.00	15.400	1.520	10.300	4.600	14.900	0.840	2.500	22.800
35.00	35.00	15.00	45.00	-30.00	15.400	1.520	10.300	4.600	14.900	0.840	2.500	22.800
35.00	40.00	15.00	45.00	-30.00	15.400	1.520	10.300	4.600	14.900	0.840	2.500	22.800
40.00	5.00	15.00	45.00	-30.00	22.100	2.180	18.200	4.900	4.300	2.080	10.400	20.700
40.00	10.00	15.00	45.00	-30.00	22.100	1.570	20.800	4.900	19.100	0.500	3.100	4.300
40.00	15.00	15.00	45.00	-30.00	22.100	1.570	18.200	4.900	17.700	2.080	17.200	11.500
40.00	20.00	15.00	45.00	-30.00	19.100	2.180	18.500	4.900	22.600	2.080	11.500	11.500
40.00	25.00	15.00	45.00	-30.00	14.900	1.520	20.800	4.100	5.800	0.840	2.500	0.100
40.00	30.00	15.00	45.00	-30.00	14.900	1.520	20.800	4.100	5.800	0.840	2.500	0.100
40.00	35.00	15.00	45.00	-30.00	14.900	1.520	20.800	4.100	5.800	0.840	2.500	0.100
40.00	40.00	15.00	45.00	-30.00	14.900	1.520	18.200	4.100	14.900	0.840	2.500	0.100
5.00	5.00	15.00	35.00	-20.00	12.200	1.520	7.300	4.900	5.800	0.840	2.500	0.100
5.00	10.00	15.00	35.00	-20.00	19.100	1.290	17.100	4.600	14.900	2.080	2.500	22.800
5.00	15.00	15.00	35.00	-20.00	12.200	1.290	7.300	4.600	14.900	0.370	11.500	22.800
5.00	20.00	15.00	35.00	-20.00	15.400	1.290	10.300	7.400	5.800	2.080	2.500	22.800
5.00	25.00	15.00	35.00	-20.00	18.400	1.520	5.800	12.200	4.300	0.840	17.600	0.100
5.00	30.00	15.00	35.00	-20.00	18.400	1.520	5.800	12.200	4.300	0.840	17.600	0.100
5.00	35.00	15.00	35.00	-20.00	18.400	1.520	5.800	12.200	4.300	0.840	17.600	0.100

5.00	40.00	15.00	35.00	-20.00	18.400	1.520	5.800	12.200	4.300	0.840	17.600	0.100
10.00	5.00	15.00	35.00	-20.00	17.900	1.310	14.400	4.600	14.900	1.020	2.500	22.800
10.00	10.00	15.00	35.00	-20.00	22.100	1.520	20.800	4.600	14.900	0.840	2.500	0.100
10.00	15.00	15.00	35.00	-20.00	14.400	1.520	10.700	7.400	7.900	0.840	2.500	0.100
10.00	20.00	15.00	35.00	-20.00	18.400	1.520	14.300	7.500	4.300	0.840	2.500	0.100
10.00	25.00	15.00	35.00	-20.00	14.400	0.560	7.300	7.300	17.200	2.200	22.000	10.700
10.00	30.00	15.00	35.00	-20.00	14.400	0.560	7.300	7.300	17.200	2.200	22.000	10.700
10.00	35.00	15.00	35.00	-20.00	14.400	0.560	7.300	7.300	17.200	2.200	22.000	10.700
10.00	40.00	15.00	35.00	-20.00	14.400	0.560	7.300	7.300	17.200	2.200	22.000	10.700
15.00	5.00	15.00	35.00	-20.00	18.400	1.520	14.300	7.500	5.800	0.840	2.500	0.100
15.00	10.00	15.00	35.00	-20.00	17.900	1.520	14.400	16.500	5.800	0.840	2.500	0.100
15.00	15.00	15.00	35.00	-20.00	13.700	1.310	10.700	4.600	14.900	1.730	3.100	22.800
15.00	20.00	15.00	35.00	-20.00	19.100	1.290	17.100	4.600	14.900	1.020	2.500	22.800
15.00	25.00	15.00	35.00	-20.00	14.400	0.560	14.400	6.300	5.800	1.020	2.500	22.800
15.00	30.00	15.00	35.00	-20.00	14.400	0.560	14.400	6.300	5.800	1.020	2.500	22.800
15.00	35.00	15.00	35.00	-20.00	14.400	0.560	14.400	6.300	5.800	1.020	2.500	22.800
15.00	40.00	15.00	35.00	-20.00	14.400	0.560	14.400	6.300	5.800	1.020	2.500	22.800
20.00	5.00	15.00	35.00	-20.00	14.400	1.520	7.300	7.400	7.900	0.840	2.500	0.100
20.00	10.00	15.00	35.00	-20.00	12.200	1.520	7.300	4.900	5.800	0.840	2.500	0.100
20.00	15.00	15.00	35.00	-20.00	12.200	0.700	4.200	6.200	16.100	2.080	22.000	5.700
20.00	20.00	15.00	35.00	-20.00	12.200	1.310	7.300	4.900	5.800	1.020	2.500	22.800
20.00	25.00	15.00	35.00	-20.00	12.700	0.560	4.200	6.200	8.900	1.150	2.500	5.700
20.00	30.00	15.00	35.00	-20.00	12.700	0.560	4.200	6.200	8.900	1.150	2.500	5.700
20.00	35.00	15.00	35.00	-20.00	12.700	0.560	4.200	6.200	8.900	1.150	2.500	5.700
20.00	40.00	15.00	35.00	-20.00	12.700	0.560	4.200	6.200	8.900	1.150	2.500	5.700
25.00	5.00	15.00	35.00	-20.00	13.700	1.520	10.300	13.200	5.800	0.840	2.500	0.100
25.00	10.00	15.00	35.00	-20.00	18.400	1.520	14.400	13.200	5.800	0.840	2.500	0.100
25.00	15.00	15.00	35.00	-20.00	12.200	1.520	7.300	7.400	5.800	0.840	2.500	0.100
25.00	20.00	15.00	35.00	-20.00	15.400	1.520	10.700	13.200	5.800	0.840	2.500	0.100
25.00	25.00	15.00	35.00	-20.00	12.200	0.700	14.400	21.500	17.200	1.170	18.100	8.300
25.00	30.00	15.00	35.00	-20.00	12.200	0.700	14.400	21.500	17.200	1.170	18.100	8.300
25.00	35.00	15.00	35.00	-20.00	12.200	0.700	14.400	21.500	17.200	1.170	18.100	8.300
25.00	40.00	15.00	35.00	-20.00	12.200	0.700	14.400	21.500	17.200	1.170	18.100	8.300
30.00	5.00	15.00	35.00	-20.00	14.900	1.520	7.300	4.100	5.800	0.840	2.500	0.100
30.00	10.00	15.00	35.00	-20.00	14.900	0.700	4.200	4.100	11.500	1.990	17.200	9.200
30.00	15.00	15.00	35.00	-20.00	14.900	1.310	13.600	4.100	17.700	2.080	10.400	8.300
30.00	20.00	15.00	35.00	-20.00	18.400	1.520	14.400	13.200	5.800	0.840	2.500	0.100
30.00	25.00	15.00	35.00	-20.00	12.200	0.700	10.700	4.600	14.900	2.310	11.500	10.200
30.00	30.00	15.00	35.00	-20.00	12.200	0.560	13.600	4.900	20.700	1.730	10.400	9.800
30.00	35.00	15.00	35.00	-20.00	12.200	0.700	10.700	4.600	14.900	2.310	11.500	10.200
30.00	40.00	15.00	35.00	-20.00	12.200	0.700	10.700	4.600	14.900	2.310	11.500	10.200
35.00	5.00	15.00	35.00	-20.00	17.900	1.570	10.700	4.900	7.200	0.500	3.100	11.100
35.00	10.00	15.00	35.00	-20.00	17.900	1.310	10.300	4.900	10.400	1.730	3.100	9.800
35.00	15.00	15.00	35.00	-20.00	17.600	1.520	20.800	6.300	5.800	0.840	2.500	11.500
35.00	20.00	15.00	35.00	-20.00	18.400	1.290	10.700	6.300	19.100	1.020	17.600	10.900
35.00	25.00	15.00	35.00	-20.00	14.900	1.570	7.300	4.100	14.900	1.150	2.500	22.800
35.00	30.00	15.00	35.00	-20.00	14.900	1.570	7.300	4.100	14.900	1.150	2.500	22.800
35.00	35.00	15.00	35.00	-20.00	14.900	1.570	7.300	4.100	14.900	1.150	2.500	22.800

35.00	40.00	15.00	35.00	-20.00	14.900	1.570	7.300	4.100	14.900	1.150	2.500	22.800
40.00	5.00	15.00	35.00	-20.00	22.200	1.570	5.800	4.600	14.900	1.150	16.300	22.800
40.00	10.00	15.00	35.00	-20.00	22.100	1.570	18.200	4.900	19.100	2.080	12.700	8.300
40.00	15.00	15.00	35.00	-20.00	17.900	1.520	18.500	4.900	5.800	0.840	2.500	0.100
40.00	20.00	15.00	35.00	-20.00	14.900	2.180	20.800	4.100	17.200	1.020	17.200	22.800
40.00	25.00	15.00	35.00	-20.00	14.900	2.180	20.800	4.100	23.000	0.370	2.500	22.800
40.00	30.00	15.00	35.00	-20.00	14.900	2.180	20.800	4.100	23.000	0.370	2.500	22.800
40.00	35.00	15.00	35.00	-20.00	14.900	2.180	20.800	4.100	23.000	0.370	2.500	22.800
40.00	40.00	15.00	35.00	-20.00	14.900	2.180	20.800	4.100	23.000	0.370	2.500	22.800
5.00	5.00	15.00	25.00	-10.00	12.200	1.290	7.300	4.600	14.900	1.020	4.300	22.800
5.00	10.00	15.00	25.00	-10.00	18.400	1.520	14.300	7.400	5.800	0.840	2.500	0.100
5.00	15.00	15.00	25.00	-10.00	12.200	1.070	7.300	4.600	14.900	2.200	2.500	22.800
5.00	20.00	15.00	25.00	-10.00	14.900	1.070	14.300	4.100	23.000	0.370	1.900	10.700
5.00	25.00	15.00	25.00	-10.00	22.200	1.520	5.800	13.200	5.800	0.840	19.600	0.100
5.00	30.00	15.00	25.00	-10.00	22.200	1.520	5.800	13.200	5.800	0.840	19.600	0.100
5.00	35.00	15.00	25.00	-10.00	22.200	1.520	5.800	13.200	5.800	0.840	19.600	0.100
5.00	40.00	15.00	25.00	-10.00	22.200	1.520	5.800	13.200	5.800	0.840	19.600	0.100
10.00	5.00	15.00	25.00	-10.00	18.400	1.520	14.300	7.400	14.900	0.840	2.500	0.100
10.00	10.00	15.00	25.00	-10.00	14.900	1.520	10.300	4.100	5.800	0.840	2.500	0.100
10.00	15.00	15.00	25.00	-10.00	18.400	1.520	14.300	7.400	5.800	0.840	17.600	0.100
10.00	20.00	15.00	25.00	-10.00	19.100	1.290	18.500	13.200	23.000	1.020	17.200	10.900
10.00	25.00	15.00	25.00	-10.00	14.400	0.560	7.300	4.900	7.900	1.150	13.700	10.200
10.00	30.00	15.00	25.00	-10.00	14.400	0.560	7.300	4.900	7.900	1.150	13.700	10.200
10.00	35.00	15.00	25.00	-10.00	14.400	0.560	7.300	4.900	7.900	1.150	13.700	10.200
10.00	40.00	15.00	25.00	-10.00	14.400	0.560	7.300	4.900	7.900	1.150	13.700	10.200
15.00	5.00	15.00	25.00	-10.00	18.400	1.520	14.300	7.400	5.800	0.840	2.500	0.100
15.00	10.00	15.00	25.00	-10.00	17.900	1.570	14.400	16.600	3.800	1.020	2.500	10.900
15.00	15.00	15.00	25.00	-10.00	17.600	1.570	14.300	4.600	14.900	0.370	18.100	4.300
15.00	20.00	15.00	25.00	-10.00	19.100	1.310	17.100	4.900	5.800	1.020	2.500	22.800
15.00	25.00	15.00	25.00	-10.00	17.900	0.700	14.400	16.600	22.600	1.170	11.500	9.200
15.00	30.00	15.00	25.00	-10.00	17.900	0.700	14.400	16.600	22.600	1.170	11.500	9.200
15.00	35.00	15.00	25.00	-10.00	17.900	0.700	14.400	16.600	22.600	1.170	11.500	9.200
15.00	40.00	15.00	25.00	-10.00	17.900	0.700	14.400	16.600	22.600	1.170	11.500	9.200
20.00	5.00	15.00	25.00	-10.00	12.200	0.700	13.600	16.500	19.100	2.080	4.300	8.300
20.00	10.00	15.00	25.00	-10.00	18.400	1.520	14.300	7.400	5.800	0.840	2.500	0.100
20.00	15.00	15.00	25.00	-10.00	15.400	1.070	14.400	6.200	11.500	1.990	10.400	8.300
20.00	20.00	15.00	25.00	-10.00	9.000	0.700	1.800	4.600	14.900	2.080	2.500	22.800
20.00	25.00	15.00	25.00	-10.00	14.900	0.700	7.300	4.100	17.200	2.310	17.600	8.300
20.00	30.00	15.00	25.00	-10.00	14.900	0.700	7.300	4.100	17.200	2.310	17.600	8.300
20.00	35.00	15.00	25.00	-10.00	14.900	0.700	7.300	4.100	17.200	2.310	17.600	8.300
20.00	40.00	15.00	25.00	-10.00	14.900	0.700	7.300	4.100	17.200	2.310	17.600	8.300
25.00	5.00	15.00	25.00	-10.00	13.700	1.310	14.400	17.500	23.000	2.080	2.500	11.500
25.00	10.00	15.00	25.00	-10.00	13.700	1.070	10.700	4.600	14.900	1.020	2.500	22.800
25.00	15.00	15.00	25.00	-10.00	12.200	1.520	7.300	7.400	5.800	0.840	2.500	0.100
25.00	20.00	15.00	25.00	-10.00	12.200	0.700	4.200	4.600	14.900	2.080	2.500	5.700
25.00	25.00	15.00	25.00	-10.00	18.400	0.560	4.200	4.600	14.900	1.730	17.600	22.800
25.00	30.00	15.00	25.00	-10.00	18.400	0.560	4.200	4.600	14.900	1.730	17.600	22.800
25.00	35.00	15.00	25.00	-10.00	18.400	0.560	4.200	4.600	14.900	1.730	17.600	22.800

25.00	40.00	15.00	25.00	-10.00	18.400	0.560	4.200	4.600	14.900	1.730	17.600	22.800
30.00	5.00	15.00	25.00	-10.00	17.900	1.070	18.200	4.900	22.600	0.500	10.400	8.300
30.00	10.00	15.00	25.00	-10.00	18.400	1.520	14.300	7.500	5.800	0.840	2.500	0.100
30.00	15.00	15.00	25.00	-10.00	18.400	1.520	14.300	7.500	5.800	0.840	2.500	0.100
30.00	20.00	15.00	25.00	-10.00	18.400	1.520	13.600	7.400	14.900	0.840	2.500	0.100
30.00	25.00	15.00	25.00	-10.00	12.200	0.700	4.200	6.300	19.100	0.370	17.200	5.700
30.00	30.00	15.00	25.00	-10.00	13.700	1.290	13.600	16.500	2.400	1.150	10.400	8.300
30.00	35.00	15.00	25.00	-10.00	12.200	0.700	4.200	6.300	19.100	0.370	17.200	5.700
30.00	40.00	15.00	25.00	-10.00	12.200	0.700	4.200	6.300	19.100	0.370	17.200	5.700
35.00	5.00	15.00	25.00	-10.00	17.900	1.570	18.500	9.300	22.600	1.730	3.100	8.300
35.00	10.00	15.00	25.00	-10.00	17.900	1.310	13.600	4.900	20.700	1.730	3.100	10.200
35.00	15.00	15.00	25.00	-10.00	15.400	1.520	10.700	7.400	5.800	0.840	2.500	0.100
35.00	20.00	15.00	25.00	-10.00	13.700	1.070	14.400	4.900	17.700	1.730	12.700	8.300
35.00	25.00	15.00	25.00	-10.00	14.900	1.570	14.400	4.100	14.900	2.200	11.500	11.500
35.00	30.00	15.00	25.00	-10.00	14.900	1.570	14.400	4.100	14.900	2.200	11.500	11.500
35.00	35.00	15.00	25.00	-10.00	14.900	1.570	14.400	4.100	14.900	2.200	11.500	11.500
35.00	40.00	15.00	25.00	-10.00	14.900	1.570	14.400	4.100	14.900	2.200	11.500	11.500
40.00	5.00	15.00	25.00	-10.00	18.400	1.290	18.500	4.900	20.700	1.730	17.600	8.300
40.00	10.00	15.00	25.00	-10.00	18.400	1.520	18.500	4.900	5.800	0.840	2.500	0.100
40.00	15.00	15.00	25.00	-10.00	18.400	1.520	18.500	4.900	5.800	0.840	2.500	0.100
40.00	20.00	15.00	25.00	-10.00	18.400	1.520	20.800	4.900	5.800	0.840	2.500	0.100
40.00	25.00	15.00	25.00	-10.00	17.900	1.310	20.800	4.900	7.200	0.500	2.500	22.800
40.00	30.00	15.00	25.00	-10.00	17.900	1.310	20.800	4.900	7.200	0.500	2.500	22.800
40.00	35.00	15.00	25.00	-10.00	17.900	1.310	20.800	4.900	7.200	0.500	2.500	22.800
40.00	40.00	15.00	25.00	-10.00	17.900	1.310	20.800	4.900	7.200	0.500	2.500	22.800
5.00	5.00	15.00	15.00	0.00	18.400	2.180	10.300	4.900	19.100	2.080	2.500	11.500
5.00	10.00	15.00	15.00	0.00	17.600	2.180	10.300	4.900	17.700	1.170	11.500	9.200
5.00	15.00	15.00	15.00	0.00	22.200	1.070	5.800	7.300	17.700	1.020	11.500	10.900
5.00	20.00	15.00	15.00	0.00	3.800	0.700	1.800	13.200	12.400	2.310	12.700	9.800
5.00	25.00	15.00	15.00	0.00	22.200	0.700	5.800	6.200	17.700	0.370	16.300	11.500
5.00	30.00	15.00	15.00	0.00	22.200	0.700	5.800	6.200	17.700	0.370	16.300	11.500
5.00	35.00	15.00	15.00	0.00	22.200	0.700	5.800	6.200	17.700	0.370	16.300	11.500
5.00	40.00	15.00	15.00	0.00	22.200	0.700	5.800	6.200	17.700	0.370	16.300	11.500
10.00	5.00	15.00	15.00	0.00	17.900	1.520	14.400	16.600	5.800	0.840	2.500	0.100
10.00	10.00	15.00	15.00	0.00	19.100	1.520	17.100	4.600	14.900	0.840	2.500	0.100
10.00	15.00	15.00	15.00	0.00	18.400	1.520	14.300	7.500	5.800	0.840	17.600	0.100
10.00	20.00	15.00	15.00	0.00	18.400	1.520	14.300	13.200	5.800	0.840	17.600	0.100
10.00	25.00	15.00	15.00	0.00	14.900	0.560	5.800	4.100	4.300	0.780	2.500	22.800
10.00	30.00	15.00	15.00	0.00	14.900	0.560	5.800	4.100	4.300	0.780	2.500	22.800
10.00	35.00	15.00	15.00	0.00	14.900	0.560	5.800	4.100	4.300	0.780	2.500	22.800
10.00	40.00	15.00	15.00	0.00	14.900	0.560	5.800	4.100	4.300	0.780	2.500	22.800
15.00	5.00	15.00	15.00	0.00	18.400	1.520	14.300	4.600	14.900	0.840	2.500	0.100
15.00	10.00	15.00	15.00	0.00	17.900	1.520	14.400	16.500	5.800	0.840	2.500	0.100
15.00	15.00	15.00	15.00	0.00	17.900	1.310	17.100	4.600	14.900	1.170	18.100	4.300
15.00	20.00	15.00	15.00	0.00	19.100	1.570	14.400	4.600	14.900	1.020	2.500	22.800
15.00	25.00	15.00	15.00	0.00	17.900	1.520	14.300	7.500	5.800	0.840	2.500	0.100
15.00	30.00	15.00	15.00	0.00	17.900	1.520	14.300	7.500	5.800	0.840	2.500	0.100
15.00	35.00	15.00	15.00	0.00	17.900	1.520	14.300	7.500	5.800	0.840	2.500	0.100

15.00	40.00	15.00	15.00	0.00	17.900	1.520	14.300	7.500	5.800	0.840	2.500	0.100
20.00	5.00	15.00	15.00	0.00	17.900	1.310	14.400	4.600	14.900	1.020	2.500	22.800
20.00	10.00	15.00	15.00	0.00	17.900	1.520	14.400	13.200	5.800	0.840	2.500	0.100
20.00	15.00	15.00	15.00	0.00	18.400	1.520	14.300	7.400	5.800	0.840	2.500	0.100
20.00	20.00	15.00	15.00	0.00	17.900	1.520	14.400	4.600	14.900	0.840	2.500	22.800
20.00	25.00	15.00	15.00	0.00	17.900	1.290	4.200	4.900	17.200	2.200	6.800	5.700
20.00	30.00	15.00	15.00	0.00	17.900	1.290	4.200	4.900	17.200	2.200	6.800	5.700
20.00	35.00	15.00	15.00	0.00	17.900	1.290	4.200	4.900	17.200	2.200	6.800	5.700
20.00	40.00	15.00	15.00	0.00	17.900	1.290	4.200	4.900	17.200	2.200	6.800	5.700
25.00	5.00	15.00	15.00	0.00	17.900	1.570	13.600	13.200	12.400	1.020	2.500	10.900
25.00	10.00	15.00	15.00	0.00	12.200	1.520	7.300	7.400	5.800	0.840	2.500	0.100
25.00	15.00	15.00	15.00	0.00	12.700	1.520	7.300	7.400	14.900	0.840	2.500	0.100
25.00	20.00	15.00	15.00	0.00	18.400	0.700	20.800	7.400	19.100	2.080	2.500	4.300
25.00	25.00	15.00	15.00	0.00	17.600	1.070	17.100	4.900	5.800	1.020	2.500	22.800
25.00	30.00	15.00	15.00	0.00	17.600	1.070	17.100	4.900	5.800	1.020	2.500	22.800
25.00	35.00	15.00	15.00	0.00	17.600	1.070	17.100	4.900	5.800	1.020	2.500	22.800
25.00	40.00	15.00	15.00	0.00	17.600	1.070	17.100	4.900	5.800	1.020	2.500	22.800
30.00	5.00	15.00	15.00	0.00	17.900	1.520	14.400	16.600	5.800	0.840	2.500	0.100
30.00	10.00	15.00	15.00	0.00	17.900	2.180	13.600	16.600	17.200	0.500	2.500	11.500
30.00	15.00	15.00	15.00	0.00	17.900	1.520	13.600	7.300	5.800	0.840	2.500	0.100
30.00	20.00	15.00	15.00	0.00	17.900	1.290	14.400	9.300	19.100	1.730	12.700	8.300
30.00	25.00	15.00	15.00	0.00	17.900	1.310	13.600	16.600	20.700	1.730	10.400	9.800
30.00	30.00	15.00	15.00	0.00	17.900	1.310	13.600	16.600	20.700	1.730	10.400	9.800
30.00	35.00	15.00	15.00	0.00	17.900	1.310	13.600	16.600	20.700	1.730	10.400	9.800
30.00	40.00	15.00	15.00	0.00	17.900	1.310	13.600	16.600	20.700	1.730	10.400	9.800
35.00	5.00	15.00	15.00	0.00	17.900	1.570	14.400	4.600	14.900	1.170	2.500	9.200
35.00	10.00	15.00	15.00	0.00	22.100	1.520	23.100	4.900	17.200	0.840	19.600	0.100
35.00	15.00	15.00	15.00	0.00	18.400	0.560	14.300	4.600	14.900	0.780	17.600	22.800
35.00	20.00	15.00	15.00	0.00	14.400	1.070	14.400	4.600	14.900	1.150	13.700	22.800
35.00	25.00	15.00	15.00	0.00	17.900	2.180	18.500	4.900	19.100	2.200	10.400	10.700
35.00	30.00	15.00	15.00	0.00	17.900	2.180	18.500	4.900	19.100	2.200	10.400	10.700
35.00	35.00	15.00	15.00	0.00	17.900	2.180	18.500	4.900	19.100	2.200	10.400	10.700
35.00	40.00	15.00	15.00	0.00	17.900	2.180	18.500	4.900	19.100	2.200	10.400	10.700
40.00	5.00	15.00	15.00	0.00	22.100	2.180	23.100	4.600	14.900	0.370	11.500	22.800
40.00	10.00	15.00	15.00	0.00	18.400	2.180	20.800	4.900	4.300	1.170	17.600	20.700
40.00	15.00	15.00	15.00	0.00	18.400	1.520	18.500	4.600	14.900	0.840	2.500	0.100
40.00	20.00	15.00	15.00	0.00	14.900	1.570	20.800	4.100	19.100	1.730	17.200	4.300
40.00	25.00	15.00	15.00	0.00	14.900	1.520	20.800	4.100	5.800	0.840	2.500	0.100
40.00	30.00	15.00	15.00	0.00	14.900	1.520	20.800	4.100	5.800	0.840	2.500	0.100
40.00	35.00	15.00	15.00	0.00	14.900	1.520	20.800	4.100	5.800	0.840	2.500	0.100
40.00	40.00	15.00	15.00	0.00	14.900	1.520	20.800	4.100	5.800	0.840	2.500	0.100
5.00	5.00	25.00	15.00	10.00	17.900	1.310	14.400	4.600	14.900	1.020	2.500	22.800
5.00	10.00	25.00	15.00	10.00	14.400	2.180	7.300	4.900	7.900	0.500	11.500	9.200
5.00	15.00	25.00	15.00	10.00	17.900	1.520	14.300	7.400	17.700	0.840	19.600	0.100
5.00	20.00	25.00	15.00	10.00	3.800	0.700	1.800	13.200	12.400	1.240	12.700	9.800
5.00	25.00	25.00	15.00	10.00	19.100	0.700	10.300	7.400	23.000	0.370	18.100	5.700
5.00	30.00	25.00	15.00	10.00	19.100	0.700	10.300	7.400	23.000	0.370	18.100	5.700
5.00	35.00	25.00	15.00	10.00	19.100	0.700	10.300	7.400	23.000	0.370	18.100	5.700

5.00	40.00	25.00	15.00	10.00	19.100	0.700	10.300	7.400	23.000	0.370	18.100	5.700
10.00	5.00	25.00	15.00	10.00	12.700	0.560	18.200	4.600	14.900	1.020	2.500	22.800
10.00	10.00	25.00	15.00	10.00	12.700	1.520	7.300	4.600	14.900	0.840	2.500	0.100
10.00	15.00	25.00	15.00	10.00	14.400	1.520	10.700	13.200	5.800	0.840	2.500	0.100
10.00	20.00	25.00	15.00	10.00	14.400	1.520	10.300	7.400	5.800	0.840	19.600	0.100
10.00	25.00	25.00	15.00	10.00	12.200	0.560	18.200	16.600	22.600	0.510	10.400	8.300
10.00	30.00	25.00	15.00	10.00	12.200	0.560	18.200	16.600	22.600	0.510	10.400	8.300
10.00	35.00	25.00	15.00	10.00	12.200	0.560	18.200	16.600	22.600	0.510	10.400	8.300
10.00	40.00	25.00	15.00	10.00	12.200	0.560	18.200	16.600	22.600	0.510	10.400	8.300
15.00	5.00	25.00	15.00	10.00	12.200	0.560	17.100	12.200	5.800	0.780	2.500	22.800
15.00	10.00	25.00	15.00	10.00	18.400	1.520	14.300	7.400	5.800	0.840	17.600	0.100
15.00	15.00	25.00	15.00	10.00	14.900	1.310	4.200	4.100	8.900	1.990	6.800	5.700
15.00	20.00	25.00	15.00	10.00	14.900	1.070	14.400	4.100	5.800	1.020	2.500	22.800
15.00	25.00	25.00	15.00	10.00	18.400	1.520	14.400	4.900	5.800	0.840	17.600	0.100
15.00	30.00	25.00	15.00	10.00	18.400	1.520	14.400	4.900	5.800	0.840	17.600	0.100
15.00	35.00	25.00	15.00	10.00	18.400	1.520	14.400	4.900	5.800	0.840	17.600	0.100
15.00	40.00	25.00	15.00	10.00	18.400	1.520	14.400	4.900	5.800	0.840	17.600	0.100
20.00	5.00	25.00	15.00	10.00	12.200	0.700	13.600	12.200	19.100	2.080	2.500	11.500
20.00	10.00	25.00	15.00	10.00	17.900	1.520	14.400	13.200	5.800	0.840	2.500	0.100
20.00	15.00	25.00	15.00	10.00	18.400	1.520	10.700	16.600	5.800	0.840	17.600	0.100
20.00	20.00	25.00	15.00	10.00	18.400	1.520	14.300	7.500	5.800	0.840	17.600	0.100
20.00	25.00	25.00	15.00	10.00	12.200	0.560	13.600	4.600	14.900	0.510	4.300	22.800
20.00	30.00	25.00	15.00	10.00	12.200	0.560	13.600	4.600	14.900	0.510	4.300	22.800
20.00	35.00	25.00	15.00	10.00	12.200	0.560	13.600	4.600	14.900	0.510	4.300	22.800
20.00	40.00	25.00	15.00	10.00	12.200	0.560	13.600	4.600	14.900	0.510	4.300	22.800
25.00	5.00	25.00	15.00	10.00	19.100	1.520	14.300	4.600	14.900	0.840	2.500	0.100
25.00	10.00	25.00	15.00	10.00	19.100	1.520	14.300	4.600	14.900	0.840	2.500	0.100
25.00	15.00	25.00	15.00	10.00	13.700	1.520	10.700	13.200	5.800	0.840	19.600	0.100
25.00	20.00	25.00	15.00	10.00	14.900	1.310	13.600	4.100	19.600	2.080	11.500	9.200
25.00	25.00	25.00	15.00	10.00	12.200	0.700	4.200	4.900	5.800	1.020	2.500	22.800
25.00	30.00	25.00	15.00	10.00	12.200	0.700	4.200	4.900	5.800	1.020	2.500	22.800
25.00	35.00	25.00	15.00	10.00	12.200	0.700	4.200	4.900	5.800	1.020	2.500	22.800
25.00	40.00	25.00	15.00	10.00	12.200	0.700	4.200	4.900	5.800	1.020	2.500	22.800
30.00	5.00	25.00	15.00	10.00	17.900	1.570	13.600	16.500	5.800	1.020	2.500	10.900
30.00	10.00	25.00	15.00	10.00	17.900	1.570	14.400	17.500	23.000	0.370	2.500	11.500
30.00	15.00	25.00	15.00	10.00	17.600	1.070	7.300	6.200	17.200	2.080	22.000	10.700
30.00	20.00	25.00	15.00	10.00	14.900	2.180	7.300	4.100	19.100	1.020	2.500	22.800
30.00	25.00	25.00	15.00	10.00	15.400	1.070	14.400	6.200	17.700	1.020	11.500	10.900
30.00	30.00	25.00	15.00	10.00	15.400	1.070	14.400	6.200	17.700	1.020	11.500	10.900
30.00	35.00	25.00	15.00	10.00	15.400	1.070	14.400	6.200	17.700	1.020	11.500	10.900
30.00	40.00	25.00	15.00	10.00	15.400	1.070	14.400	6.200	17.700	1.020	11.500	10.900
35.00	5.00	25.00	15.00	10.00	12.200	0.560	18.500	4.900	20.700	1.730	10.400	8.300
35.00	10.00	25.00	15.00	10.00	17.600	2.180	7.300	4.900	7.200	2.200	2.500	11.500
35.00	15.00	25.00	15.00	10.00	12.200	0.560	13.600	4.900	17.200	2.200	4.300	10.700
35.00	20.00	25.00	15.00	10.00	19.100	1.520	13.600	4.900	5.800	0.840	2.500	0.100
35.00	25.00	25.00	15.00	10.00	17.900	1.290	18.200	4.900	17.700	2.080	12.700	10.200
35.00	30.00	25.00	15.00	10.00	17.900	1.290	18.200	4.900	17.700	2.080	12.700	10.200
35.00	35.00	25.00	15.00	10.00	17.900	1.290	18.200	4.900	17.700	2.080	12.700	10.200

35.00	40.00	25.00	15.00	10.00	17.900	1.290	18.200	4.900	17.700	2.080	12.700	10.200
40.00	5.00	25.00	15.00	10.00	14.900	1.570	20.800	4.100	16.100	0.500	4.300	4.300
40.00	10.00	25.00	15.00	10.00	18.400	2.180	20.800	4.900	4.300	0.370	17.600	20.700
40.00	15.00	25.00	15.00	10.00	22.100	1.520	20.800	4.900	5.800	0.840	2.500	0.100
40.00	20.00	25.00	15.00	10.00	17.900	1.570	13.600	4.600	14.900	1.020	2.500	10.900
40.00	25.00	25.00	15.00	10.00	19.100	1.520	18.500	4.600	14.900	0.840	2.500	0.100
40.00	30.00	25.00	15.00	10.00	19.100	1.520	18.500	4.600	14.900	0.840	2.500	0.100
40.00	35.00	25.00	15.00	10.00	19.100	1.520	18.500	4.600	14.900	0.840	2.500	0.100
40.00	40.00	25.00	15.00	10.00	19.100	1.520	18.500	4.600	14.900	0.840	2.500	0.100
5.00	5.00	35.00	15.00	20.00	17.900	1.570	14.400	4.900	19.100	1.020	2.500	10.900
5.00	10.00	35.00	15.00	20.00	22.200	2.180	14.300	7.500	5.800	1.020	2.500	22.800
5.00	15.00	35.00	15.00	20.00	18.400	1.310	10.300	7.300	10.400	1.020	17.600	22.800
5.00	20.00	35.00	15.00	20.00	3.800	0.700	1.800	13.200	20.700	1.730	10.400	8.300
5.00	25.00	35.00	15.00	20.00	19.100	0.160	13.600	4.900	5.800	1.020	2.500	22.800
5.00	30.00	35.00	15.00	20.00	19.100	0.160	13.600	4.900	5.800	1.020	2.500	22.800
5.00	35.00	35.00	15.00	20.00	19.100	0.160	13.600	4.900	5.800	1.020	2.500	22.800
5.00	40.00	35.00	15.00	20.00	19.100	0.160	13.600	4.900	5.800	1.020	2.500	22.800
10.00	5.00	35.00	15.00	20.00	12.200	1.520	7.300	4.900	19.100	0.840	2.500	0.100
10.00	10.00	35.00	15.00	20.00	18.400	1.520	7.300	6.300	5.800	0.840	17.600	0.100
10.00	15.00	35.00	15.00	20.00	18.400	1.520	10.300	9.300	5.800	0.840	17.600	0.100
10.00	20.00	35.00	15.00	20.00	13.700	1.290	10.700	13.700	19.100	0.370	17.200	22.800
10.00	25.00	35.00	15.00	20.00	19.100	1.570	14.400	17.500	17.200	2.200	10.400	10.700
10.00	30.00	35.00	15.00	20.00	19.100	1.570	14.400	17.500	17.200	2.200	10.400	10.700
10.00	35.00	35.00	15.00	20.00	19.100	1.570	14.400	17.500	17.200	2.200	10.400	10.700
10.00	40.00	35.00	15.00	20.00	19.100	1.570	14.400	17.500	17.200	2.200	10.400	10.700
15.00	5.00	35.00	15.00	20.00	12.200	0.560	17.100	12.200	5.800	0.780	2.500	22.800
15.00	10.00	35.00	15.00	20.00	12.200	1.520	7.300	4.900	5.800	0.840	19.600	0.100
15.00	15.00	35.00	15.00	20.00	12.200	0.010	4.200	21.700	17.200	2.310	6.800	5.700
15.00	20.00	35.00	15.00	20.00	19.100	1.310	17.100	4.900	5.800	1.020	2.500	22.800
15.00	25.00	35.00	15.00	20.00	18.400	1.520	14.400	7.400	5.800	0.840	2.500	0.100
15.00	30.00	35.00	15.00	20.00	18.400	1.520	14.400	7.400	5.800	0.840	2.500	0.100
15.00	35.00	35.00	15.00	20.00	18.400	1.520	14.400	7.400	5.800	0.840	2.500	0.100
15.00	40.00	35.00	15.00	20.00	18.400	1.520	14.400	7.400	5.800	0.840	2.500	0.100
20.00	5.00	35.00	15.00	20.00	12.200	0.700	13.600	12.200	4.300	2.080	2.500	22.800
20.00	10.00	35.00	15.00	20.00	17.900	1.520	14.300	13.200	5.800	0.840	19.600	0.100
20.00	15.00	35.00	15.00	20.00	17.900	1.520	14.300	13.200	5.800	0.840	19.600	0.100
20.00	20.00	35.00	15.00	20.00	17.900	1.310	14.400	4.900	17.700	1.020	17.200	10.900
20.00	25.00	35.00	15.00	20.00	12.200	0.560	14.400	6.300	5.800	1.020	2.500	22.800
20.00	30.00	35.00	15.00	20.00	12.200	0.560	14.400	6.300	5.800	1.020	2.500	22.800
20.00	35.00	35.00	15.00	20.00	12.200	0.560	14.400	6.300	5.800	1.020	2.500	22.800
20.00	40.00	35.00	15.00	20.00	12.200	0.560	14.400	6.300	5.800	1.020	2.500	22.800
25.00	5.00	35.00	15.00	20.00	17.900	1.070	18.500	16.600	3.800	2.080	2.500	8.300
25.00	10.00	35.00	15.00	20.00	17.900	1.520	14.400	13.200	5.800	0.840	19.600	0.100
25.00	15.00	35.00	15.00	20.00	18.400	2.180	14.400	17.500	17.200	1.730	2.500	8.300
25.00	20.00	35.00	15.00	20.00	18.400	1.520	13.600	12.200	5.800	0.840	17.600	0.100
25.00	25.00	35.00	15.00	20.00	14.400	0.560	14.300	7.500	5.800	1.020	2.500	22.800
25.00	30.00	35.00	15.00	20.00	14.400	0.560	14.300	7.500	5.800	1.020	2.500	22.800
25.00	35.00	35.00	15.00	20.00	14.400	0.560	14.300	7.500	5.800	1.020	2.500	22.800

25.00	40.00	35.00	15.00	20.00	14.400	0.560	14.300	7.500	5.800	1.020	2.500	22.800
30.00	5.00	35.00	15.00	20.00	17.900	1.570	13.600	16.500	5.800	2.080	2.500	11.500
30.00	10.00	35.00	15.00	20.00	17.900	1.570	14.400	16.600	19.100	1.020	2.500	10.900
30.00	15.00	35.00	15.00	20.00	17.900	1.570	14.400	16.600	20.700	2.080	12.700	8.300
30.00	20.00	35.00	15.00	20.00	17.900	1.070	18.500	9.300	20.700	1.730	12.700	8.300
30.00	25.00	35.00	15.00	20.00	15.400	1.520	10.300	6.400	5.800	0.840	2.500	0.100
30.00	30.00	35.00	15.00	20.00	15.400	1.520	10.300	6.400	5.800	0.840	2.500	0.100
30.00	35.00	35.00	15.00	20.00	15.400	1.520	10.300	6.400	5.800	0.840	2.500	0.100
30.00	40.00	35.00	15.00	20.00	15.400	1.520	10.300	6.400	5.800	0.840	2.500	0.100
35.00	5.00	35.00	15.00	20.00	22.100	1.070	23.100	4.900	17.700	1.170	17.200	8.300
35.00	10.00	35.00	15.00	20.00	12.200	0.560	13.600	4.600	14.900	0.510	11.500	9.200
35.00	15.00	35.00	15.00	20.00	12.700	1.520	13.600	4.900	5.800	0.840	19.600	0.100
35.00	20.00	35.00	15.00	20.00	14.900	0.100	4.200	4.100	12.400	2.310	11.500	9.200
35.00	25.00	35.00	15.00	20.00	12.700	1.520	17.100	4.900	5.800	0.840	2.500	0.100
35.00	30.00	35.00	15.00	20.00	12.700	1.520	17.100	4.900	5.800	0.840	2.500	0.100
35.00	35.00	35.00	15.00	20.00	12.700	1.520	17.100	4.900	5.800	0.840	2.500	0.100
35.00	40.00	35.00	15.00	20.00	12.700	1.520	17.100	4.900	5.800	0.840	2.500	0.100
40.00	5.00	35.00	15.00	20.00	14.900	1.290	20.800	4.100	4.300	0.370	17.600	20.700
40.00	10.00	35.00	15.00	20.00	22.100	1.310	18.200	4.900	22.600	1.730	3.100	9.800
40.00	15.00	35.00	15.00	20.00	22.100	1.520	18.200	4.900	5.800	0.840	19.600	0.100
40.00	20.00	35.00	15.00	20.00	17.900	1.310	18.500	4.900	22.600	1.150	3.100	9.800
40.00	25.00	35.00	15.00	20.00	14.900	1.520	20.800	4.100	14.900	0.840	2.500	0.100
40.00	30.00	35.00	15.00	20.00	14.900	1.520	20.800	4.100	14.900	0.840	2.500	0.100
40.00	35.00	35.00	15.00	20.00	14.900	1.520	20.800	4.100	14.900	0.840	2.500	0.100
40.00	40.00	35.00	15.00	20.00	14.900	1.520	20.800	4.100	14.900	0.840	2.500	0.100
5.00	5.00	45.00	15.00	30.00	17.900	1.570	14.400	4.600	14.900	0.370	17.200	10.200
5.00	10.00	45.00	15.00	30.00	18.400	1.570	10.300	7.400	10.400	2.080	2.500	11.500
5.00	15.00	45.00	15.00	30.00	22.100	1.290	20.800	4.600	14.900	1.020	2.500	22.800
5.00	20.00	45.00	15.00	30.00	3.800	0.700	1.800	13.200	20.700	0.510	10.400	8.300
5.00	25.00	45.00	15.00	30.00	22.100	0.560	23.100	4.900	19.100	1.020	17.200	10.900
5.00	30.00	45.00	15.00	30.00	22.100	0.560	23.100	4.900	19.100	1.020	17.200	10.900
5.00	35.00	45.00	15.00	30.00	22.100	0.560	23.100	4.900	19.100	1.020	17.200	10.900
5.00	40.00	45.00	15.00	30.00	22.100	0.560	23.100	4.900	19.100	1.020	17.200	10.900
10.00	5.00	45.00	15.00	30.00	19.100	1.070	7.300	4.600	14.900	1.020	2.500	22.800
10.00	10.00	45.00	15.00	30.00	14.900	2.180	7.300	4.100	14.900	2.080	2.500	11.500
10.00	15.00	45.00	15.00	30.00	12.700	1.520	7.300	4.600	14.900	0.840	2.500	0.100
10.00	20.00	45.00	15.00	30.00	17.900	1.570	14.400	13.200	4.300	0.780	2.500	22.800
10.00	25.00	45.00	15.00	30.00	17.600	1.070	7.300	4.900	5.800	1.020	2.500	22.800
10.00	30.00	45.00	15.00	30.00	17.600	1.070	7.300	4.900	5.800	1.020	2.500	22.800
10.00	35.00	45.00	15.00	30.00	17.600	1.070	7.300	4.900	5.800	1.020	2.500	22.800
10.00	40.00	45.00	15.00	30.00	17.600	1.070	7.300	4.900	5.800	1.020	2.500	22.800
15.00	5.00	45.00	15.00	30.00	12.200	0.560	17.100	12.200	5.800	2.080	2.500	22.800
15.00	10.00	45.00	15.00	30.00	12.200	1.520	7.300	7.400	19.100	0.840	19.600	0.100
15.00	15.00	45.00	15.00	30.00	17.900	1.520	14.300	7.500	5.800	0.840	2.500	0.100
15.00	20.00	45.00	15.00	30.00	19.100	1.070	18.500	4.600	14.900	1.020	2.500	22.800
15.00	25.00	45.00	15.00	30.00	17.900	1.070	14.400	4.900	17.700	0.370	3.100	10.700
15.00	30.00	45.00	15.00	30.00	17.900	1.070	14.400	4.900	17.700	0.370	3.100	10.700
15.00	35.00	45.00	15.00	30.00	17.900	1.070	14.400	4.900	17.700	0.370	3.100	10.700

15.00	40.00	45.00	15.00	30.00	17.900	1.070	14.400	4.900	17.700	0.370	3.100	10.700
20.00	5.00	45.00	15.00	30.00	12.200	0.700	13.600	12.200	5.800	2.080	2.500	22.800
20.00	10.00	45.00	15.00	30.00	17.900	1.520	14.400	13.200	3.800	0.840	2.500	0.100
20.00	15.00	45.00	15.00	30.00	17.900	1.520	14.300	13.200	5.800	0.840	19.600	0.100
20.00	20.00	45.00	15.00	30.00	12.200	1.520	7.300	7.400	19.100	0.840	2.500	0.100
20.00	25.00	45.00	15.00	30.00	14.400	1.070	13.600	16.600	19.100	2.080	13.700	8.300
20.00	30.00	45.00	15.00	30.00	14.400	1.070	13.600	16.600	19.100	2.080	13.700	8.300
20.00	35.00	45.00	15.00	30.00	14.400	1.070	13.600	16.600	19.100	2.080	13.700	8.300
20.00	40.00	45.00	15.00	30.00	14.400	1.070	13.600	16.600	19.100	2.080	13.700	8.300
25.00	5.00	45.00	15.00	30.00	17.900	1.070	18.500	8.400	19.100	1.020	2.500	22.800
25.00	10.00	45.00	15.00	30.00	17.900	1.070	18.500	8.400	5.800	2.080	2.500	22.800
25.00	15.00	45.00	15.00	30.00	18.400	1.520	14.300	13.200	5.800	0.840	17.600	0.100
25.00	20.00	45.00	15.00	30.00	18.400	1.520	14.300	7.400	5.800	0.840	17.600	0.100
25.00	25.00	45.00	15.00	30.00	19.100	1.070	18.500	16.500	22.600	0.030	10.400	8.300
25.00	30.00	45.00	15.00	30.00	19.100	1.070	18.500	16.500	22.600	0.030	10.400	8.300
25.00	35.00	45.00	15.00	30.00	19.100	1.070	18.500	16.500	22.600	0.030	10.400	8.300
25.00	40.00	45.00	15.00	30.00	19.100	1.070	18.500	16.500	22.600	0.030	10.400	8.300
30.00	5.00	45.00	15.00	30.00	17.900	1.570	13.600	13.700	19.100	1.020	2.500	10.900
30.00	10.00	45.00	15.00	30.00	17.900	1.070	18.200	17.500	20.700	1.170	2.500	11.500
30.00	15.00	45.00	15.00	30.00	17.900	1.570	14.400	16.600	20.700	0.500	10.400	8.300
30.00	20.00	45.00	15.00	30.00	17.900	1.310	14.400	4.600	14.900	1.020	2.500	22.800
30.00	25.00	45.00	15.00	30.00	22.100	2.180	14.300	7.300	23.000	0.370	17.200	8.300
30.00	30.00	45.00	15.00	30.00	22.100	2.180	14.300	7.300	23.000	0.370	17.200	8.300
30.00	35.00	45.00	15.00	30.00	22.100	2.180	14.300	7.300	23.000	0.370	17.200	8.300
30.00	40.00	45.00	15.00	30.00	22.100	2.180	14.300	7.300	23.000	0.370	17.200	8.300
35.00	5.00	45.00	15.00	30.00	22.100	1.520	23.100	4.900	22.600	1.020	2.500	10.900
35.00	10.00	45.00	15.00	30.00	12.200	0.700	14.400	4.900	22.600	1.730	2.500	9.800
35.00	15.00	45.00	15.00	30.00	15.400	1.520	10.300	6.400	5.800	0.840	19.600	0.100
35.00	20.00	45.00	15.00	30.00	17.600	1.520	10.700	6.200	5.800	0.840	19.600	0.100
35.00	25.00	45.00	15.00	30.00	12.700	1.520	18.500	4.600	14.900	0.840	19.600	0.100
35.00	30.00	45.00	15.00	30.00	12.700	1.520	18.500	4.600	14.900	0.840	19.600	0.100
35.00	35.00	45.00	15.00	30.00	12.700	1.520	18.500	4.600	14.900	0.840	19.600	0.100
35.00	40.00	45.00	15.00	30.00	12.700	1.520	18.500	4.600	14.900	0.840	19.600	0.100
40.00	5.00	45.00	15.00	30.00	22.100	2.180	18.200	4.900	5.800	1.020	2.500	22.800
40.00	10.00	45.00	15.00	30.00	18.400	1.520	18.500	4.900	5.800	0.840	17.600	0.100
40.00	15.00	45.00	15.00	30.00	22.100	1.520	18.200	4.900	5.800	0.840	19.600	0.100
40.00	20.00	45.00	15.00	30.00	18.400	1.520	18.500	4.600	14.900	0.840	17.600	0.100
40.00	25.00	45.00	15.00	30.00	14.900	1.520	20.800	4.100	5.800	0.840	17.600	0.100
40.00	30.00	45.00	15.00	30.00	14.900	1.520	20.800	4.100	5.800	0.840	17.600	0.100
40.00	35.00	45.00	15.00	30.00	14.900	1.520	20.800	4.100	5.800	0.840	17.600	0.100
40.00	40.00	45.00	15.00	30.00	14.900	1.520	20.800	4.100	5.800	0.840	17.600	0.100
5.00	5.00	55.00	15.00	40.00	17.900	1.290	17.100	4.900	5.800	0.500	17.200	9.200
5.00	10.00	55.00	15.00	40.00	17.900	1.290	14.300	7.400	19.100	0.370	2.500	10.200
5.00	15.00	55.00	15.00	40.00	17.900	1.570	13.600	4.600	14.900	0.370	11.500	10.200
5.00	20.00	55.00	15.00	40.00	12.200	0.700	14.400	9.300	2.400	2.310	3.100	8.300
5.00	25.00	55.00	15.00	40.00	22.100	1.070	23.100	12.200	23.000	0.780	11.500	10.200
5.00	30.00	55.00	15.00	40.00	22.100	1.070	23.100	12.200	23.000	0.780	11.500	10.200
5.00	35.00	55.00	15.00	40.00	22.100	1.070	23.100	12.200	23.000	0.780	11.500	10.200

5.00	40.00	55.00	15.00	40.00	22.100	1.070	23.100	12.200	23.000	0.780	11.500	10.200
10.00	5.00	55.00	15.00	40.00	17.900	1.520	13.600	16.500	22.600	0.840	19.600	0.100
10.00	10.00	55.00	15.00	40.00	13.700	1.290	13.600	16.600	23.000	0.370	17.200	8.300
10.00	15.00	55.00	15.00	40.00	18.400	1.570	7.300	6.300	5.800	1.020	2.500	22.800
10.00	20.00	55.00	15.00	40.00	17.900	0.700	10.300	4.900	19.100	0.370	11.500	9.200
10.00	25.00	55.00	15.00	40.00	18.400	0.560	17.100	4.600	14.900	2.080	2.500	11.500
10.00	30.00	55.00	15.00	40.00	18.400	0.560	17.100	4.600	14.900	2.080	2.500	11.500
10.00	35.00	55.00	15.00	40.00	18.400	0.560	17.100	4.600	14.900	2.080	2.500	11.500
10.00	40.00	55.00	15.00	40.00	18.400	0.560	17.100	4.600	14.900	2.080	2.500	11.500
15.00	5.00	55.00	15.00	40.00	17.900	1.520	14.400	16.600	5.800	0.840	19.600	0.100
15.00	10.00	55.00	15.00	40.00	12.200	1.520	7.300	4.900	5.800	0.840	2.500	0.100
15.00	15.00	55.00	15.00	40.00	12.200	0.560	17.100	4.900	19.100	0.370	17.200	10.200
15.00	20.00	55.00	15.00	40.00	19.100	1.290	17.100	4.900	5.800	1.020	2.500	22.800
15.00	25.00	55.00	15.00	40.00	22.200	0.100	5.800	16.500	19.100	2.310	17.200	22.200
15.00	30.00	55.00	15.00	40.00	22.200	0.100	5.800	16.500	19.100	2.310	17.200	22.200
15.00	35.00	55.00	15.00	40.00	22.200	0.100	5.800	16.500	19.100	2.310	17.200	22.200
15.00	40.00	55.00	15.00	40.00	22.200	0.100	5.800	16.500	19.100	2.310	17.200	22.200
20.00	5.00	55.00	15.00	40.00	12.200	0.560	17.100	13.200	19.100	2.080	2.500	22.800
20.00	10.00	55.00	15.00	40.00	17.900	1.520	14.400	16.500	5.800	0.840	19.600	0.100
20.00	15.00	55.00	15.00	40.00	14.900	1.520	7.300	4.100	14.900	0.840	2.500	0.100
20.00	20.00	55.00	15.00	40.00	18.400	1.520	14.300	13.200	5.800	0.840	17.600	0.100
20.00	25.00	55.00	15.00	40.00	12.200	0.560	10.700	16.600	23.000	1.020	17.200	10.900
20.00	30.00	55.00	15.00	40.00	12.200	0.560	10.700	16.600	23.000	1.020	17.200	10.900
20.00	35.00	55.00	15.00	40.00	12.200	0.560	10.700	16.600	23.000	1.020	17.200	10.900
20.00	40.00	55.00	15.00	40.00	12.200	0.560	10.700	16.600	23.000	1.020	17.200	10.900
25.00	5.00	55.00	15.00	40.00	17.900	1.070	18.500	8.400	17.700	2.200	2.500	22.800
25.00	10.00	55.00	15.00	40.00	17.900	1.520	14.400	16.500	5.800	0.840	19.600	0.100
25.00	15.00	55.00	15.00	40.00	15.400	1.520	10.700	13.200	5.800	0.840	19.600	0.100
25.00	20.00	55.00	15.00	40.00	15.400	1.520	10.300	6.400	5.800	0.840	2.500	0.100
25.00	25.00	55.00	15.00	40.00	17.900	1.070	13.600	12.200	19.600	0.780	10.400	8.300
25.00	30.00	55.00	15.00	40.00	17.900	1.070	13.600	12.200	19.600	0.780	10.400	8.300
25.00	35.00	55.00	15.00	40.00	17.900	1.070	13.600	12.200	19.600	0.780	10.400	8.300
25.00	40.00	55.00	15.00	40.00	17.900	1.070	13.600	12.200	19.600	0.780	10.400	8.300
30.00	5.00	55.00	15.00	40.00	17.900	1.520	14.300	13.200	5.800	0.840	19.600	0.100
30.00	10.00	55.00	15.00	40.00	18.400	1.070	18.500	16.600	5.800	2.080	2.500	9.200
30.00	15.00	55.00	15.00	40.00	22.100	1.520	14.300	4.600	14.900	0.840	19.600	0.100
30.00	20.00	55.00	15.00	40.00	19.100	1.520	14.400	4.600	14.900	1.020	2.500	22.800
30.00	25.00	55.00	15.00	40.00	12.200	0.560	7.300	17.500	19.100	2.200	4.300	10.700
30.00	30.00	55.00	15.00	40.00	12.200	0.560	7.300	17.500	19.100	2.200	4.300	10.700
30.00	35.00	55.00	15.00	40.00	12.200	0.560	7.300	17.500	19.100	2.200	4.300	10.700
30.00	40.00	55.00	15.00	40.00	12.200	0.560	7.300	17.500	19.100	2.200	4.300	10.700
35.00	5.00	55.00	15.00	40.00	17.600	2.180	10.300	8.400	17.700	0.370	2.500	22.800
35.00	10.00	55.00	15.00	40.00	18.400	1.310	10.700	6.200	10.400	1.170	17.600	11.500
35.00	15.00	55.00	15.00	40.00	14.900	2.180	7.300	4.100	14.900	1.150	2.500	22.800
35.00	20.00	55.00	15.00	40.00	17.900	1.070	13.600	16.500	5.800	1.150	10.400	8.300
35.00	25.00	55.00	15.00	40.00	14.900	1.520	7.300	4.100	5.800	0.840	19.600	0.100
35.00	30.00	55.00	15.00	40.00	14.900	1.520	7.300	4.100	5.800	0.840	19.600	0.100
35.00	35.00	55.00	15.00	40.00	14.900	1.520	7.300	4.100	5.800	0.840	19.600	0.100

35.00	40.00	55.00	15.00	40.00	14.900	1.520	7.300	4.100	5.800	0.840	19.600	0.100
40.00	5.00	55.00	15.00	40.00	22.100	1.570	18.200	4.900	17.700	2.200	3.100	10.200
40.00	10.00	55.00	15.00	40.00	22.100	1.310	20.800	4.900	4.300	1.170	18.100	20.700
40.00	15.00	55.00	15.00	40.00	14.900	1.570	20.800	4.100	23.000	0.370	3.100	4.300
40.00	20.00	55.00	15.00	40.00	22.100	1.520	20.800	4.900	5.800	0.840	19.600	0.100
40.00	25.00	55.00	15.00	40.00	14.900	1.520	20.800	4.100	5.800	0.840	17.600	0.100
40.00	30.00	55.00	15.00	40.00	14.900	1.520	20.800	4.100	5.800	0.840	17.600	0.100
40.00	35.00	55.00	15.00	40.00	14.900	1.520	20.800	4.100	5.800	0.840	17.600	0.100
40.00	40.00	55.00	15.00	40.00	14.900	1.520	20.800	4.100	5.800	0.840	17.600	0.100
5.00	5.00	65.00	15.00	50.00	17.900	1.290	18.500	6.200	23.000	0.370	2.500	8.300
5.00	10.00	65.00	15.00	50.00	15.400	1.310	14.400	4.600	14.900	1.990	22.000	20.700
5.00	15.00	65.00	15.00	50.00	17.900	1.570	14.400	7.400	5.800	2.080	17.200	10.200
5.00	20.00	65.00	15.00	50.00	22.100	0.700	18.200	17.500	23.000	0.370	3.100	8.300
5.00	25.00	65.00	15.00	50.00	17.900	1.070	14.300	21.700	20.700	0.500	1.900	8.300
5.00	30.00	65.00	15.00	50.00	17.900	1.070	14.300	21.700	20.700	0.500	1.900	8.300
5.00	35.00	65.00	15.00	50.00	17.900	1.070	14.300	21.700	20.700	0.500	1.900	8.300
5.00	40.00	65.00	15.00	50.00	17.900	1.070	14.300	21.700	20.700	0.500	1.900	8.300
10.00	5.00	65.00	15.00	50.00	18.400	1.520	13.600	16.600	19.100	0.840	17.600	0.100
10.00	10.00	65.00	15.00	50.00	18.400	1.310	10.700	4.600	14.900	0.510	17.600	22.800
10.00	15.00	65.00	15.00	50.00	17.900	1.570	13.600	16.600	20.700	1.020	2.500	10.900
10.00	20.00	65.00	15.00	50.00	19.100	1.310	14.400	4.900	5.800	1.020	2.500	22.800
10.00	25.00	65.00	15.00	50.00	19.100	0.700	17.100	7.300	23.000	0.370	18.100	10.700
10.00	30.00	65.00	15.00	50.00	19.100	0.700	17.100	7.300	23.000	0.370	18.100	10.700
10.00	35.00	65.00	15.00	50.00	19.100	0.700	17.100	7.300	23.000	0.370	18.100	10.700
10.00	40.00	65.00	15.00	50.00	19.100	0.700	17.100	7.300	23.000	0.370	18.100	10.700
15.00	5.00	65.00	15.00	50.00	12.200	0.560	17.100	4.900	5.800	1.020	2.500	22.800
15.00	10.00	65.00	15.00	50.00	12.200	1.520	7.300	4.600	14.900	1.020	2.500	22.800
15.00	15.00	65.00	15.00	50.00	12.200	0.560	17.100	4.900	23.000	0.370	17.200	8.300
15.00	20.00	65.00	15.00	50.00	22.100	1.070	23.100	17.500	20.700	0.030	10.400	8.300
15.00	25.00	65.00	15.00	50.00	19.100	0.700	14.400	4.900	5.800	1.020	2.500	22.800
15.00	30.00	65.00	15.00	50.00	19.100	0.700	14.400	4.900	5.800	1.020	2.500	22.800
15.00	35.00	65.00	15.00	50.00	19.100	0.700	14.400	4.900	5.800	1.020	2.500	22.800
15.00	40.00	65.00	15.00	50.00	19.100	0.700	14.400	4.900	5.800	1.020	2.500	22.800
20.00	5.00	65.00	15.00	50.00	12.200	0.560	17.100	13.200	5.800	0.780	2.500	22.800
20.00	10.00	65.00	15.00	50.00	17.900	1.520	14.400	16.500	23.000	0.840	2.500	0.100
20.00	15.00	65.00	15.00	50.00	17.600	1.520	10.700	4.600	14.900	0.840	2.500	0.100
20.00	20.00	65.00	15.00	50.00	17.900	1.310	14.400	4.900	19.100	1.020	2.500	22.800
20.00	25.00	65.00	15.00	50.00	12.700	0.560	14.400	16.500	5.800	2.080	2.500	22.800
20.00	30.00	65.00	15.00	50.00	12.700	0.560	14.400	16.500	5.800	2.080	2.500	22.800
20.00	35.00	65.00	15.00	50.00	12.700	0.560	14.400	16.500	5.800	2.080	2.500	22.800
20.00	40.00	65.00	15.00	50.00	12.700	0.560	14.400	16.500	5.800	2.080	2.500	22.800
25.00	5.00	65.00	15.00	50.00	17.900	1.070	18.500	6.300	5.800	2.080	2.500	22.800
25.00	10.00	65.00	15.00	50.00	17.900	1.070	18.500	4.900	5.800	1.020	2.500	22.800
25.00	15.00	65.00	15.00	50.00	14.400	1.520	7.300	4.900	5.800	0.840	19.600	0.100
25.00	20.00	65.00	15.00	50.00	14.900	1.070	14.300	4.100	14.900	1.730	3.100	22.800
25.00	25.00	65.00	15.00	50.00	17.900	1.290	18.500	21.500	17.700	0.500	12.700	8.300
25.00	30.00	65.00	15.00	50.00	17.900	1.290	18.500	21.500	17.200	0.500	12.700	8.300
25.00	35.00	65.00	15.00	50.00	17.900	1.290	18.500	21.500	17.200	0.500	12.700	8.300

25.00	40.00	65.00	15.00	50.00	17.900	1.290	18.500	21.500	17.200	0.500	12.700	8.300
30.00	5.00	65.00	15.00	50.00	17.900	2.180	10.700	12.200	5.800	1.020	2.500	22.800
30.00	10.00	65.00	15.00	50.00	17.900	1.070	18.200	16.600	23.000	1.020	2.500	10.900
30.00	15.00	65.00	15.00	50.00	17.900	1.520	13.600	9.300	7.200	0.840	2.500	0.100
30.00	20.00	65.00	15.00	50.00	17.900	1.570	13.600	12.200	23.000	2.080	17.200	10.200
30.00	25.00	65.00	15.00	50.00	22.100	0.700	18.200	4.600	14.900	1.170	18.100	22.800
30.00	30.00	65.00	15.00	50.00	22.100	0.700	18.200	4.600	14.900	1.170	18.100	22.800
30.00	35.00	65.00	15.00	50.00	22.100	0.700	18.200	4.600	14.900	1.170	18.100	22.800
30.00	40.00	65.00	15.00	50.00	22.100	0.700	18.200	4.600	14.900	1.170	18.100	22.800
35.00	5.00	65.00	15.00	50.00	17.900	1.070	10.700	7.400	10.400	1.170	17.200	11.100
35.00	10.00	65.00	15.00	50.00	17.900	1.070	14.400	16.600	3.800	1.150	10.400	8.300
35.00	15.00	65.00	15.00	50.00	17.900	1.290	14.400	6.200	5.800	0.500	3.100	10.200
35.00	20.00	65.00	15.00	50.00	17.900	1.520	14.400	4.900	5.800	0.840	19.600	0.100
35.00	25.00	65.00	15.00	50.00	12.200	1.520	17.100	4.900	3.800	0.840	2.500	0.100
35.00	30.00	65.00	15.00	50.00	12.200	1.520	17.100	4.900	3.800	0.840	2.500	0.100
35.00	35.00	65.00	15.00	50.00	12.200	1.520	17.100	4.900	3.800	0.840	2.500	0.100
35.00	40.00	65.00	15.00	50.00	12.200	1.520	17.100	4.900	3.800	0.840	2.500	0.100
40.00	5.00	65.00	15.00	50.00	14.900	1.310	20.800	4.100	4.300	0.370	11.500	22.800
40.00	10.00	65.00	15.00	50.00	22.100	1.310	18.200	4.900	17.700	1.730	3.100	11.500
40.00	15.00	65.00	15.00	50.00	14.900	1.520	23.100	4.100	14.900	0.840	2.500	22.800
40.00	20.00	65.00	15.00	50.00	19.100	1.520	18.500	4.600	14.900	0.840	19.600	0.100
40.00	25.00	65.00	15.00	50.00	14.900	1.520	20.800	4.100	3.800	0.840	2.500	0.100
40.00	30.00	65.00	15.00	50.00	14.900	1.520	20.800	4.100	3.800	0.840	2.500	0.100
40.00	35.00	65.00	15.00	50.00	14.900	1.520	20.800	4.100	3.800	0.840	2.500	0.100
40.00	40.00	65.00	15.00	50.00	14.900	1.520	20.800	4.100	3.800	0.840	2.500	0.100
5.00	5.00	75.00	15.00	60.00	19.100	1.570	13.600	7.300	7.200	0.030	17.200	8.300
5.00	10.00	75.00	15.00	60.00	19.100	1.570	14.400	4.900	19.100	1.170	2.500	10.200
5.00	15.00	75.00	15.00	60.00	14.400	1.070	13.600	4.900	3.800	2.200	13.700	10.700
5.00	20.00	75.00	15.00	60.00	22.100	0.010	14.300	21.700	21.600	0.510	1.900	8.300
5.00	25.00	75.00	15.00	60.00	7.800	0.160	14.400	4.600	14.900	1.170	2.500	11.500
5.00	30.00	75.00	15.00	60.00	7.800	0.160	14.400	4.600	14.900	1.170	2.500	11.500
5.00	35.00	75.00	15.00	60.00	7.800	0.160	14.400	4.600	14.900	1.170	2.500	11.500
5.00	40.00	75.00	15.00	60.00	7.800	0.160	14.400	4.600	14.900	1.170	2.500	11.500
10.00	5.00	75.00	15.00	60.00	19.100	1.570	13.600	17.500	20.700	0.030	3.100	8.300
10.00	10.00	75.00	15.00	60.00	17.900	1.570	13.600	17.500	22.600	1.730	3.100	11.500
10.00	15.00	75.00	15.00	60.00	19.100	1.310	14.400	4.600	14.900	1.020	2.500	22.800
10.00	20.00	75.00	15.00	60.00	14.900	1.310	10.300	4.100	5.800	1.020	2.500	22.800
10.00	25.00	75.00	15.00	60.00	22.100	0.560	18.200	7.300	17.200	2.200	2.500	22.800
10.00	30.00	75.00	15.00	60.00	22.100	0.560	18.200	7.300	17.200	2.200	2.500	22.800
10.00	35.00	75.00	15.00	60.00	22.100	0.560	18.200	7.300	17.200	2.200	2.500	22.800
10.00	40.00	75.00	15.00	60.00	22.100	0.560	18.200	7.300	17.200	2.200	2.500	22.800
15.00	5.00	75.00	15.00	60.00	17.900	1.570	14.400	16.600	20.700	0.500	10.400	8.300
15.00	10.00	75.00	15.00	60.00	12.200	1.520	7.300	7.400	5.800	0.840	2.500	0.100
15.00	15.00	75.00	15.00	60.00	9.000	1.310	7.300	4.600	14.900	1.020	17.200	22.800
15.00	20.00	75.00	15.00	60.00	19.100	1.520	14.300	4.600	14.900	0.840	19.600	0.100
15.00	25.00	75.00	15.00	60.00	19.100	0.700	14.400	4.600	14.900	1.020	2.500	22.800
15.00	30.00	75.00	15.00	60.00	19.100	0.700	14.400	4.600	14.900	1.020	2.500	22.800
15.00	35.00	75.00	15.00	60.00	19.100	0.700	14.400	4.600	14.900	1.020	2.500	22.800

15.00	40.00	75.00	15.00	60.00	19.100	0.700	14.400	4.600	14.900	1.020	2.500	22.800
20.00	5.00	75.00	15.00	60.00	12.200	0.560	17.100	12.200	5.800	2.080	2.500	22.800
20.00	10.00	75.00	15.00	60.00	17.900	1.070	18.500	4.600	14.900	1.020	2.500	22.800
20.00	15.00	75.00	15.00	60.00	18.400	1.520	14.400	13.200	19.100	0.840	2.500	0.100
20.00	20.00	75.00	15.00	60.00	17.900	1.310	14.400	4.900	5.800	1.020	2.500	10.900
20.00	25.00	75.00	15.00	60.00	13.700	1.070	14.400	17.500	20.700	1.730	12.700	22.800
20.00	30.00	75.00	15.00	60.00	13.700	1.070	14.400	17.500	20.700	1.730	12.700	22.800
20.00	35.00	75.00	15.00	60.00	13.700	1.070	14.400	17.500	20.700	1.730	12.700	22.800
20.00	40.00	75.00	15.00	60.00	13.700	1.070	14.400	17.500	20.700	1.730	12.700	22.800
25.00	5.00	75.00	15.00	60.00	17.900	1.070	18.500	6.200	19.100	0.370	2.500	22.800
25.00	10.00	75.00	15.00	60.00	17.900	1.070	18.500	4.900	5.800	1.020	2.500	22.800
25.00	15.00	75.00	15.00	60.00	18.400	2.180	18.200	16.600	23.000	2.080	17.600	9.200
25.00	20.00	75.00	15.00	60.00	18.400	1.520	14.300	7.500	5.800	0.840	2.500	0.100
25.00	25.00	75.00	15.00	60.00	17.900	1.070	18.500	13.700	19.100	2.080	2.500	8.300
25.00	30.00	75.00	15.00	60.00	19.100	1.070	18.500	16.600	23.000	0.370	18.100	8.300
25.00	35.00	75.00	15.00	60.00	19.100	1.070	18.500	16.600	23.000	0.370	18.100	8.300
25.00	40.00	75.00	15.00	60.00	19.100	1.070	18.500	16.600	23.000	0.370	18.100	8.300
30.00	5.00	75.00	15.00	60.00	17.900	1.070	18.200	17.500	5.800	2.080	2.500	10.200
30.00	10.00	75.00	15.00	60.00	17.900	1.070	18.500	16.600	23.000	0.370	2.500	11.500
30.00	15.00	75.00	15.00	60.00	17.900	1.570	14.400	16.600	17.700	0.370	10.400	8.300
30.00	20.00	75.00	15.00	60.00	15.400	1.070	14.400	6.400	23.000	0.370	2.500	8.300
30.00	25.00	75.00	15.00	60.00	17.900	1.520	14.400	7.400	5.800	0.840	19.600	0.100
30.00	30.00	75.00	15.00	60.00	17.900	1.520	14.400	7.400	5.800	0.840	19.600	0.100
30.00	35.00	75.00	15.00	60.00	17.900	1.520	14.400	7.400	5.800	0.840	19.600	0.100
30.00	40.00	75.00	15.00	60.00	17.900	1.520	14.400	7.400	5.800	0.840	19.600	0.100
35.00	5.00	75.00	15.00	60.00	17.900	2.180	14.400	9.300	4.300	1.150	2.500	22.800
35.00	10.00	75.00	15.00	60.00	17.900	1.070	20.800	4.900	22.600	2.200	3.100	4.300
35.00	15.00	75.00	15.00	60.00	14.400	2.180	7.300	4.600	14.900	2.080	2.500	22.800
35.00	20.00	75.00	15.00	60.00	22.100	1.290	23.100	4.900	22.600	2.080	17.200	11.500
35.00	25.00	75.00	15.00	60.00	17.900	1.520	17.100	4.900	2.400	0.840	2.500	0.100
35.00	30.00	75.00	15.00	60.00	17.900	1.520	17.100	4.900	2.400	0.840	2.500	0.100
35.00	35.00	75.00	15.00	60.00	17.900	1.520	17.100	4.900	2.400	0.840	2.500	0.100
35.00	40.00	75.00	15.00	60.00	17.900	1.520	17.100	4.900	2.400	0.840	2.500	0.100
40.00	5.00	75.00	15.00	60.00	19.100	2.180	18.500	4.900	17.200	2.200	2.500	22.800
40.00	10.00	75.00	15.00	60.00	22.100	1.520	18.200	4.900	5.800	0.840	19.600	0.100
40.00	15.00	75.00	15.00	60.00	14.900	1.520	20.800	4.100	5.800	0.840	17.600	0.100
40.00	20.00	75.00	15.00	60.00	14.900	1.520	20.800	4.100	5.800	0.840	17.600	0.100
40.00	25.00	75.00	15.00	60.00	14.900	1.520	20.800	4.100	4.300	0.840	2.500	0.100
40.00	30.00	75.00	15.00	60.00	14.900	1.520	20.800	4.100	4.300	0.840	2.500	0.100
40.00	35.00	75.00	15.00	60.00	14.900	1.520	20.800	4.100	4.300	0.840	2.500	0.100
40.00	40.00	75.00	15.00	60.00	14.900	1.520	20.800	4.100	4.300	0.840	2.500	0.100
5.00	5.00	85.00	15.00	70.00	19.100	1.310	18.200	6.200	20.700	2.080	18.800	9.800
5.00	10.00	85.00	15.00	70.00	17.900	1.310	13.600	6.300	22.600	1.020	11.500	10.900
5.00	15.00	85.00	15.00	70.00	15.400	1.290	14.400	7.400	5.800	1.020	2.500	22.800
5.00	20.00	85.00	15.00	70.00	3.800	0.700	1.800	7.400	19.100	0.510	10.400	8.300
5.00	25.00	85.00	15.00	70.00	7.800	0.160	17.100	4.600	14.900	1.170	17.200	22.800
5.00	30.00	85.00	15.00	70.00	7.800	0.160	17.100	4.600	14.900	1.170	17.200	22.800
5.00	35.00	85.00	15.00	70.00	7.800	0.160	17.100	4.600	14.900	1.170	17.200	22.800

5.00	40.00	85.00	15.00	70.00	7.800	0.160	17.100	4.600	14.900	1.170	17.200	22.800
10.00	5.00	85.00	15.00	70.00	18.400	1.520	13.600	13.200	5.800	0.840	2.500	11.500
10.00	10.00	85.00	15.00	70.00	14.900	1.070	13.600	4.100	17.700	0.370	2.500	9.200
10.00	15.00	85.00	15.00	70.00	19.100	1.570	14.400	4.900	5.800	2.080	2.500	22.800
10.00	20.00	85.00	15.00	70.00	15.400	1.520	10.700	4.600	14.900	1.020	19.600	22.800
10.00	25.00	85.00	15.00	70.00	18.400	1.520	7.300	17.500	12.400	0.840	17.600	0.100
10.00	30.00	85.00	15.00	70.00	18.400	1.520	7.300	17.500	12.400	0.840	17.600	0.100
10.00	35.00	85.00	15.00	70.00	18.400	1.520	7.300	17.500	12.400	0.840	17.600	0.100
10.00	40.00	85.00	15.00	70.00	18.400	1.520	7.300	17.500	12.400	0.840	17.600	0.100
15.00	5.00	85.00	15.00	70.00	18.400	1.570	10.300	6.200	19.100	0.370	2.500	9.200
15.00	10.00	85.00	15.00	70.00	14.400	1.310	7.300	6.200	5.800	2.080	2.500	22.800
15.00	15.00	85.00	15.00	70.00	14.900	1.310	10.700	4.100	3.800	2.080	18.100	11.500
15.00	20.00	85.00	15.00	70.00	18.400	1.070	18.500	4.600	14.900	0.030	17.600	22.800
15.00	25.00	85.00	15.00	70.00	19.100	0.700	17.100	4.600	14.900	1.020	2.500	22.800
15.00	30.00	85.00	15.00	70.00	19.100	0.700	17.100	4.600	14.900	1.020	2.500	22.800
15.00	35.00	85.00	15.00	70.00	19.100	0.700	17.100	4.600	14.900	1.020	2.500	22.800
15.00	40.00	85.00	15.00	70.00	19.100	0.700	17.100	4.600	14.900	1.020	2.500	22.800
20.00	5.00	85.00	15.00	70.00	12.200	0.560	17.100	12.200	4.300	2.080	2.500	22.800
20.00	10.00	85.00	15.00	70.00	17.900	1.070	18.500	4.600	14.900	1.020	2.500	22.800
20.00	15.00	85.00	15.00	70.00	3.800	1.430	2.100	13.200	5.800	1.020	2.500	10.900
20.00	20.00	85.00	15.00	70.00	12.700	1.070	10.300	9.300	8.900	1.170	18.100	10.700
20.00	25.00	85.00	15.00	70.00	12.200	0.560	14.400	6.300	17.700	0.370	11.500	10.200
20.00	30.00	85.00	15.00	70.00	12.200	0.560	14.400	6.300	17.700	0.370	11.500	10.200
20.00	35.00	85.00	15.00	70.00	12.200	0.560	14.400	6.300	17.700	0.370	11.500	10.200
20.00	40.00	85.00	15.00	70.00	12.200	0.560	14.400	6.300	17.700	0.370	11.500	10.200
25.00	5.00	85.00	15.00	70.00	17.900	1.070	18.500	6.300	5.800	0.500	2.500	22.800
25.00	10.00	85.00	15.00	70.00	17.900	1.570	14.400	16.500	22.600	0.500	17.200	8.300
25.00	15.00	85.00	15.00	70.00	14.900	2.180	7.300	4.100	14.900	1.020	2.500	22.800
25.00	20.00	85.00	15.00	70.00	17.900	1.310	14.400	4.600	14.900	1.020	2.500	22.800
25.00	25.00	85.00	15.00	70.00	18.400	1.070	18.500	16.600	19.100	0.370	2.500	8.300
25.00	30.00	85.00	15.00	70.00	18.400	1.070	18.500	16.600	19.100	0.370	2.500	8.300
25.00	35.00	85.00	15.00	70.00	18.400	1.070	18.500	16.600	19.100	0.370	2.500	8.300
25.00	40.00	85.00	15.00	70.00	18.400	1.070	18.500	16.600	19.100	0.370	2.500	8.300
30.00	5.00	85.00	15.00	70.00	17.900	1.070	18.500	17.500	19.100	1.020	2.500	10.900
30.00	10.00	85.00	15.00	70.00	18.400	2.180	10.300	6.200	19.100	1.020	2.500	22.800
30.00	15.00	85.00	15.00	70.00	19.100	1.520	10.700	6.300	5.800	0.840	19.600	0.100
30.00	20.00	85.00	15.00	70.00	17.900	1.570	14.400	17.500	20.700	1.730	11.500	10.200
30.00	25.00	85.00	15.00	70.00	17.900	1.520	14.400	4.900	5.800	0.840	19.600	0.100
30.00	30.00	85.00	15.00	70.00	17.900	1.520	14.400	4.900	5.800	0.840	19.600	0.100
30.00	35.00	85.00	15.00	70.00	17.900	1.520	14.400	4.900	5.800	0.840	19.600	0.100
30.00	40.00	85.00	15.00	70.00	17.900	1.520	14.400	4.900	5.800	0.840	19.600	0.100
35.00	5.00	85.00	15.00	70.00	15.400	2.180	7.300	6.400	11.500	2.080	22.000	10.200
35.00	10.00	85.00	15.00	70.00	19.100	1.070	10.300	4.900	3.800	2.200	3.100	10.700
35.00	15.00	85.00	15.00	70.00	17.900	1.290	14.400	4.900	22.600	1.020	2.500	22.800
35.00	20.00	85.00	15.00	70.00	12.200	0.560	14.400	4.900	20.700	1.730	12.700	9.800
35.00	25.00	85.00	15.00	70.00	17.900	2.180	17.100	4.900	19.100	0.370	2.500	22.800
35.00	30.00	85.00	15.00	70.00	17.900	2.180	17.100	4.900	19.100	0.370	2.500	22.800
35.00	35.00	85.00	15.00	70.00	17.900	2.180	17.100	4.900	19.100	0.370	2.500	22.800

35.00	40.00	85.00	15.00	70.00	17.900	2.180	17.100	4.900	19.100	0.370	2.500	22.800
40.00	5.00	85.00	15.00	70.00	17.900	1.310	18.500	4.900	17.200	1.730	2.500	9.800
40.00	10.00	85.00	15.00	70.00	22.100	1.290	17.100	4.900	4.300	0.500	17.200	22.800
40.00	15.00	85.00	15.00	70.00	14.900	1.520	20.800	4.100	5.800	0.840	19.600	0.100
40.00	20.00	85.00	15.00	70.00	17.900	1.520	18.500	4.600	14.900	0.840	19.600	0.100
40.00	25.00	85.00	15.00	70.00	14.900	1.520	20.800	4.100	5.800	0.840	17.600	0.100
40.00	30.00	85.00	15.00	70.00	14.900	1.520	20.800	4.100	5.800	0.840	17.600	0.100
40.00	35.00	85.00	15.00	70.00	14.900	1.520	20.800	4.100	5.800	0.840	17.600	0.100
40.00	40.00	85.00	15.00	70.00	14.900	1.520	20.800	4.100	5.800	0.840	17.600	0.100
5.00	5.00	95.00	15.00	80.00	14.900	1.070	13.600	4.100	14.900	1.990	17.200	22.800
5.00	10.00	95.00	15.00	80.00	17.900	1.310	18.200	4.900	3.800	2.200	12.700	10.200
5.00	15.00	95.00	15.00	80.00	13.700	1.070	10.300	4.900	5.800	2.080	2.500	22.800
5.00	20.00	95.00	15.00	80.00	3.800	0.700	1.800	7.400	20.700	0.510	10.400	8.300
5.00	25.00	95.00	15.00	80.00	12.200	0.560	14.400	4.600	14.900	1.170	2.500	22.800
5.00	30.00	95.00	15.00	80.00	12.200	0.560	14.400	4.600	14.900	1.170	2.500	22.800
5.00	35.00	95.00	15.00	80.00	12.200	0.560	14.400	4.600	14.900	1.170	2.500	22.800
5.00	40.00	95.00	15.00	80.00	12.200	0.560	14.400	4.600	14.900	1.170	2.500	22.800
10.00	5.00	95.00	15.00	80.00	15.400	1.070	13.600	6.400	5.800	1.020	2.500	22.800
10.00	10.00	95.00	15.00	80.00	19.100	1.520	18.200	13.200	17.700	0.840	19.600	0.100
10.00	15.00	95.00	15.00	80.00	13.700	1.070	13.600	13.700	22.600	0.510	10.400	8.300
10.00	20.00	95.00	15.00	80.00	22.100	1.070	20.800	7.300	23.000	0.370	22.000	4.300
10.00	25.00	95.00	15.00	80.00	19.100	1.310	14.400	16.500	19.100	0.030	12.700	9.800
10.00	30.00	95.00	15.00	80.00	19.100	1.310	14.400	16.500	19.100	0.030	12.700	9.800
10.00	35.00	95.00	15.00	80.00	19.100	1.310	14.400	16.500	19.100	0.030	12.700	9.800
10.00	40.00	95.00	15.00	80.00	19.100	1.310	14.400	16.500	19.100	0.030	12.700	9.800
15.00	5.00	95.00	15.00	80.00	14.900	1.310	10.300	4.100	19.100	0.370	2.500	9.200
15.00	10.00	95.00	15.00	80.00	17.600	1.310	10.300	7.400	14.900	2.080	2.500	22.800
15.00	15.00	95.00	15.00	80.00	14.400	1.570	7.300	4.900	5.800	2.080	2.500	22.800
15.00	20.00	95.00	15.00	80.00	22.100	1.520	20.800	7.400	5.800	0.840	2.500	0.100
15.00	25.00	95.00	15.00	80.00	19.100	0.700	17.100	4.600	14.900	1.020	2.500	22.800
15.00	30.00	95.00	15.00	80.00	19.100	0.700	17.100	4.600	14.900	1.020	2.500	22.800
15.00	35.00	95.00	15.00	80.00	19.100	0.700	17.100	4.600	14.900	1.020	2.500	22.800
15.00	40.00	95.00	15.00	80.00	19.100	0.700	17.100	4.600	14.900	1.020	2.500	22.800
20.00	5.00	95.00	15.00	80.00	9.000	0.700	4.200	4.600	14.900	0.370	2.500	22.800
20.00	10.00	95.00	15.00	80.00	17.900	1.070	18.500	4.600	14.900	1.020	2.500	22.800
20.00	15.00	95.00	15.00	80.00	12.200	1.520	7.300	6.300	19.100	1.020	2.500	22.800
20.00	20.00	95.00	15.00	80.00	12.200	1.520	7.300	7.400	23.000	0.840	2.500	11.500
20.00	25.00	95.00	15.00	80.00	12.200	0.560	14.400	12.500	16.100	1.150	4.300	8.300
20.00	30.00	95.00	15.00	80.00	12.200	0.560	14.400	12.500	16.100	1.150	4.300	8.300
20.00	35.00	95.00	15.00	80.00	12.200	0.560	14.400	12.500	16.100	1.150	4.300	8.300
20.00	40.00	95.00	15.00	80.00	12.200	0.560	14.400	12.500	16.100	1.150	4.300	8.300
25.00	5.00	95.00	15.00	80.00	17.900	1.070	18.500	4.900	19.100	1.020	2.500	22.800
25.00	10.00	95.00	15.00	80.00	17.900	1.570	14.400	16.500	23.000	0.370	2.500	8.300
25.00	15.00	95.00	15.00	80.00	17.900	1.070	18.500	4.600	14.900	1.020	2.500	22.800
25.00	20.00	95.00	15.00	80.00	17.900	1.070	14.300	4.600	14.900	0.370	10.400	22.800
25.00	25.00	95.00	15.00	80.00	17.900	0.700	18.200	4.600	14.900	2.080	12.700	22.800
25.00	30.00	95.00	15.00	80.00	17.900	0.700	18.200	4.600	14.900	2.080	12.700	22.800
25.00	35.00	95.00	15.00	80.00	17.900	0.700	18.200	4.600	14.900	2.080	12.700	22.800

25.00	40.00	95.00	15.00	80.00	17.900	0.700	18.200	4.600	14.900	2.080	12.700	22.800
30.00	5.00	95.00	15.00	80.00	17.900	1.070	18.500	16.500	19.100	1.020	2.500	10.900
30.00	10.00	95.00	15.00	80.00	17.900	1.570	14.400	16.500	22.600	2.080	2.500	9.200
30.00	15.00	95.00	15.00	80.00	18.400	1.520	14.300	4.600	14.900	0.840	17.600	0.100
30.00	20.00	95.00	15.00	80.00	14.400	2.180	7.300	4.600	14.900	0.500	13.700	22.800
30.00	25.00	95.00	15.00	80.00	17.900	1.070	14.400	7.300	19.100	1.020	2.500	22.800
30.00	30.00	95.00	15.00	80.00	17.900	1.070	14.400	7.300	19.100	1.020	2.500	22.800
30.00	35.00	95.00	15.00	80.00	17.900	1.070	14.400	7.300	19.100	1.020	2.500	22.800
30.00	40.00	95.00	15.00	80.00	17.900	1.070	14.400	7.300	19.100	1.020	2.500	22.800
35.00	5.00	95.00	15.00	80.00	17.900	2.180	14.400	9.300	5.800	1.020	2.500	22.800
35.00	10.00	95.00	15.00	80.00	17.900	1.290	18.500	8.400	5.500	0.500	3.100	8.300
35.00	15.00	95.00	15.00	80.00	17.900	1.520	14.300	7.500	5.800	0.840	19.600	0.100
35.00	20.00	95.00	15.00	80.00	22.100	1.520	23.100	4.900	5.800	0.840	19.600	0.100
35.00	25.00	95.00	15.00	80.00	14.400	2.180	17.100	4.900	4.300	1.020	2.500	22.800
35.00	30.00	95.00	15.00	80.00	14.400	2.180	17.100	4.900	4.300	1.020	2.500	22.800
35.00	35.00	95.00	15.00	80.00	14.400	2.180	17.100	4.900	4.300	1.020	2.500	22.800
35.00	40.00	95.00	15.00	80.00	14.400	2.180	17.100	4.900	4.300	1.020	2.500	22.800
40.00	5.00	95.00	15.00	80.00	18.400	1.520	18.200	4.600	14.900	0.840	17.600	0.100
40.00	10.00	95.00	15.00	80.00	19.100	1.520	18.500	4.900	5.800	0.840	19.600	0.100
40.00	15.00	95.00	15.00	80.00	18.400	1.520	18.500	4.900	5.800	0.840	17.600	0.100
40.00	20.00	95.00	15.00	80.00	19.100	1.310	18.200	4.900	20.700	2.200	3.100	10.700
40.00	25.00	95.00	15.00	80.00	19.100	1.520	18.500	4.600	14.900	0.840	19.600	0.100
40.00	30.00	95.00	15.00	80.00	19.100	1.520	18.500	4.600	14.900	0.840	19.600	0.100
40.00	35.00	95.00	15.00	80.00	19.100	1.520	18.500	4.600	14.900	0.840	19.600	0.100
40.00	40.00	95.00	15.00	80.00	19.100	1.520	18.500	4.600	14.900	0.840	19.600	0.100
5.00	5.00	105.00	15.00	90.00	18.400	1.520	17.100	6.300	2.400	1.020	2.500	10.900
5.00	10.00	105.00	15.00	90.00	17.900	1.570	14.400	7.300	7.200	0.500	2.500	11.500
5.00	15.00	105.00	15.00	90.00	12.700	0.560	20.800	4.900	8.900	0.750	4.300	4.300
5.00	20.00	105.00	15.00	90.00	3.800	0.700	1.800	7.400	20.700	0.510	10.400	8.300
5.00	25.00	105.00	15.00	90.00	12.200	0.560	14.400	4.900	5.800	1.020	2.500	10.900
5.00	30.00	105.00	15.00	90.00	12.200	0.560	14.400	4.900	5.800	1.020	2.500	10.900
5.00	35.00	105.00	15.00	90.00	12.200	0.560	14.400	4.900	5.800	1.020	2.500	10.900
5.00	40.00	105.00	15.00	90.00	12.200	0.560	14.400	4.900	5.800	1.020	2.500	10.900
10.00	5.00	105.00	15.00	90.00	17.900	1.570	14.400	13.200	17.200	1.020	3.100	10.900
10.00	10.00	105.00	15.00	90.00	19.100	1.310	18.500	4.900	23.000	0.370	17.200	9.800
10.00	15.00	105.00	15.00	90.00	12.200	0.560	18.200	12.200	19.100	1.020	3.100	10.900
10.00	20.00	105.00	15.00	90.00	12.700	0.560	14.400	4.600	14.900	1.020	2.500	22.800
10.00	25.00	105.00	15.00	90.00	12.700	0.560	14.400	4.900	5.800	1.020	2.500	22.800
10.00	30.00	105.00	15.00	90.00	12.700	0.560	14.400	4.900	5.800	1.020	2.500	22.800
10.00	35.00	105.00	15.00	90.00	12.700	0.560	14.400	4.900	5.800	1.020	2.500	22.800
10.00	40.00	105.00	15.00	90.00	12.700	0.560	14.400	4.900	5.800	1.020	2.500	22.800
15.00	5.00	105.00	15.00	90.00	19.100	1.310	13.600	16.600	17.700	0.030	11.500	9.200
15.00	10.00	105.00	15.00	90.00	19.100	1.290	18.500	7.400	17.700	1.020	2.500	10.900
15.00	15.00	105.00	15.00	90.00	19.100	2.180	10.300	7.300	10.400	2.080	2.500	9.200
15.00	20.00	105.00	15.00	90.00	17.900	1.570	10.300	7.400	19.100	1.170	2.500	11.500
15.00	25.00	105.00	15.00	90.00	22.100	1.070	23.100	6.300	20.700	0.510	18.800	8.300
15.00	30.00	105.00	15.00	90.00	22.100	1.070	23.100	6.300	20.700	0.510	18.800	8.300
15.00	35.00	105.00	15.00	90.00	22.100	1.070	23.100	6.300	20.700	0.510	18.800	8.300

15.00	40.00	105.00	15.00	90.00	22.100	1.070	23.100	6.300	20.700	0.510	18.800	8.300
20.00	5.00	105.00	15.00	90.00	22.200	1.310	5.800	6.200	5.800	1.020	2.500	22.800
20.00	10.00	105.00	15.00	90.00	17.900	1.070	18.500	4.600	14.900	1.020	2.500	22.800
20.00	15.00	105.00	15.00	90.00	9.000	0.700	4.200	4.900	19.100	1.020	2.500	10.900
20.00	20.00	105.00	15.00	90.00	15.400	1.520	10.300	4.600	14.900	1.020	2.500	22.800
20.00	25.00	105.00	15.00	90.00	17.600	1.070	7.300	12.200	3.800	2.080	3.100	8.300
20.00	30.00	105.00	15.00	90.00	17.600	1.070	7.300	12.200	3.800	2.080	3.100	8.300
20.00	35.00	105.00	15.00	90.00	17.600	1.070	7.300	12.200	3.800	2.080	3.100	8.300
20.00	40.00	105.00	15.00	90.00	17.600	1.070	7.300	12.200	3.800	2.080	3.100	8.300
25.00	5.00	105.00	15.00	90.00	17.900	1.070	18.500	6.200	17.700	1.020	2.500	22.800
25.00	10.00	105.00	15.00	90.00	17.900	1.570	14.400	16.500	20.700	0.500	3.100	8.300
25.00	15.00	105.00	15.00	90.00	17.900	1.570	14.400	16.600	19.600	0.500	11.500	9.200
25.00	20.00	105.00	15.00	90.00	17.900	1.070	14.300	4.600	14.900	0.500	3.100	22.800
25.00	25.00	105.00	15.00	90.00	18.400	1.070	5.800	7.400	5.800	1.020	2.500	22.800
25.00	30.00	105.00	15.00	90.00	18.400	1.070	5.800	7.400	5.800	1.020	2.500	22.800
25.00	35.00	105.00	15.00	90.00	18.400	1.070	5.800	7.400	5.800	1.020	2.500	22.800
25.00	40.00	105.00	15.00	90.00	18.400	1.070	5.800	7.400	5.800	1.020	2.500	22.800
30.00	5.00	105.00	15.00	90.00	19.100	2.180	10.700	4.600	14.900	2.080	2.500	22.800
30.00	10.00	105.00	15.00	90.00	17.900	1.570	13.600	12.200	23.000	1.020	2.500	10.900
30.00	15.00	105.00	15.00	90.00	17.900	1.570	13.600	9.300	19.100	0.500	17.200	9.200
30.00	20.00	105.00	15.00	90.00	12.200	0.700	14.400	9.300	22.600	1.170	2.500	11.500
30.00	25.00	105.00	15.00	90.00	19.100	1.310	13.600	16.600	20.700	0.030	2.500	10.200
30.00	30.00	105.00	15.00	90.00	19.100	1.310	13.600	16.600	20.700	0.030	2.500	10.200
30.00	35.00	105.00	15.00	90.00	19.100	1.310	13.600	16.600	20.700	0.030	2.500	10.200
30.00	40.00	105.00	15.00	90.00	19.100	1.310	13.600	16.600	20.700	0.030	2.500	10.200
35.00	5.00	105.00	15.00	90.00	12.700	1.070	10.300	7.400	4.300	1.020	2.500	22.800
35.00	10.00	105.00	15.00	90.00	18.400	2.180	10.700	7.400	19.100	1.020	2.500	22.800
35.00	15.00	105.00	15.00	90.00	22.100	1.520	14.300	7.500	5.800	0.840	19.600	0.100
35.00	20.00	105.00	15.00	90.00	12.200	0.560	18.500	4.900	20.700	1.730	12.700	8.300
35.00	25.00	105.00	15.00	90.00	12.200	1.570	17.100	4.900	17.700	0.370	2.500	22.800
35.00	30.00	105.00	15.00	90.00	12.200	1.570	17.100	4.900	17.700	0.370	2.500	22.800
35.00	35.00	105.00	15.00	90.00	12.200	1.570	17.100	4.900	17.700	0.370	2.500	22.800
35.00	40.00	105.00	15.00	90.00	12.200	1.570	17.100	4.900	17.700	0.370	2.500	22.800
40.00	5.00	105.00	15.00	90.00	19.100	1.520	18.500	4.900	5.800	0.840	19.600	0.100
40.00	10.00	105.00	15.00	90.00	14.900	1.310	14.400	4.100	14.900	2.080	2.500	22.800
40.00	15.00	105.00	15.00	90.00	19.100	1.520	18.500	4.600	14.900	0.840	19.600	0.100
40.00	20.00	105.00	15.00	90.00	14.900	1.520	20.800	4.100	5.800	0.840	17.600	0.100
40.00	25.00	105.00	15.00	90.00	17.900	1.520	18.500	4.600	14.900	0.840	19.600	0.100
40.00	30.00	105.00	15.00	90.00	17.900	1.520	18.500	4.600	14.900	0.840	19.600	0.100
40.00	35.00	105.00	15.00	90.00	17.900	1.520	18.500	4.600	14.900	0.840	19.600	0.100
40.00	40.00	105.00	15.00	90.00	17.900	1.520	18.500	4.600	14.900	0.840	19.600	0.100
5.00	5.00	115.00	15.00	100.00	22.100	1.570	23.100	4.900	17.700	2.080	2.500	22.800
5.00	10.00	115.00	15.00	100.00	22.100	1.570	23.100	4.900	5.800	1.020	2.500	10.900
5.00	15.00	115.00	15.00	100.00	14.400	1.070	13.600	7.400	7.900	0.510	13.700	8.300
5.00	20.00	115.00	15.00	100.00	3.800	0.700	1.800	13.200	5.800	1.170	18.100	11.100
5.00	25.00	115.00	15.00	100.00	7.800	0.160	17.100	4.600	14.900	2.080	2.500	11.500
5.00	30.00	115.00	15.00	100.00	7.800	0.160	17.100	4.600	14.900	2.080	2.500	11.500
5.00	35.00	115.00	15.00	100.00	7.800	0.160	17.100	4.600	14.900	2.080	2.500	11.500

5.00	40.00	115.00	15.00	100.00	7.800	0.160	17.100	4.600	14.900	2.080	2.500	11.500
10.00	5.00	115.00	15.00	100.00	17.900	1.570	14.400	6.300	5.800	1.020	2.500	22.800
10.00	10.00	115.00	15.00	100.00	18.400	1.310	17.100	6.300	5.800	1.020	2.500	10.900
10.00	15.00	115.00	15.00	100.00	13.700	1.070	13.600	13.700	12.400	0.510	2.500	10.200
10.00	20.00	115.00	15.00	100.00	15.400	1.070	14.400	12.200	17.700	0.780	2.500	11.500
10.00	25.00	115.00	15.00	100.00	12.200	0.560	13.600	12.200	23.000	0.780	17.200	11.500
10.00	30.00	115.00	15.00	100.00	12.200	0.560	13.600	12.200	23.000	0.780	17.200	11.500
10.00	35.00	115.00	15.00	100.00	12.200	0.560	13.600	12.200	23.000	0.780	17.200	11.500
10.00	40.00	115.00	15.00	100.00	12.200	0.560	13.600	12.200	23.000	0.780	17.200	11.500
15.00	5.00	115.00	15.00	100.00	14.900	1.070	13.600	4.100	5.800	1.020	2.500	22.800
15.00	10.00	115.00	15.00	100.00	19.100	1.310	14.300	13.200	5.800	1.170	17.200	11.500
15.00	15.00	115.00	15.00	100.00	18.400	1.570	14.300	7.500	5.800	1.020	2.500	10.900
15.00	20.00	115.00	15.00	100.00	18.400	1.520	17.100	7.400	19.100	0.840	2.500	0.100
15.00	25.00	115.00	15.00	100.00	19.100	0.700	17.100	4.600	14.900	1.020	2.500	22.800
15.00	30.00	115.00	15.00	100.00	19.100	0.700	17.100	4.600	14.900	1.020	2.500	22.800
15.00	35.00	115.00	15.00	100.00	19.100	0.700	17.100	4.600	14.900	1.020	2.500	22.800
15.00	40.00	115.00	15.00	100.00	19.100	0.700	17.100	4.600	14.900	1.020	2.500	22.800
20.00	5.00	115.00	15.00	100.00	12.700	0.560	17.100	4.600	14.900	1.020	2.500	22.800
20.00	10.00	115.00	15.00	100.00	18.400	1.070	7.300	7.300	22.600	1.170	17.600	22.800
20.00	15.00	115.00	15.00	100.00	14.900	1.310	7.300	4.100	23.000	0.370	17.200	10.200
20.00	20.00	115.00	15.00	100.00	12.200	1.310	7.300	4.900	5.800	1.020	2.500	10.900
20.00	25.00	115.00	15.00	100.00	17.600	1.070	7.300	16.600	3.800	0.500	11.500	10.200
20.00	30.00	115.00	15.00	100.00	17.600	1.070	7.300	16.600	3.800	0.500	11.500	10.200
20.00	35.00	115.00	15.00	100.00	17.600	1.070	7.300	16.600	3.800	0.500	11.500	10.200
20.00	40.00	115.00	15.00	100.00	17.600	1.070	7.300	16.600	3.800	0.500	11.500	10.200
25.00	5.00	115.00	15.00	100.00	17.900	1.070	18.500	6.200	5.800	1.020	2.500	22.800
25.00	10.00	115.00	15.00	100.00	17.900	1.570	14.400	17.500	23.000	0.370	2.500	8.300
25.00	15.00	115.00	15.00	100.00	17.600	1.070	7.300	4.900	5.800	1.020	2.500	22.800
25.00	20.00	115.00	15.00	100.00	12.700	1.070	10.300	12.200	23.000	0.780	2.500	8.300
25.00	25.00	115.00	15.00	100.00	17.900	1.290	13.600	16.600	17.200	0.500	2.500	8.300
25.00	30.00	115.00	15.00	100.00	17.900	1.290	13.600	16.600	19.100	0.500	2.500	9.200
25.00	35.00	115.00	15.00	100.00	17.900	1.290	13.600	16.600	19.100	0.500	2.500	9.200
25.00	40.00	115.00	15.00	100.00	17.900	1.290	13.600	16.600	19.100	0.500	2.500	9.200
30.00	5.00	115.00	15.00	100.00	17.900	1.520	13.600	6.200	5.800	0.840	19.600	0.100
30.00	10.00	115.00	15.00	100.00	18.400	2.180	10.300	6.200	19.100	1.020	2.500	22.800
30.00	15.00	115.00	15.00	100.00	17.900	1.520	13.600	7.400	5.800	0.840	2.500	0.100
30.00	20.00	115.00	15.00	100.00	17.900	1.070	14.300	7.500	23.000	0.370	2.500	8.300
30.00	25.00	115.00	15.00	100.00	19.100	1.070	13.600	16.600	19.100	0.370	2.500	10.200
30.00	30.00	115.00	15.00	100.00	17.900	1.290	13.600	16.600	20.700	1.730	2.500	9.200
30.00	35.00	115.00	15.00	100.00	19.100	1.070	13.600	16.600	19.100	0.370	2.500	10.200
30.00	40.00	115.00	15.00	100.00	19.100	1.070	13.600	16.600	19.100	0.370	2.500	10.200
35.00	5.00	115.00	15.00	100.00	17.900	1.310	14.400	16.600	22.600	1.150	2.500	11.500
35.00	10.00	115.00	15.00	100.00	14.900	1.520	10.300	4.100	5.800	0.840	19.600	0.100
35.00	15.00	115.00	15.00	100.00	17.900	1.570	14.400	17.500	23.000	1.020	2.500	10.900
35.00	20.00	115.00	15.00	100.00	15.400	1.070	17.100	6.400	5.800	1.020	2.500	22.800
35.00	25.00	115.00	15.00	100.00	12.200	1.520	18.200	4.900	19.100	1.020	2.500	22.800
35.00	30.00	115.00	15.00	100.00	12.200	1.520	18.200	4.900	19.100	1.020	2.500	22.800
35.00	35.00	115.00	15.00	100.00	12.200	1.520	18.200	4.900	19.100	1.020	2.500	22.800

35.00	40.00	115.00	15.00	100.00	12.200	1.520	18.200	4.900	19.100	1.020	2.500	22.800
40.00	5.00	115.00	15.00	100.00	9.000	1.520	20.800	4.900	5.800	0.840	19.600	0.100
40.00	10.00	115.00	15.00	100.00	22.100	1.070	20.800	4.900	16.100	1.170	18.100	22.800
40.00	15.00	115.00	15.00	100.00	18.400	1.520	18.500	4.900	5.800	0.840	17.600	0.100
40.00	20.00	115.00	15.00	100.00	22.100	1.290	20.800	4.900	22.600	0.500	3.100	11.500
40.00	25.00	115.00	15.00	100.00	14.900	1.520	20.800	4.100	5.800	0.840	19.600	0.100
40.00	30.00	115.00	15.00	100.00	14.900	1.520	20.800	4.100	5.800	0.840	19.600	0.100
40.00	35.00	115.00	15.00	100.00	14.900	1.520	20.800	4.100	5.800	0.840	19.600	0.100
40.00	40.00	115.00	15.00	100.00	14.900	1.520	20.800	4.100	5.800	0.840	19.600	0.100

Appendix D: Optimal Policy for Adaptive Lateral Control

Table D.1: Optimal Policy for Adaptive Lateral Control

$s_1 = V_x$ (m/s)	$a_1 = k_{prev}$	$a_2 = k_p$	$a_3 = k_d$
5.0	6.100	0.620	0.040
10.0	9.900	0.330	0.020
15.0	6.500	0.330	0.070
20.0	7.200	0.310	0.070
25.0	8.200	0.250	0.070
35.0	8.400	0.190	0.070
40.0	8.100	0.190	0.070

Bibliography

[Ackermann et al 1995] Ackermann J., Guldner J., Sienel W., Steinhauser R., Utkin V.I. "Linear and nonlinear controller design for robust automatic steering". In *IEEE Transactions on Control Systems Technology*, Vol 3, Issue 1, March, pp 132 – 143, 1995.

[Ackermann 1990] Ackermann J. "Robust car steering by yaw rate control". In *Proceedings of the 29th Conference on Decision and Control*. Honolulu, Hawaii, December, pp 2033-2034. 1990.

[Anitescu & Potra] Anitescu M. and Potra F.R. "Formulating dynamic multi-rigid-body contact problems with friction as solvable linear complementariry problems". In *ASME Nonlinear Dynamics*, Vol 14 pp 231-247, 1997.

[Aström & Wittenmark 1994] Aström K. J., Wittenmark B., *Adaptive Control*, Addison-Wesley. 1994.

[Arkin 1998] Arkin, R.C., Sutton. *Behavior-based robotics*. The MIT Press. Cambridge, MA, USA.1998.

[Bakker et al 1987] Bakker, E., Nyborg, L., Pacejka, H. B. "Tyre Modelling for Use in Vehicle Dynamics Studies", *SAE Technical Paper Series*, no 870421. 1987.

[Baraff 1994] Baraff, D. "Fast Contact Force Computation for Nonpenetrating Rigid Bodies". In *Computer Graphics Proceedings, Annual Conference Series*: pp 23-34, 1994.

[Bellman 1957a] Bellman R.E. *Dynamic Programming*. Princeton University Press, Princeton, NJ, 1957.

[Bellman 1957b] Bellman R. E. "A Markov decision process". In *Journal of Mathematical Mech*., Vol 6 pp 679-684. 1957.

[Bollinger & Duffie 1988] Bollinger, J.G. and Duffie, N.A. *Computer Control of Machines and Processes*. Addison-Wesley Publishing. 1988.

[Brenan et al 1989] Brenan K.E., Campbell S.L., Petzold L.R. *Numerical solution of initial-value problems in differential-algebraic equations*. North-Holland, New York, 1989

[Brooks 1991] Brooks R A. "New Approaches to Robotics." In *Science*, 253, pp 1227-1232, 1991.

[Brooks 1986] Brooks R A. "A Robust Layered Control Systems for a Mobile Robot." In *Journal of Robotics and Automation*, 2, pp 14-23, 1986.

[Chu 1974] Chu K. C. "Decentralized control of high speed vehicle strings", In *Transportation Science*, Vol 8, Issue 4, pp. 361-383, June, 1974.

[Chrstos & Grygier 1997] Chrstos, J. P. and Grygier, P. A. "Experimental Testing of a 1994 Ford Taurus for NADSdyna Validation", *SAE Paper No. 970563*, February 1997.

[Ellis 2005] Ellis J.R., *Vehicle Dynamics*, London Business Books Ltd. 1969.

[Erleben 2005] Erleben K. Stable, Robust, and Versatile Multibody Dynamics Animation. *PhD thesis*, Department of Computer Science, University of Copenhagen (DIKU), Universitetsparken 1, DK-2100 Copenhagen, Denmark, March 2005.

[Fenton & Selim 1988] Fenton, R.E.; Selim, I. () "On the optimal design of an automotive lateral controller", In *IEEE Transactions on Vehicular Technology*, Volume 37, Issue 2, May Page(s):108 – 113. 1988.

[Fenton et al 1976] Fenton R. E., Melocik G. C., and Olson K. W., "On the steering of automated vehicles: Theory and experiment", In *IEEE Trans. on Automatic Control*, vol. 21, no. 3, pp. 306-315. 1976.

[Fehlberg 1969] Fehlberg E, "Low-order Classical Runge-Kutta Formulas with Stepsize Control." In *NASA Technical Report R-315*, 1969.

[Franke et al 1995] Franke U., Bottiger F., Zomotor Z., Seeberger D. "Truck platooning in mixed traffic". In *Proceedings of the Intelligent Vehicles '95 Symposium*, Detroit, MI, USA, pp 1-6, 1995.

[Fritz et al 2004] Fritz H., Gern A., Schiemenz H., Bonnet C. "CHAUFFEUR Assistant: a driver assistance system for commercial vehicles based on fusion of advanced ACC and lane keeping". In *Proceedings of 2004 IEEE Intelligent Vehicles Symposium*, pp 495-500, 2004.

[Fritz 1999] Fritz H. "Longitudinal and lateral control of heavy duty trucks for automated vehicle following in mixed traffic: experimental results from the CHAUFFEUR project". In *Proceedings of the 1999 IEEE International Conference on Control Applications*, Kohala Coast, HI, USA, Vol. 2, pp 1348-1352, 1999.

[Gillespie 1992] Gillespie T.D. *Fundamentals of Vehicle Dynamics*, SAE R-114, USA. 1992.

[Ginsberg 1995] Ginsberg, J.H., *Advanced Engineering Dynamics 2nd Edition*, Cambridge University Press, 1995.

[Grantham & Vincent 1993] Grantham, W.J., Vincent, T.L. *Modern Control Systems: Analysis and Design*. John Wiley & Sons, USA. 1993.

[Guldner et al 1999] Guldner J., Sienel W., Tan H.-S., Ackermann J., Patwardhan S., and Bünte T. "Robust automatic steering control for look-down reference systems with front and rear sensors". In *IEEE Transactions on Control Systems Technology*, Vol 7, no. 1, pp 2-11. 1999.

[Guldner et al 1997] Guldner J., Tan H.S. and Patwardhan S. "Study of Design Directions for Lateral Vehicle Control". In *Proceedings of the 36th Conference on Decision & Control*, San Diego, California USA December, pp 4732-4737. 1997.

[Guldner et al 1994] Guldner J., Utkin V.I., and Ackermann J. "A Sliding Mode Control Approach to Automatic Car Steering". In *Proc. American Control Conf.*, Baltimore, Maryland, USA, June, pp. 1969-1973. 1994.

[Harker 2001] Harker B.J. "PROMOTE-CHAUFFEUR II & 5.8 GHz vehicle to vehicle communications system". In *Proceeding of Advanced Driver Assistance Systems, 2001. International Conference on ADAS.* (IEE Conf. Publ. No. 483), Birmingham, UK, pp 81-85, 2001.

[Haug 1990] Haug, E. J., "Feasibility Study and Conceptual Design of a National Advanced Driving Simulator", NHTSA Contract DTNH22-89-07352, Report No. DOT-HS-807-597, March. 1990.

[Hedrick et al 1994] Hedrick J.K., Tomizuka M., Varaiya P. "Control issues in automated highway systems". In *IEEE Control Systems Magazine*, Volume: 14, Issue: 6, Dec, pp 21-32, 1994

[Ioannou & Chien 1993] Ioannu P.A. and Chien C.C. "Autonomous Intelligent Cruise Control". In *IEEE Transactions on Vehicular Technology*, Vol 42, NO. 4, Nov, pp 657-672, 1993.

[Jochem et al 1995] Jochem T., Pomerleau D., Kumar B., and Armstrong J., "PANS: A portable navigation platform", In *Proc. Intelligent Vehicles Symposium*, pp. 107-112, Detroit, MI, USA. 1995.

[Kargels 1960] Kargels, G., "Automatic Car Controls for Electronic Highways", In *GMR276*, General Motors Research Labs, June, Warren, MI, 1960.

[Kato et al 2002] Kato, S., Tsugawa S., Tokuda, K., Matsui T. Fujii, H. "Cooperative Driving of Automated Vehicles with Inter-vehicle Communications". In *IEEE Transactions on Intelligent Transportation Systems*. Volume: 3, Issue: 3, pp 155- 161, 2002.

[Khalil 1996] Khalil H.K. *Nonlinear Systems*. 3rd Edition. Prentice Hall, 1996, 2002.

[Khatir & Davison 2006] Khatir, M. E., Davison, E. J. (2006) 'A Decentralized Lateral-Longitudinal Controller for a Platoon of Vehicles Operating on a Plane'. In *Proceedings of 2006 American Control Conference*, June 14-16, Minneapolis, Minnesota, USA. 2006.

[Laumonier et al 2006] Laumonier, J., C. Desjardins and B. Chaib-draa. (2006). Cooperative Adaptive Cruise Control: a Reinforcement Learning Approach. In: *Proceedings of 4th Workshop in Traffic and Transportation, AAMAS'06*. Hakodate, Hokkaido, Japan, May 2006.

[Levine & Athans 1966] Levine J. and Athans M., "On the optimal error regulation of a string of moving vehicles," In *IEEE Transactions on Automatic Control*, Vol. AC-11, No. 11, pp. 355-361, Nov. 1966.

[Lin & Canny 1991] Lin M. and Canny J. "A fast algorithm for incremental distance calculation". In *Proceedings of IEEE Conference on Robotics and Automation*, pp 1008-1014, 1991.

[Liu et al 2001] Liu X; Goldsmith A., Mahal S.S., Hedrick J.K., "Effects of communication delay on string stability in vehicle platoons". In *Proceedings of 2001 IEEE Intelligent Transportation* Systems, Oakland, CA, USA, pp 625 – 630, 2001.

[Maciuca & Hedrick 1995] Maciuca D.B., Hedrick, J.K. 'Advanced Nonlinear Brake System Control for Vehicle Platooning'. In *Proceedings of the third European Control Conference* (ECC 1995), Rome, Italy. 1995.

[Mackworth 1993] Mackworth A. "On Seeing Robots". In *Computer Vision: Systems, Theory and Applications*, World Scientific Press, pp. 1-13, 1993.

[Mahadevan & Connell 1991a] Mahadevan S. and Connell J. "Scaling reinforcement learning to robotics by exploiting the subsumption architecture". In *Proceedings of the Eighth International Workshop on Machine Learning*, pages 328-332, 1991.

[Mahadevan & Connell 1991b] Mahadevan S. and Connell J. "Automatic programming of behavior-based robots using reinforcement learning". In *Proceedings of the Ninth National Conference on Artificial Intelligence*, Anaheim, CA, USA, pp 768-773, 1991.

[Mammar 1997] Mammar, S. "Lateral vehicle control using gain scheduled H∞ controllers", In *IEEE Conference on Intelligent Transportation System, ITSC 97*, 9-12 Nov 1997 Page(s):248 – 253, 1997.

[Meier et al 2004] Meier, G., Roppenecker, G., Wurmthaler, C. "Automatic lateral vehicle guidance using tracking control - a modular approach to separate driver- and vehicle-dependent dynamics." In *2004 IEEE Intelligent Vehicles Symposium*, Page(s): 145 – 149, 14-17 June 2004.

[McMahon & Hedrick 1989] McMahon, Donn H; Hedrick, J K., "Longitudinal model development for automated roadway vehicles", *PATH research report; UCB-ITS-PRR-89-5*, California Department of Transportation, 1989.

[Melzer & Kuo 1971] Melzer S. M. and Kuo B. C. "Optimal regulations of systems described by a countably infinite number of objects," In *Automatica*, Vol. 7, pp359-366, 1971.

[Michaud et al 2006] Michaud, F., Lepage, P., Frenette, P., Létourneau, D., Gaubert, N., "Coordinated maneuvering of automated vehicles in platoon," In *IEEE Transactions on Intelligent Transportation Systems, Special Issue on Cooperative Intelligent Vehicles*, 7(4):437-447, 2006.

[Michel 2004] Michel, O. "Cyberbotics Ltd. Webotstm: Professional Mobile Robot Simulation". In: International Journal of Advanced Robotic Systems. Vol 1 Number 1 pp 39-42, 2004.

[Minorsky 1922] Minorsky, N., "Directional Stability and Automatically Steered Bodies," J. Am. Soc. Nav. Eng., vol. 34, p. 280, 1922.

[NAHS Research Program 1998] National Automated Highway System Research Program. "A Review Committee for a Review of the National Automated Highway System Consortium Research Program." In *Transport Research Board Special Report 253*. National Research Council (U.S.), Washington, D.C.,1998.

[Netto et al 2004] Netto M. S., Chaib S., Mammar S. "Lateral adaptive control for vehicle lane keeping", In *Proceeding of the 2004 American Control Conference*. pp 2693-2698, Boston, USA. 2004.

[Ng et al 2004] Ng A..Y., Coates A., Diel M., Ganapathi V., Schulte J, Tse B., Berger E. and Liang E., Inverted autonomous helicopter flight via reinforcement learning, by. In *International Symposium on Experimental Robotics*, 2004.

[Ng et al 2006] Ng L., Clark C., D'Eleuterio G.M.T, Huissoon J.P., "A Decentralized Reinforcement Learning Controller for Collaborative Driving". In *Proceedings of 1st IFAC Workshop on Multi-Vehicle Systems 2006 MVS '06*. Oct 2-3, Salvador, Bahia, Brazil, 2006.

[Parker 2000] Parker L. E., "Current State of the Art in Distributed Robot Systems", In *Distributed Autonomous Robotic Systems 4*, Lynne E. Parker, George Bekey, and Jacob Barhen (eds.), Springer, pp 3-12, 2000.

[Peng & Tomizuka 1991] Peng H. and Tomizuka M. "Optimal Preview Control For Vehicle Lateral Guidance". In *Research Reports: Paper UCB-ITS-PRR-91-16*, Institute of Transportation Studies California Partners for Advanced Transit and Highways (PATH), University of California, Berkeley, USA, 1991

[Peng et al 1992] Peng H., Zhang W.B., Arai A., Lin Y., Hessburg T., Devlin P., Tomizuka M., Shladover S. "Experimental Automatic Lateral Control System for an Automobile", In *Research Reports: UCB-ITS-PRR-92-11*, Institute of Transportation Studies California Partners for Advanced Transit and Highways (PATH), University of California, Berkeley, USA, 1992.

[Pham et al 1997] Pham H., Tomizuka M., Hedrick K., "Integrated Maneuvering Control for Automated Highway Systems Based on a Magnetic Reference Sensing System". In *Research Reports: UCB-ITS-PRR-97-28*, Institute of Transportation Studies California Partners for Advanced Transit and Highways (PATH), University of California, Berkeley, USA, 1997.

[Pham et al 1996] Pham H., Hedrick J. K. "A Robust Optimal Lateral Vehicle Control Strategy". In *Proceedings of the 1996 IEEE international Conference on Control Applications*, Dearborn, MI September 15-18, pp 361-366. 1996.

[Pham et al 1994] Pham H., Hedrick K., Tomizuka M. "Combined lateral and longitudinal control of vehicles for IVHS". In *Proceedings of the 1994 American Control Conference*, Vol.2, pp1205 – 1206, 1994.

[Rajamani et al 2000] Rajamani R., Tan H.S., Law B.K., Zhang W.B. "Demonstration of integrated longitudinal and lateral control for the operation of automated vehicles in platoons". In *IEEE Transactions on Control Systems Technology*. Vol 8, Issue 4, July, pp 695-708, 2000.

[Raza & Ioannou 1996] Raza H. and Ioannou P. "Vehicle following control design for automated highway systems". In *IEEE Control Systems Magazine*, Vol 16, Issue 6, Dec, pp 43-60, 1996.

[Raza & Ioannou 1997] Raza H. and Ioannou P. "Vehicle following control design for automated highway systems". In *Proceedings of 1997 IEEE 47th Vehicular Technology Conference*, Phoenix, AZ, USA, Vol 2, pp 904-908, 1997.

[Reidmiller et al 2001] Riedmiller M., Merke A., Meier D., Homan A.., Sinner A.., Thate O., and Ehrmann R. "Karlsruhe brainstormers—a reinforcement learning approach to robotic soccer". In *RoboCup-2000: Robot soccer world cup IV*, P. Stone, T. Balch and G. Kraetszchmar (Eds.), pp 367–372. Berlin: Springer Verlag, 2001.

[Ren & Green 1994] Ren W. and Green D. "Continuous platooning: a new evolutionary operating concept for automated highway systems". In *Proceedings of 1994 American Control Conference*, Vol 1, pp 21 – 25, 1994.

[Rummery &Niranjan 1994] Rummery G.A. and Niranjan M. "On-Line Q-Learning using connectionist systems". In: *Technical Report CUED/F-INFENG/TR 166*. Engineering Department, Cambridge University, 1994.

[Safonov 1980] Safonov M.G. Stability and robustness of multivariable feedback systems. *MIT Press Series in Signal Processing , Optimization and Control*. 1980.

[Salaani et al 2001] Salaani, M. K., Grygier, P. A., Heydinger, G. J. "Model Validation of the 1998 Chevrolet Malibu for the National Advanced Driving Simulator", *SAE Paper 2001-01-0141*. March 2001.

[Salaani & Heydinger 2000] Salaani, M. K., Heydinger, G. J. "Model Validation of the 1997 Jeep Cherokee for the National Advanced Driving Simulator". *SAE Paper No. 2000-01-0700*, March. 2000.

[Selim and Fenton 1984] Selim, I. and Fenton, R.E. "On the optimal design of a vehicle lateral controller", In Proceedings of *34th IEEE Vehicular Technology Conference*. Volume 34, 21-23 May 1984 Page(s):291 – 298. 1984.

[Shampine et al 1976] Shampine L., Watts H., Davenport S. "Solving Non-stiff Ordinary Differential Equations - The State of the Art." In *SIAM Review*, Volume 18, pages 376-411, 1976.

[Shladover et al 1991] Shladover S. E., Desoer C. A., Hedrick J. K., Tomizuka M., Walrand J., Zhang W.B., McMahon D. H., Peng H., Sheikholeslam S., and McKeown N. "Automatic vehicle control developments in the PATH program," In *IEEE Transactions in Vehicular Technology*. Vol. 40, no. 1, pp. 114-130, 1991.

[Sutton & Barto 1998] Sutton, R.S. and Barto A.G. *Reinforcement Learning: An Introduction*. A Bradford Book. The MIT Press. Cambridge, MA, USA.1998.

[Stewart & Trinkle 2000] Stewart D. and Trinkle J.C. "An Implicit Time-Stepping Scheme for Rigid Body Dynamics with Coulomb Friction". In *Proceeding of the 2000 IEEE International Conference on Robotics and Automation*. pp 162-169, San Francisco, CA, USA, April, 2000.

[Swaroop & Hedrick 1996] Swaroop D. and Hedrick J.K. "String stability of interconnected systems". In *IEEE Transactions on Automatic Control*, Vol 41, Issue 3, March, pp 349 – 357, 1996.

[Swaroop & Hedrick 1994] Swaroop D., Hedrick J.K. 'Direct Adaptive Longitudinal Control for Vehicle Platoons'. *IEEE Conference on Decision and Control*, December. 1994.

[Tan et al 1998] Tan H.S., Rajamani R., Zhang W.B. "Demonstration of an automated highway platoon system". In *Proceedings of the American Control Conference 1998*. Philadelphia, PA, USA, vol.3, pp 1823-1827, 1998.

[Thorpe et al 1997] Thorpe C., Jochem T., Pomerleau, D. The 1997 automated highway free agent demonstration. In *Proceedings of IEEE Conference on Intelligent Transportation System ITSC 97*. Boston, MA, USA, pp 495-501, 1997.

[Tsugawa et al 2000] Tsugawa S., Kato S., Matsui T., Naganawa H., Fujii, H. "An architecture for cooperative driving of automated vehicles". In *Proceedings of 2000 IEEE Intelligent Transportation Systems*. Dearborn, MI, USA, pp 422-427, 2000.

[Uchibe 1999] Uchibe E. "Cooperative Behavior Acquisition by Learning and Evolution in a Multi-Agent Environment for Mobile Robots". *Ph.D. Thesis*, Osaka University, January, 1999.

[Unyelioglu et al 1996] Unyelioglu K. A., Hatipoglu C., and Ozguner U., "Design and stability analysis of a lane following controller", In *IEEE Trans. on Control Systems Technology*. 1996.

[Variya 1993] Varaiya, P. "Smart cars on smart roads: problems of control". In: *IEEE Transactions on Automatic Control*. Vol 32, Mar 1993.

[Watkins 1989] Watkins C.J.C.H. "Learning from Delayed Rewards". *Ph.D. Thesis*. Cambridge University, 1989.

[Zhang & Ioannou 2005] Zhang J. and Ioannou P.A. "Adaptive Vehicle Following Control System with Variable Time Headways". In *Proceedings of 44th IEEE Conference on Decision and Control and 2005 European Control Conference. CDC-ECC '05*. pp 3880 – 3885, 2005.

[Zhang & Parsons 1990] Zhang W. and Parsons R.E., "An intelligent roadway reference system for vehicle lateral guidance/control". In Proc. *American Control Conf.*, San Diego, CA, USA, 1990, pp. 281-286. 1990.